BIOKINETIC MODELING, LABORATORY EXAMINATION AND FIELD ANALYSIS OF DNA, RNA AND PROTEIN AS ROBUST MOLECULAR BIOMARKERS OF CHLOROETHENE REDUCTIVE DECHLORINATION IN *DEHALOCOCCOIDES MCCARTYI*

A Dissertation

Presented to the Faculty of the Graduate School

of Cornell University

In Partial Fulfillment of the Requirements for the Degree of

Doctor of Philosophy

by

Gretchen Lee Watson Heavner

May 2013

BIOKINETIC MODELING, LABORATORY EXAMINATION AND FIELD ANALYSIS OF DNA, RNA AND PROTEIN AS ROBUST MOLECULAR BIOMARKERS OF CHLOROETHENE REDUCTIVE DECHLORINATION IN *DEHALOCOCCOIDES MCCARTYI*

Gretchen Lee Watson Heavner, Ph. D.

Cornell University 2013

DNA, RNA and protein were tested as specific and robust biomarkers of anaerobic reductive dechlorination by *Dehalococcoides* (DMC) species in predictive modeling, with mixed microbial cultures and at a field site. A comprehensive biokinetic model of a community containing DMC strain 195 was updated to describe continuously fed reactors with specific biomass levels based on quantitative PCR (qPCR)-based population data (DNA and RNA). The model was calibrated and validated with subsets of chemical and molecular biological data from various continuous feed experiments (n=24) with different loading rates of the electron acceptor (1.5 to 482 μeeq/L-h), types of electron acceptor (PCE, TCE, *cis*-DCE) and electron donor to electron acceptor ratios. Based on early model results, both competitive inhibition of chloroethene degradation and empirically derived mRNA "adjustment factors" were added to the model.

Quantitative reverse-transcriptase polymerase chain reaction (qRT-PCR) data were taken from microcosms containing the KB-1^{TM} consortium (SiREM Labs of Guelph, Ontario, Canada), operated under continuous, chlorinated ethene feed conditions, with the aim of clarifying

relationships and creating more robust set of biomarkers that could be used at field sites bioaugmented with the KB-1™ culture. The correlation between respiration rate and mRNA transcript number was upheld for the hydrogenase HupL, and significant differences were observed for reductive dehalogenases (RDases) TceA and DET1545 when comparing the two mixed cultures studied (KB-1™ and D2). A correlation was also observed for RDase VcrA expression compared to respiration rate in the KB-1™ mixed culture. Additionally, correlation trends for HupL and VcrA were upheld when looking at proteomic ion intensities as compared to respiration rates, though protein changes were not as drastic as they were for mRNA transcripts.

Additional experiments were conducted to quantify these biomarkers under stress conditions (presence of oxygen or low pH). Addition of stressors caused respiration rates to decrease significantly, whereas transcript abundances exhibited a slow decay (0.02-0.03 per hr) over the time period studied, indicating that transcript abundance alone cannot predict respiration rate in stressed conditions within hours to days following stress.

A successful proteomics-based method was developed for identifying DMC and *Geobacter* biomarkers of reductive dechlorination at a trichloroethene-contaminated industrial site in Ft. Erie, Ontario that had been bio-augmented with the commercially-available KB-1™ microbial culture two years prior. Samples were obtained from two wells with high hydraulic connectivity to the enhanced in-situ bioremediation system, and two with low hydraulic connectivity. The DNA and RNA biomarkers detected were a set of reductive dehalogenases, and the highly-conserved hydrogenase, HupL. Proteomic biomarkers of organohalide respiration were detected in all four field samples' metaproteomes, and the key reductive dehalogenases present in the bioaugmentation culture were the most highly detected proteins overall, suggesting that deployed DMC strains maintain devotion to high RDase concentrations in the field.

BIOGRAPHICAL SKETCH

Gretchen Lee Watson Heavner was born on July 10, 1977 in Rochester, MN to C. Thomas Watson and Kristy Beth Anderson Watson. Gretchen moved from Rochester to Bellevue, WA, Lafayette, CA, back to Bellevue, WA and then graduated from Lawrence Central High School in Indianapolis, IN in 1995. She earned a Bachelor of Science degree in Chemistry from the University of Puget Sound in 1999. Gretchen earned a Master of Science degree in Civil and Environmental Engineering from the University of Colorado, Boulder in 2002. Gretchen matriculated at Cornell University in 2006 after working as a consulting environmental engineer in Anchorage, Alaska for three years.

Dedicated to Ben and Eli, with love,
for their support and distraction…

ACKNOWLEDGMENTS

First I would like to thank my thesis advisor, Dr. Ruth Richardson, for the many years of invaluable instruction, feedback, and encouragement she has provided during my time in her lab. Ruth is a dedicated advisor, and has always given freely of her time, consistently providing thoughtful and helpful feedback on experiments and manuscripts.

I would also like to thank the other members of my special committee: Drs. James Gossett and Daniel Buckley. Jim was especially involved in my project and has provided much needed expertise and feedback, as well as encouragement.

I owe so much to the PSS Posse, Annie Rowe and Cresten Mansfeldt. I am incredibly lucky to have been given the opportunity to work with such talented, intelligent and supportive people – I never would have made it without you!

I also would like to thank my office mates and CEE peeps, in particular Cloelle Sausville-Giddings, Po-Hsun Lin, Gabriela Hidalgo Casanueva, Deborah Sills and Wan Lutfi Bin Wan Johari who made each day much more enjoyable. It is an amazing thing to have co-workers that are also dear friends.

I also have to thank all of the wonderful friends I made while in Ithaca - especially everyone in the Brewing Conspiracy that I may not have mentioned yet (Mike Booth, Heather Fullerton, Madeline Galac, Sarah Short, Matt Rendina, Rick Pampuro, Ben Logsdon, Punita Juneja, Arend Van Der Zande). You made my time in Ithaca AWESOME and I miss you so much.

I would also like to thank my family. My parents have encouraged me in everything I have ever set out to do (including moving to Alaska alone) and have been

a constant source of reassurance and support. They have always loved me for who I am and I have always known I could count on them for anything, two things I will always be grateful for.

I would also like to acknowledge my son, Eli, to whom this dissertation is dedicated. The first two years have been fun! I look forward to many more!

Finally, I would like to thank my partner in everything and best friend, Ben, who has motivated and supported me throughout my Ph.D. He has made every difficult part of the past six (seven?) years more bearable and every fun part that much more wonderful. He inspires me every day, and I am immensely thankful to have him in my life.

TABLE OF CONTENTS

LIST OF TABLES

LIST OF FIGURES

CHAPTER 1:

Background and Objectives

1.A. Introduction

Humans have caused the release of numerous toxic chemicals to the environment. These waste streams threaten drinking water supplies and natural ecosystems – both terrestrial and aquatic. Attempts have been made both to remediate past releases, and to stop the occurrence of new releases. However, the cost of remediation is often prohibitive – particularly because traditional methods often involve removal of the contaminated substances for treatment. Great strides have been made in recent years towards *in situ* remediation methods – especially with regards to subsurface contamination, which is more challenging to remedy than surface contamination. In recent years, successful *in situ* bioremediation has been documented for common and wide-ranging groundwater contaminants, including chlorinated solvents.[1] This bioremediation can include bioaugmentation and/or biostimulation of naturally occurring microbial populations. Detection of *Dehalococcoides mccartyi* (DMC) DNA at a site indicates that conditions could be favorable for reductive dechlorination.[1,2]

This dissertation seeks to test DNA, RNA and protein as specific and robust biomarkers of anaerobic reductive dechlorination by *Dehalococcoides* species in predictive modeling, with mixed microbial cultures, and at a field site. As a paper-based dissertation, each of the following chapters (Chapters 2-4), presents a complete story describing the specific research objective addressed. The first paper chapter (Chapter 2) describes the development of a biokinetic model utilizing molecular biologically derived (DNA) specific populations levels. The resulting model accurately predicts dechlorination, fermentation and methanogenesis under a variety of conditions in a DMC strain 195 (DMC195)-containing mixed culture (D2) and also incorporates

relevant inhibition parameters and an RNA adjustment factor. The correlation between respiration rate and mRNA transcript abundance has been extensively studied for the Cornell mixed culture (D2).[3–5] Chapter 3 expands this previous work[3–5] to include similar studies with the *Dehalococcoides*-containing mixed culture KB-1™ (SiREM Labs of Guelph, Ontario, Canada) that is commercially available for bioaugmentation at field sites and contains multiple strains of DMC.[6] The third paper chapter (Chapter 4) takes our knowledge of biomarkers of reductive dechlorination and applies them to samples from a trichloroethene (TCE)-contaminated field site, where we report on the first successful proteomics-based method for identifying *Dehalococcoides* and *Geobacter* biomarkers of reductive dechlorination at a trichloroethene-contaminated industrial site in Ft. Erie, Ontario that had been bio-augmented with the commercially-available KB-1™ microbial culture. The purpose of the final chapter (Chapter 5) is to link the three paper chapters into a complete story and provide future directions of this work. The following sections in this chapter provide a contextual background that highlights the importance of the work, and provide a rationale for the chosen research objectives and the approaches taken to carry them out.

1.B. Environmental Contamination with Chloroethenes

Chloroethenes have been widely used as dry-cleaning and degreasing solvents since the 1930s because they are both non-flammable and chemically stable.[7,8] Their widespread use and a historical lack of proper disposal methods cause them to be the most common contaminants observed in soils, sediments, and groundwater aquifers around the world. A recent study by the United States Geological Survey (USGS) suggests that tetrachloroethene (PCE) and TCE are also some of the most common contaminants detected above the Environmental Protection Agency's (EPA's) maximum contaminant levels (MCLs) in untreated groundwater.[1,9,10] PCE,

TCE, *cis*-dichloroethene (*cis*-DCE) and vinyl chloride (VC) are all included on the EPA and Agency for Toxic Substances and Disease Registry (ATSDR) 2011 Substance Priority List, with PCE, TCE and VC in the top 40.[11] This list prioritizes substances based on a combination of their prevalence, toxicity and potential for human exposure. VC is the highest listed organic contaminant, listed fourth after arsenic, lead and mercury.[11]

1.C. Reductively Dechlorinating Microorganisms

The only organisms able to produce a non-toxic end-product (ethene) from PCE and/or TCE through the process of anaerobic reductive dechlorination are members of the genus *Dehalococcoides*[8,12] *Dehalococcoides mccartyi* strain 195 (DMC195) can convert PCE to ethene.[13–15] DMC strains FL2[16], VS[17–19], GT[17] and the mixed culture KB-1[6] can convert TCE to ethene. DMC strain BAV1 can convert DCE to ethene (Figure 1.1).[20] Degradation of PCE or TCE by other species, or DMC strain CBDB1[21–23], often stalls at DCE or VC, suspected and known carcinogens, respectively. Additionally, DMC strain MB produces *trans*-DCE, rather than *cis*-DCE.[24] The DMC isolates, along with numerous environmental and mixed-culture samples, have highly similar 16S rRNA gene sequences. However, Hendrickson et al. divided them into three phylogenetic subgroups based on sequence signatures in hypervariable regions 2 and 6 of the 16S rRNA gene: the Cornell (DMC195), Victoria (DMC strain VS) and Pinellas (DMC strains CBDB1, BAV1, GT and FL2) subgroups.[1,25,26] Other obligate organohalide respirers exist, such as the non-DMC chloroflexi *Dehalogenimonas*, and the Gram-positive *Dehalobacter*.[27,28] However, DMC are still the only organisms to completely dechlorinate PCE or TCE. Thus, evaluating natural attenuation and/or enhanced bioremediation at a field site and establishing engineering procedures for remediation can be closely linked to an understanding of the organisms carrying out transformation of lesser-chlorinated ethenes.[29]

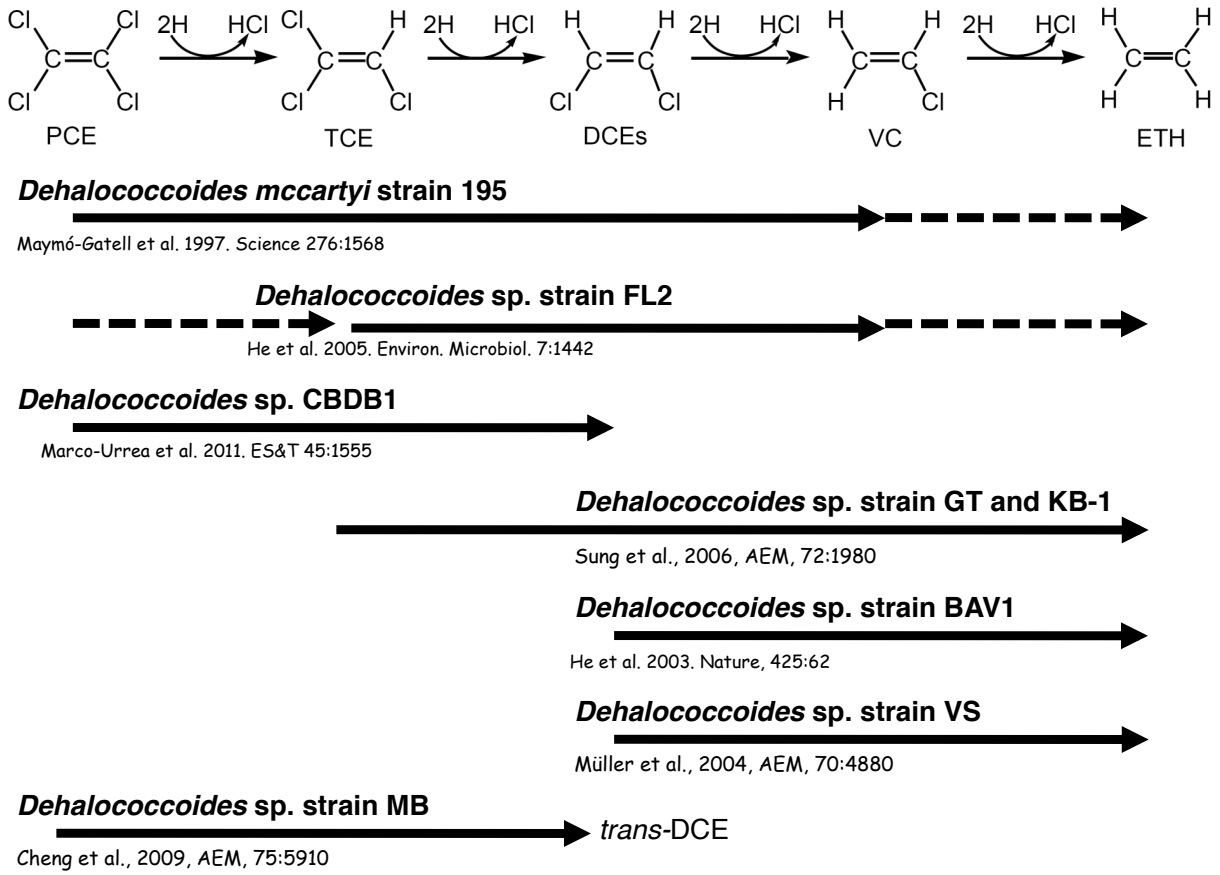

Figure 1.1. *Dehalococcoides* strains catalyze different steps of PCE/TCE dechlorination.

1.D. Biomarkers of Reductive Dechlorination

To prove to a regulatory agency that bioremediation is occurring at a site, three conditions must be met: organisms that are capable of degrading the contaminant under site conditions must be present, loss of the contaminant of interest must be documented, and the organism must be actively expressing its bioremediation capability *in situ*.[30] The third piece of evidence is the most difficult to demonstrate conclusively. Costly microcosms have generally been used to demonstrate it, but biomarkers may serve as the key piece of evidence.

Biomarkers are biomolecules (DNA, RNA or protein) that correspond to a specific microbial process or state. Several studies have been conducted regarding detection of 16S rRNA

genes at field sites. 16S rRNA gene sequences are highly conserved among strains of DMC, forming a distinct phylogenetic group.[1] Hendrickson et al. observed that there is a strong correlation between the presence of the DMC 16S rRNA gene at a site, and the reductive dechlorination of chlorinated ethenes to ethene.[1] However, presence of the 16S rRNA gene does not necessarily mean that dechlorination will occur – present conditions may not be favorable and the targeted electron acceptor differs among strains (phylogeny does not necessarily predict physiology), making it challenging to predict whether or not dechlorination will occur or is occurring at a certain site without more information.[1,31–34] The physiological differences are attributed to the numerous reductive dehalogenases (RDases) coded for in the genomes of each strain of DMC (12-36 per strain).[26] Reductive dehalogenases are the enzymes produced by DMC that allow for respiration of chlorinated organics.

In line with the central dogma of microbiology, the genes for bioremediation may be present, but bioremediation may not be occurring. As a result, the mRNA or protein produced from these genes is a more appropriate indicator of organism activity.[31] Analysis of the mRNA transcripts or proteins for genes other than those directly involved in respiration may be able to give insight into conditions at the site. For example, targeting genes that are related to pH or O_2 stress could give an indication of why a contaminated site is not showing dechlorination when the DNA for the appropriate organisms is present.[31] Several studies have been conducted that examine the quantitative correlation between reductive dechlorination and specific rRNA transcripts.[3–5,35–41] Based on these studies, a preliminary suite of potential field biomarkers can be generated that includes RDases, including VC RDase enzymes that have been linked to successful biological dechlorination of VC to ethene in groundwater systems, and the Ni-Fe hydrogenase, HupL, which is the only predicted periplasm-facing hydrogenase in DMC.[33] The

mechanism of VC dechlorination is important in bioremediation because VC is the most toxic of the chlorinated ethenes, and the VC to ethene step is often rate-limiting.[33] RNA and protein for genes linked to the VC to ethene step of reductive dechlorination (VcrA and BvcA) may serve as the most logical biomarkers for complete remediation of chlorinated ethenes.[33]

1.E. Models of Reductive Dechlorination

In addition to requiring halogenated organics as electron acceptors, all DMC strains require hydrogen as the electron donor. In the mixed community modeled in this study (D2), hydrogen is provided to DMC195, the only DMC strain present,[42] by fermentation of butyrate to acetate and hydrogen (Figure 1.2). There are many putative fermenters in this culture as assessed by 16S rRNA-based clone library, of which *Syntrophomonas* is a dominant member that is able to perform ß-oxidation of butyrate to hydrogen and acetate.[42,43] The other key members of this mixed community are strains of the acetoclastic methanogen *Methanosaeta* (MS) and the hydrogenotrophic methanogen *Methanospirillum* (MHU).[42] Methanogens are common members of dechlorinating communities and methanogenesis is commonly stimulated at PCE/TCE-contaminated sites when fermentable electron donor is provided.[44]

As discussed in Chapter 2, biokinetic models are useful tools for forecasting contaminant conversion rates and studying mixed community dynamics such as anaerobic dechlorination supported by interspecies hydrogen transfer. Various models have been developed that describe reductive dechlorination of chlorinated ethenes.[19,45–59] Several of these models examined high chloroethene concentrations, and thus observed substrate inhibition or toxicity to the dechlorinator,[48,51,55–58] while others examined competitive inhibition among chloroethenes.[46–49,53,54,57,59] However, only two models have been presented that examine the syntrophic community as a whole: Fennell and Gossett[45] (on which this current study is based) and Lee et

al.[47] Additionally, with the exception of Schaefer et al. and Haest et al., component biomass levels in these models were calibrated to total protein (mg total protein) or milligrams volatile suspended solids (mgVSS) in the mixed cultures, and attempts were not made to experimentally quantify individual population components in the community utilizing molecular biology techniques.[54,55]

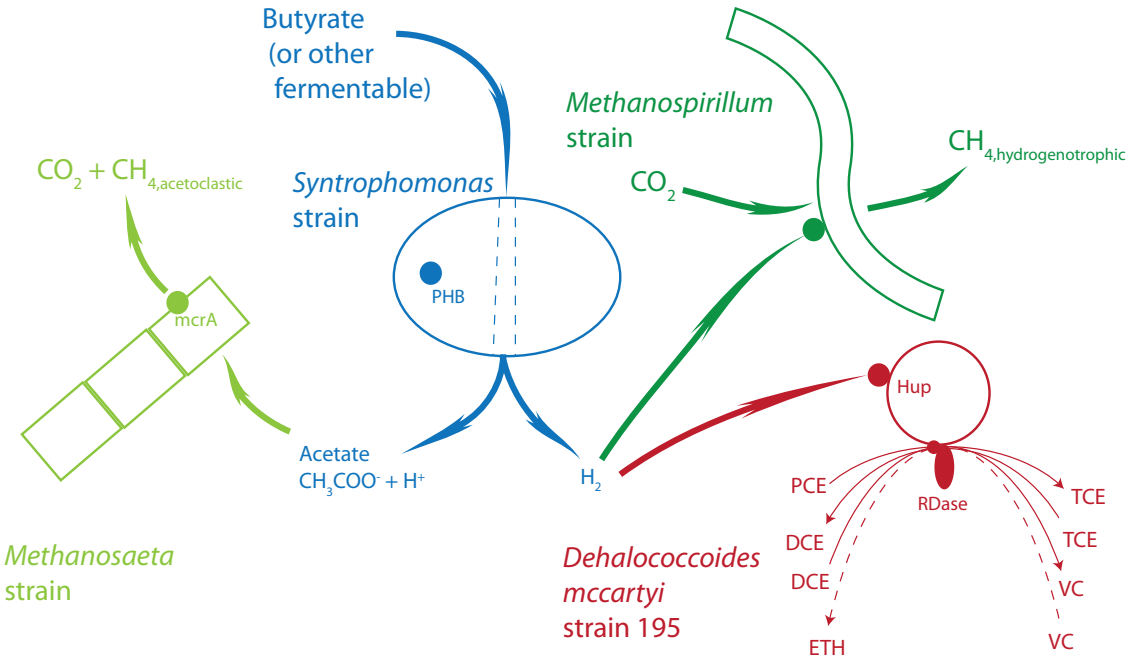

Figure 1.2. Electron and metabolite flow in the *Dehaloccoides mccartyi* strain 195-containing mixed community D2 that is maintained at Cornell University.

1.F. D2 vs. KB-1

Several *Dehalococcoides*-containing mixed communities have been studied by various groups over the years. These mixed cultures differ in the *Dehalococcoides* strains they contain, and thus their degradation capabilities. Two mixed cultures that are able to degrade PCE/TCE to ethene are the D2 culture which is maintained at Cornell University, and the KB-1™ mixed culture that is commercially available for bioaugmentation at field sites[60] and was started from

the KB-1 mixed culture studied at the University of Toronto.[61] These KB-1 cultures differ from the D2 culture in that they contain more than one DMC strain, and are able to gain energy from the reductive dechlorination of VC to ethene.[37,61] It has been observed that multiple reductive dehalogenases are expressed in the KB-1 lab cultures when they are fed TCE, *cis*-DCE, VC or 1,2-dichloroethane, and that two RDases (VcrA and BvcA) are expressed under all the studied conditions.[37]

1.G. Proteomics

Detection of low abundance protein biomarkers is difficult. Several studies have been conducted that examined the quantification of DMC genes and transcripts at a TCE-contaminated field site[35] and the quantitative correlation between reductive dechlorination and specific RNA transcripts.[3–5,35–41] Additionally, several studies have been conducted concerning the proteome of DMC.[5,62–66] Morris et al. examined the metaproteome of the DMC195 pure culture and three other DMC-containing cultures and discovered that HupL is one of the most highly expressed genes in all DMC strains.[62,63] Werner et al. developed a mass spectrometry-based Multiple Reaction Monitoring (MRM) method for absolute quantification of low abundance proteins in complex mixed microbial communities and compared the DMC195-containing mixed culture, D2, and the KB-1 mixed culture.[64] Rowe et al. expanded on this MRM method, and examined the quantitative correlation between reductive dechlorination and the expression of specific genes in DMC195. They also developed *in vivo* enzymatic rate parameters for key RDases TceA and PceA.[5] Previously, the use of proteomic methods in environmental samples has been prohibited by the lack of metagenomic data.[67] However, to date, the genomes of five DMC strains have been sequenced in addition to the metagenomes of three mixed DMC communities (D2, KB-1 and ANAS).[68–72] This allows for the generation of an extensive

reference database for against which to compare peptides for protein identification.

1.H. Rationale for Approach

DNA, mRNA and protein each have benefits and drawbacks as biomarkers. Proteins are the best indicator of potential for activity – they are the functional unit of activity. However, detection of low abundance protein biomarkers is difficult. Conversely, amplification of signal from DNA or mRNA does allow for detection of low abundance biomarkers. Additionally, mRNA can be considered a more sensitive biomarker as it has a much shorter half-life than DNA or protein and is less likely to produce residual signals (this also makes it more difficult to preserve and analyze samples that need to be transported to a lab from the field). Longer half-lives of DNA and protein can make inference of instantaneous activity difficult.

In addition to desiring biomarkers that are specific, robust and indicative of current activity, it would be helpful to have quantitative, high-throughput methods of measuring them. Along this vein, qRT-PCR and microarrays are well-established techniques for analysis. Although microarrays are high-throughput, they are only semi-quantitative. Proteomic methods are also high-throughput, but not as well established, and have not been documented in field samples with DMC previously.

1.I. Research Objectives

The main objective of this study is to test DNA, RNA and protein as specific and robust biomarkers of anaerobic reductive dechlorination by *Dehalococcoides* strains in predictive modeling, with mixed microbial cultures, and at a field site. The specific objectives undertaken to achieve this are:

1) Develop a mechanistic model of the D2 mixed community based on species-specific molecular biological data (DNA and RNA) that also incorporates competitive inhibition
2) Develop robust empirical relationships between mRNA levels and instant respiration rates. This will provide a suite of robust biomarkers of reductive dechlorination that target multiple strains of DMC.
3) Detect field proteomes for DMC (which has not yet been successfully done) and make a comparison of DNA, mRNA and protein biomarker detection in samples from a TCE-contaminated site in Ft. Erie, Canada.

REFERENCES

(1) Hendrickson, E. R.; Payne, J. A.; Young, R. M.; Starr, M. G.; Perry, M. P.; Fahnestock, S.; Ellis, D. E.; Ebersole, R. C. Molecular analysis of *Dehalococcoides* 16S ribosomal DNA from chloroethene-contaminated sites throughout North America and Europe. *Appl. Environ. Microb.* **2002**, *68*, 485–495.

(2) Fennell, D.; Carroll, A.; Gossett, J.; Zinder, S. Assesment of Indigenous Reductive Dechlorinating Potential at a TCE-Contaminated Site Using Microcosms, Polymerase Chain Reaction Analysis, and Site Data. *Environ. Sci. Technol.* **2001**, *35*, 1830–1839.

(3) Rahm, B. G.; Richardson, R. E. Correlation of respiratory gene expression levels and pseudo-steady-state PCE respiration rates in *Dehalococcoides ethenogenes*. *Environ. Sci. Technol.* **2008**, *42*, 416–421.

(4) Rahm, B. G.; Richardson, R. E. Gene Transcripts As Quantitative Bioindicators of Tetrachloroethene, Trichloroethene, and cis-1,2-Dichloroethene Dehalorespiration Rates. *Environ. Sci. Technol.* **2008**, *42*, 5099–5105.

(5) Rowe, A. R.; Heavner, G. L.; Mansfeldt, C. B.; Werner, J. J.; Richardson, R. E. Relating Chloroethene Respiration Rates in *Dehalococcoides* to Protein and mRNA Biomarkers. *Environ. Sci. Technol.* **2012**, *46*, 9388–9397.

(6) Duhamel, M.; Mo, K.; Edwards, E. Characterization of a highly enriched *Dehalococcoides*-containing culture that grows on vinyl chloride and trichloroethene. *Appl. Environ. Microb.* **2004**, *70*, 5538–5545.

(7) Doherty, R. E. A History of the Production and Use of Carbon Tetrachloride, Tetrachloroethylene, Trichloroethylene and 1,1,1-Trichloroethane in the United States: Part 1--Historical Background; Carbon Tetrachloride and Tetrachloroethylene. *Environmental Forensics* **2000**, *1*, 69–81.

(8) Löffler, F. E.; Edwards, E. A. Harnessing microbial activities for environmental cleanup. *Current Opinion in Biotechnology* **2006**, *17*, 274–284.

(9) Squillace, P. J.; Moran, M. J.; Lapham, W. W.; Price, C. V.; Clawges, R. M.; Zogorski, J. S. Volatile Organic Compounds in Untreated Ambient Groundwater of the United States, 1985−1995. *Environ. Sci. Technol.* **1999**, *33*, 4176–4187.

(10) Moran, M. J.; Zogorski, J. S.; Squillace, P. J. Chlorinated Solvents in Groundwater of the United States. *Environ. Sci. Technol.* **2007**, *41*, 74–81.

(11) ATSDR – Priority List of Hazardous Substances **2011**.

(12) Maphosa, F.; De Vos, W. M.; Smidt, H. Exploiting the ecogenomics toolbox for environmental diagnostics of organohalide-respiring bacteria. *Trends in Biotechnology* **2010**.

(13) Maymo-Gatell, X.; Chien, Y.; Gossett, J. M.; Zinder, S. H. Isolation of a bacterium that reductively dechlorinates tetrachloroethene to ethene. *Science* **1997**, *276*, 1568–1571.

(14) Maymo-Gatell, X.; Anguish, T.; Zinder, S. H. Reductive dechlorination of chlorinated ethenes and 1, 2-dichloroethane by *Dehalococcoides ethenogenes* 195. *Appl. Environ. Microb.* **1999**, *65*, 3108–3113.

(15) Fennell, D. E.; Nijenhuis, I.; Wilson, S. F.; Zinder, S. H.; Häggblom, M. M.

Dehalococcoides ethenogenes Strain 195 Reductively Dechlorinates Diverse Chlorinated Aromatic Pollutants. *Environ. Sci. Technol.* **2004**, *38*, 2075–2081.
(16) He, J.; Sung, Y.; Krajmalnik-Brown, R.; Ritalahti, K. M.; Loffler, F. E. Isolation and characterization of *Dehalococcoides* sp. strain FL2, a trichloroethene (TCE)- and 1,2-dichloroethene-respiring anaerobe. *Environ. Microbiol.* **2005**, *7*, 1442–1450.
(17) Sung, Y.; Ritalahti, K. M.; Apkarian, R. P.; Loffler, F. E. Quantitative PCR Confirms Purity of Strain GT, a Novel Trichloroethene-to-Ethene-Respiring *Dehalococcoides* Isolate. *Appl. Environ. Microb.* **2006**, *72*, 1980–1987.
(18) Müller, J. A.; Rosner, B. M.; Von Abendroth, G.; Meshulam-Simon, G.; McCarty, P. L.; Spormann, A. M. Molecular identification of the catabolic vinyl chloride reductase from *Dehalococcoides* sp. strain VS and its environmental distribution. *Appl. Environ. Microb.* **2004**, *70*, 4880–4888.
(19) Cupples, A. M.; Spormann, A. M.; McCarty, P. L. Comparative evaluation of chloroethene dechlorination to ethene by *Dehalococcoides*-like microorganisms. *Environ. Sci. Technol.* **2004**, *38*, 4768–4774.
(20) He, J.; Ritalahti, K. M.; Yang, K.-L.; Koenigsberg, S. S.; Loffler, F. E. Detoxification of vinyl chloride to ethene coupled to growth of an anaerobic bacterium. *Nature* **2003**, *424*, 62–65.
(21) Adrian, L.; Szewzyk, U.; Wecke, J.; Gorisch, H. Bacterial dehalorespiration with chlorinated benzenes. *Nature* **2000**, *408*, 580–583.
(22) Bunge, M.; Adrian, L.; Kraus, A.; Opel, M.; Lorenz, W. G.; Andreesen, J. R.; Görisch, H.; Lechner, U. Reductive dehalogenation of chlorinated dioxins by an anaerobic bacterium. *Nature* **2003**, *421*, 357–360.
(23) Marco-Urrea, E.; Nijenhuis, I.; Adrian, L. Transformation and Carbon Isotope Fractionation of Tetra- and Trichloroethene to Trans-Dichloroethene by *Dehalococcoides* sp. Strain CBDB1. *Environ. Sci. Technol.* **2011**, *45*, 1555–1562.
(24) Cheng, D.; He, J. Z. Isolation and Characterization of "Dehalococcoides" sp Strain MB, Which Dechlorinates Tetrachloroethene to trans-1,2-Dichloroethene. *Appl. Environ. Microb.* **2009**, *75*, 5910–5918.
(25) Hug, L. A.; Salehi, M.; Nuin, P.; Tillier, E. R.; Edwards, E. A. Design and Verification of a Pangenome Microarray Oligonucleotide Probe Set for *Dehalococcoides* spp. *Appl. Environ. Microb.* **2011**, *77*, 5361–5369.
(26) Loffler, F. E.; Yan, J.; Ritalahti, K. M.; Adrian, L.; Edwards, E. A.; Konstantinidis, K. T.; Muller, J. A.; Fullerton, H.; Zinder, S. H.; Spormann, A. M. *Dehalococcoides mccartyi* gen. nov., sp. nov., obligate organohalide-respiring anaerobic bacteria, relevant to halogen cycling and bioremediation, belong to a novel bacterial class, Dehalococcoidetes classis nov., within the phylum Chloroflexi. *Int. J. Syst. Evol. Micr.* **2012**.
(27) Siddaramappa, S.; Challacombe, J. F.; Delano, S. F.; Green, L. D.; Daligault, H.; Bruce, D.; Detter, C.; Tapia, R.; Han, S. S.; Goodwin, L.; Han, J.; Woyke, T.; Pitluck, S.; Pennacchio, L.; Nolan, M.; Land, M.; Chang, Y. J.; Kyrpides, N. C.; Ovchinnikova, G.; Hauser, L.; Lapidus, A.; Yan, J.; Bowman, K. S.; Da Costa, M. S.; Rainey, F. A.; Moe, W. M. Complete genome sequence of *Dehalogenimonas lykanthroporepellens* type strain (BL-DC-9(T)) and comparison to *Dehalococcoides* strains. *Standards in Genomic Sciences* **2012**, *6*, 251–264.

(28) Holliger, C.; Hahn, D.; Harmsen, H.; Ludwig, W.; Schumacher, W.; Tindall, B.; Vazquez, F.; Weiss, N.; Zehnder, A. J. B. *Dehalobacter restrictus* gen. nov. and sp. nov., a strictly anaerobic bacterium that reductively dechlorinates tetra- and trichloroethene in an anaerobic respiration. *Archives of Microbiology* **1998**, *169*, 313–321.
(29) Cupples, A.; Spormann, A.; McCarty, P. Growth of a *Dehalococcoides*-like microorganism on vinyl chloride and cis-dichloroethene as electron acceptors as determined by competetive PCR. *Appl. Environ. Microb.* **2003**, *69*, 4342–4342.
(30) Committee on In Situ Bioremediation, National Research Council *In Situ Bioremediation: When Does it Work?*; The National Academies Press: Washington, D.C., 1993.
(31) Lovley, D. R. Cleaning up with genomics: applying molecular biology to bioremediation. *Nat Rev Micro* **2003**, *1*, 35–44.
(32) Lu, X.; Wilson, J. T.; Kampbell, D. H. Relationship between *Dehalococcoides* DNA in ground water and rates of reductive dechlorination at field scale. *Water Res.* **2006**, *40*, 3131–3140.
(33) Scheutz, C.; Durant, N.; Dennis, P.; Hansen, M. H.; Jorgensen, T.; Jakobsen, R.; Bjerg, P. L. Concurrent ethene generation and growth of *Dehalococcoides* containing vinyl chloride reductive dehalogenase genes during an enhanced reductive dechlorination field demonstration. *Environ. Sci. Technol* **2008**, *42*, 9302–9309.
(34) Tas, N.; Van Eekert, M. H. .; De Vos, W. M.; Smidt, H. The little bacteria that can–diversity, genomics and ecophysiology of *Dehalococcoides* spp. in contaminated environments. *Microbial Biotechnology*.
(35) Lee, P. K. H.; Macbeth, T. W.; Sorenson, K. S.; Deeb, R. A.; Alvarez-Cohen, L. Quantifying Genes and Transcripts To Assess the In Situ Physiology of *Dehalococcoides* spp. in a Trichloroethene-Contaminated Groundwater Site. *Appl. Environ. Microb.* **2008**, *74*, 2728–2739.
(36) Rahm, B. G.; Morris, R. M.; Richardson, R. E. Temporal Expression of Respiratory Genes in an Enrichment Culture Containing *Dehalococcoides ethenogenes*. *Appl. Environ. Microb.* **2006**, *72*, 5486–5491.
(37) Waller, A. S.; Krajmalnik-Brown, R.; Loffler, F. E.; Edwards, E. A. Multiple Reductive-Dehalogenase-Homologous Genes Are Simultaneously Transcribed during Dechlorination by *Dehalococcoides*-Containing Cultures. *Appl. Environ. Microb.* **2005**, *71*, 8257–8264.
(38) Behrens, S.; Azizian, M. F.; McMurdie, P. J.; Sabalowsky, A.; Dolan, M. E.; Semprini, L.; Spormann, A. M. Monitoring abundance and expression of *Dehalococcoides* species chloroethene-reductive dehalogenases in a tetrachloroethene-dechlorinating flow column. *Appl. Environ. Microb.* **2008**, *74*, 5695–5703.
(39) Fung, J. M.; Morris, R. M.; Adrian, L.; Zinder, S. H. Expression of Reductive Dehalogenase Genes in *Dehalococcoides ethenogenes* Strain 195 Growing on Tetrachloroethene, Trichloroethene, or 2,3-Dichlorophenol. *Appl. Environ. Microb.* **2007**, *73*, 4439–4445.
(40) Johnson, D. R.; Lee, P. K. .; Holmes, V. F.; Fortin, A. C.; Alvarez-Cohen, L. Transcriptional expression of the tceA gene in a *Dehalococcoides*-containing microbial enrichment. *Appl. Environ. Microb.* **2005**, *71*, 7145.

(41) Johnson, D. R.; Lee, P. K. .; Holmes, V. F.; Alvarez-Cohen, L. An internal reference technique for accurately quantifying specific mRNAs by real-time PCR with application to the tceA reductive dehalogenase gene. *Appl. Environ. Microb.* **2005**, *71*, 3866.
(42) Rowe, A. R.; Lazar, B. J.; Morris, R. M.; Richardson, R. E. Characterization of the Community Structure of a Dechlorinating Mixed Culture and Comparisons of Gene Expression in Planktonic and Biofloc-Associated *Dehalococcoides* and *Methanospirillum* Species. *Appl. Environ. Microb.* **2008**, *74*, 6709–6719.
(43) Sieber, J. R.; Sims, D. R.; Han, C.; Kim, E.; Lykidis, A.; Lapidus, A. L.; McDonnald, E.; Rohlin, L.; Culley, D. E.; Gunsalus, R.; McInerney, M. J. The genome of *Syntrophomonas wolfei*: new insights into syntrophic metabolism and biohydrogen production. *Environ. Microbiol.* **2010**, 2289–2301.
(44) Henry, B. M. In *In Situ Remediation of Chlorinated Solvent Plumes*; Stroos, H. F.; Ward, C. H., Eds.; Springer, 2010; pp. 357–423.
(45) Fennell, D.; Gossett, J. Modeling the production of and competition for hydrogen in a dechlorinating culture. *Environ. Sci. Technol.* **1998**, *32*, 2450–2460.
(46) Cupples, A. M.; Spormann, A. M.; McCarty, P. L. Vinyl chloride and cis-dichloroethene dechlorination kinetics and microorganism growth under substrate limiting conditions. *Environ. Sci. Technol.* **2004**, *38*, 1102–1107.
(47) Lee, I.-S.; Bae, J.-H.; Yang, Y.; McCarty, P. L. Simulated and experimental evaluation of factors affecting the rate and extent of reductive dehalogenation of chloroethenes with glucose. *J. Contam. Hydrol.* **2004**, *74*, 313–331.
(48) Yu, S.; Semprini, L. Kinetics and modeling of reductive dechlorination at high PCE and TCE concentrations. *Biotechnol. Bioeng.* **2004**, *88*, 451–464.
(49) Yu, S.; Dolan, M. E.; Semprini, L. Kinetics and Inhibition of Reductive Dechlorination of Chlorinated Ethylenes by Two Different Mixed Cultures. *Environ. Sci. Technol.* **2005**, *39*, 195–205.
(50) Becker, J. G. A Modeling Study and Implications of Competition between *Dehalococcoides ethenogenes* and Other Tetrachloroethene-Respiring Bacteria. *Environ. Sci. Technol.* **2006**, *40*, 4473–4480.
(51) Amos, B. K.; Christ, J. A.; Abriola, L. M.; Pennell, K. D.; Löffler, F. E. Experimental Evaluation and Mathematical Modeling of Microbially Enhanced Tetrachloroethene (PCE) Dissolution. *Environ. Sci. Technol.* **2007**, *41*, 963–970.
(52) Becker, J. G.; Seagren, E. A. Modeling the effects of microbial competition and hydrodynamics on the dissolution and detoxification of dense nonaqueous phase liquid contaminants. *Environ. Sci. Technol.* **2009**, *43*, 870–877.
(53) Huang, D.; Becker, J. G. Determination of intrinsic monod kinetic parameters for two heterotrophic tetrachloroethene (PCE)-respiring strains and insight into their application. *Biotechnol. Bioeng.* **2009**, *104*, 301–311.
(54) Schaefer, C. E.; Condee, C. W.; Vainberg, S.; Steffan, R. J. Bioaugmentation for chlorinated ethenes using *Dehalococcoides* sp.: Comparison between batch and column experiments. *Chemosphere* **2009**, *75*, 141–148.
(55) Haest, P.; Springael, D.; Smolders, E. Dechlorination kinetics of TCE at toxic TCE concentrations: Assessment of different models. *Water Res.* **2010**, *44*, 331–339.
(56) Huang, D.; Becker, J. G. Dehalorespiration Model That Incorporates the Self-

Inhibition and Biomass Inactivation Effects of High Tetrachloroethene Concentrations. *Environ. Sci. Technol.* **2011**, *45*, 1093–1099.
(57) Sabalowsky, A. R.; Semprini, L. Trichloroethene and cis-1,2-dichloroethene concentration-dependent toxicity model simulates anaerobic dechlorination at high concentrations: I. batch-fed reactors. *Biotechnol. Bioeng.* **2010**, *107*, 529–539.
(58) Sabalowsky, A. R.; Semprini, L. Trichloroethene and cis-1,2-dichloroethene concentration-dependent toxicity model simulates anaerobic dechlorination at high concentrations. II: Continuous flow and attached growth reactors. *Biotechnol. Bioeng.* **2010**, *107*, 540–549.
(59) Popat, S. C.; Deshusses, M. A. Kinetics and Inhibition of Reductive Dechlorination of Trichloroethene, cis-1, 2-Dichloroethene and Vinyl Chloride in a Continuously Fed Anaerobic Biofilm Reactor. *Environ. Sci. Technol.* **2011**, *45*, 1569–1578.
(60) Major, D. W.; McMaster, M. L.; Cox, E. E.; Edwards, E. A.; Dworatzek, S. M.; Hendrickson, E. R.; Starr, M. G.; Payne, J. A.; Buonamici, L. W. Field Demonstration of Successful Bioaugmentation To Achieve Dechlorination of Tetrachloroethene To Ethene. *Environ. Sci. Technol.* **2002**, *36*, 5106–5116.
(61) Duhamel, M.; Wehr, S. D.; Yu, L.; Rizvi, H.; Seepersad, D.; Dworatzek, S.; Cox, E. E.; Edwards, E. A. Comparison of anaerobic dechlorinating enrichment cultures maintained on tetrachloroethene, trichloroethene, cis-dichloroethene and vinyl chloride. *Water Res.* **2002**, *36*, 4193–4202.
(62) Morris, R.; Sowell, S.; Barofsky, D.; Zinder, S.; Richardson, R. Transcription and mass-spectroscopic proteomic studies of electron transport oxidoreductases in *Dehalococcoides ethenogenes*. *Environ. Microbiol.* **2006**, *8*, 1499–1509.
(63) Morris, R. M.; Fung, J. M.; Rahm, B. G.; Zhang, S.; Freedman, D. L.; Zinder, S. H.; Richardson, R. E. Comparative Proteomics of *Dehalococcoides* spp. Reveals Strain-Specific Peptides Associated with Activity. *Appl. Environ. Microb.* **2007**, *73*, 320–326.
(64) Werner, J. J.; Ptak, A. C.; Rahm, B. G.; Zhang, S.; Richardson, R. E. Absolute quantification of *Dehalococcoides* proteins: enzyme bioindicators of chlorinated ethene dehalorespiration. *Environmental Microbiology* **2009**, *11*, 2687–2697.
(65) Lee, P. K. H.; Dill, B. D.; Louie, T. S.; Shah, M.; VerBerkmoes, N. C.; Andersen, G. L.; Zinder, S. H.; Alvarez-Cohen, L. Global Transcriptomic and Proteomic Responses of *Dehalococcoides ethenogenes* Strain 195 to Fixed Nitrogen Limitation. *Appl. Environ. Microb.* **2012**, *78*, 1424–1436.
(66) Men, Y. J.; Feil, H.; VerBerkmoes, N. C.; Shah, M. B.; Johnson, D. R.; Lee, P. K. H.; West, K. A.; Zinder, S. H.; Andersen, G. L.; Alvarez-Cohen, L. Sustainable syntrophic growth of *Dehalococcoides ethenogenes* strain 195 with *Desulfovibrio vulgaris Hildenborough* and *Methanobacterium congolense*: global transcriptomic and proteomic analyses. *Isme Journal* **2012**, *6*, 410–421.
(67) Wilkins, M. J.; VerBerkmoes, N. C.; Williams, K. H.; Callister, S. J.; Mouser, P. J.; Elifantz, H.; N'Guessan, A. L.; Thomas, B. C.; Nicora, C. D.; Shah, M. B.; Abraham, P.; Lipton, M. S.; Lovley, D. R.; Hettich, R. L.; Long, P. E.; Banfield, J. F. Proteogenomic Monitoring of *Geobacter* Physiology during Stimulated Uranium Bioremediation. *Appl. Environ. Microb.* **2009**, *75*, 6591–6599.
(68) Seshadri, R.; Adrian, L.; Fouts, D. E.; Eisen, J. A.; Phillippy, A. M.; Methe, B. A.;

Ward, N. L.; Nelson, W. C.; Deboy, R. T.; Khouri, H. M.; Kolonay, J. F.; Dodson, R. J.; Daugherty, S. C.; Brinkac, L. M.; Sullivan, S. A.; Madupu, R.; Nelson, K. E.; Kang, K. H.; Impraim, M.; Tran, K.; Robinson, J. M.; Forberger, H. A.; Fraser, C. M.; Zinder, S. H.; Heidelberg, J. F. Genome Sequence of the PCE-Dechlorinating Bacterium *Dehalococcoides ethenogenes*. *Science* **2005**, *307*, 105–108.

(69) Kube, M.; Beck, A.; Zinder, S. H.; Kuhl, H.; Reinhardt, R.; Adrian, L. Genome sequence of the chlorinated compound–respiring bacterium *Dehalococcoides* species strain CBDB1. *Nature Biotechnology* **2005**, *23*, 1269–1273.

(70) McMurdie, P. J.; Behrens, S. F.; Müller, J. A.; Göke, J.; Ritalahti, K. M.; Wagner, R.; Goltsman, E.; Lapidus, A.; Holmes, S.; Löffler, F. E.; Spormann, A. M. Localized Plasticity in the Streamlined Genomes of Vinyl Chloride Respiring *Dehalococcoides*. *PLoS Genet* **2009**, *5*, e1000714.

(71) Hug, L. A.; Beiko, R. G.; Rowe, A. R.; Richardson, R. E.; Edwards, E. A. Comparative metagenomics of three *Dehalococcoides*-containing enrichment cultures: the role of the non-dechlorinating community. *BMC Genomics* **2012**, *13*, 327.

(72) Brisson, V. L.; West, K. A.; Lee, P. K. H.; Tringe, S. G.; Brodie, E. L.; Alvarez-Cohen, L. Metagenomic analysis of a stable trichloroethene-degrading microbial community. *ISME Journal* **2012**, *6*, 1702–1714.

CHAPTER 2:

Molecular Biomarker-Based Biokinetic Modeling of a PCE-Dechlorinating and Methanogenic Mixed Culture

2.A. Abstract

Bioremediation of chlorinated ethenes via anaerobic reductive dechlorination relies upon the activity of specific microbial populations – most notably *Dehalococcoides* (DMC) strains. In the lab and field *Dehalococcoides* grow most robustly in mixed communities which usually contain both fermenters and methanogens. Recently, researchers have been developing quantitative molecular biomarkers to aid in field site diagnostics and it is hoped that these biomarkers could aid in the modeling of anaerobic reductive dechlorination. A comprehensive biokinetic model of a community containing *Dehalococcoides mccartyi* (formerly *D. ethenogenes*) was updated to describe continuously fed reactors with specific biomass levels based on quantitative PCR (qPCR)-based population data (DNA and RNA). The model was calibrated and validated with subsets of chemical and molecular biological data from various continuous feed experiments (n=24) with different loading rates of the electron acceptor (1.5 to 482 μeeq/L-h), types of electron acceptor (PCE, TCE, *cis*-DCE) and electron donor to electron acceptor ratios. The resulting model predicted the sum of dechlorination products vinyl chloride (VC) and ethene (ETH) well. However, VC alone was under-predicted and ETH was over-predicted. Consequently, competitive inhibition among chlorinated ethenes was examined and then added to the model. Additionally, as 16S rRNA gene copy numbers did not provide accurate model fits in all cases, we examined whether an improved fit could be obtained if mRNA levels for key functional enzymes could be used to infer respiration rates. The resulting empirically-derived mRNA "adjustment factors" were added to the model for both DMC and the main methanogen in the culture (a *Methanosaeta* species) to provide a more nuanced prediction

of activity. Results of this study suggest that at higher feeding rates competitive inhibition is important and mRNA provides a more accurate indicator of a population's instantaneous activity than 16S rRNA gene copies alone as biomass estimates.

2.B. Introduction

Tetrachloroethene (PCE) and trichloroethene (TCE) are two of the most common contaminants observed in soils, sediments and groundwater aquifers around the world.[1] *In situ* bioremediation is gaining in acceptance as a method for treating groundwater contaminated with PCE and TCE. The only isolated microorganisms known to completely dechlorinate PCE to non-toxic ethene (ETH) are strains of *Dehalococcoides* (DMC), through the process of anaerobic reductive dechlorination. However, DMC strains grow most robustly as part of a mixed microbial community (in both environmental systems and enrichment cultures), likely due to critical growth factors produced by other community members, higher *in situ* hydrogen levels as a result of interspecies hydrogen transfer, or protection from oxidative stress under shifting redox conditions.[2–7] In the process of reductive dechlorination, chlorine atoms are sequentially replaced by hydrogen atoms, forming TCE, dichloroethene (DCE), vinyl chloride (VC) and ethene. There are other genera of microorganisms that can catalyze different steps of PCE/TCE dechlorination; however, degradation stops at DCE. Understanding the factors affecting transformation of lesser-chlorinated ethenes is informative for the evaluation of natural attenuation and for the establishment of engineering procedures for remediation.[8]

In addition to requiring halogenated organics as electron acceptors, all DMC strains require hydrogen as the electron donor. In the mixed community studied (D2), hydrogen is provided to *Dehalococcoides mccartyi* strain 195 (DMC195), the only DMC strain present,[9] by fermentation of butyrate to acetate and hydrogen. There are many putative fermenters in this culture as assessed by 16S rRNA-based clone library, of which *Syntrophomonas* is a dominant

member that is able to perform ß-oxidation of butyrate to hydrogen and acetate.[9,10] The other key members of this mixed community are strains of the acetoclastic methanogen *Methanosaeta* (MS) and the hydrogenotrophic methanogen *Methanospirillum* (MHU).[9] Methanogenesis is commonly stimulated at PCE/TCE-contaminated sites when excess fermentable electron donor is provided.[11]

Biokinetic models are useful tools for forecasting contaminant conversion rates and studying mixed community dynamics such as anaerobic dechlorination supported by interspecies hydrogen transfer. Various models have been developed that describe reductive dechlorination of chlorinated ethenes.[12–27] Several of these models examined high chloroethene concentrations, and thus observed substrate inhibition or toxicity to the dechlorinator,[16,19,23–26] while others examined competitive inhibition among chloroethenes.[13,15–17,21,22,25,27] However, only two models have been presented that examine the syntrophic community as a whole: Fennell and Gossett[12] (on which this current study is based) and Lee et al.[15] Additionally, with the exception of Schaefer et al. and Haest et al., all of these models were developed based on total protein (mg total protein per L) or milligrams volatile suspended solids (mgVSS) in the mixed cultures, and attempts were not made to experimentally quantify individual populations in the community utilizing molecular biology techniques.[22,23]

The objective of this study was to develop a biokinetic model utilizing molecular biologically-derived specific population levels that accurately predicts dechlorination, fermentation and methanogenesis under a variety of conditions in a DMC195-containing mixed culture (D2), that also incorporates relevant inhibition parameters. The model was tested with three chlorinated electron acceptors (PCE, TCE, *cis*-DCE) continuously fed to the culture at a variety of feed rates and varying electron donor to electron acceptor ratios. The fit of the model

to data sets was numerically evaluated for chloroethenes, butyrate, acetate, methane and hydrogen. In cases of poor model fits (methane, PCE or butyrate/acetate) mRNA expression data were examined to explore whether mRNA biomarkers more accurately reflect specific populations' activities. The mRNA targets chosen as biomarkers of methanogenesis and dechlorination were coenzyme-M reductase (McrA - MS) and a Ni/Fe hydrogenase (HupL - DMC), respectively. McrA is a subunit of a key functional enzyme in methane generation.[28] HupL is a hydrogenase found in all DMC strains. Previous work comparing HupL transcripts (mRNA per mL) to respiration rates showed a power relationship (on a log-log scale) with a correlation score (Pearson's *r*) of 0.88 over three orders of magnitude.[29–31] The current study generated a similar empirical relationship for McrA transcripts versus methanogenesis and tested it in the biokinetic model as predictors of actual methanogenesis rates.

2.C. Materials and Methods

2.C.1. Continuous Feed (Pseudo-Steady State) Experiments.

An enrichment culture (D2) containing DMC195 was maintained on PCE and butyrate as described previously.[32,33] Subcultures (100-mL) of the D2 stock culture were established in 160-mL serum bottles, and continuous feed experiments were carried out as described previously.[30,29,31] Yeast extract and vitamin solution were pulse fed at the beginning of the experiment, and periodically thereafter as needed. Liquid and headspace samples were collected for sample analysis and to maintain the culture volume (no increase of more than 10%).[31] Experimental parameters for the continuous feed experiments are presented in Table A1.1 in Appendix I.

2.C.2. Analytical Methods.

Chlorinated ethenes, ethene, and methane were analyzed from 100-µL headspace samples via gas chromatography as described by DiStefano[34] and Smatlak,[35] and modified by Rahm and

Rowe.[31,32] Hydrogen was analyzed from 50-μL headspace samples via reduction gas detector (RGD, Trace Analytical RGD2).[33] Butyrate and acetate were analyzed via a Dionex Ion Chromatograph (IC).[36]

2.C.3. Biokinetic Model.

A comprehensive physiological model of the D2 mixed community[12,37] was reworked to include molecular biological data for population densities (cells/mL) and kinetic rate constants (μmole/cell-h), and updated to describe continuously fed reactors instead of batch microcosms. The model describes dechlorination, fermentation, competition for H_2 by DMC and hydrogenotrophic methanogens, and generation of methane. It is based on Monod-type kinetics, and utilizes both H_2 thresholds and thermodynamic limitations on butyrate fermentation.[12] Kinetic equations described by Fennell[12,37] still apply, except for the changes described below. The units of biomass have been changed from mgVSS to 16S rRNA gene copies, and this was incorporated into the kinetic constants as described below. The model keeps track of volatile compounds in both the gaseous and aqueous phases, and interphase transport is modeled using mass transfer coefficients, as described by Fennell.[37]

2.C.4. Cell Concentration Determination.

Cell concentrations for *Dehalococcoides* (X_{DMC195}), *Methanospirillum* (X_{MHU}) and *Methanosaeta* (X_{Ms}) were obtained using quantitative polymerase chain reaction (qPCR) for 16S rRNA genes specific to those populations. DNA extractions were performed using the UltraClean Microbial DNA Isolation Kit (Mo Bio Laboratories) or the AllPrep DNA/RNA Mini Kit (Qiagen). 16S rRNA gene copies were quantified by amplification of DNA with iQ SYBR Green Supermix (Bio-Rad) and primers as described previously.[32,31,9,38] Triplicate amplifications of all samples were conducted on the iCycler iQ Multicolor Real-Time PCR Detection System

(Bio-Rad). Transcript levels were determined with the help of Data Analysis for Real-Time PCR (DART-PCR), available at http://www.gene-quantification.de/download.html#dart.[30,39] Number of copies were converted to cells by dividing by the number of copies of the 16S rRNA gene in the available genomes of the same genus as well as the D2-specific metagenome (available at JGI IMG http://img.jgi.doe.gov). DMC195 has one 16S rRNA gene copy per genome, MHU was assumed to have four copies per genome, and MS was assumed to have two copies per genome. Fermenter population numbers were estimated by subtracting the DMC195, MHU, and MS population numbers from the total culture population as determined previously by FISH with DAPI counterstaining.[9]

2.C.5. Calculation of Kinetic Parameters.

Yield parameters for DMC195 were determined from growth experiments under non-limiting PCE concentrations over a 24-hour period.[29] Kinetic parameters for the dechlorinators (k_{max} and K_S) were calculated by nonlinear regression of Equation 1. k_{max} and K_S for VC were calculated from batch experiments where triplicate bottles were fed increasing amounts of VC as in Yu, 2005[17], but with the inclusion of hydrogen as a second limiting substrate as in Fennell.[12] The generic equation for microbial transformation of a chloroethene is:

$$\frac{\frac{dM_{W,CE}}{dt}}{\frac{(C_{W,H_2} - H_2 Threshold_{DMC195})}{K_{S,H_2,DMC195} + (C_{W,H_2} - H_2 Threshold_{DMC195})} * X_{DMC195}} = -\frac{k_{CE} C_{W,CE}}{K_{S,CE} + C_{W,CE}} \qquad (1)$$

where k_{CE} is the maximum specific rate of chloroethene utilization (µmol/cell-h); $C_{W,CE}$ is the aqueous chloroethene concentration (µmol/L); $K_{S,CE}$ is the half velocity constant for chloroethene use (µmol/L); $M_{W,CE}$ is the total amount of chloroethene (PCE, TCE, DCE or VC) in the aqueous phase (µmol); X_{DMC195} is the total DMC195 biomass contained in the serum bottle (cells); C_{W,H_2} is the aqueous H_2 concentration (µmol/L); $K_{S,H_2,DMC195}$ is the half-velocity constant

for H_2 use by DMC195 (μmol/L); and H_2 $Threshold_{DMC195}$ is the thermodynamic threshold for H_2 use by dechlorinators (μmol/L).[12]

k_{max} for the methanogens was calculated using Equation 2. K_S values for the methanogens and fermenters were the same as those utilized in the original model.[12] k_{max} values for the hydrogenotrophic and acetoclastic methanogens were determined experimentally in batch cultures that were fed H_2/CO_2 only or acetate only, respectively. The generic equation for methanogenesis is:

$$\frac{d[CH_4]}{dt} = \frac{k_{\max} X S}{K_S + S} \tag{2}$$

where $[CH_4]$ is the total amount of methane in the bottle (μmol); X is the total methanogen biomass (acetoclastic or hydrogenotrophic) contained in the serum bottle (cells); S is the limiting substrate (acetate or H_2) concentration (μmol/L); k_{max} (μmol/cell-h) and K_S (μmol/L) are the maximum specific rate of substrate utilization and half velocity coefficients for methanogenesis (acetoclastic or methanogenic), respectively. Modeling of hydrogenotrophic methanogenesis also includes a hydrogen threshold (8 nM) as described by Fennell.[12]

Modeling of electron donor fermentation includes a factor (Φ) incorporating the influence of the thermodynamics of product formation (ΔG_{rxn} and $\Delta G_{critical}$) on the rate of fermentation as in Fennell et al.[12] Φ was calculated from pseudo steady-state experiments in which butyrate was pulse-fed and butyrate, acetate, and H_2 were measured. The equation for fermentation is:

$$\frac{dS}{dt} = \frac{-k_{\max} X_{ferm} S \Phi}{K_S + S} \quad \text{where } \Phi = 1 - \exp\left(\frac{\Delta G_{rxn} - \Delta G_{critical}}{RT}\right) \tag{3}$$

where X_{ferm} is the total fermenter biomass (assumed to be *Syntrophomonas*) contained in the serum bottle (cells); S is the mass of electron donor (butyrate) in the bottle; k_{max} (μmol/cell-h) and K_S (μmol/L) are the maximum specific rate of substrate utilization and half velocity

coefficients for fermentation, respectively.

In order to determine the yield (Y) in units of cells/µmol, the specific growth rates (µ, per hour) for the methanogens and fermenters were calculated using the original values for k_{max} and yield (4.9 µmol/mgVSS-h and 0.00279 mgVSS/µmol, respectively) that were used in the Fennell model.[12] A new yield (cells per µmole substrate) was then calculated using that specific growth rate, and the newly calculated k_{max} using Equation 4.

$$\mu = \frac{Yk_{\max}S}{K_S + S} - b \tag{4}$$

where b is the decay parameter which was assumed to be 0.001 per hour.[12]

The nonlinear regressions and 95 percent confidence intervals for the kinetic parameters were calculated using the Curve Fitting Toolbox in MATLAB (Math Works) (Table 2.1, Figure A1.1).

Table 2. 1. Kinetic Parameters Used for Modeling

	kmax	95% Confidence Interval		Ks	95% Confidence Interval		Yield	Units in terms of:	16S rRNA gene copies /cell	Cells/mL culture
	µmol/cell-h	Lower	Upper	µmol/L	Lower	Upper	cells/µmol			
H_2-Methanogens	9.4E-10	n/a	n/a	0.5[35]	n/a	n/a	6.08E+07	H2	4	1.70E+08
Ac-Methanogens	3.3E-09	2.6E-09	3.9E-09	557	236	878	4.19E+05	acetate	2	5.65E+07
Fermenters	1.1E-08	8.8E-09	1.4E-08	261	154	454	1.26E+06	butyrate	3	1.64E+07
DMC-PCE	3.5E-10	3.0E-10	4.1E-10	22	14	34	1.60E+08[29]	chloride or H2	1	2.73E+08
DMC-TCE	2.2E-10	1.8E-10	2.6E-10	0.18	0.074	0.40	1.60E+08[29]	chloride or H2	1	"
DMC-DCE	2.2E-10	1.8E-10	2.6E-10	2.9	0.89	12	1.60E+08[29]	chloride or H2	1	"
DMC-VC	1.0E-10	6.7E-11	1.5E-10	101	21	314	0	-	1	"

2.C.6. Inhibition Parameters.

A competitive inhibition model was parameterized by conducting batch experiments in which two electron acceptors were fed concurrently at varying concentrations (as in Yu, 2005).[17]

Butyrate was fed in excess to prevent hydrogen being rate-limiting. Competitive inhibition was then included in the model using the following equation

$$\frac{dM_{W,CE}}{dt} = -\frac{k_{CE} X_{DMC195} C_{W,CE}}{K_{S,CE}\left(1+\frac{S_{I,1}}{K_{I,1}}+\frac{S_{I,2}}{K_{I,2}}\right)+C_{W,CE}} \quad (5)$$

where $S_{I,1}$ and $S_{I,2}$ are the aqueous concentrations of chloroethenes that inhibit the chloroethene of interest (μmol/L). The inhibition constants of each chloroethene are expressed as $K_{I,1}$ and $K_{I,2}$ (μmol/L), and were set to the respective half-saturation constants from uninhibited experiments, as done previously.[17,16]

A Haldane inhibition model for acetoclastic methanogenesis was parameterized by conducting batch experiments in which only acetate was fed at varying concentrations. The kinetic equation for acetoclastic methanogenesis was modified to include this parameter as follows:

$$\frac{d[CH_4]}{dt} = \frac{k_{\max} X S}{K_S + S + S^2/K_I} \quad (6)$$

2.C.7. Estimating Fermentable Electron Equivalents Provided by Yeast Extract (YE) and Endogenous Decay of Biomass.

Endogenous decay was included as a source of hydrogen in the model as previously described, but with a conversion from cell numbers to mg VSS (by morphology, making assumptions of % dry weight per cell) and then to μmol butyrate.[12,2,40] Electron equivalents (eeqs) provided by yeast extract were calculated from batch reactors fed yeast extract and PCE only. Total reduction products (H_2, lesser chlorinated ethenes, organic acids and methane) were summed after 24 hours, and the eeqs provided per μL of yeast extract were calculated.

2.C.8. Evaluation of Fit.

The fit of the model to experimental data was evaluated using Pearson's chi-squared (χ^2) test for goodness of fit, calculated using Matlab.

2.C.9. Evaluation of mRNA Expression.

RNA extractions were performed using the bacterial protocol of the RNeasy Mini Kit (Qiagen) or the AllPrep DNA/RNA Mini Kit (Qiagen) with modifications and DNase treatments as previously described.[32] For the genes of interest from MS and *Syntrophomonas* (McrA and PHB Synthase, respectively), homologs were found within the D2 metagenome available at http://img.jgi.doe.gov under "PCEOT." Primers were designed for the D2 metagenome homolog using IDT PrimerQuest, and were then checked for specificity using BLAST with the nucleotide collection (nr/nt) database (McrA-F: 5'-AACAATCCAGCCATGCAGCAGTTC-3', McrA-R: 5'-TGTTGATGGTCTCGGGTGTGACTT-3', PHB-F: 5'-TTGCCAAACGCATAGTGAGCAAGG-3' and PHB-R: 5'-TTCCACAAATGCGGTCATGCCTTC-3'). Expression of the hydrogenase HupL in DMC195 was evaluated using primers described previously.[41]

2.D. Results and Discussion

2.D.1. Calculation of Kinetic Parameters.

The Monod curves for PCE, TCE, *cis*-DCE and VC transformation, and fermentation, and a Haldane model for acetoclastic methanogenesis by the D2 culture are shown in Figure A1.1. The curves show good fits for all metabolites. Table 2.1 presents k_{max} and K_S values for the D2 culture for each process included in the model.

For comparison, kinetic parameter values from the literature were recalculated according to Duhamel et al.[2] assuming protein content of 50% and conversion factors of 4.2×10^{-15} and 7.4×10^{-14} g dry weight of cell per 16S rRNA gene copy for DMC195 and *Syntrophomonas*, respectively. In the literature, k_{max} values for chloroethenes ranged from 6×10^{-14} to 6.5×10^{-9}

μmol/cell-h.[12,16,42,23,14,6] The k_{max} and yield values for butyrate fermentation by *Syntrophomonas* were 2.8 x 10^{-9} μmol/cell-h and 3.1 x 10^{6} cells/μmol, respectively.[43]

Substrate inhibition of acetate was observed for acetoclastic methanogenesis (Figure A1.1F), and model fits suggested a K_I of 17.2 mM (95% CI of 6.0 to 28.4 mM). Haldane inhibition was also examined for the chloroethenes (PCE in particular), as it was included in the model presented by Yu.[16] It was found that at the range of PCE concentrations observed in this study, substrate inhibition was not applicable – a K_I of 4 mM was calculated, which is much higher than the highest observed PCE concentration, and the saturated PCE concentration of 904 μM. Observed inhibition was highest in experimental bottles where PCE reached saturating levels (HLH1_INHIB and HLH2_INHIB in Table A1.1) but this is more likely attributable to solvent toxicity than to true substrate inhibition.

2.D.2. Fate of Electron Donor eeqs.

In the D2 mixed culture, butyrate is fermented to acetate and hydrogen, and methane is produced from both acetate and hydrogen. Hydrogen is also used for anaerobic reductive dechlorination. Calculated from model results, 80-90% of the methane produced was from acetate, as long as the culture was not electron donor limited (consistent with previous findings).[11] When electron donor was limited (no butyrate or yeast extract provided) a small amount of methane was produced, but nearly all of it (99%) was from acetate. Hydrogen is also used by the dechlorinators to reductively dechlorinate the chloroethenes. Depending on the ratio of electron donor to electron acceptor, between 8 and 76% of the hydrogen eeqs were used for dechlorination, as calculated from model results. (At a low electron donor to electron acceptor ratio, more eeqs were used for dechlorination and at a higher ratio, more eeqs were available for methanogenesis). Experimental results are discussed in more detail by Rowe.[31]

2.D.3. Model Fits

"Bare bones" model (no competitive inhibition, no eeqs from yeast extract, no endogenous decay).

The "bare bones" model is the Fennell model[12] converted to include molecular biological data for population densities and kinetic rate, and updated to describe continuously fed reactors. As shown in Figure 2.1, VC+ETH was predicted fairly well in the "bare bones" model (no competitive inhibition, no eeqs from yeast extract, no endogenous decay) over a wide range of feeding rates (1.5 to 183 μeeq/L-h), and for all electron acceptors fed (PCE, TCE, *cis*-DCE). As done previously for DMC195[30], VC and ethene were plotted together because in DMC195, the VC to ethene step is cometabolic, and no energy is produced.[6,44,45] However, as the feeding rate increased, the χ^2 value also increased (χ^2 values are presented in Table A1.2, 'No INH' column). At the lowest feeding rates, the χ^2 value ranged from 0.014 to 0.58. At the medium feeding rates, the χ^2 value ranged from 0.33 to 1.9. At the highest feeding rate for PCE (HLH3), VC+ETH was not predicted as well, with a χ^2 value of 122, whereas for *cis*-DCE (D3A2) and TCE (T3A1) the high feeding rate χ^2 values were 10 and 1.7, respectively. Poor fits at higher feeding rates were likely caused by competitive inhibition of PCE degradation by buildup of TCE and/or DCE, which normally are below detection limits (20-40 nM aqueous) at low feeding rates. At low feeding rates (~2-10 μeeq/L-h), the respiration rate was generally equal to the feeding rate – the concentration of substrate limited the reaction rate (first-order kinetics). However, at higher feeding rates, the concentration of substrate no longer limited the reaction rate (zero-order kinetics) and higher chlorinated ethenes accumulated to detectable levels.

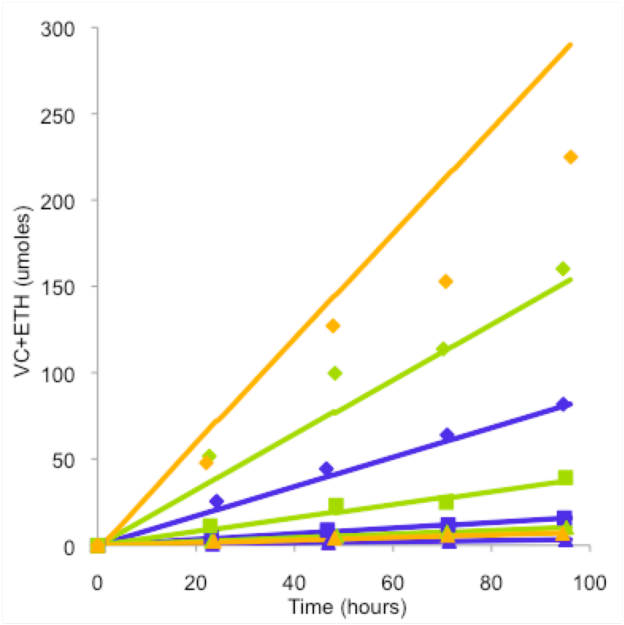

Figure 2. 1. VC+ETH model predictions (lines) as compared to experimental data (points) for high (diamond or solid line), medium (square or long dashed line) and low (triangle or short dashed line) feeding rates of PCE (orange), TCE (blue) or DCE (green). The VC+ETH is a running total for bottles with high feeding rates that were purged when VC+ETH > 50 µmole/bottle (0.5 mM nominal). Bottles included in the figure are HLH3, HLL1, T3A1, T3B1, T3C1, D3A2, T3B2, T3C2.

Inclusion of electron equivalents from yeast extract and biomass endogenous decay.

Three experiments that were fed PCE at low feeding rates (~5 µeeq/L-h) were used to examine the inclusion of eeqs from yeast extract and biomass endogenous decay: no electron donor or yeast extract added (P0FY01), no electron donor, but with yeast extract added (P0FYY1), and an experiment with butyrate and yeast extract added (HLL1). Even when no butyrate was fed it was observed that dechlorination and methanogenesis did occur (Figure 2.2A,B). In fact, researchers have suggested that endogenous decay of *in situ* biomass can fuel dechlorination.[46] Consequently, endogenous decay and available eeqs from yeast extract (~1.5 µeeq/µL fed) were included in the model. As shown in Figure 2.2, the addition of eeqs from endogenous decay to the case where no electron donor and no yeast extract were fed to the culture resulted in accurate prediction of PCE and VC+ETH (Figure 2.2A). Though methane was

greatly overpredicted in the endogenous decay only example, in any experiment where an electron donor was added (yeast extract or butyrate) this overprediction became insignificant (Figures 2.2B and C).

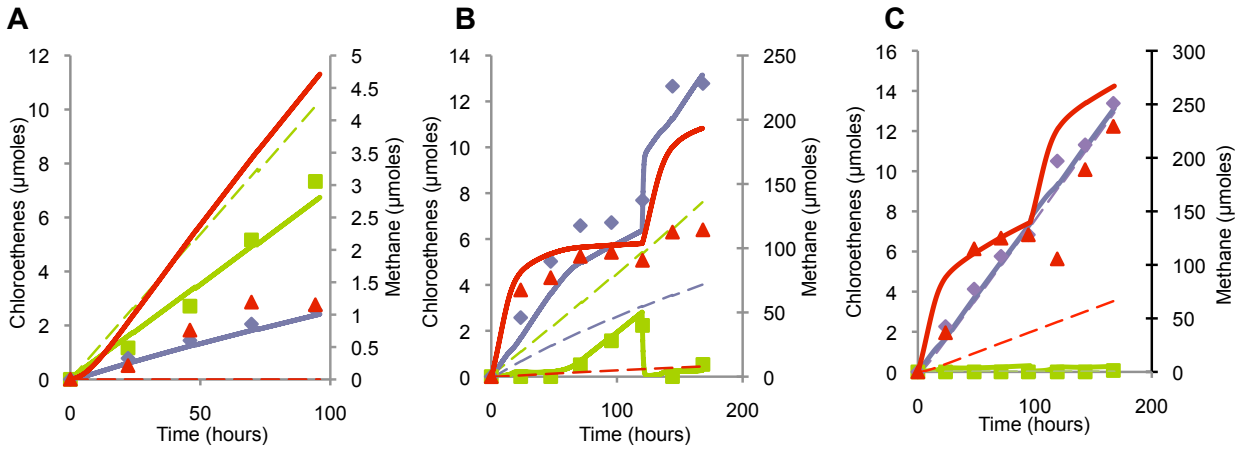

Figure 2. 2. Effects of inclusion of endogenous decay and yeast extract eeqs to the model. In each case the points are experimental data, the dashed lines are model predictions without inclusion of endogenous decay or yeast extract eeqs, and the solid lines are model predictions including endogenous decay and/or yeast extract eeqs, as appropriate. PCE is shown in green (squares), VC+ETH is blue (diamonds), and methane is red (triangles). TCE and DCE are not shown as their concentrations were consistently an order of magnitude lower than PCE.
A – experiment with no electron donor, showing addition of variable endogenous decay (P0FY01)
B – experiment with no electron donor, fed YE at 0 &120 hours (P0FYY1)
C – experiment with continuous feed of butyrate as electron donor, fed YE at 0 &100 hours (HLL1)

Figure 2.2B shows that PCE, VC+ETH or methane were not predicted well in the case where yeast extract was provided to the culture and variable endogenous decay was the sole source of reducing equivalents in the model. However, when reducing equivalents were also provided by yeast extract in the model, all the fits improved.

Figure 2.2C shows that when both butyrate and yeast extract were fed, a model that doesn't include eeqs from yeast extract predicted PCE and VC+ETH well, but not methane. The addition of eeqs from endogenous decay and yeast extract to the model greatly improved the methane fit.

Inclusion of competitive inhibition.

Though VC+ETH was generally predicted well in the model ("bare bones" and with endogenous decay and yeast extract eeqs), VC and ETH individually were not predicted well – especially at higher electron acceptor feed rates. Experiments were conducted to develop a competitive inhibition model for DMC195. Results of inhibition studies are shown in the Supporting Results Section in Appendix I and Figure A1.2. The observed inhibition patterns among chloroethenes are summarized in Figure A1.3.

Previously, inhibition models were proposed for the PM and EV mixed cultures, maintained on TCE and PCE, respectively,[17,16] and the commercially available Shaw SDC-9 culture,[27] which contain different DMC strains than the D2 mixed culture (though all three contain a DMC strain that produces TceA and VcrA). All three inhibition models showed TCE inhibition of DCE and VC degradation. The most significant difference was that in our mixed culture (and the PM and EV mixed cultures), there was a strong inhibition of the VC to ETH step by DCE, and this was not shown in the Popat inhibition model.[17,16,27] The differences in these inhibition models are likely due to strain-specific reductive dehalogenases catalyzing the step-wise reductive dechlorination of PCE to ethene. However, it was surprising to see a similar trend in TCE inhibition of VC in cultures (PM, EV and Shaw SDC-9, e.g.) that contain a separate VC-specializing RDase (VcrA or BvcA). As done previously, measured Ks values reported above were used as putative competitive inhibition constants in the model, as shown in Equation 5.[17,16]

The community model was run both with and without competitive inhibition, and the fits compared. Inclusion of competitive inhibition in the model improved the overall fit for VC and ETH individually at higher feeding rates (Figures 2.3A-C), without affecting good fits at lower feeding rates (Figures 2.3D-F). χ^2 values are presented in Table A1.2 and model fits for all

metabolites and experiments are presented in Figure A1.6.

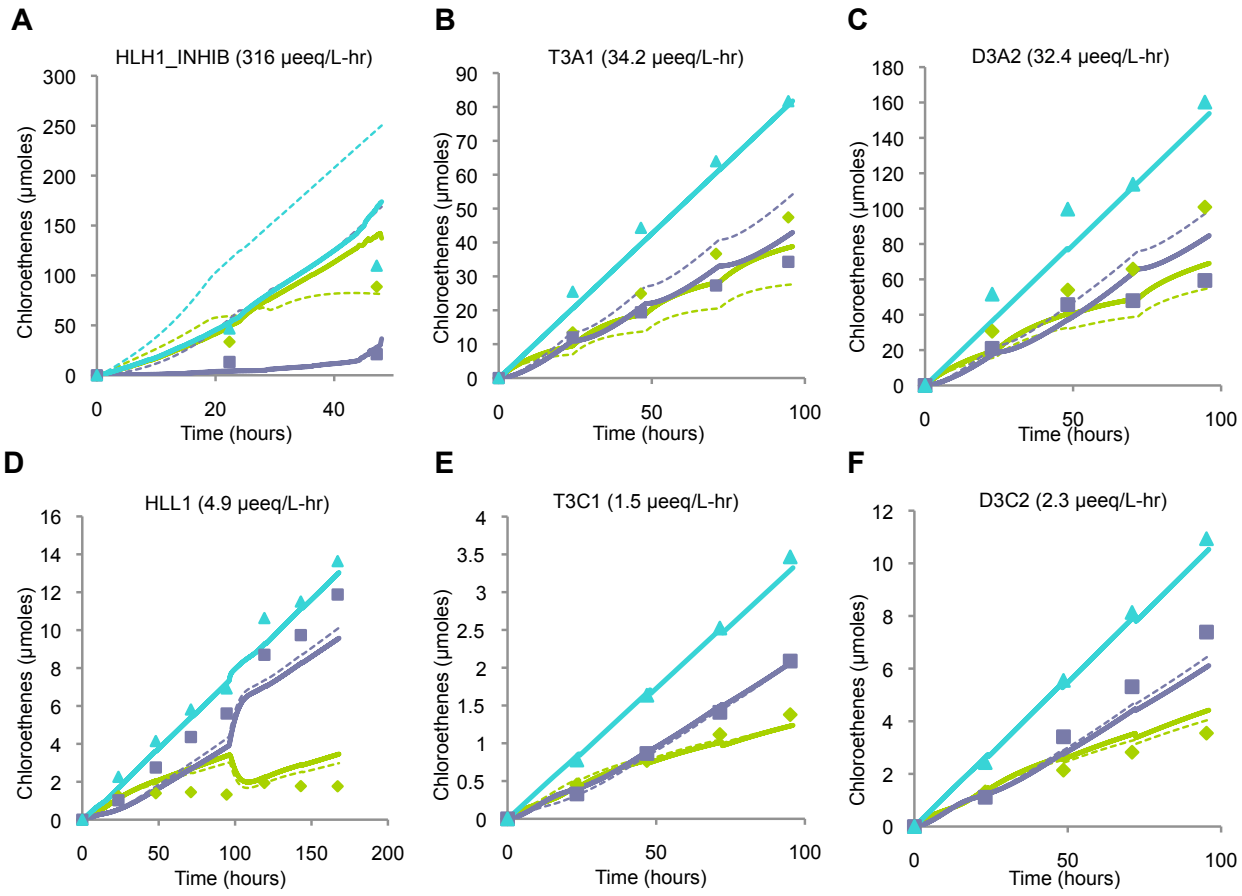

Figure 2. 3. Model fits (lines) compared to data for high (A-C) and low (D-F) feeding rates and differing electron acceptors. Solid lines include competitive inhibition and dashed lines do not. For the high feeding rates, the data/model fits are running totals of purge events. Green/diamonds are VC, purple/squares are ETH, and blue/triangles are VC+ETH. TCE and DCE are not shown as their concentrations were consistently an order of magnitude lower than PCE. Note different y-axis scales.

Biomass predictions.

Average 16S rRNA gene copy numbers from the experiments listed in Table A1.1 were used for estimating biomasses in running the model. These were 2.73±2.37 x 10^8 cells/mL, 1.64±1.58 x 10^7 cells/mL, 1.70±1.32 x 10^8 cells/mL, and 5.65±6.14 x 10^7 cells/mL for DMC195, fermenters (*Syntrophomonas* sp.), MHU and MS, respectively, where the range indicates standard deviation across samples collected over a two year period. Though clone libraries suggested several candidate fermenters, microarray data (unpublished results), metagenome

libraries and metaproteome spectral counts suggested *Syntrophomonas* to be a dominant representative (JGI IMG/M ER: http://img.jgi.doe.gov/mer).

Biomass predictions of the model compared as percent change over the experimental time course were generally good (Figure A1.4). Biomass predictions failed at high PCE feeding rates (HLH1, HLH2 and HLH3), when population abundance (measured as 16S rRNA gene copies) becomes decoupled from population activity, assessed by measurement of respiration products.[6]

2.D.4. mRNA Biomarkers.

The model based on 16S rRNA gene copies is an advancement over mgVSS or mg protein-based models, but there are several cases where it over-predicts DMC195 and methanogen activity, especially at higher feeding rates where model fits and biomass predictions are poor (Figure 2.5, dashed lines, and Figure A1.4, respectively). Poor fits for methanogenesis can potentially be explained by toxicity to *Methanosaeta* in cultures when DCE or PCE levels build up (DCE fed experiments or high PCE feeding rates).[47] As stated above, 80-90% of the total methane produced is thought to be by acetoclastic methanogens. As a metric of instant metabolic activity, we monitored transcript levels of a key gene at the end of MS's methanogenesis pathway – McrA.[28] A linear trend is observed for the plot of McrA expression in units of mRNA copies/DNA copy versus actual methanogenesis rate (slope=22.2, R^2=0.80), but not for McrA expression versus model-predicted respiration rate, indicating that mRNA biomarkers are more sensitive indicators of actual activity than MS 16S rRNA gene copy numbers (Figure 2.4A).

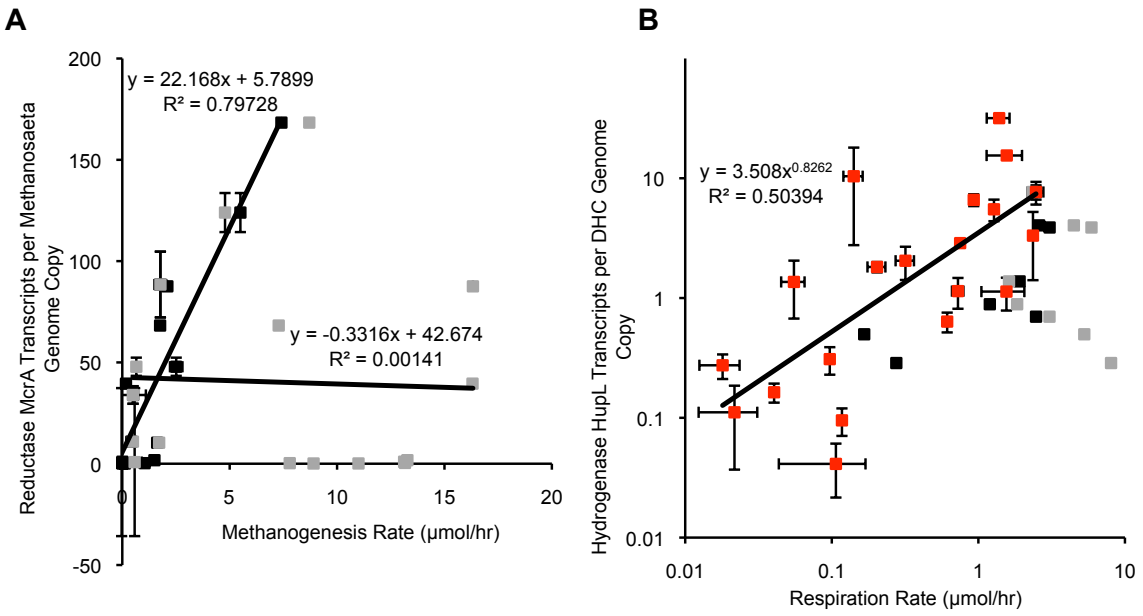

Figure 2. 4. (A) McrA expression as mRNA copies/DNA copy as compared to the actual methanogenesis rate (black squares) and the model-predicted methanogenesis rate (gray squares) and (B) HupL expression as copies/16S rRNA gene copies as compared to the actual respiration rate (red squares and black squares for inhibited bottles) and the model-predicted respiration rate for inhibited bottles (gray squares). In all cases the respiration rates were calculated over the last 24 hours of the experiment prior to sampling.

Poor fits for chloroethenes (e.g., Figure 2.5, dashed lines) can be explained by solvent toxicity stress on DMC195 organisms at high chloroethene concentrations as solvents approach solubility limits. If HupL, a key hydrogenase, is used as representative of DMC195 activity as suggested in previous work,[30,29,31] a trend should be observed for HupL expression relative to chloroethene respiration rate. A trend is observed for all bottles with the exception of HLH1-2, HLH2-2 and HLH3-7, which have the highest feeding rates tested (316, 482 and 183 µeeq/L-h, respectively). Based on chloroethene timecourses, HLH1-2 and HLH2-2 were just beginning to be inhibited after 2 days - for the first 24 hours, the model predictions were fairly good, but then the PCE concentrations reached an inhibitory/toxic level, and the fits became much poorer (Figure 2.5). The chloroethene sampling frequency may not have been tight enough to capture a drop in respiration rate that correlated with the HupL expression measured at that time point.

Additionally, the HupL expression was lower for the 7-day samples than for the 2-day samples of HLH1 and HLH2, and in all cases was lower than for lower feeding rates, indicating that DMC195 was under stress, likely due to solvent toxicity. Even though HLH1-2, HLH2-2 and HLH3-7 are outliers for the trend observed for other bottles, when plotted with their actual respiration rate they are closer to the trend line than when plotted with their model-predicted respiration rate (Figure 2.4B).

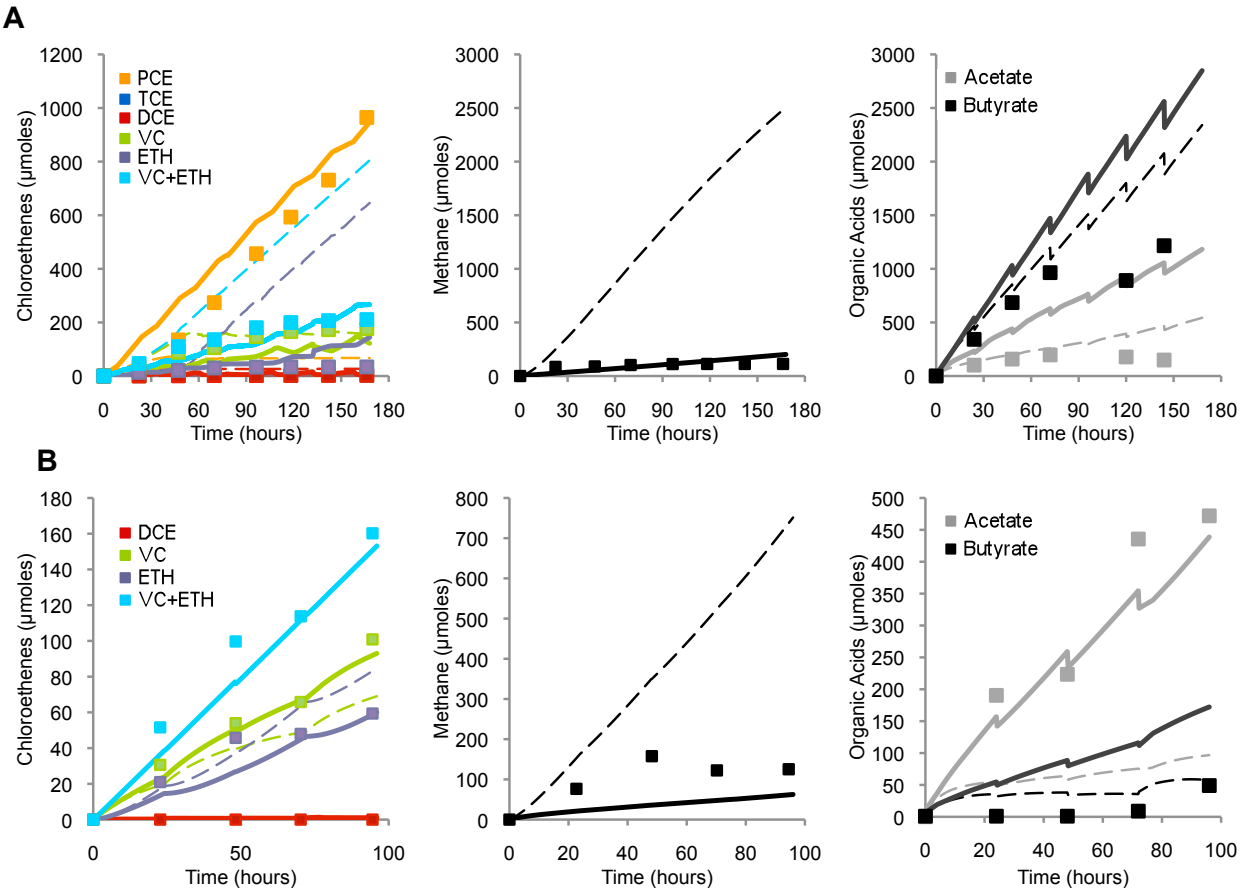

Figure 2. 5. Timecourses for experiments HLH1 (A) and D3A2 (B) showing improved model fits (solid lines) when an mRNA adjustment factor is included in the model, as compared to the data (squares) and model fits before the mRNA adjustment factor was included in the model (dashed lines). χ^2 values for model fits are presented in Table A1.3.

It was observed that at higher electron donor feeding rates, butyrate and/or acetate fits were poor and that many butyrate eeqs were unaccounted for in the measured metabolic products (Figure 2.5 and Figure A1.5). *Syntrophomonas* has been shown to produce polyhydroxybutyrate

(PHB) granules to store alkanoic acids when they are exposed to a transient substrate supply, like the batch feeding of our mixed culture.[48,49] A key enzyme in PHB production is PHB synthase (3-hydroxybutyryl-CoA dehydratase (Locus ID: Swol_1936) in *Syntrophomonas)*.[50] The homolog of this gene in the D2 metagenome is PCEOTH_1714030. After designing new primers we looked at mRNA expression levels for PHB synthase in these experiments. It was observed that at higher electron donor feeding rates, which correspond to greater amounts of missing eeqs, PHB synthase expression was up-regulated relative to time zero (Figure A1.5).

2.D.5. mRNA Adjustment of the Modeled Respiration Rates.

As shown above, mRNA is a more nuanced activity indicator that, if incorporated into the model, could improve predictions of an individual population's activity – particularly at high chloroethene feeding rates and/or concentrations. Incorporating mRNA into a kinetic model is challenging, however. The relationship between mRNA and kinetics is not directly mechanistic. Instead, mRNA biomarker levels for acetoclastic methanogenesis and reductive dechlorination were included as an adjustment factor on biomass activity as shown below in Equations 11 and 12, respectively.

$$\frac{d\,[CH_4]_{MS}}{dt} = MIN\left[\frac{k_{\max} X_{MS} S}{K_S + S + S^2/K_I}; \left(\frac{McrA_{transcripts}}{cell} * B\right)\right] \qquad (11)$$

$$\frac{d\ Mw_{PCE}}{dt} = MIN\left[\begin{array}{l}\dfrac{k_{PCE} X_{DMC195} C_{W,PCE}}{K_{S,PCE}\left(1+\dfrac{C_{W,TCE}}{K_{I,TCE}}\right)+C_{W,PCE}} * \dfrac{\left(C_{W,H_2} - H_2Threshold_{DMC195}\right)}{K_{S,H_2,DMC195}\left(C_{W,H_2} - H_2Threshold_{DMC195}\right)}; \\ \left(\dfrac{HupL_{transcripts}}{cell} * D\right)\end{array}\right] \qquad (12)$$

McrA/cell or HupL/cell are the mRNA expression levels measured just before the final time point of the experiment, when mRNA expression has typically reached a steady level in

continuous feed experiments.[29–31] B and D are the slopes in Figures 4A and 4B, respectively. A "switch" was also added to the model so that at lower feeding rates, when the expression may be lower than maximum, but the fit was good, the adjustment factor didn't affect the model. The adjustment factor replaced the kinetic expression at high feeding rates, if the mRNA expression indicated that respiration was occurring at a rate lower than expected. Generally, at lower feeding rates first-order kinetics were observed – the substrate was rate limiting. But at higher feeding rates, zero-order kinetics were observed – the substrate was no longer rate limiting, and the reaction was going at k_{max}. Some high feed rate cultures did not respire at k_{max}, and so the adjustment factor was applied to model the suppressed respiration rates (i.e. HLH1, HLH2, HLH3, D3A2). Figure 2.5 shows timecourses for HLH1 and D3A2. Inclusion of the empirically-derived mRNA adjustment factor drastically improved the fit of the model to the data for both methanogenesis and dechlorination, as shown in Figure 2.5 with χ^2 values presented in Table A1.3. At lower feed rates McrA adjustment and DNA-based Monod kinetics predicted activity equally well (data not shown). mRNA levels can be used as part of a predictive tool.

In summary, a biokinetic model was developed based on qPCR-quantified 16S rRNA gene copies for population densities and kinetic rate constants that accurately predicts dechlorination, fermentation, methanogenesis and biomass changes under a variety of conditions. The model incorporates competitive inhibition of chloroethenes and mRNA expression data for key metabolic pathway enzymes. The model was tested with three electron acceptors (PCE, TCE, *cis*-DCE) at a variety of feed rates with varying electron donor to electron acceptor ratios. The use of mRNA as a biomarker of specific respiratory activity was especially valuable in cases of high chloroethene concentrations, where there was potential for toxicity to various community members and a purely biokinetic model overpredicted dechlorination and methanogenesis.

mRNA levels (McrA and HupL) served as good biomarkers of methanogenesis and dechlorination rates, and improved model fits significantly. This work demonstrates one possible strategy for bringing quantitative molecular biomarkers and biokinetic modeling in mixed cultures forward.

2.E. Acknowledgements

This project was supported by the U.S. Department of Defense (DOD) and the National Science Foundation (NSF) CBET Program (CB1ET-0731169). Portions of this research were performed in the Environmental Molecular Sciences Laboratory (EMSL), a DOE/BER national scientific user facility located at Pacific Northwest National Laboratory (PNNL) in Richland, Washington. PNNL is a multi-program national laboratory operated by Battelle for the DOE under Contract DE-ACO5-76RLO 1830.

REFERENCES

(1) Hendrickson, E. R.; Payne, J. A.; Young, R. M.; Starr, M. G.; Perry, M. P.; Fahnestock, S.; Ellis, D. E.; Ebersole, R. C. Molecular analysis of *Dehalococcoides* 16S ribosomal DNA from chloroethene-contaminated sites throughout North America and Europe. *Appl. Environ. Microb.* **2002**, *68*, 485–495.

(2) Duhamel, M.; Mo, K.; Edwards, E. Characterization of a highly enriched *Dehalococcoides*-containing culture that grows on vinyl chloride and trichloroethene. *Appl. Environ. Microb.* **2004**, *70*, 5538–5545.

(3) Chen, G. Reductive dehalogenation of tetrachloroethylene by microorganisms: current knowledge and application strategies. *Appl. Microbiol. Biot.* **2004**, *63*, 373–377.

(4) He, J.; Holmes, V. F.; Lee, P. K. H.; Alvarez-Cohen, L. Influence of Vitamin B12 and Cocultures on the Growth of *Dehalococcoides* Isolates in Defined Medium. *Appl. Environ. Microb.* **2007**, *73*, 2847–2853.

(5) Holmes, V. F.; He, J.; Lee, P. K. H.; Alvarez-Cohen, L. Discrimination of Multiple *Dehalococcoides* Strains in a Trichloroethene Enrichment by Quantification of Their Reductive Dehalogenase Genes. *Appl. Environ. Microb.* **2006**, *72*, 5877–5883.

(6) Maymo-Gatell, X.; Chien, Y.; Gossett, J. M.; Zinder, S. H. Isolation of a bacterium that reductively dechlorinates tetrachloroethene to ethene. *Science* **1997**, *276*, 1568–1571.

(7) Becker, J. G.; Berardesco, G.; Rittmann, B. E.; Stahl, D. A. The Role of Syntrophic Associations in Sustaining Anaerobic Mineralization of Chlorinated Organic Compounds. *Environ. Health Persp.* **2004**, *113*, 310–316.

(8) Cupples, A.; Spormann, A.; McCarty, P. Growth of a *Dehalococcoides*-like microorganism on vinyl chloride and cis-dichloroethene as electron acceptors as determined by competetive PCR. *Appl. Environ. Microb.* **2003**, *69*, 4342–4342.

(9) Rowe, A. R.; Lazar, B. J.; Morris, R. M.; Richardson, R. E. Characterization of the Community Structure of a Dechlorinating Mixed Culture and Comparisons of Gene Expression in Planktonic and Biofloc-Associated "*Dehalococcoides* and *Methanospirillum* Species. *Appl. Environ. Microb.* **2008**, *74*, 6709–6719.

(10) Sieber, J. R.; Sims, D. R.; Han, C.; Kim, E.; Lykidis, A.; Lapidus, A. L.; McDonnald, E.; Rohlin, L.; Culley, D. E.; Gunsalus, R.; McInerney, M. J. The genome of Syntrophomonas wolfei: new insights into syntrophic metabolism and biohydrogen production. *Environ. Microbiol.* **2010**, 2289–2301.

(11) Henry, B. M. In *In Situ Remediation of Chlorinated Solvent Plumes*; Stroos, H. F.; Ward, C. H., Eds.; Springer, 2010; pp. 357–423.

(12) Fennell, D.; Gossett, J. Modeling the production of and competition for hydrogen in a dechlorinating culture. *Environ. Sci. Technol.* **1998**, *32*, 2450–2460.

(13) Cupples, A. M.; Spormann, A. M.; McCarty, P. L. Vinyl chloride and cis-dichloroethene dechlorination kinetics and microorganism growth under substrate limiting conditions. *Environ. Sci. Technol.* **2004**, *38*, 1102–1107.

(14) Cupples, A. M.; Spormann, A. M.; McCarty, P. L. Comparative evaluation of chloroethene dechlorination to ethene by *Dehalococcoides*-like microorganisms. *Environ. Sci. Technol.* **2004**, *38*, 4768–4774.

(15) Lee, I.-S.; Bae, J.-H.; Yang, Y.; McCarty, P. L. Simulated and experimental evaluation of factors affecting the rate and extent of reductive dehalogenation of chloroethenes

with glucose. *J. Contam. Hydrol.* **2004**, *74*, 313–331.
(16) Yu, S.; Semprini, L. Kinetics and modeling of reductive dechlorination at high PCE and TCE concentrations. *Biotechnol. Bioeng.* **2004**, *88*, 451–464.
(17) Yu, S.; Dolan, M. E.; Semprini, L. Kinetics and Inhibition of Reductive Dechlorination of Chlorinated Ethylenes by Two Different Mixed Cultures. *Environ. Sci. Technol.* **2005**, *39*, 195–205.
(18) Becker, J. G. A Modeling Study and Implications of Competition between *Dehalococcoides ethenogenes* and Other Tetrachloroethene-Respiring Bacteria. *Environ. Sci. Technol.* **2006**, *40*, 4473–4480.
(19) Amos, B. K.; Christ, J. A.; Abriola, L. M.; Pennell, K. D.; Löffler, F. E. Experimental Evaluation and Mathematical Modeling of Microbially Enhanced Tetrachloroethene (PCE) Dissolution. *Environ. Sci. Technol.* **2007**, *41*, 963–970.
(20) Becker, J. G.; Seagren, E. A. Modeling the effects of microbial competition and hydrodynamics on the dissolution and detoxification of dense nonaqueous phase liquid contaminants. *Environ. Sci. Technol.* **2009**, *43*, 870–877.
(21) Huang, D.; Becker, J. G. Determination of intrinsic monod kinetic parameters for two heterotrophic tetrachloroethene (PCE)-respiring strains and insight into their application. *Biotechnol. Bioeng.* **2009**, *104*, 301–311.
(22) Schaefer, C. E.; Condee, C. W.; Vainberg, S.; Steffan, R. J. Bioaugmentation for chlorinated ethenes using *Dehalococcoides* sp.: Comparison between batch and column experiments. *Chemosphere* **2009**, *75*, 141–148.
(23) Haest, P.; Springael, D.; Smolders, E. Dechlorination kinetics of TCE at toxic TCE concentrations: Assessment of different models. *Water Res.* **2010**, *44*, 331–339.
(24) Huang, D.; Becker, J. G. Dehalorespiration Model That Incorporates the Self-Inhibition and Biomass Inactivation Effects of High Tetrachloroethene Concentrations. *Environ. Sci. Technol.* **2011**, *45*, 1093–1099.
(25) Sabalowsky, A. R.; Semprini, L. Trichloroethene and cis-1,2-dichloroethene concentration-dependent toxicity model simulates anaerobic dechlorination at high concentrations: I. batch-fed reactors. *Biotechnol. Bioeng.* **2010**, *107*, 529–539.
(26) Sabalowsky, A. R.; Semprini, L. Trichloroethene and cis-1,2-dichloroethene concentration-dependent toxicity model simulates anaerobic dechlorination at high concentrations. II: Continuous flow and attached growth reactors. *Biotechnol. Bioeng.* **2010**, *107*, 540–549.
(27) Popat, S. C.; Deshusses, M. A. Kinetics and Inhibition of Reductive Dechlorination of Trichloroethene, cis-1, 2-Dichloroethene and Vinyl Chloride in a Continuously Fed Anaerobic Biofilm Reactor. *Environ. Sci. Technol.* **2011**, *45*, 1569–1578.
(28) Freitag, T. E.; Prosser, J. I. Correlation of Methane Production and Functional Gene Transcriptional Activity in a Peat Soil. *Appl. Environ. Microb.* **2009**, *75*, 6679–6687.
(29) Rahm, B. G.; Richardson, R. E. Gene Transcripts As Quantitative Bioindicators of Tetrachloroethene, Trichloroethene, and cis-1,2-Dichloroethene Dehalorespiration Rates. *Environ. Sci. Technol.* **2008**, *42*, 5099–5105.
(30) Rahm, B. G.; Richardson, R. E. Correlation of respiratory gene expression levels and pseudo-steady-state PCE respiration rates in *Dehalococcoides ethenogenes*. *Environ. Sci. Technol.* **2008**, *42*, 416–421.
(31) Rowe, A. R.; Heavner, G. L.; Mansfeldt, C. B.; Werner, J. J.; Richardson, R. E.

Relating Chloroethene Respiration Rates in *Dehalococcoides* to Protein and mRNA Biomarkers. *Environ. Sci. Technol.* **2012**, *46*, 9388–9397.
(32) Rahm, B. G.; Morris, R. M.; Richardson, R. E. Temporal Expression of Respiratory Genes in an Enrichment Culture Containing *Dehalococcoides ethenogenes*. *Appl. Environ. Microb.* **2006**, *72*, 5486–5491.
(33) Fennell, D. E.; Gossett, J. M.; Zinder, S. H. Comparison of butyric acid, ethanol, lactic acid, and propionic acid as hydrogen donors for the reductive dechlorination of tetrachloroethene. *Environ. Sci. Technol.* **1997**, *31*, 918–926.
(34) DiStefano, T. D.; Gossett, J. M.; Zinder, S. H. Reductive dechlorination of high concentrations of tetrachloroethene to ethene by an anaerobic enrichment culture in the absence of methanogenesis. *Appl. Environ. Microb.* **1991**, *57*, 2287–2292.
(35) Smatlak, C. R.; Gossett, J. M.; Zinder, S. H. Comparative kinetics of hydrogen utilization for reductive dechlorination of tetrachloroethene and methanogenesis in an anaerobic enrichment culture. *Environ. Sci. Technol.* **1996**, *30*, 2850–2858.
(36) Rowe, A. R.; Mansfeldt, C. B.; Heavner, G.; Richardson, R. E. *Methanospirillum* respiratory mRNA biomarkers correlate with hydrogenotrophic methanogenesis rate during growth and competition for hydrogen in an organochlorine-respiring mixed culture. *Environ. Sci. Technol.* **2012**, 10.1021/es303061y.
(37) Fennell, D. Comparison of Alternative Hydrogen Donors for Anaerobic Reductive Dechlorination of Tetrachloroethene. Ph.D. Dissertation, Cornell University: Ithaca, NY, 1998.
(38) Adrian, L.; Hansen, S. K.; Fung, J. M.; Gorisch, H.; Zinder, S. H. Growth of *Dehalococcoides* strains with chlorophenols as electron acceptors. *Environ. Sci. Technol.* **2007**, *41*, 2318–2323.
(39) Peirson, S. N.; Butler, J. N.; Foster, R. G. Experimental validation of novel and conventional approaches to quantitative real-time PCR data analysis. *Nucleic Acids Res.* **2003**, *31*, 1–7.
(40) Loferer-Krossbacher, M.; Klima, J.; Psenner, R. Determination of bacterial cell dry mass by transmission electron microscopy and densitometric image analysis. *Appl. Environ. Microb.* **1998**, *64*, 688–694.
(41) Morris, R.; Sowell, S.; Barofsky, D.; Zinder, S.; Richardson, R. Transcription and mass-spectroscopic proteomic studies of electron transport oxidoreductases in *Dehalococcoides ethenogenes*. *Environ. Microbiol.* **2006**, *8*, 1499–1509.
(42) Haston, Z.; McCarty, P. Chlorinated ethene half-velocity coefficients (Ks) for reductive dehalogenation. *Environ. Sci. Technol.* **1999**, *33*, 223–226.
(43) Beaty, P. S.; McInerney, M. J. Effects of organic acid anions on the growth and metabolism of Syntrophomonas wolfei in pure culture and in defined consortia. *Appl. Environ. Microb.* **1989**, *55*, 977–983.
(44) Magnuson, J. K.; Stern, R. V.; Gossett, J. M.; Zinder, S. H.; Burris, D. R. Reductive dechlorination of tetrachloroethene to ethene by a two-component enzyme pathway. *Appl. Environ. Microb.* **1998**, *64*, 1270–1275.
(45) Maymo-Gatell, X.; Anguish, T.; Zinder, S. H. Reductive dechlorination of chlorinated ethenes and 1, 2-dichloroethane by *Dehalococcoides ethenogenes* 195. *Appl. Environ. Microb.* **1999**, *65*, 3108–3113.
(46) Sleep, B. E.; Brown, A. J.; Lollar, B. S. Long-term tetrachlorethene degradation

sustained by endogenous cell decay. *J. Environ. Eng. Sci.* **2005**, *4*, 11–17.
(47) Blum, D. J. W.; Speece, R. A database of chemical toxicity to environmental bacteria and its use in interspecies comparisons and correlations. *Res. J. Water Pollut. C.* **1991**, 198–207.
(48) Beccari, M.; Majone, M.; Massanisso, P.; Ramadori, R. A bulking sludge with high storage response selected under intermittent feeding. *Water Res.* **1998**, *32*, 3403–3413.
(49) Beun, J.; Dircks, K.; Van Loosdrecht, M.; Heijnen, J. Poly-[beta]-hydroxybutyrate metabolism in dynamically fed mixed microbial cultures. *Water Res.* **2002**, *36*, 1167–1180.
(50) Dias, J. M. L.; Serafim, L. S.; Lemos, P. C.; Reis, M. A. M.; Oliveira, R. Mathematical modelling of a mixed culture cultivation process for the production of polyhydroxybutyrate. *Biotechnol. Bioeng.* **2005**, *92*, 209–222.

CHAPTER 3:

Biomarkers of Reductive Dechlorination in Bioaugmentation Culture KB-1™

3.A. Abstract

Transcriptional biomarkers can be informative for the evaluation of natural attenuation and for the establishment of engineering procedures for remediation at contaminated sites – including those with chlorinated solvents PCE and TCE. The presence of daughter products, cis-dichloroethene (DCE), vinyl chloride (VC) or ethene, at a site indicates that reductive dechlorination has occurred sometime in the past. Site conditions could be such that it is not presently occurring or active organisms may no longer be present.

Dehalococcoides mccartyi (DMC) gene transcripts corresponding to 16S rRNA, the hydrogenase (H2ase) Hup, and reductive dehalogenases (RDases) TceA, VcrA and homologs to DET1545 in *Dehalococcoides mccartyi* strain 195 (DMC195) hold promise as potential biomarkers of the *in situ* dehalorespiration of chlorinated ethenes, as previously reported.[1–3] Here, we present quantitative reverse-transcriptase polymerase chain reaction (qRT-PCR) data taken from microcosms containing the KB-1™ consortium, operated under continuous, chlorinated ethene feed conditions, with the aim of clarifying relationships and creating more robust set of biomarkers that can be used at field sites bioaugmented with the KB-1™ culture. Candidate biomarkers from KB-1™ demonstrate a variety of trends in terms of transcript abundance as a function of respiration rate over a respiration rate range of 7.7×10^{-12} to 5.9×10^{-10} μeeq/cell-hr, with an average DMC population size of 1.5×10^{8} cells/mL. TceA transcripts were sparsely detected. Linear trends on a log-log plot were observed for VcrA, HupL and 16S rRNA, indicating a positive correlation between respiration rate and transcript abundance. Across strains of DMC, transcript abundances per cell were similar for the dominant RDases

(VcrA and RdhA5/DET1545 in KB-1™ and TceA in DMC195) as were 16S rRNA and HupL levels. Metaproteomic data supports the trends observed at the transcript level.

Additional experiments were conducted to quantify these biomarkers under stress conditions (presence of oxygen or low pH). Addition of stressors caused respiration rates to decrease significantly, whereas transcript abundances exhibited a slow decay (0.02-0.03 per hr) over the time period studied, indicating that transcript abundance alone cannot predict respiration rate in stressed conditions within hours to days following stress.

3.B. Introduction

In situ bioremediation of groundwater contaminated with tetrachloroethene (PCE) and trichloroethene (TCE), two of the most common subsurface contaminants in the world, has gained acceptance as a valid treatment method.[4] The only organisms able to produce a non-toxic end-product (ethene) from PCE and/or TCE through the process of anaerobic reductive dechlorination are members of the genus *Dehalococcoides*.[5–7] *Dehalococcoides mccartyi* strain 195 (DMC195) can convert PCE to ethene.[8–10] *Dehalococcoides mccartyi* (DMC) strains FL2[11], VS[12–14], GT[12] and the multiple strains in the mixed culture KB-1[15] can convert TCE to ethene. DMC strain BAV1 can convert DCE to ethene.[16] Degradation of PCE or TCE by other species, or DMC strain CBDB1[17–19], often stalls at DCE or VC, suspected and known carcinogens, respectively. The VC to ethene step is cometabolic for both DMC195 and DMC strain FL2.[9,11] 16S rRNA gene sequences are highly conserved among strains of DMC, forming a distinct phylogenetic group.[4] However, Hendrickson et al. divided them into three phylogenetic subgroups based on sequence signatures in hypervariable regions 2 and 6 of the 16S rRNA gene: the Cornell (DMC195), Victoria (DMC strain VS) and Pinellas (DMC strains CBDB1, BAV1, GT and FL2) subgroups.[4,5,20] Thus, evaluating natural attenuation and/or enhanced

bioremediation at a field site and establishing engineering procedures for remediation can be closely linked to an understanding of the organisms carrying out transformation of lesser-chlorinated ethenes.[21]

Finding daughter products at an anaerobic site, *cis*-DCE, VC or ethene, only indicates that reductive dechlorination has occurred sometime in the past. Site conditions could be such that it is not occurring now or active organisms may no longer be present.[22] To prove that bioremediation is occurring at a site, three criteria must be met: there must be a demonstrated loss of contaminant mass from the site, organisms that are capable of degrading the contaminant must be present, and the organisms must be expressing the capability to degrade the contaminant *in situ*.[23] The third piece of evidence is the most difficult to demonstrate conclusively. Biomarkers may serve as the key piece of evidence and may even inform quantitative forecasting of *in situ* rates of bioremediation.

Biomarkers are biomolecules (DNA, RNA or protein) that correspond to a specific microbial process or state. Several studies have been conducted regarding detection of 16S rRNA genes at field sites.[4,24–28] Hendrickson et al. observed that there is a strong correlation between the presence of the DMC 16S rRNA gene at a site, and the reductive dechlorination of chlorinated ethenes to ethene.[4] However, the presence of the 16S rDNA does not necessarily mean that complete dechlorination will occur – conditions may not be favorable and the capability for use of the various chloroethene electron acceptors differs among strains (phylogeny does not necessarily predict physiology), making it impossible to predict whether or not dechlorination will occur at a certain site without more information.[4,28–31] Additionally, there are numerous reductive dehalogenases (12-36 per strain) coded for in the genomes of each strain of DMC.[5] Reductive dehalogenases (RDases) are the enzymes produced by DMC that allow for

respiration of chlorinated organics. As a result, targeting the mRNA or protein produced from these genes may be better indicators of organism activity.[29] Analysis of the mRNA transcripts or proteins for genes other than those directly involved in bioremediation (e.g. stress response genes) may also be able to give insight into conditions at the site.

Several studies have been conducted that examine the quantitative correlation between reductive dechlorination and specific RNA transcripts.[1–3,32–38] Based on these studies, a preliminary suite of potential field biomarkers can be generated that includes RDases, especially VC RDase enzymes that have been linked to successful biological dechlorination of VC to ethene in groundwater systems, and other targets.[30] The mechanism of VC dechlorination is important in bioremediation because VC is the most toxic of the chlorinated ethenes, and the VC to ethene step is often rate-limiting.[30] Genes linked to the VC-to-ethene step of reductive dechlorination (VcrA, BvcA, etc.) may serve as useful biomarkers for complete remediation of chlorinated ethenes.[30]

The correlation between respiration rate and mRNA transcript number has been extensively studied for the Cornell mixed culture (D2).[1–3] However, due to the genetic similarity among *Dehalococcoides* strains, the variation in the electron acceptors they can reductively dechlorinate, and type and number of reductive dehalogenases they contain, finding robust biomarkers for reductive dechlorination of chloroethenes is challenging. To that end, we have expanded previous work with DMC195[1–3] to include similar studies with the *Dehalococcoides*-containing mixed culture KB-1™ that is commercially available for bioaugmentation at field sites. KB-1™ differs from the D2 culture in that it contains more than one DMC strain, some of which can gain energy from the reductive dechlorination of VC to ethene.[34,39] It has been observed that multiple reductive dehalogenases are expressed when the KB-1 lab cultures

maintained at the University of Toronto (in this paper referred to as KB1-UT) are fed TCE, *cis*-DCE, VC or 1,2-dichloroethane, and that two (VcrA and BvcA) are expressed under all studied conditions.[34] The development of a suite of robust biomarkers of reductive dechlorination, that allows for the variation (both phylogenetic and phenotypic) among different strains would assist in the application of *in situ* bioremediation at contaminated field sites. The ultimate objective is to be able to use mRNA levels of robust biomarkers to infer *in situ* respiration rates at field sites, including testing mRNA responses under common stresses to DMC activity.

3.C. Materials and Methods

3.C.1. Analytical Methods.

Chlorinated ethenes, ethene, and methane were analyzed from 100-µL headspace samples via gas chromatography as described by DiStefano[40] and Smatlak,[41] and modified by Rahm and Rowe.[3,33] Hydrogen was analyzed from 50-µL headspace samples via reduction gas detector (RGD, Trace Analytical RGD2) or by a TCD at higher concentrations.[42,43] During the oxygen stress experiment, oxygen was analyzed via gas chromatography as described by Gossett.[44]

3.C.2. Microbial Culture.

KB-1™ culture was provided by SiREM Labs of Guelph, Ontario, Canada. The culture contains at least two DMC strains, a *Geobacter* strain, and a wide variety of other microorganisms.[39,45,46] A metagenome library is available for a related lab culture at the University of Toronto (DCKB1, http://genome.jgi-psf.org/aqukb/aqukb.home.html).

3.C.3. Continuous Feed Experiments.

Continuous (TCE) feed experiments were conducted as in Rowe 2012, with the exception that 100-mL subcultures of undiluted KB-1™ culture were used, and electron donor and a carbon source were pulse-fed as hydrogen gas and acetate, respectively, at the beginning of the

experiment, and periodically thereafter as needed (rather than continuously fed as with the D2 culture experiments in Rowe 2012).[3] Experimental parameters for the continuous feed experiments are presented in Table 3.1.

Table 3. 1. Experimental Parameters

Experiment	Culture Title	Length of Experiment (Hours)	EA	Calculated EA Feed Rate (µeeq/L-hr)	ED	Carbon Source	Respiration Rate (µeeq/L-hr)	Respiration Rate After Stress (µeeq/L-hr)
KB1 2 Rates	K2A1	23.3	TCE	4.6	MeOH /EtOH	MeOH /EtOH	4.5	-
	K2A2	23.5		1.7			1.6	-
	K2C1	24.5		129			128.0	-
	K2C2	24.7		124			121.8	-
KB1 3 Rates	K3A1	26.7	TCE	16.4	H2	Acetate	16.0	-
	K3A2	27.0		16.6			16.5	-
	K3B1	27.2		42.8			35.3	-
	K3B2	27.4		39.3			30.5	-
	K3C1	27.6		99.9			46.7	-
	K3C2	27.8		98.2			62.5	-
Acid Stress	ACA1	19.7	TCE	9.5	H2	Acetate	1.3	-
	ACA2	43.8		3.1			1.5	1.9
	ACB1	30.8		2.8			1.6	0.4
	ACB2	31.0		2.5			1.4	0.5
	ACC1	44.0		2.3			1.5	0.2
	ACC2	44.2		0.6			1.0	-0.1
Oxygen Stress Batch	O2A1	20.0	TCE	-	H2	Acetate	59.6	-
	O2A2	48.6		-			71.2	29.9
	O2B1	27.1		-			69.0	0.4
	O2B2	27.3		-			71.6	0.4
	O2C1	192.7		-			68.2	2.5
	O2C2	192.8		-			76.6	2.2

3.C.4. Calculation of Respiration Rates.

Because the KB-1™ culture contains both a *Geobacter* strain, and at least two DMC strains, respiration rates were calculated differently from previous studies where DMC195 was the sole dechlorinator.[3] From the perspective of DMC respiration, it was conservatively assumed that the *Geobacter* strain was responsible for all TCE to DCE conversion, and that the DMC strains were solely responsible for all DCE to VC to ethene conversions. Additionally, for the D2 culture, the VC to ethene step is assumed to be co-metabolic,[8] whereas energy is gained from the VC to ethene step in the KB1-UT culture.[34,39] Consequently, in this study, respiration rates in

terms of electron equivalents (eeq) for DMC strains were based on measured chloroethenes and utilized the following formula for DCE:

$$rDCE = \frac{d(2 * VC + 4 * ETH)}{dt} \quad (1)$$

where rDCE is the DCE respiration rate (μeeq/L-hr), and VC and ethene are the vinyl chloride and ethene concentrations (μmol/L), respectively.

3.C.5. Stress Experiments.

Stress experiments were conducted both in batch and continuous feed modes.

Oxygen Stress.

Six subcultures were batch-fed electron acceptor, electron donor and a carbon source (TCE, hydrogen and acetate, respectively). After one feeding (and approximately 24 hours), the cultures were purged anaerobically, re-fed, and the stressor (1.6 mg/L aqueous oxygen) was added. One control was sacrificed for proteomic and microarray analysis just prior to purging, and a second, unstressed control was sacrificed after approximately 50 hours total. Duplicate experimental bottles were sacrificed for proteomic and microarray analysis approximately eight hours after the stressor was added. The final duplicate experimental bottles were sacrificed when the DMC populations were appearing to recover (VC and ethene were being produced). The second control was sacrificed approximately 24 after the second TCE spike so that the results were representative of an active culture, not an idle, inactive culture. At this point TCE was no longer present, but DCE and VC were.

Acid Stress.

Six subcultures were continuously fed electron acceptor (TCE), and batch-fed electron donor and a carbon source (hydrogen and acetate, respectively). After approximately 22 hours, the stressor (1 M HCl) was added, lowering the pH of the subcultures to ~5.3. One control was

sacrificed for proteomic and microarray analysis just prior to the addition of the stressor. The second control was sacrificed approximately 24 hours after the addition of the stressor (46 hours total). Duplicate experimental bottles were sacrificed 10 hours after the addition of the stressor, and the final duplicate experimental bottles were sacrificed approximately 24 hours after the addition of the stressor.

3.C.6. Nucleic Acid Extraction and Quantification.

DNA and RNA extractions were performed using the AllPrep DNA/RNA Mini Kit (Qiagen) with modifications and DNase treatments as previously described.[3,33] Total DNA was quantified using the Quant-iT™ Picogreen® double stranded DNA assay (Invitrogen). RNA quality and quantity was analyzed using the Agilent 2100 BioAnlyzer. DNase treatment, cDNA synthesis, qPCR set up and qPCR run conditions were performed as previously described.[1–3] Prior to qPCR, all DNA and cDNA samples were diluted 1 to 5 with molecular grade water. Primers and annealing temperatures used in this study are listed in Table A2.1. Analysis of qPCR data was performed as outlined previously, utilizing luciferase mRNA quantities to estimate overall mRNA recovery and reverse transcription efficiency.[38] Transcript levels were calculated from raw fluorescence data using the Data Analysis for Real-time PCR (DART-PCR) method.[1,47,48] Long amplicons (for 16S, TceA, 1545, VcrA) or D2 mixed culture DNA extracts (for HupL) were used to generate standard curves for each target to convert R_0 to copies. Primers and annealing temperatures used to generate long amplicons are listed in Table A2.2.

3.C.7. Proteomic Analysis.

Protein extractions were performed on cell pellets of 50 mL culture (14,000 x *g*, 10 minutes). The culture was pelleted, decanted, and then frozen at -20°C. The frozen pellets were shipped overnight on dry ice to the Environmental Molecular Sciences Laboratory (EMSL) at the

Pacific Northwest National Laboratory for proteome extraction and analysis.

Urea Sample Digestion.

Cell pellets were resuspended in 9 M urea and vortexed into suspension. Each sample was added to a barocycle pulse tube (Pressure Biosciences Inc., South Easton, MA) and barocycled for 10 cycles (20 seconds at 35,000 psi and then back down to ambient pressure for 10 seconds) for cell lysis. The sample was transferred to a centrifuge tube and spun at 5,000 x *g* for 5 minutes to collect debris, and the supernatant was transferred to a fresh tube and assayed with bicinchoninic acid (BCA) (Thermo Scientific, Rockford, IL) to determine the protein concentration. The sample was then reduced with 10 mM dithiothreitol (DTT) (Sigma, St. Louis, MO) with incubation at 60˚C for 30 minutes with constant shaking at 800 rpm. Samples were then diluted 10-fold for preparation for digestion with 100 mM NH_4HCO_3; 1 mM $CaCl_2$ and sequencing-grade modified porcine trypsin (Promega, Madison, WI) were added to all protein samples at a 1:50 (w/w) trypsin-to-protein ratio for 3 h at 37˚C. The resulting peptides were cleaned using Discovery C18 (50 mg, 1 mL) solid phase extraction tubes (Supelco, St.Louis, MO), using the following protocol: 3 mL of methanol was added for conditioning followed by 2 mL of 0.1% TFA in H_2O. The samples were then loaded onto each column followed by 4 mL of 95:5: H_2O:ACN, 0.1% TFA. Samples were eluted with 1 mL 80:20 ACN:H_2O. The samples were concentrated down to ~30 µL using a Speed Vac and a final assay was performed to determine the peptide concentration. An equal mass of each sample was aliquoted into fresh centrifuge tubes.

TMT Isobaric Tag Labeling.

The continuous-feed and stress experiments (sample sets of 6) were labeled using amine-reactive Thermo Scientific Tandem Mass Tag (TMT) Isobaric Mass Tagging Kits (Thermo

Scientific, Rockford, IL) according to the manufacturer's instructions.[49] Briefly, 41 µL of anhydrous acetonitrile was added to each reagent (TMT 126 to 131), vortexed and allowed to dissolve for 5 minutes with occasional vortexing. Reagents were then added to the samples and incubated for 1 hour at room temperature. The tagging reaction was quenched by adding 8 µL of 5% hydroxylamine to the sample with incubation for 15 minutes at room temperature. The samples within each set were then combined and dried in the Speed Vac to remove the organic solvents. Each of the 4 samples were then cleaned using Discovery C18 (50 mg, 1 mL) solid phase extraction tubes as described above and once again assayed with bicinchoninic acid to determine the final peptide concentration.

2D-LC-MS/MS Analysis.

The 2D-LC system was custom built using two Agilent 1200 nanoflow pumps and one 1200 capillary pump (Agilent Technologies, Santa Clara, CA), various Valco valves (Valco Instruments Co., Houston, TX) and a PAL autosampler (Leap Technologies, Carrboro, NC). Full automation was made possible by custom software that allows for parallel event coordination providing near 100% MS duty cycle through use of two trapping and analytical columns. All columns were manufactured in-house by slurry packing media into fused silica (Polymicro Technologies Inc., Phoenix, AZ) using a 1 cm sol-gel frit for media retention. The columns used consisted of a first dimension SCX column: 5-µm PolySULFOETHYL A, 15-cm x 360 µm outer diameter (o.d.) x 150 µm inner diameter (i.d.) (PolyLC Inc., Columbia, MD); trapping columns: 5-µm Jupiter C_{18}, 4 cm x 360 µm o.d. x 150 µm i.d. (Phenomenex, Torrence, CA); and second dimension reversed-phase columns: 3-µm Jupiter C_{18}, 35-cm x 360 µm o.d. x 75 µm i.d. (Phenomenex, Torrence, CA). Mobile phases consisted of 0.1 mM NaH_2PO_4 (A) and 0.3 M NaH_2PO_4 (B) for the first dimension and 0.1% formic acid in water (A) and 0.1% formic acid in

acetonitrile (B) for the second dimension.

MS analysis was performed using a LTQ Orbitrap Velos ETD mass spectrometer (Thermo Scientific, San Jose, CA) fitted with a custom electrospray ionization (ESI) interface. Electrospray emitters were custom made using 150 μm o.d. x 20 μm i.d. chemically etched fused silica.[50] The heated capillary temperature and spray voltage were 275°C and 2.2 kV, respectively. Data was acquired for 100 minutes, beginning 65 minutes after sample injection and 15 minutes into gradient. Orbitrap spectra (AGC $1x10^6$) were collected from 400-2000 m/z at a resolution of 60k followed by data dependent ion trap CID MS/MS (collision energy 35%, AGC $3x10^4$) of the ten most abundant ions. A dynamic exclusion time of 60 seconds was used to discriminate against previously analyzed ions.

Data Analysis.

MS/MS data was searched using SEQUEST against a peptide database constructed from a series of isolate genomes and metagenomic datasets and other known RDase sequences, using relatively conservative filters [Xcorr values of 1.9 (+1), 2.2 (+2), and 3.5 (+3)]. The following metagenomic data was used in these searches: *Dehalococcoides mccartyi* strains CBDB1 and 195, the KB1-UT metagenomic sequences (DCKB1 at JGI), *Geobacter lovleyi*, *Methanoregula boonei*, *Methanosaeta thermophila*, *Methanospirillum hungatei*, D2 metagenomic sequences (PCEDH *and* PCEOT at JGI), *Spirochaeta thermophila*, *Sporomusa* str. KB1, *Syntrophomonas wolfei*, and *Syntrophus aciditrophicus*. Resulting peptide identifications were filtered using an MS-GF[51] cutoff value to 1×10^{-10}.[51]

TMT ion intensities, acquired using the tool MASIC (MS/MS Automated Selected Ion Chromatogram), were used to measure relative peptide abundance in the continuous feed and stress experiment samples.[49] The intensity associated with each reporter ion is proportional to the

contribution of each of the component samples to the total peptide abundance. Aggregation of the relative abundance measurements for all peptides detected for a given protein can be used to measure the relative amounts of each of the identified proteins.

Relative protein quantities of biomarkers in shotgun proteomic samples were estimated by calculating the normalized spectral abundance factor (NSAF).[52] This technique adjusts for biases in peptide detection arising from protein length.[53]

3.C.8. Transcriptomic Analysis.

The transcriptomic data for this study was generated using microarrays designed to capture all known DMC genes' transcripts.[20] In brief, 50 mL of each experimental KB-1™ culture was pelleted. The RNA was extracted and purified using a method previously outlined.[1–3,54] After DNA digestion by the TurboTM DNase (Ambion) and quantification using the RNA 2000 kit on a Bioanalyzer (Agilent Technologies), the RNA was reverse transcribed using Superscript II (Invitrogen) with the substitution of the amino allyl-dUTP (Ambion) for a portion of the dTTP nucleotide concentration, as previously described.[54,55]

The resulting complementary DNA (cDNA) pool was base-hydrolyzed to remove residual RNA, purified using GFX Columns with sodium bicarbonate as the elution buffer (GE Healthcare), and quantified using a ThermoScientific NanoDrop 2000c. The purified cDNA was labeled with either cyanine-3 or -5 (GE Healthcare) for the control or experimental cultures, respectively.[54] The labeled cDNA was purified using an additional GFX Column with the manufacturer provided elution buffer. The final sample cDNA was quantified using the nanodrop. For each sample, 800 ng of both the experiment (Cy5) and the control (Cy3) was hybridized to a 2-Color Agilent 4 x 44 K microarray (GSE42136)[20], as previously described.[54] The microarray was scanned using an Agilent Technologies Scanner (G2505C) with data

reported by Agilent Feature Extraction Software. The raw median intensity values were LOESS normalized within the array and replicate spots were geometrically averaged, as previously reported.[54] The raw and normalized data is freely available at the NCBI GEO Database (http://www.ncbi.nlm.nih.gov/geo/) under the accession GSE42136.

3.D. Results and Discussion

3.D.1. Correlations Between mRNA Biomarkers and Respiration Rate.

To relate DMC biomarkers to respiration rates in KB-1, subcultures were taken from the commercially available mixed culture provided by SiREM (KB-1^{TM}). The subcultures were continuously fed electron acceptor (TCE) and batch fed electron donor and carbon source (hydrogen and acetate, respectively) in excess (Table 3.1). Over the course of these approximately 24-hour experiments RNA biomarkers reached a pseudo-steady-state (PSS) concentration, which occurred after an initial up-regulation period for mRNA biomarkers (Figure 3.1). Additionally, *Dehalococcoides* cell density did not change statistically over the experiments conducted (examples provided in Figure 3.1). Respiration rates ranged from 1.8 to 128 μeeq/L-hr (9.00×10^{-13} to 2.88×10^{-12} (μmol/cell-hr). These experiments extended previous work[1–3] in the DMC195-containing D2 mixed culture by generating biomarker response curves for a different *Dehalococcoides*-containing culture (KB-1^{TM}), potentially increasing the robustness of certain biomarkers.

The biomarkers examined were 16S rRNA, HupL, TceA, a DET1545 homolog (an RDase of unknown function) and VcrA. Trends were previously determined for four of the five biomarkers examined for the D2 culture (with the exception of VcrA, as it is not found in the DMC195 genome for D2 metagenome).[1–3] On log-log plots, linear trends were observed for HupL and VcrA with correlation scores (Pearson's *r*) of 0.945 and 0.819, respectively (Figures 3

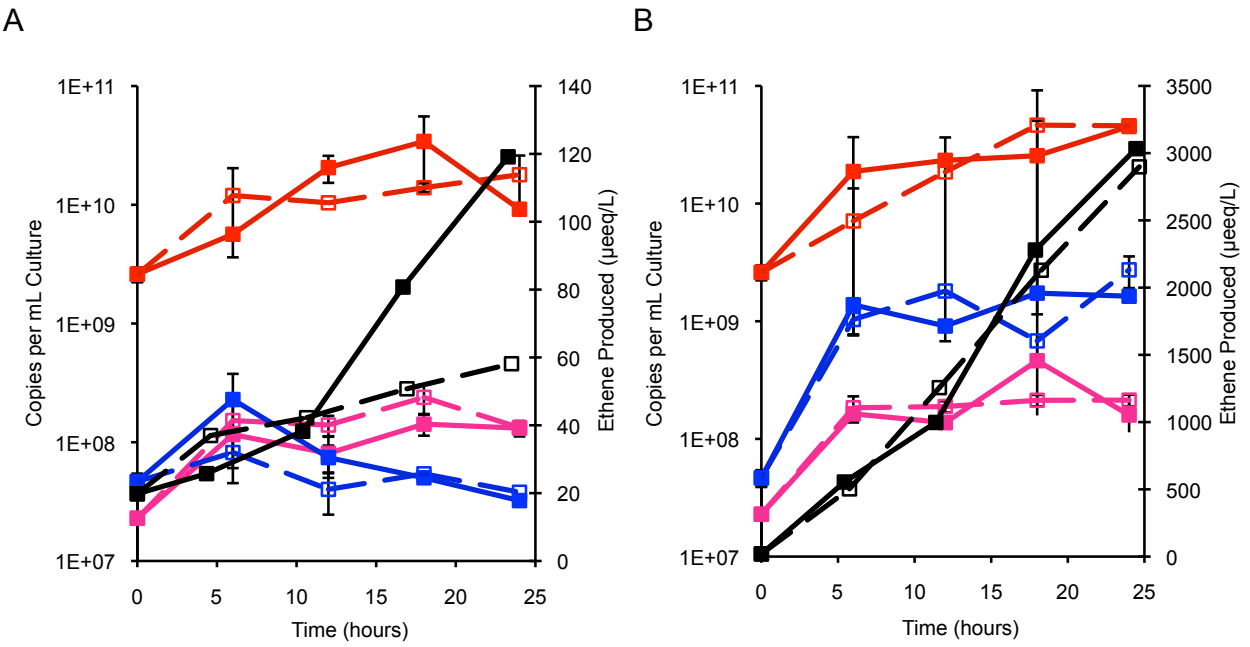

Figure 3. 1. Nucleic acid biomarker levels in duplicate continuously fed reactors. The reactors were fed TCE at approximately 2.5-5 µeeq/L-hr (A) and 125 µeeq/L-hr (B). Ethene produced is also displayed (right axis). Error bars represent standard errors of duplicate extractions. Ethene produced is in black, 16S rRNA gene is in pink, 16S rRNA is in red and hupL is in blue. Solid and dashed lines represent the different duplicates.

.2A and B). HupL expression (0.1 to 10 copies per cell) in the KB-1^{TM} culture was indistinguishable from expression in the D2 culture for respiration rates ranging over three orders of magnitude. PSS transcript levels ranged from 2 to 50 copies per cell for VcrA. The 1545 RDase homolog detected by our primers was expressed at a constant level (approximately 10 copies per cell) over the respiration rates observed, at a similar order of magnitude as the peak expression values for the D2 culture (Figure 3.2C). This is in sharp contrast to the expression pattern observed for the D2 culture, where 1545 expression peaks at a low to mid respiration rate (Figure 3.2C).[2,3] TceA was expressed in KB-1^{TM} at a very low level (less than 0.01 transcripts per cell), especially as compared to the D2 mixed culture (Figure 3.2D). Ribosome content (per mL) also remained relatively constant (equal to around 100 copies per cell), and was indistinguishable from the D2 culture over the range of respiration rates studied (Figure 3.2E).

Cell densities (based on 16S rRNA gene copies per mL) did not change significantly within or across experiments and were slightly lower than in the D2 mixed culture (Figure 3.2F). This indicates that the populations are relatively steady over the time frames and range of respiration rates studied, and that changes in the RNA levels are due to up-regulation, not due to an increase in cell density.

BvcA and the *Geobacter* RDase PceA were not examined by qPCR in this study. *Geobacter* is a non-*Dehalococcoides* dechlorinating population in the KB-1 culture that dechlorinates PCE and TCE to *cis*-DCE via a PceA enzyme.[46] Since we are most concerned with the VC to ethene step of the dechlorination process, as VC is a known carcinogen and ethene is non-toxic, this RDase was not included as a biomarker. A BvcA homolog is present in KB-1.[34] However, at the time the work was conducted, evidence for the function of BvcA was not as strong as for VcrA, and thus it was not included in our original suite of potential biomarkers. However, just recently the function of BvcA in BAV1 was identified as catalyzing the dechlorination of all chloroethene isomers in cultures of strain BAV1 growing on chlorethenes, as it was the only detected RDase.[56]

3.D.2. Stress Responses.

Oxygen Stress.

The six subcultures in this experiment had batch respiration rates of 69.4 ± 5.6 μeeq/L-hr with VC and ethene as the main products prior to the addition of oxygen. After headspace purging and re-feeding, the control had a respiration rate of 29.9 μeeq/L-hr. After addition of the stressor, the experimental bottles were all inactivated (Figures 3.3A). The medium was initially pink in the oxygen-amended bottles, indicating that the redox indicator resazurin had been oxidized, whereas the resazurin remained colorless in the control bottles. The measured

respiration rates for bottles B1 and B2 (sacrificed 8 hours after addition of the stressor) dropped to 0.44 and 0.39 µeeq/L-hr, respectively. The measured respiration rates for bottles C1 and C2 (sacrificed 170 hours after the addition of the stressor) were 2.5 and 2.2 µeeq/L-hr, respectively, indicating that dechlorination past DCE was again occurring in the bottles. Additionally, prior to recovery, the medium in bottles C1 and C2 returned to a black color, indicating the oxygen in the

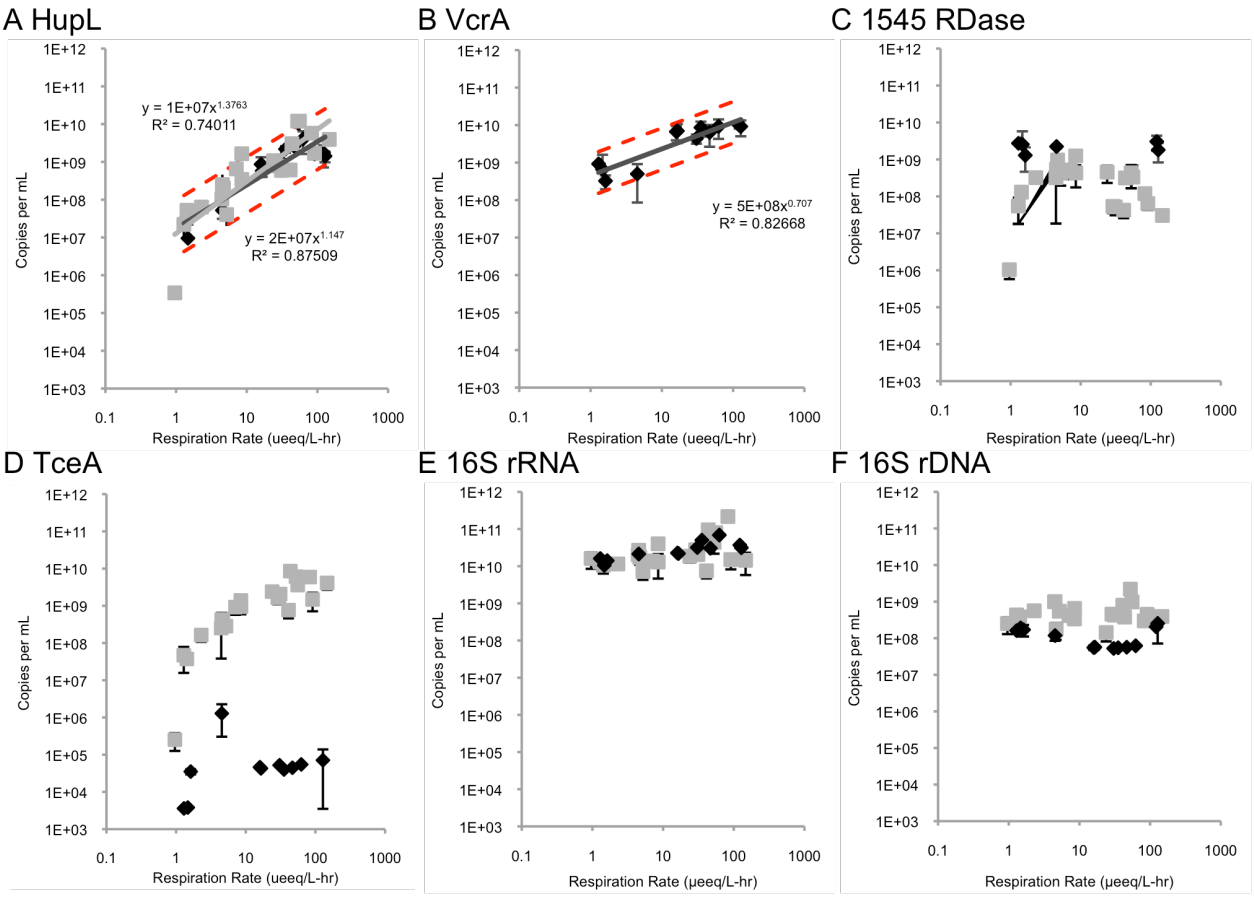

Figure 3. 2. Pseudo-steady-state mRNA concentrations (copies per mL) of specific targets: hydrogenase HupL (A); reductive dehalogenases VcrA (B), 1545 (C), and TceA (D); and 16S ribosomal RNA subunit (E) and 16S rDNA (F) vs. steady-state respiration rates (µeeq/L-hr) for the KB-1 culture (black diamonds) and D2 culture (grey squares). Error bars represent standard error of average respiration rates between replicate reactors (X-error bars) and standard deviations of PSS mRNA measurements over time for replicate reactors (Y-error bars). Power law trend lines for KB-1 (solid black line) and D2 (solid grey line) and 95% confidence intervals around the KB-1 trend (dashed red line) are displayed where appropriate. Note that reductive dehalogenase VcrA is not present in the D2 DMC strain's genome.

bottles had been consumed, and the redox indicator resazurin was no longer oxidized. GC data for all six subcultures is presented in Figures 3.3A. Oxygen levels for the six subcultures are presented in Figures 3.3B. It is important to note that the culture became anaerobic again at between 48 and 115 hours, which corresponded to a return to activity for the stressed subcultures. TCE degradation began again in this time period (Figure A2.1). However, as this portion of the degradation pathway was likely carried out by the *Geobacter* strain present in the mixed culture, we waited until *cis*-DCE degradation resumed (observed as VC production) prior to sacrificing the bottles for further analysis [170 hours after the stressor was added (Figure A2.1)].

Time courses of target biomarker expression levels (VcrA, HupL and 1545) are also presented in Figures 3.3C-E. For all three targets, the control bottle (A2) remained at a higher expression level longer than the experimental bottles (B1, B2, C1 and C2) after the experimental bottles were stressed. The eventual decrease in expression levels for the control bottle is likely due to starvation of the batch culture as the chloroethenes were consumed, which has been seen previously in the D2 culture.[3] The trend of HupL declining in transcripts more rapidly than RDases has also been seen previously.[33]

Acid Stress.

Six subcultures were continuously fed TCE had respiration rates of 1.4 ± 0.2 μeeq/L-hr prior to the addition of acid. After the addition of acid, the experimental bottles dropped to respiration rates of 0.2 ± 0.3 μeeq/L-hr while the control had a respiration rate of 1.9 μeeq/L-hr. GC data for all six subcultures are presented in Supporting Information (SI) Figure A2.2A.

Time courses for the target biomarker expression levels are also presented in SI Figure A2.2B-D. A clear trend is not observed for the expression of target biomarkers in the

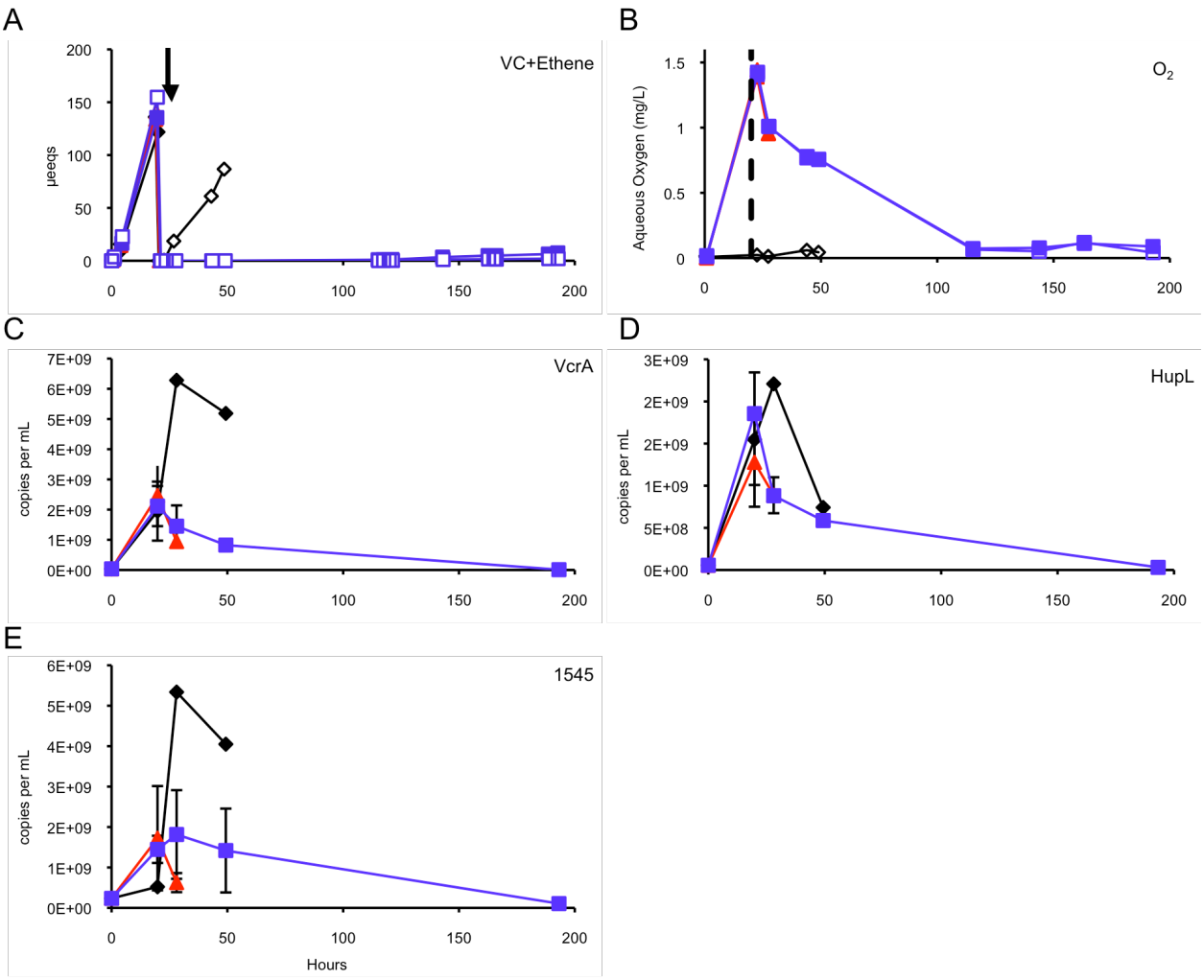

Figure 3. 3. Timecourses of metabolite and mRNA concentrations for specific targets in oxygen stress experiments. The control is in black, and the stressed bottles are in red (sacrificed ~12 hours after stress) and blue (sacrificed at end of the experiment). Note the culture was starting to recover ~100 hours after the oxygen stress. The arrow (vertical dashed line in B) indicates when the stress was added. Error bars represent standard error of duplicate reactors.

experimental bottles as compared to the control bottles. The length of the experiment (short) and low feeding rate may not have given enough time for an observable change in transcript levels. The low feed rate translates to less active cells – the total transcript levels for HupL and VcrA were lower in the acid-stress control subcultures as compared to the oxygen stress control subcultures (Figures 4 vs. S2). Prior to addition of the stressor, the transcript levels for HupL, VcrA and 1545 were $4.01 \times 10^6 \pm 1.98 \times 10^6$, $4.98 \times 10^8 \pm 2.38 \times 10^8$ and $1.18 \times 10^9 \pm 7.10 \times 10^8$

copies per mL, respectively for all the bottles. The expected values after 10.5 hours, based on the decay rates inferred from Figures 3.4, were $3.24x10^6$, $4.64x10^8$ and $1.00x10^9$ copies per mL for HupL, VcrA and 1545, respectively. These values are within the standard deviation of the valuesprior to the addition of the stressor, suggesting a limited ability to resolve such declines with the qRT-PCR method.

3.D.3. Endogenous mRNA Decay.

RNA decay rates for DMC were calculated from batch reactors after addition of oxygen (1.6 mg/L) caused the subcultures to become inactive (Figures 3.3A). RNA decay rates in KB-1™ for VcrA, HupL and 1545 (Figures 3.4) were found to be 0.02-0.03 per hr (half lives of 20-30 hours), slightly lower than those observed previously for D2's DMC population for the time period following peak expression (0.03-0.06 per hr), and the same as those post purging of reactors for D2 (0.02 per hr).[3] These RNA decay rates are also much higher than cell DNA decay rates 0.003 to 0.004 per hr previously found for D2.[57]

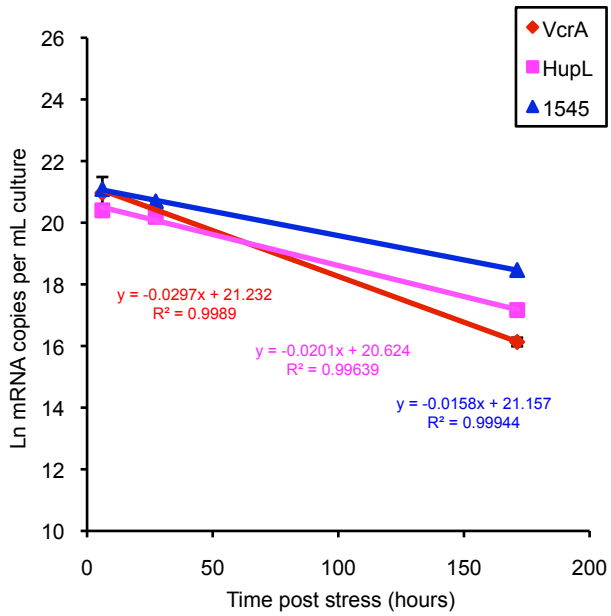

Figure 3. 4. Quantification of mRNA biomarker levels in batch reactors following addition oxygen (3.14 mg) with exponential decay fits (Ln mRNA vs. time) demonstrating endogenous mRNA degradation. Error bars represent standard error based on biological replicates.

3.D.4. Proteomic Biomarker Validation.

Shotgun metaproteomic data for KB-1™ supports the trends observed at the transcript level (NSAF scores are presented in Table 3.2). The most abundant reductive dehalogenases detected in KB-1™ were the VcrA and 1545 homologs followed by BvcA. TceA was detected, but at a very low level (NSAF of 4.88E-04) – especially compared to samples from the D2 culture analyzed in the same way (NSAF of 0.152). The HupL homologs were the third most abundant biomarker of interest detected. Twelve other RDase homologs were also found in the metaproteome, including the *Geobacter* RDase PceA.

Table 3. 2. Detected Biomarkers In Shotgun KB-1™ Metaproteome Sample. The NSAF is a sum of NSAF's for all detected homologs. With the exception of the hydrogenase, HupL, the biomarkers are reductive dehalogenases.

Homolog	NSAF x 10^5
VcrA	4723
1545	4684
HupL	959
BvcA	923
Geobacter PceA	94
KB1_8, KB1_9	66
DET0180	62
KB1_1	57
TceA	49
KB1_1549	13
DET1528	8.4
KB1_7	7.7
DET1519	2.2
DET1538	1.1
cbdbA80	1.1

The 1545 homolog is interesting because it is highly conserved among DMC strains (e.g. cbdbA1638/DhcVS_1436) and has been detected at field sites previously[32] whereas VcrA and BvcA are less ubiquitous RDases. The 46 1545-homolog peptides that were detected in the KB-1™ culture align with homologs from the Cornell, Victora and Pinellas subgroups (1545-C,

1545-V and 1545-P, respectively): one peptide hits 1545-C alone, 25 peptides align with all groups, nine peptides align with 1545-P (but not 1545-C and 1545-V), one peptide aligns with 1545-P and 1545-V but not 1545-C (Table A2.3). Consequently, DMC strains in KB-1^{TM} could be differentiated by virtue of slight differences in the 1545 homologs' peptides. Consensus peptides were generated from aligning detected peptides with identical overlapping sequences (Table 3.3). Five regions of the 1545 sequence had strain specificity in the detected peptides (red boxes A-E in Figures 3.5). In region A, 6 peptides were detected, one was specific for 1545-C, and the other 5 were specific for 1545-P and the homolog in the KB-1 mixed culture. In region D, 6 three peptides were detected that are specific for 1545-P. In regions C and E, one peptide was detected that was specific for 1545-P. Two regions were found to be highly conserved, and highly detected. In regions F and G, 12 and 9 peptides, respectively, were detected that aligned with homologs from all groups (1545-C, 1545-V and 1545-P).

3.D.5. Transcriptomic Biomarker Discovery.

Microarray analysis of the oxygen stress experiment showed that as the C bottles started to recover, the RDases that were highly upregulated (average C's compared to average B's) were homologs of DET0173, 1545 and BvcA. The most downregulated RDases were 1545 and VcrA. 1545 being both highly up and down-regulated is likely due to multiple strains of DMC in the KB-1 culture.[34,54] The most upregulated 1545 probes target both 1545-C and 1545-V. The most downregulated 1545 probes target 1545-P (Table 3.4).

Table 3. 3. Consensus 1545 Homolog Peptides Detected in Shotgun KB-1™ Sample. Peptides are highlighted based on their specificity the Cornell group (green) or the Pinellas group (orange), and peptides highlighted in blue are highly conserved. See Figure 3.5 for peptide locations.

Peptide Numbers	Highlighted Region in Figure 3.5	Consensus Sequence	Combined Spectral Counts for Peptide	Cornell Group	Victoria Group	Pinellas Group and KB-1 Mixed Culture
13, 27, 26, 10, 9	A	GTIANIPLFNTYFYK	14			X
28	A	NVSLFNTYFYK	2	X		
14, 21, 20, 19, 37, 36, 45, 25, 24, 23, 22, 30	F	QKLYTLTPEYGAPGRLYGVLTDLPLEPTHPIDAGIYR	31	X	X	X
46, 12, 31, 44	B	YLGYQLIGTIGNDARYVGSEGGAAIMAGLGEASR	410	X	X*	X
32	C	SAGTLLGGMANGNTFYN	1			X
34, 15, 11, 18, 17, 16		LVIPNVPLWEIALSTQGSNELWR	8	X	X	X**
29, 43, 42	D	YIGTTIPVTAARPIVFENVPK	3			X
41		WTGTPEEASR	5	X		X
40		VSQGTSPGWAETK	2		X	X***
33, 35, 5, 4, 2, 1, 8, 39, 38	G	VLGAAALSAAELAERTASNYPGYTYR	81	X	X	X
3	E	AIYYGADR	1		X	X
7		ERPIDDPTIEVDF	1	X	X	X
6		DTAVQPRPWWVK	4	X	X	X

*3 of the detected peptides that form this consensus peptide don't hit VS, but 1 does

**5 of the detected peptides that form this consensus peptide don't hit FL2, but 1 does

***This peptide does not hit FL2

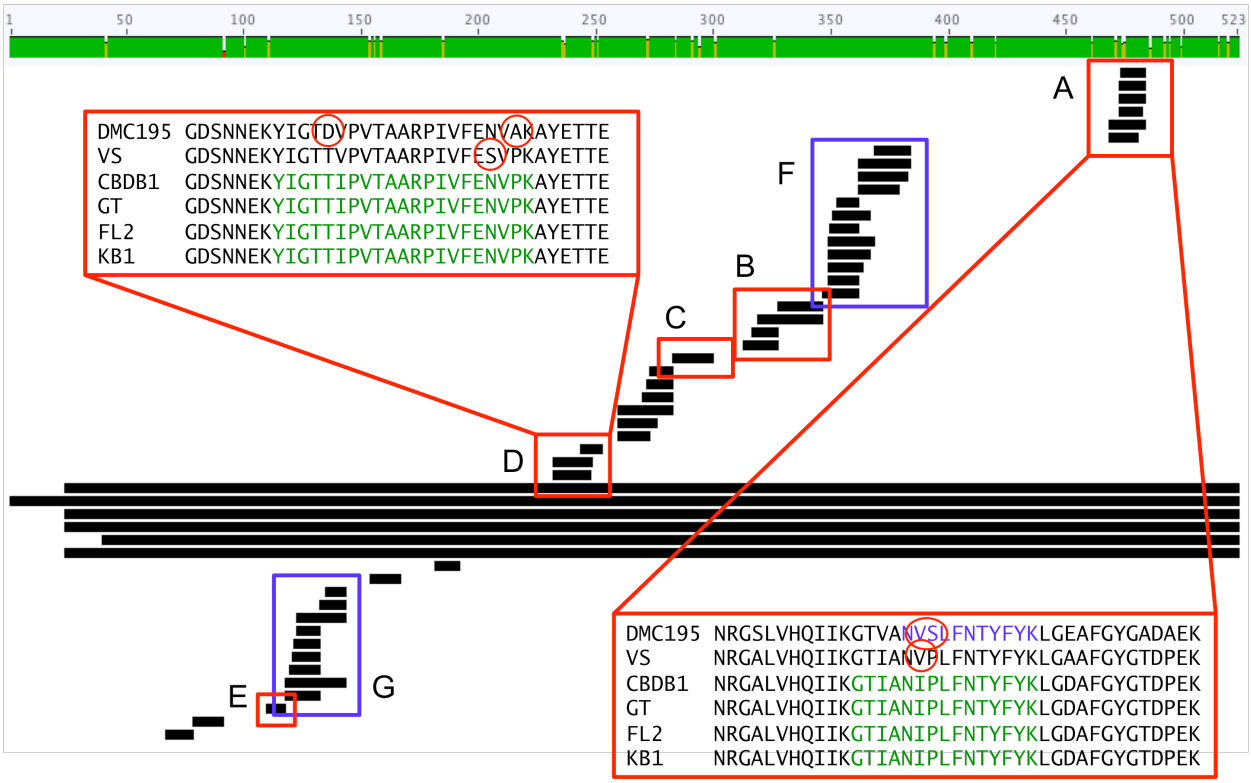

Figure 3. 5. A comparison of 1545-homolog peptides detected in the KB-1 culture sample to the 1545-homolog sequences in genomes of DMC195, DMC strains VS, CBDB1, GT, FL2 and the KB-1 mixed culture. Peptides boxed in red (A-E) show strain specificity, whereas peptides boxed in blue (F and G) are highly conserved and align across all strains. In the insets, detected consensus peptides are highlighted in green, and variations that were detected are highlighted in blue, with the differences circled in red. This figure was created using Geneious version 5.0.4 created by Biomatters.

Table 3. 4. Nucleotide Percent Identity Between Microarray Probe Targets and *Dehalococcoides mccartyi* strains for the 1545 homologs.

	Cornell Group	Victoria Group	Pinellas Group				Fold Change Following Oxygen Recovery
	DMC195	VS	BAV1	CBDB1	GT	KB-1	
panDhc_506_RC	69.4	85.7	69.4	100.0	100.0	100.0	0.03
KB1_0072	73.3	93.3	73.3	100.0	100.0	100.0	0.05
panDhc_506	85.7	87.8	85.7	100.0	100.0	100.0	0.34
gi147669941	91.7	95.0	100.0	98.3	98.3	85.0	3.49
panDhc_502	100.0	87.8	91.8	83.7	83.7	81.6	9.58
panDhc_502_RC	100.0	85.7	100.0	83.7	83.7	83.7	6.88
panDhc_422	85.7	100.0	83.7	83.7	83.7	83.7	25.48

3.D.6. Multiplexed Proteomic Analysis.

Continuous Feed Experiments.

To relate DMC biomarker protein levels to respiration rates in KB-1™, plots were generated of TMT ion intensities for HupL, VcrA, 1545 and TceA versus respiration rates (from 1.8 to 128 μeeq/L-hr) (Figure A2.3). Similar trends were observed for HupL, VcrA and TceA relative protein levels as for mRNA expression levels versus respiration rate, though proteins showed a smaller magnitude of change over the range of respiration rates tested. A difference between mRNA and protein trends was that ion intensities for 1545 increased as respiration rates increased, whereas their mRNA expression levels stayed relatively constant (Figures A2.3C and 3.2C, respectively).

Oxygen Stress Experiment.

Similarities were observed between the microarray results and multiplex protein results for the oxygen stress experiment. A comparison of the recovering bottles (average C's) to the stressed bottles (average B's) was made. In both the microarray results and protein results, the abundance ratio of the recovering bottles to the stressed bottles was high for the 1545 homolog and BvcA and low for VcrA (Figure 3.6). These three RDases were the only RDases detected in both the proteome and transcriptome of the oxygen stress bottles. The B bottles were sacrificed only 8 hours after the stress was added, which is not enough time for protein turnover to show in samples. Protein decay rates were previously calculated for RDases in the D2 culture, and were found to be approximately 0.0025 per hour.[3] Thus, the bottles sacrificed at 8 hours can be thought of as representative of the maximum protein levels observed. In the B bottles, the ion intensities for VcrA and BvcA are similar, with 1545 approximately an order of magnitude lower. In C bottles (sacrificed approximately 170 hours after the stressor was added), VcrA has

decreased, whereas the 1545 homolog and BvcA are at similar levels to the B bottles. As the cultures have been inactive for a great portion of this time prior to recovery, you would expect a decrease in enzyme levels due to decay. The VcrA ion intensities have decreased from $1.43 \times 10^7 \pm 1.90 \times 10^6$ to $8.38 \times 10^6 \pm 8.39 \times 10^6$. The expected values after 165 hours, based on the decay rates calculated previously, are 1.04×10^7 (within the error bars of the measured final time point). However, that is not the case for the 1545 homolog and VcrA, which are at similar levels to their maximum for this experiment when the bottles were sacrificed after recovery. Thus, it appears that the DMC strains in KB-1™ that contain 1545-C and BvcA homologs are recovering faster than the strain containing the VcrA gene.

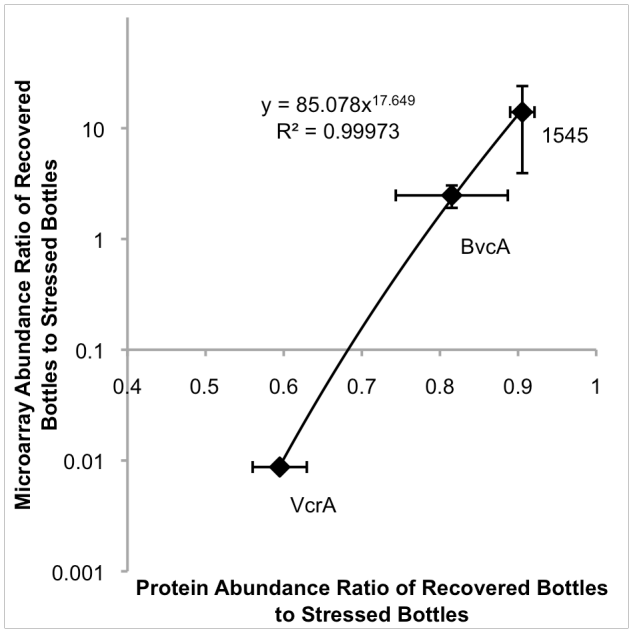

Figure 3. 6. Microarray probe intensity ratio of recovered bottles to stressed bottles vs. protein abundance ratio of recovered bottles to oxygen stressed bottles for the reductive dehalogenases detected in both the protein and microarray results (1545, BvcA and VcrA only). In both cases the same reductive dehalogenases are recovering (1545 and BvcA) and VcrA is not recovering yet. The 1545 homolog targeted by the microarray probes is specific for 1545-C and 1545-V.

A total of 11 1545-homolog peptides were detected in the oxygen stress samples. Three were specific for the 1545-C, and one was specific for the CBDB1 strain. Three of the specific

peptides are from the same region of the 1545 homolog (Figure 3.7). In this region, the peptides detected in the KB-1™ mixed culture sample were specific for the VS and Pinellas groups. In the oxygen stress samples, two peptides were detected that are specific for 1545-C, and the third was specific for 1545-V and 1545-P. One peptide was detected in another region of the 1545

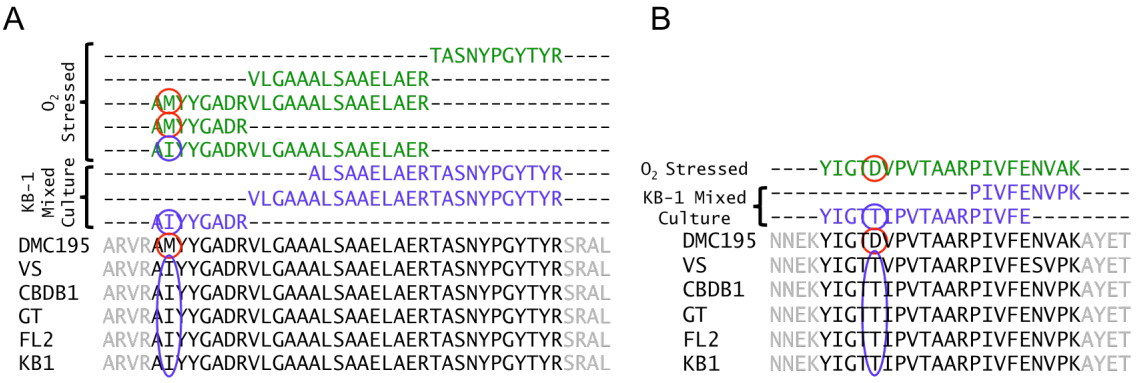

Figure 3. 7. Two regions of the 1545-homolog where peptides were detected in the oxygen stress samples (green) as compared to the peptides detected in the KB-1™ mixed culture sample (blue). Six homologs from DMC genomes, and the KB-1 metagenome are shown in black. The amino acids that differ are circled in red if they match the DMC195 sequence and in blue if they match the remaining sequences. Panel A represents regions D and F in Figure 3.5, and Panel B represents region C in Figure 3.5.

gene that was specific for 1545-C in the oxygen stress samples, whereas a variant of that peptide that was specific for 1545-V and 1545-P was detected in the KB-1™ mixed culture sample. The microarray and proteomic results indicate that a strain with a Cornell group 1545 homolog and BvcA is selectively surviving after oxygen stress.

The key results of this study are that the correlation between respiration rate and mRNA transcript number is upheld for HupL, and significant differences are observed for TceA and 1545 when comparing the two mixed cultures studied (KB-1™ and D2). A correlation is also observed for VcrA expression compared to respiration rate in the KB-1™ mixed culture. Additionally, correlation trends for HupL and VcrA are upheld when looking at proteomic ion intensities as compared to respiration rates, though for the overall magnitude of difference at the protein level are smaller than for mRNA transcripts.

Addition of stressors caused respiration rates to decrease significantly, but mRNA lingered – indicating that transcript abundance alone cannot predict respiration rate in stressed conditions within hours to days following stress. Furthermore, both transcriptomic and proteomic data indicated initial recovery post oxygen stress of DMC strains that have homologs for 1545 and BvcA as opposed to a strain with VcrA.

3.E. Acknowledgements

This project was supported by the National Science Foundation (NSF) CBET Program (CBET-0731169) and the U.S. Department of Defense (DOD) (W911NF-07-1-0249). Culture used in this research was provided by Philip C. Dennis at SiREM Laboratories in Guelph, Ontario, Canada. Portions of this research were performed at the Environmental Molecular Sciences Laboratory (EMSL), a DOE/BER national scientific user facility located at Pacific Northwest National Laboratory (PNNL) in Richland, Washington. PNNL is a multi-program national laboratory operated by Battelle for the DOE under Contract DE-ACO5-76RLO 1830. We would also like to thank Julie Brown of Cornell University, Department of Microbiology, for 1545 primer design.

REFERENCES

(1) Rahm, B. G.; Richardson, R. E. Correlation of respiratory gene expression levels and pseudo-steady-state PCE respiration rates in *Dehalococcoides ethenogenes*. *Environ. Sci. Technol.* **2008**, *42*, 416–421.

(2) Rahm, B. G.; Richardson, R. E. Gene Transcripts As Quantitative Bioindicators of Tetrachloroethene, Trichloroethene, and cis-1,2-Dichloroethene Dehalorespiration Rates. *Environ. Sci. Technol.* **2008**, *42*, 5099–5105.

(3) Rowe, A. R.; Heavner, G. L.; Mansfeldt, C. B.; Werner, J. J.; Richardson, R. E. Relating Chloroethene Respiration Rates in *Dehalococcoides* to Protein and mRNA Biomarkers. *Environ. Sci. Technol.* **2012**, *46*, 9388–9397.

(4) Hendrickson, E. R.; Payne, J. A.; Young, R. M.; Starr, M. G.; Perry, M. P.; Fahnestock, S.; Ellis, D. E.; Ebersole, R. C. Molecular analysis of *Dehalococcoides* 16S ribosomal DNA from chloroethene-contaminated sites throughout North America and Europe. *Appl. Environ. Microb.* **2002**, *68*, 485–495.

(5) Loffler, F. E.; Yan, J.; Ritalahti, K. M.; Adrian, L.; Edwards, E. A.; Konstantinidis, K. T.; Muller, J. A.; Fullerton, H.; Zinder, S. H.; Spormann, A. M. *Dehalococcoides mccartyi* gen. nov., sp. nov., obligate organohalide-respiring anaerobic bacteria, relevant to halogen cycling and bioremediation, belong to a novel bacterial class, Dehalococcoidetes classis nov., within the phylum Chloroflexi. *Int. J. Syst. Evol. Micr.* **2012**.

(6) Maphosa, F.; De Vos, W. M.; Smidt, H. Exploiting the ecogenomics toolbox for environmental diagnostics of organohalide-respiring bacteria. *Trends in Biotechnology* **2010**.

(7) Löffler, F. E.; Edwards, E. A. Harnessing microbial activities for environmental cleanup. *Current Opinion in Biotechnology* **2006**, *17*, 274–284.

(8) Maymo-Gatell, X.; Chien, Y.; Gossett, J. M.; Zinder, S. H. Isolation of a bacterium that reductively dechlorinates tetrachloroethene to ethene. *Science* **1997**, *276*, 1568–1571.

(9) Maymo-Gatell, X.; Anguish, T.; Zinder, S. H. Reductive dechlorination of chlorinated ethenes and 1, 2-dichloroethane by *Dehalococcoides ethenogenes* 195. *Appl. Environ. Microb.* **1999**, *65*, 3108–3113.

(10) Fennell, D. E.; Nijenhuis, I.; Wilson, S. F.; Zinder, S. H.; Häggblom, M. M. *Dehalococcoides ethenogenes* Strain 195 Reductively Dechlorinates Diverse Chlorinated Aromatic Pollutants. *Environ. Sci. Technol.* **2004**, *38*, 2075–2081.

(11) He, J.; Sung, Y.; Krajmalnik-Brown, R.; Ritalahti, K. M.; Loffler, F. E. Isolation and characterization of *Dehalococcoides* sp. strain FL2, a trichloroethene (TCE)- and 1,2-dichloroethene-respiring anaerobe. *Environ. Microbiol.* **2005**, *7*, 1442–1450.

(12) Sung, Y.; Ritalahti, K. M.; Apkarian, R. P.; Loffler, F. E. Quantitative PCR Confirms Purity of Strain GT, a Novel Trichloroethene-to-Ethene-Respiring *Dehalococcoides* Isolate. *Appl. Environ. Microb.* **2006**, *72*, 1980–1987.

(13) Müller, J. A.; Rosner, B. M.; Von Abendroth, G.; Meshulam-Simon, G.; McCarty, P. L.; Spormann, A. M. Molecular identification of the catabolic vinyl chloride reductase from *Dehalococcoides* sp. strain VS and its environmental distribution. *Appl. Environ. Microb.* **2004**, *70*, 4880–4888.

(14) Cupples, A. M.; Spormann, A. M.; McCarty, P. L. Comparative evaluation of chloroethene dechlorination to ethene by *Dehalococcoides*-like microorganisms. *Environ. Sci. Technol.* **2004**, *38*, 4768–4774.
(15) Duhamel, M.; Mo, K.; Edwards, E. Characterization of a highly enriched *Dehalococcoides*-containing culture that grows on vinyl chloride and trichloroethene. *Appl. Environ. Microb.* **2004**, *70*, 5538–5545.
(16) He, J.; Ritalahti, K. M.; Yang, K.-L.; Koenigsberg, S. S.; Loffler, F. E. Detoxification of vinyl chloride to ethene coupled to growth of an anaerobic bacterium. *Nature* **2003**, *424*, 62–65.
(17) Adrian, L.; Szewzyk, U.; Wecke, J.; Gorisch, H. Bacterial dehalorespiration with chlorinated benzenes. *Nature* **2000**, *408*, 580–583.
(18) Bunge, M.; Adrian, L.; Kraus, A.; Opel, M.; Lorenz, W. G.; Andreesen, J. R.; Görisch, H.; Lechner, U. Reductive dehalogenation of chlorinated dioxins by an anaerobic bacterium. *Nature* **2003**, *421*, 357–360.
(19) Marco-Urrea, E.; Nijenhuis, I.; Adrian, L. Transformation and Carbon Isotope Fractionation of Tetra- and Trichloroethene to Trans-Dichloroethene by *Dehalococcoides* sp. Strain CBDB1. *Environ. Sci. Technol.* **2011**, *45*, 1555–1562.
(20) Hug, L. A.; Salehi, M.; Nuin, P.; Tillier, E. R.; Edwards, E. A. Design and Verification of a Pangenome Microarray Oligonucleotide Probe Set for *Dehalococcoides* spp. *Appl. Environ. Microb.* **2011**, *77*, 5361–5369.
(21) Cupples, A.; Spormann, A.; McCarty, P. Growth of a *Dehalococcoides*-like microorganism on vinyl chloride and cis-dichloroethene as electron acceptors as determined by competetive PCR. *Appl. Environ. Microb.* **2003**, *69*, 4342–4342.
(22) Fennell, D.; Carroll, A.; Gossett, J.; Zinder, S. Assesment of Indigenous Reductive Dechlorinating Potential at a TCE-Contaminated Site Using Microcosms, Polymerase Chain Reaction Analysis, and Site Data. *Environ. Sci. Technol.* **2001**, *35*, 1830–1839.
(23) Committee on In Situ Bioremediation, National Research Council *In Situ Bioremediation: When Does it Work?*; The National Academies Press: Washington, D.C., 1993.
(24) Ellis, D. E.; Lutz, E. J.; Odom, J. M.; Buchanan Jr, R. J.; Bartlett, C. L.; Lee, M. D.; Harkness, M. R.; DeWeerd, K. A. Bioaugmentation for accelerated in situ anaerobic bioremediation. *Environ. Sci. Technol.* **2000**, *34*, 2254–2260.
(25) Major, D. W.; McMaster, M. L.; Cox, E. E.; Edwards, E. A.; Dworatzek, S. M.; Hendrickson, E. R.; Starr, M. G.; Payne, J. A.; Buonamici, L. W. Field Demonstration of Successful Bioaugmentation To Achieve Dechlorination of Tetrachloroethene To Ethene. *Environ. Sci. Technol.* **2002**, *36*, 5106–5116.
(26) Lendvay, J. M.; Löffler, F. E.; Dollhopf, M.; Aiello, M. R.; Daniels, G.; Fathepure, B. Z.; Gebhard, M.; Heine, R.; Helton, R.; Shi, J.; others. Bioreactive barriers: a comparison of bioaugmentation and biostimulation for chlorinated solvent remediation. *Environ. Sci. Technol* **2003**, *37*, 1422–1431.
(27) Lu, X.; Wilson, J. T.; Kampbell, D. H. Relationship between geochemical parameters and the occurrence of *Dehalococcoides* DNA in contaminated aquifers. *Water Resour. Res.* **2006**, *42*.
(28) Lu, X.; Wilson, J. T.; Kampbell, D. H. Relationship between *Dehalococcoides* DNA in ground water and rates of reductive dechlorination at field scale. *Water Res.* **2006**,

40, 3131–3140.
(29) Lovley, D. R. Cleaning up with genomics: applying molecular biology to bioremediation. *Nat Rev Micro* **2003**, *1*, 35–44.
(30) Scheutz, C.; Durant, N.; Dennis, P.; Hansen, M. H.; Jorgensen, T.; Jakobsen, R.; Bjerg, P. L. Concurrent ethene generation and growth of *Dehalococcoides* containing vinyl chloride reductive dehalogenase genes during an enhanced reductive dechlorination field demonstration. *Environ. Sci. Technol* **2008**, *42*, 9302–9309.
(31) Tas, N.; Van Eekert, M. H. .; De Vos, W. M.; Smidt, H. The little bacteria that can–diversity, genomics and ecophysiology of *Dehalococcoides* spp. in contaminated environments. *Microbial Biotechnology*.
(32) Lee, P. K. H.; Macbeth, T. W.; Sorenson, K. S.; Deeb, R. A.; Alvarez-Cohen, L. Quantifying Genes and Transcripts To Assess the In Situ Physiology of *Dehalococcoides* spp. in a Trichloroethene-Contaminated Groundwater Site. *Appl. Environ. Microb.* **2008**, *74*, 2728–2739.
(33) Rahm, B. G.; Morris, R. M.; Richardson, R. E. Temporal Expression of Respiratory Genes in an Enrichment Culture Containing *Dehalococcoides ethenogenes*. *Appl. Environ. Microb.* **2006**, *72*, 5486–5491.
(34) Waller, A. S.; Krajmalnik-Brown, R.; Loffler, F. E.; Edwards, E. A. Multiple Reductive-Dehalogenase-Homologous Genes Are Simultaneously Transcribed during Dechlorination by *Dehalococcoides*-Containing Cultures. *Appl. Environ. Microb.* **2005**, *71*, 8257–8264.
(35) Behrens, S.; Azizian, M. F.; McMurdie, P. J.; Sabalowsky, A.; Dolan, M. E.; Semprini, L.; Spormann, A. M. Monitoring abundance and expression of *Dehalococcoides* species chloroethene-reductive dehalogenases in a tetrachloroethene-dechlorinating flow column. *Appl. Environ. Microb.* **2008**, *74*, 5695–5703.
(36) Fung, J. M.; Morris, R. M.; Adrian, L.; Zinder, S. H. Expression of Reductive Dehalogenase Genes in *Dehalococcoides ethenogenes* Strain 195 Growing on Tetrachloroethene, Trichloroethene, or 2,3-Dichlorophenol. *Appl. Environ. Microb.* **2007**, *73*, 4439–4445.
(37) Johnson, D. R.; Lee, P. K. H.; Holmes, V. F.; Fortin, A. C.; Alvarez-Cohen, L. Transcriptional expression of the tceA gene in a *Dehalococcoides*-containing microbial enrichment. *Appl. Environ. Microb.* **2005**, *71*, 7145.
(38) Johnson, D. R.; Lee, P. K. H.; Holmes, V. F.; Alvarez-Cohen, L. An internal reference technique for accurately quantifying specific mRNAs by real-time PCR with application to the tceA reductive dehalogenase gene. *Appl. Environ. Microb.* **2005**, *71*, 3866.
(39) Duhamel, M.; Wehr, S. D.; Yu, L.; Rizvi, H.; Seepersad, D.; Dworatzek, S.; Cox, E. E.; Edwards, E. A. Comparison of anaerobic dechlorinating enrichment cultures maintained on tetrachloroethene, trichloroethene, cis-dichloroethene and vinyl chloride. *Water Res.* **2002**, *36*, 4193–4202.
(40) DiStefano, T. D.; Gossett, J. M.; Zinder, S. H. Reductive dechlorination of high concentrations of tetrachloroethene to ethene by an anaerobic enrichment culture in the absence of methanogenesis. *Appl. Environ. Microb.* **1991**, *57*, 2287–2292.
(41) Smatlak, C. R.; Gossett, J. M.; Zinder, S. H. Comparative kinetics of hydrogen utilization for reductive dechlorination of tetrachloroethene and methanogenesis in an

anaerobic enrichment culture. *Environ. Sci. Technol.* **1996**, *30*, 2850–2858.
(42) Fennell, D. E.; Gossett, J. M.; Zinder, S. H. Comparison of butyric acid, ethanol, lactic acid, and propionic acid as hydrogen donors for the reductive dechlorination of tetrachloroethene. *Environ. Sci. Technol.* **1997**, *31*, 918–926.
(43) Fennell, D. Comparison of Alternative Hydrogen Donors for Anaerobic Reductive Dechlorination of Tetrachloroethene. Ph.D. Dissertation, Cornell University: Ithaca, NY, 1998.
(44) Gossett, J. M. Sustained aerobic oxidation of vinyl chloride at low oxygen concentrations. *Environ. Sci. Technol.* **2010**, *44*, 1405–1411.
(45) Duhamel, M.; Edwards, E. A. Microbial composition of chlorinated ethene-degrading cultures dominated by *Dehalococcoides*. *FEMS Microbiol. Ecol.* **2006**, *58*, 538–549.
(46) Duhamel, M.; Edwards, E. A. Growth and Yields of Dechlorinators, Acetogens, and Methanogens during Reductive Dechlorination of Chlorinated Ethenes and Dihaloelimination of 1,2-Dichloroethane. *Environ. Sci. Technol.* **2007**, *41*, 2303–2310.
(47) Peirson, S. N.; Butler, J. N.; Foster, R. G. Experimental validation of novel and conventional approaches to quantitative real-time PCR data analysis. *Nucleic Acids Res.* **2003**, *31*, 1–7.
(48) Schefe, J. H.; Lehmann, K. E.; Buschmann, I. R.; Unger, T.; Funke-Kaiser, H. Quantitative real-time RT-PCR data analysis: current concepts and the novel "gene expression's C T difference" formula. *J. Mol. Med.* **2006**, *84*, 901–910.
(49) Thompson, A.; Schaefer, J.; Kuhn, K.; Kienle, S.; Schwarz, J.; Schmidt, G.; Neumann, T.; Johnstone, R. A. W.; Mohammed, A. K. A.; Hamon, C. Tandem Mass Tags: A Novel Quantification Strategy for Comparative Analysis of Complex Protein Mixtures by MS/MS. *Analytical Chemistry* **2006**, *78*, 4235–4235.
(50) Kelly, R. T.; Page, J. S.; Luo, Q.; Moore, R. J.; Orton, D. J.; Tang, K.; Smith, R. D. Chemically Etched Open Tubular and Monolithic Emitters for Nanoelectrospray Ionization Mass Spectrometry. *Analytical Chemistry* **2006**, *78*, 7796–7801.
(51) Kim, S.; Gupta, N.; Pevzner, P. A. Spectral Probabilities and Generating Functions of Tandem Mass Spectra: A Strike against Decoy Databases. *Journal of Proteome Research* **2008**, *7*, 3354–3363.
(52) Zybailov, B.; Mosley, A. L.; Sardiu, M. E.; Coleman, M. K.; Florens, L.; Washburn, M. P. Statistical Analysis of Membrane Proteome Expression Changes in *Saccharomyces cerevisiae*. *Journal of Proteome Research* **2006**, *5*, 2339–2347.
(53) Wilkins, M. J.; VerBerkmoes, N. C.; Williams, K. H.; Callister, S. J.; Mouser, P. J.; Elifantz, H.; N'Guessan, A. L.; Thomas, B. C.; Nicora, C. D.; Shah, M. B.; Abraham, P.; Lipton, M. S.; Lovley, D. R.; Hettich, R. L.; Long, P. E.; Banfield, J. F. Proteogenomic Monitoring of *Geobacter* Physiology during Stimulated Uranium Bioremediation. *Appl. Environ. Microb.* **2009**, *75*, 6591–6599.
(54) Mansfeldt, C. B. Data driven hypothesis modelling of *Dehalococcoides mccartyi* : predicted biology and biomarkers of stress in two mixed microbial communities, Cornell University: Ithaca, NY, 2013.
(55) Waller, A. S. Molecular Investigation of Chloroethene Reductive Dehalogenation by the Mixed Microbial Community KB1, University of Toronto: Toronto, Ontario, Canada, 2009.
(56) Tang, S.; Chan, W. W. M.; Fletcher, K. E.; Seifert, J.; Liang, X.; Loffler, F. E.;

Edwards, E. A.; Adrian, L. Functional Characterization of Reductive Dehalogenases by Using Blue Native Polyacrylamide Gel Electrophoresis. *Appl. Environ. Microb.* **2012**, *79*, 974–981.

(57) Rowe, A. R. Molecular Biomarkers for Respiration in *Dehalococcoides ethenogenes* and *Methanospirillum hungatei*: Comparing Protein and Messenger-RNA Abundance in Anaerobes, Cornell University: Ithaca, NY, 2011.

CHAPTER 4:

Detection of Organohalide-Respiring Enzyme Biomarkers at a TCE-Contaminated Field Site that has been Bioaugmented with the Mixed Microbial Consortium KB-1™

4.A. Abstract

Implementation of chloroethene bioremediation requires methods for monitoring the structure and activity of the subsurface microbial communities that are responsible for reductive dechlorination. Here we report on a successful proteomics-based method for identifying *Dehalococcoides* and *Geobacter* biomarkers of reductive dechlorination at a trichloroethene (TCE)-contaminated industrial site in Ft. Erie, Ontario that had been bio-augmented with the commercially available KB-1™ microbial culture, and compare the detected proteomic biomarkers to DNA and RNA biomarkers in the same samples. Samples were obtained from two wells with high hydraulic connectivity to the enhanced in-situ bioremediation system, and two with low hydraulic connectivity. The DNA and RNA biomarkers detected were a set of reductive dehalogenases, and the highly conserved Ni-Fe hydrogenase, HupL. Proteomic biomarkers of organohalide respiration were detected in all four field samples' metaproteomes, and the key reductive dehalogenases present in the bioaugmentation culture were the most highly detected proteins overall, suggesting that deployed *Dehalococcoides mccartyi* strains maintain devotion to high RDase concentrations in the field.

4.B. Introduction

Biomarkers are biomolecules (DNA, RNA or proteins) that correspond to a specific microbial process or state. Several studies have been conducted regarding detection of 16S rRNA genes at field sites. 16S rRNA gene sequences are highly conserved among strains of *Dehalococcoides mccartyi* (DMC), forming a distinct phylogenetic group.[1] As early as 2001,

researchers observed that there is a strong correlation between the presence of the DMC 16S rRNA gene at a site, and the reductive dechlorination of chlorinated ethenes to ethene.[2] However, the presence of the 16S rRNA gene does not necessarily mean that dechlorination will occur – conditions may not be favorable and the capability of using specific chloroethene electron acceptors differs among strains (phylogeny does not necessarily predict physiology), making it difficult to predict whether or not dechlorination will occur at a certain site without more information.[2–6] Additionally, there are numerous reductive dehalogenases (12-36 per strain) coded for in the genomes of each strain of DMC.[1] Reductive dehalogenases (RDases) are the enzymes produced by DMC that allow for respiration of chlorinated hydrocarbons.

Due to the central dogma of microbiology, proteins are expected to be the best indicators of activity as they are the functional mediators of activity. However, detection of low abundance protein biomarkers is difficult, and thus far no field sampling efforts have yielded metaproteome libraries successfully. Several studies have been conducted that examine the quantitative correlation between reductive dechlorination activity and specific rRNA transcripts[7–16] and the quantification of DMC genes and transcripts at a trichloroethene (TCE)-contaminated field site.[8] Additionally, several studies have been conducted in our lab concerning the proteome of DMC.[16–19] Morris et al. examined the metaproteome of the DMC strain 195 (DMC195) pure culture, and discovered that HupL is one of the most highly expressed genes in batch cultures.[18] Werner et al. developed a method for quantifying low abundance proteins in complex mixed microbial communities and compared the DMC195-containing mixed culture, D2, and the KB-1 mixed culture.[19] Rowe et al. expanded on this method, and examined the quantitative correlation between reductive dechlorination and the expression of specific genes in DMC195.[16] Based on these studies, a preliminary suite of potential field biomarkers can be generated that includes

RDases, including vinyl chloride (VC) RDase enzymes that have been linked to successful biological dechlorination of VC to ethene in groundwater systems, and other targets.[5] The mechanism of VC dechlorination is important in bioremediation because VC is the most toxic of the chlorinated ethenes, and the VC to ethene step is often rate-limiting.[5] Genes linked to the VC to ethene step of reductive dechlorination (VcrA, BvcA, etc.) may be the best biomarkers for complete remediation of chlorinated ethenes.[5]

Many genes are highly conserved between DMC strains (e.g. HupL and 1545 homologs), making them ideal biomarkers of anaerobic reductive dechlorination. However, phylogeny does not necessarily inform physiology. Thus, a method for detecting strain variation is necessary. Proteomic biomarkers may provide this method. From one sample, much more information can be gained as to gene sequence than with qPCR alone - multiple compatible primer sets would be needed just for one gene to effectively test for all variants of each gene homolog. Additionally, the presence of protein is a good indicator of organism activity, at least on the time scale of field sites.

In this study, groundwater samples were collected from a well-characterized, TCE-contaminated industrial site in southwestern Ontario, Canada (ISSO).[20] High concentrations of TCE, *cis*-dichloroethene (*cis*-DCE) and VC have been detected in the groundwater, and the presence of cDCE and VC indicates that dechlorination by native microorganisms at the site might have occurred. An enhanced in-situ bioremediation (EISB) system was installed at the site in 2008. DMC DNA and mRNA were quantified and field metaproteomes were extracted, digested with trypsin and analyzed by mass spectrometry. The field metaproteomes were compared with proteomes of the KB-1^{TM} seed culture.

4.C. Materials and Methods

4.C.1. Site Description.

The EISB system extracts groundwater from the TCE-contaminated site through three wells located downgradient of the assumed source area (Figure 4.1).[20] The extracted groundwater was amended with eletron donor, and re-injected into the aquifer through recharge wells (IW in Figure 4.1) located in the vicinity of the source area, and upgradient of the extraction wells. Select recharge wells were bioaugmented with the commercially-available KB-1™ microbial culture in October 2009 to boost bioremediation rates for the detected chloroethenes (TCE, cDCE and VC) to ethene.

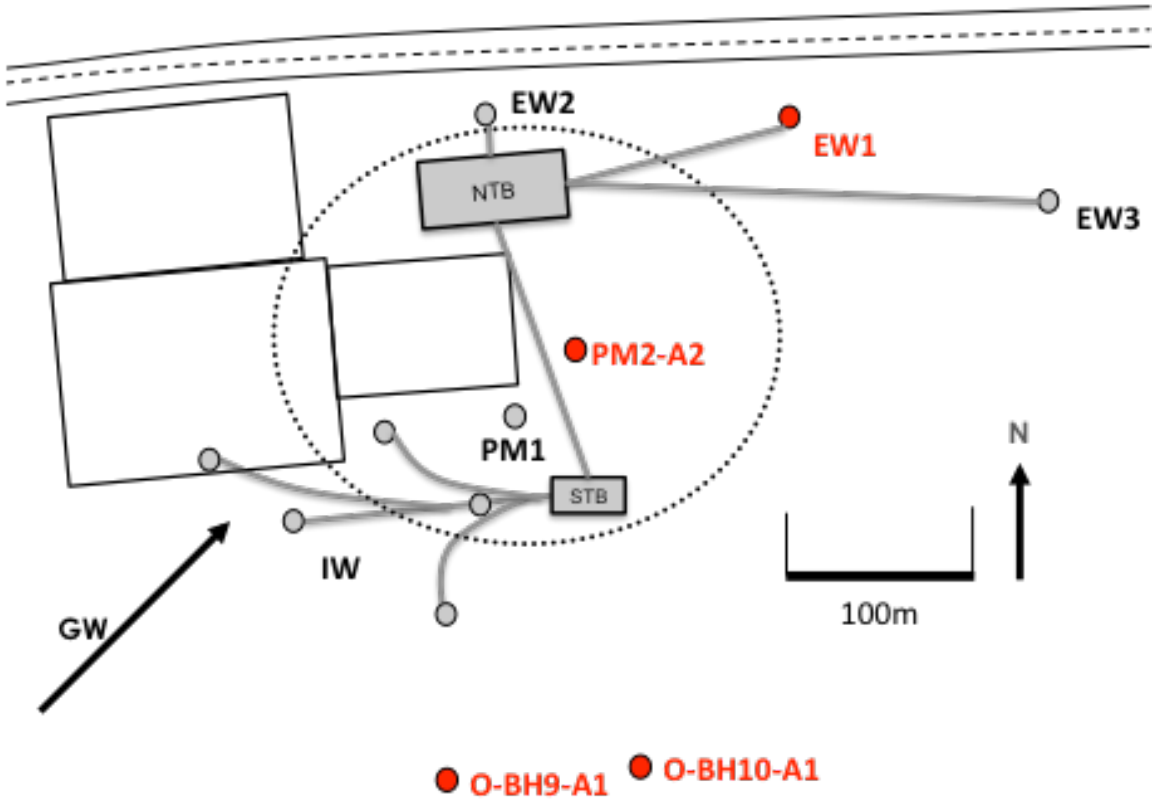

Figure 4. 1. Sketch of the field site (ISSO). Groundwater is extracted from the northern portion of the property (EW wells) and transferred through buried piping to the northern treatment building (NTB) where it is combined, filtered, and amended with chlorine dioxide (ClO2) to control biofouling. The groundwater is then transferred to the southern treatment building (STB) through a central forcemain where the groundwater is amended with electron donor (ethanol) and distributed to individual recharge wells (IW). The wells sampled for this study were PM2-A2, EW1, O-BH9-A1 and O-BH10-A1.

4.C.2. Groundwater Sample Collection.

Groundwater samples were collected approximately two years after bioaugmentation at the site. Samples were obtained from established wells using dedicated inertial lift pumps, with traditional groundwater purging methods. Groundwater was purged from the well until water quality parameters (e.g. temperature, pH, DO, redox potential, conductivity and turbidity) had stabilized when measured using a flow-through cell attached to a multi-parameter sensor, which usually occurred after 2-4 well volumes had been purged. Additionally, the water level was monitored before and after sampling. Between 8 and 12 liters of groundwater were collected in collapsible, 5 gallon containers and transported to the North Treatment Building (NTB) on the site.

For each sample, 8-12 liters of groundwater were filtered through a prefilter (1.2 μm pore size, 142 mm diameter, Versapor® Acrylic Copolymer Membrane Disc Filters; Pall Corporation, NY) followed by a filter (0.2 μm pore size, 142 mm diameter, Supor® PES Membrane Disc Filters; Pall Corporation, NY). Exact volumes filtered are presented in Table 4.1. The groundwater was pumped at approximately 0.5 L/min. Each filter was then removed from the filtering apparatus, folded and placed in a sterile 50 mL conical tube, and flash frozen in an ethanol/dry ice bath before being placed on dry ice. A total of 10 standard hole punches (11 for well EW-1) were removed as subsamples for nucleic acid extraction and the remaining filters were shipped overnight on dry ice to the Environmental Molecular Sciences Laboratory (EMSL) at the Pacific Northwest National Laboratory for proteomic analysis.

Table 4. 1. Groundwater sample volumes and recoveries of DNA, RNA and protein

Well	Volume Filtered (L)	Hole Punches Extracted for Nucleic Acids	DNA recovered (ng)		RNA recovered (µg)		Protein recovered (µg)	
			F	PF	F	PF	F	PF
PM2A2	9.5	5	102	38	2.6	2.1	30	n/a
EW1	12	5	46	13	1.9	1.5	46	n/a
O-BH09-A1	11.25	5	2.8	2.5	bd	bd	60	n/a
O-BH10-A1	8.25	5	2.4	3.4	bd	bd	60	n/a

*bd means that RNA was below detection in extractant fluid.

4.C.3. Nucleic Acid Extraction and Quantification.

DNA and RNA extractions were performed using the AllPrep DNA/RNA Mini Kit (Qiagen) with modifications and DNase treatments as previously described.[9,16] In place of a cell pellet, 5 hole punches (1.3% of the filter surface area) were placed in the cell lysis tube for nucleic acid extraction. Total DNA was quantified using the Quant-iT™ Picogreen® double stranded DNA assay (Invitrogen). RNA quality and quantity was analyzed using the Agilent 2100 BioAnlyzer. DNase treatment, cDNA synthesis, qPCR set up and qPCR run conditions were performed as previously described.[7,10,16] Prior to qPCR, all DNA and cDNA samples were diluted 1 to 5. Primers and annealing temperatures used in this study are listed in Table A2.1 and Table A3.1. Analysis of qPCR data was performed as outlined previously using the iCycler iQ Multicolor Real-Time PCR Detection System (Bio-Rad).[15] Transcript levels were calculated from raw fluorescence data using the Data Analysis for Real-time PCR (DART-PCR) method.[10,21,22] Long amplicon or D2 mixed culture DNA extracts (for HupL and DET1559) were used to generate standard curves for each target to convert R_0 to copies. Primers and annealing temperatures for long amplicons are listed in Table A2.2 and Table A3.1.

4.C.4. Sequencing of qPCR Products.

qPCR products from amplification of DNA from the EW1 and O-BH9-A1 wells were purified using the QIAquick PCR Purification Kit (Qiagen). DNA sequencing was performed

using an Applied Biosystems Automated 3730 DNA Analyzer at the Cornell University Life Sciences Core Laboratories Center.

4.C.5. Proteomic Analysis.

Proteomic Sample Preparation of Samples PM2A2 and EW1.

Various tests were performed on filters PM2A2 and EW1 to determine the most appropriate filter extraction method. Filters were cut in half for two different procedures and subsequently cut into pieces for extraction. Urea (9 M) was added, and the samples were vortexed and sonicated. The cells in the supernatant were lysed via Pressure Cycling Technology (PCT) using a barocylcer (Pressure BioSciences Inc., South Easton, MA). The suspended cells were subjected to 20 seconds of high pressure at 35 kpsi followed by 10 seconds of ambient pressure for 10 cycles. The protein concentration was determined by a Coomassie assay (Thermo Scientific, Rockford, IL) and reduced by adding fresh dithiothreitol (DTT) to a final concentration of 10 mM. Samples were incubated at 60°C for 30 minutes, then diluted 10-fold with NH_4HCO_3 (100 mM, pH 8.4) to reduce the urea concentration. $CaCl_2$ was added to the diluted sample to a final concentration of 1 mM, and the sample was digested for 3 hours at 37°C using sequencing grade trypsin (USB, Santa Clara, CA) at a ratio of 1 unit of trypsin per 50 units of protein (1 unit = ~1 μg of protein). Following incubation, digested samples were desalted using an appropriately sized C-18 SPE column using Discovery C18 (50 mg, 1 mL) solid phase extraction tubes (Supelco, St.Louis, MO), using the following protocol: 3 mL of methanol was added for conditioning followed by 2 mL of 0.1% TFA in H_2O. The samples were then loaded onto each column followed by 4 mL of 95:5 H_2O:ACN, 0.1% TFA. Samples were eluted with 1 mL 80:20 ACN:H_2O, 0.1% TFA. The samples were concentrated down to ~0.1 mL using a Speed Vac (ThermoSavant, Holbrook, NY). The final peptide concentration was determined by

bicinchoninic acid (BCA) assay (Thermo Scientific, Rockford, IL).

Filter Aided Sample Preparation (FASP) was used as an alternative sample preparation method.[23] The second half of the filters had 2 mL UPX buffer (Expedeon, San Diego, CA) added, and were sonicated, vortexed and barocycled as described above and incubated at 95°C for 5 minutes. Amicon Ultra-15 10K MWCO centrifuge devices (Millipore, Billerica, MA) were used for buffer exchange. The sample was added to the filter unit with urea (8 M, pH 8.5) at 15% of the total volume. The unit was centrifuged at 4000 x *g* for 40 minutes (until it reached the dead volume of 200 uL). Another 10 mL of urea (8 M, pH 8.0) was added. The unit was spun at 4000 x *g* for 40 minutes and this was repeated 3 times followed by 3 rinses with NH_4HCO_3 (100 mM, pH 8.0). A BCA assay was used to determine the protein concentration and enough 25mM NH_4HCO_3 was added to the filter unit to cover the filter. The flow-through collection tube was thoroughly cleaned and the sample was tryptically digested in a 1:50 (w/w) ratio with 1 mM CaCl2 and was allowed to incubate overnight at 37°C. The following day the much smaller peptide sample was centrifuged at 4000 x *g* for 30 minutes and the peptides were collected in the flow through. The filter was rinsed with NH_4HCO_3 (25 mM), and the flow-through was pooled. The sample was then cleaned via Strong Cation Exchange (SCX) Solid Phase Extraction (SPE) (Supelco). Each column (100 mg, 1 mL) was conditioned with MeOH, rinsed in varying sequences and amounts with ammonium formate in 25% ACN (10 mM, pH 3.0), ammonium formate in 25% ACN (500 mM), and nanopure water. Samples were acidified to a pH of 4.0 by adding 20% formic acid. Samples were then introduced to the columns and washed with ammonium formate in 25% ACN (10 mM, pH 3.0). Excess liquid was removed from the columns under vacuum. Peptides were eluted with 80:15:5 MeOH:H_2O:NH_4OH and concentrated to ~100 µL using a SpeedVac. Final peptide concentrations were determined using

a BCA protein assay.

Both extraction methods resulted in column contamination so the peptides from both methods were combined and used for offline high pH RP C-18 fractionation to remove contamination (described below).

Proteomic Sample Preparation of Samples O-BH9-A1 and O-BH10-A1.

Frozen filter pieces were crushed and added to a 50-mL falcon tube. Five mL of Universal Protein Extraction (UPX) buffer (Expedeon) was added to each and incubated at 40°C for 2 hours to extract the sample. The solution was pipetted out, barocycled and incubated at 95°C for 5 minutes. FASP was performed as described previously, however the proteins were removed prior to digestion in order to perform a methanol/chloroform extraction to remove large contaminants that are not removed through buffer exchanges. Cold methanol was added at 4 times the sample volume followed by cold chloroform (equal volume to cold methanol) and cold water (3 times the volume of the cold methanol). The samples were then vortexed and centrifuged at 14,000 x *g* for 3 minutes. The upper layer was removed, followed by another addition of cold methanol, and the samples were vortexed, sonicated and spun again to collect the protein pellet. The supernatant was drawn off and the protein pellet was dried lightly under N_2. The sample was urea digested and C18 SPE cleaned as described above.

High pH RP C-18 Fractionation.

Samples were diluted to a volume of 900 µL with ammonium formate buffer (10 mM, pH 10.0), and resolved on a XBridge C18 (250x4.6 mm, 5 µM with 4.6x20 mm guard column, Waters, Milford, MA). Separations were performed at 0.5 mL/min using an Agilent 1100 series HPLC system (Agilent Technologies, Santa Clara, CA) with mobile phases (A) ammonium formate (10 mM, pH 10.0) and (B) 10:90 ammonium formate (10 mM, pH 10.0):acetonitrile.

The gradient was adjusted from 100% A to 95% A over the first 10 min, 95% A to 65% A over minutes 10 to 70, 65% A to 30% A over minutes 70 to 85, maintained at 30% A over minutes 85 to 95, re-equilibrated with 100% A over minutes 95 to 105, and held at 100% A until minute 120. Fractions were collected every 1.25 minutes (96 fractions total). All fractions were dried to half their volume under vacuum, and every five fractions were pooled starting at 40 minutes to ensure the contamination peaks were not collected. The fractions were then completely dried down and 15 µL of ammonium bicarbonate (25 mM) was added to each fraction for storage at -20°C until LC-MS/MS analysis.

2D-LC-MS/MS Analysis.

MS analysis was performed using a LTQ Orbitrap Velos ETD mass spectrometer (Thermo Scientific, San Jose, CA) fitted with a custom electrospray ionization (ESI) interface as described in Chapter 3.

Data Analysis.

MS/MS data was searched as described in Chapter 3. The following genomic data was used in the searches for spectra matches: *Dehalococcoides mccartyi* strains CBDB1 and 195, the KB1-UT metagenomic sequences (DCKB1 at JGI), *Geobacter lovleyi*, *Methanoregula boonei*, *Methanosaeta thermophila*, *Methanospirillum hungatei*, D2 metagenomic sequences (PCEDH *and* PCEOT at JGI), *Spirochaeta thermophila*, *Sporomusa* str. KB1, *Syntrophomonas wolfei*, and *Syntrophus aciditrophicus*. Relative protein quantities of biomarkers in shotgun proteomic samples were estimated by calculating the normalized spectral abundance factor (NSAF).[24] This technique accounts for for biases arising from protein length.[25]

4.D. Results and Discussion

Four monitoring wells (Figure 4.1) were sampled about two years after bioaugmentation

was effected at the site: two with high hydraulic connectivity to the EISB (PM2A2 and EW1) and two with low hydraulic connectivity to the EISB (O-BH09-A1 and O-BH10-A1), based on bromine tracer tests previously conducted by Geosyntec Consultants (Guelph, Ontario, Canada). Monitoring well EW1 is actually an extraction well for the EISB. All four samples came from anaerobic locations with documented TCE contamination and dechlorination activity (Figure 4.2). Degradation of chloroethenes was observed in wells PM2A2 and EW1 starting with electron donor addition in July 2008 (Figure 4.2A-B). After bioaugmentation in October 2009, the rate of degradation rapidly increased and by July 2010 almost all the chloroethenes had been converted to ethene (Figure 4.2A-B). Degradation was observed over this time period in wells O-BH09-A1 and O-BH10-A1, though to a lesser degree (Figure 4.2C-D). The site is known to have a native DMC population (hence the biostimulation prior to bioaugmentation).[26]

4.D.1. Nucleic Acid Results.

As shown in Figure 4.3, the most prevalent DNA biomarkers observed in groundwater samples from the ISSO site were genes for 16S rRNA gene of DMC, VcrA and the 1545 homolog. BvcA, HupL and DET1559 homologs were detected, but at lower levels. TceA was not detected above a detection limit of 100 copies per milliliter of groundwater filtered. A previous study looked at 16S rRNA gene and RDase gene abundances at another bioaugmented, TCE-contaminated field site and found similar results – the 16S rRNA, VcrA and 1545 homolog genes were the most abundant, with BvcA and TceA detected at lower levels.[8] Varying levels of DNA biomarkers are due to the presence of multiple strains of DMC at the ISSO site. The 16S primers used in this study hit all strains of DMC – however, the other biomarkers are not present in all strains.

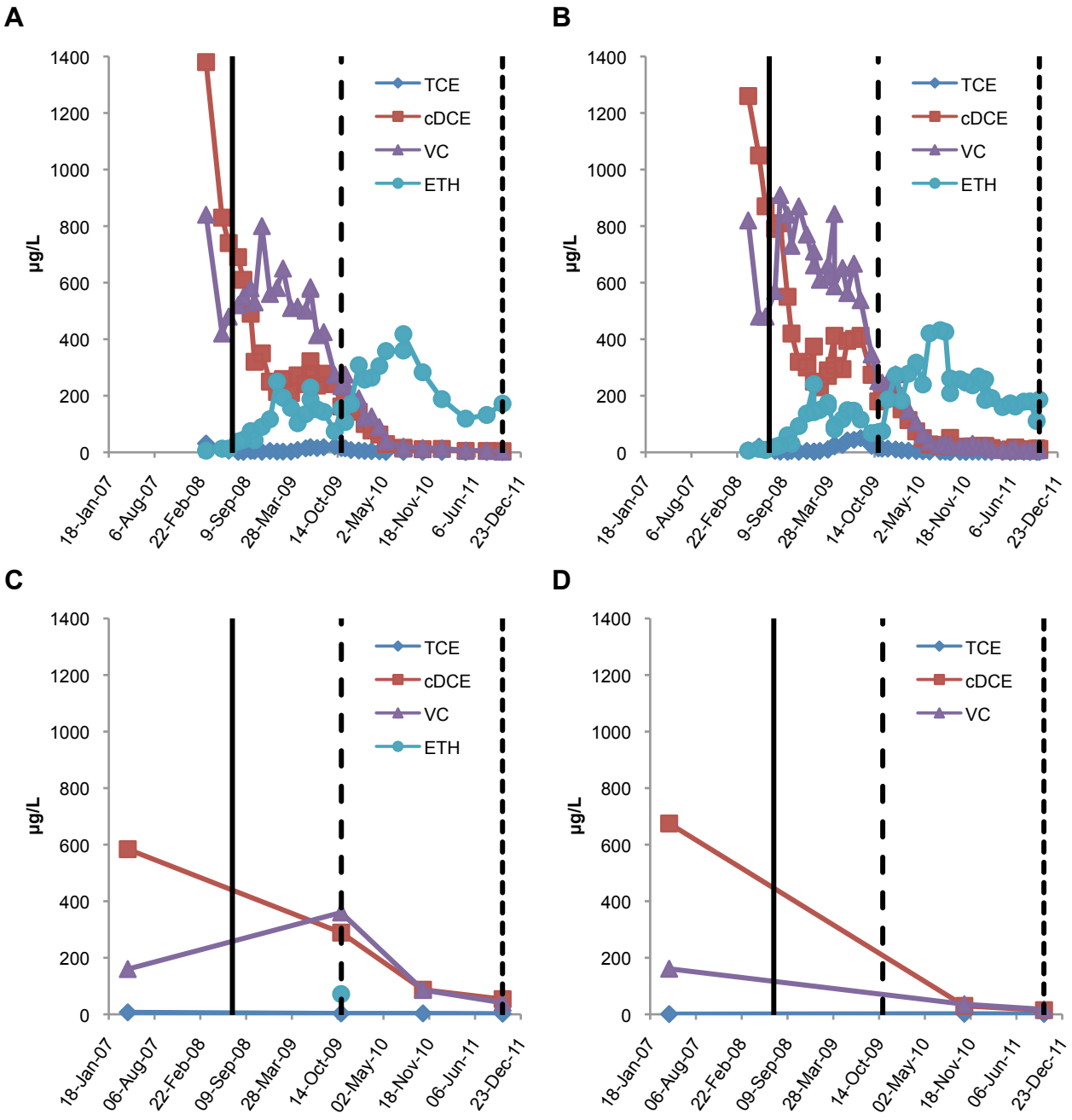

Figure 4. 2. Chlorinated ethene concentrations over time for monitoring well PM2-A2 (A), extraction well EW1 (B), and background wells O-BH9-A1 (C) and O-BH10-A1 (D) at an industrial site in southwestern Ontario, Canada. Electron donor addition began in July 2008 (solid vertical line) and bioaugmentation with KB-1 occurred in October 2009 (dashed vertical line). Samples were collected for nucleic acid and proteomic analysis in October 2011 (dotted line). Note that ethene was not analyzed in well O-BH10-A1.

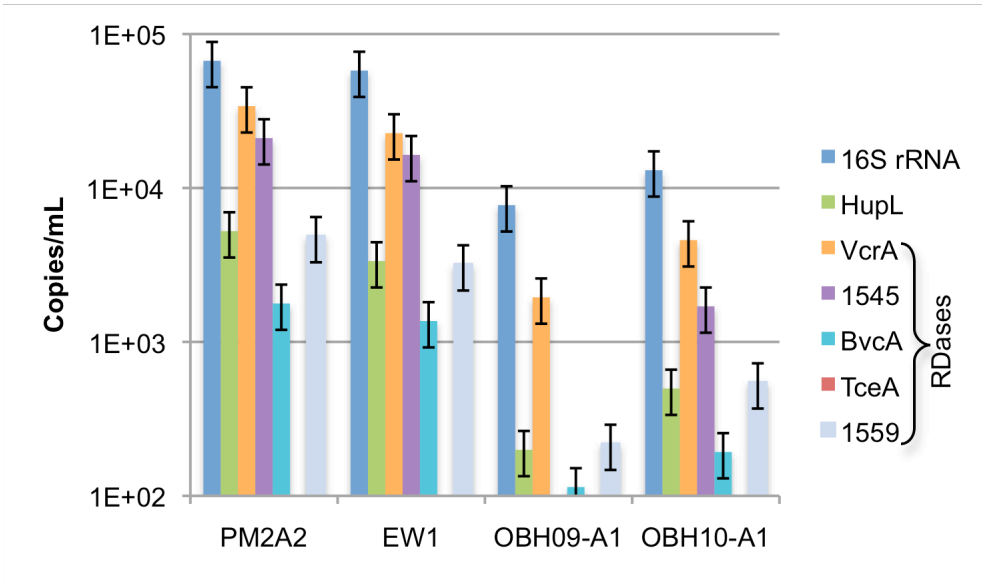

Figure 4. 3. DNA biomarkers detected in filtered groundwater collected from monitoring and extraction wells at an industrial site in southwestern Ontario, Canada. The data in this figure are from DNA extracted off the filters (as opposed to the pre-filters). The detection limit is approximately 100 copies/mL. Error bars represent average standard deviations of replicate samples (n=3-6) of 10-20 experimental groups.

The 1545 primers used in this study hit all strains of DMC with the 1545 homolog (DMC195, VS, CBDB1, GT, FL2 and BAV1, in which the gene is interrupted) and the KB-1 mixed culture – they do not hit any RDase from strain MB (which produces *trans*-DCE rather than *cis*-DCE).[27] In contrast, the HupL forward primer is specific for DMC195 (one mismatch at the last nucleotide when compared to CBDB1, GT, BAV1 and KB-1), and the reverse primer is specific for DMC195 and strain VS (two mismatches in the middle when compared to other strains). The specificity of the HupL primers used likely explains the low levels of HupL observed (Figure 4.3). BLASTs of the sequenced qPCR products showed that the expected qPCR products were produced with the VcrA and 1545 primers for both wells and for TceA primers for the O-BH9-A1 well, but that the expected qPCR products were not produced with the HupL primers.

RNA was successfully recovered in samples from monitoring wells EW1 and PM2A2.

Both the filter and the pre-filter were extracted, and RNA was detected in both samples (Table 4.1). The RNA extracted from wells O-BH9-A1 and O-BH10-A1 was either degraded or below quantification limits, and could not be analyzed further. Before qPCR analysis could be performed, the tube containing cDNA from well PM2A2's filter was lost. Consequently, results could only be provided for the cDNA from the pre-filter of this well. However, strong correlations were observed between the filter and pre-filter samples for both DNA from wells PM2A2 and EW1 (Figure 4.4A) and cDNA from well EW1 (Figure 4.4B) with R^2 values of 0.95 and 0.98, respectively, and results suggest that approximately one third of the DMC (<0.5 µm in diameter) are being retained on the 1.2 µm pore size pre-filters.

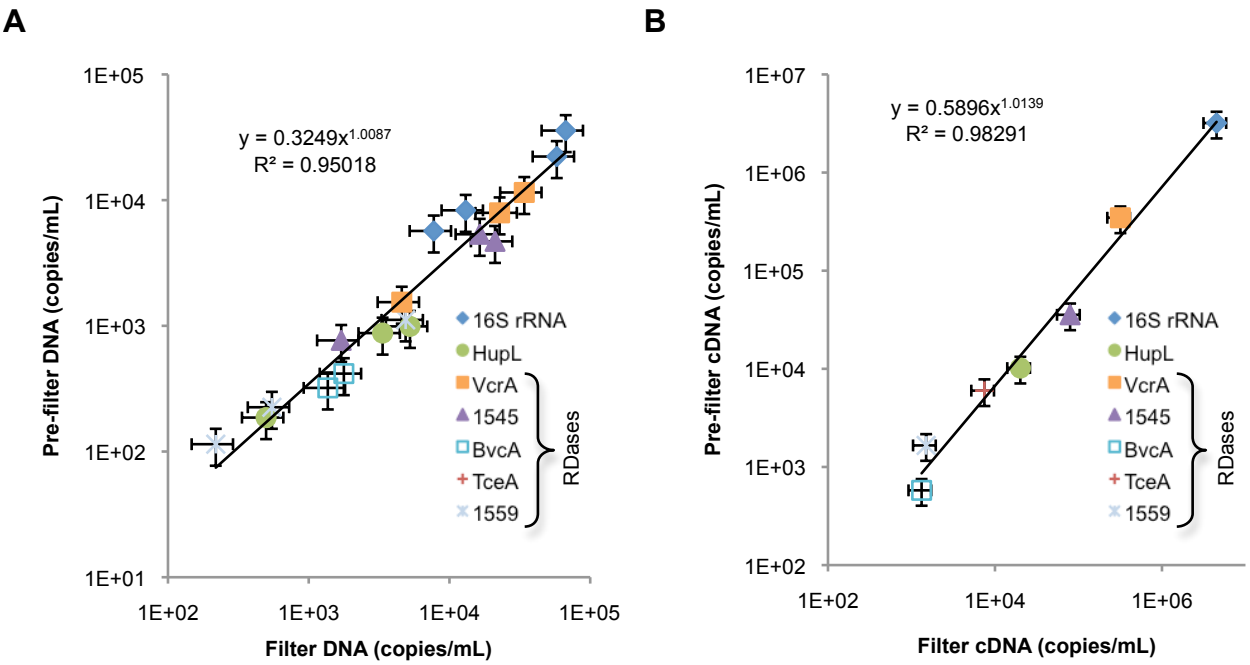

Figure 4. 4. Correlation of copies per mL on the filter to the pre-filter for DNA (A) and cDNA (B) for detected biomarkers. Points are colored by qPCR target. Error bars represent average standard deviations of replicate samples.

As shown in Figure 4.5, the most prevalent RNA biomarkers observed in ground water samples for the ISSO site 16S rRNA, VcrA and the 1545-homolog. BvcA, HupL, TceA and DET1559 homologs were detected, but at lower levels. These trends follow closely with those observed for DNA. However the difference in order of magnitude was larger for cDNA than for

DNA. As shown in Figure 4.6, cDNA copies per DNA copy ranged from approximately 200 for 16S rRNA down to 0.5 for the DET1559 homolog (TceA was not detected). These ratios are similar to those found at another bioaugmented, TCE-contaminated field site and actively growing lab cultures.[8,16]

4.D.2. Proteomic Results.

Comparison of Field Proteome to Lab Proteome.

A total of 507, 298, 1779 and 871 proteins were detected in the PM2A2, EW1, O-BH9-A1 and O-BH10-A1 samples, respectively, as compared to 3911 in the KB-1^{TM} culture sample. These lower numbers are likely due to the complexity of the field samples (both phylogenetic complexity and geochemical complexity) and an insufficient metagenomic database for the soil microbial community. Surprisingly, higher total numbers of proteins were detected in the O-BH9-A1 and O-BH10-A1 samples as compared to the PM2A2 and EW1 samples, despite an order of magnitude lower total populations of DMC (~1 x 10^4 DMC/mL versus 1 x 10^5 DMC/mL). As discussed in the Materials and Methods section, the protein extraction methods for these sets of samples differed due to issues originally encountered with the PM2A2 and EW1 samples as a result of precipitated minerals in these samples. Therefore, it is possible that material was lost in the extraction and digestion processes for those two samples (See Table 4.1 for total material extracted). The low DMC protein count may also be due to its relative (not just absolute) population density. Many other phylogenetic groups are stimulated during EISB.

Of the 1596 proteins detected in the field samples, but not in the KB-1^{TM} culture sample, 392 were identified as part of the KB-1 metagenome (Table A3.2). However, only 133 out of 392 were detected in more than one sample or had spectral counts greater than one. The remaining peptides not detected in the KB-1^{TM} culture sample, but identified as part of the KB-1

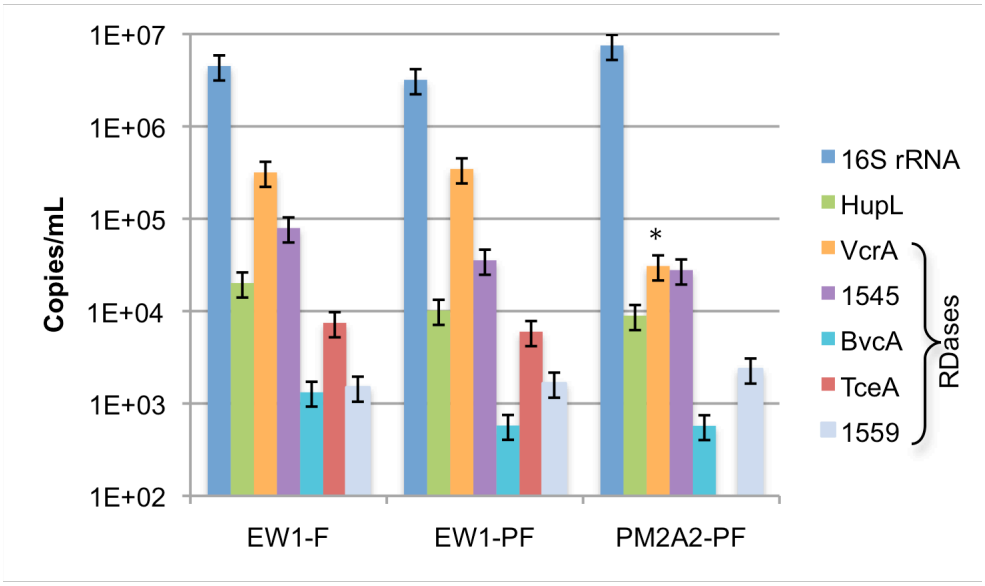

Figure 4. 5. cDNA biomarkers detected in groundwater collected from monitoring and extraction wells at the ISSO site in southwestern Ontario, Canada. The detection limit is approximately 100 copies/mL. Error bars represent average standard deviations of replicate samples. The star indicates that the efficiency of the VcrA sample for PM2A2-PF was outside the accepted range of 0.8-1.2, and that the value may be erring low.

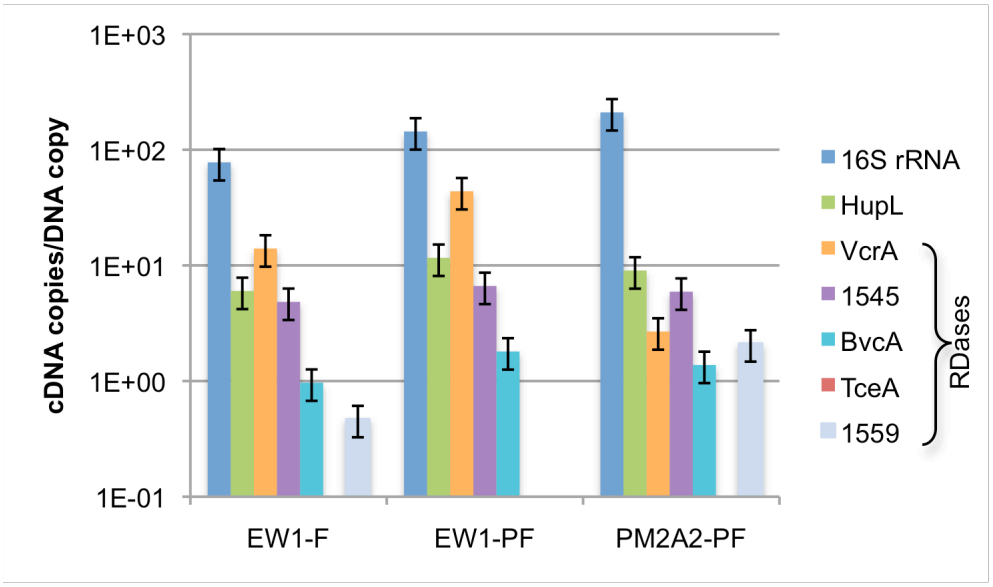

Figure 4. 6. cDNA copies per DNA copy for detected biomarkers in the PM2A2 and EW1 groundwater samples. Error bars represent average standard deviations of replicate samples.

metagenome were identified as belonging to DMC (179), *Geobacter* (40), or other KB-1 community members, methanogens, fermenters or spirochaetes (985). Figure 4.7 presents how the detected proteins overlap among the samples. 78 total proteins were detected in all five

samples (Table A3.3). These include VcrA and the 1545 homolog from DMC, and several ATP synthases and methyl-accepting chemotaxis proteins from various phylogenetic groups.

Biomarker comparison.

As with the DNA results, the most prevalent proteomic biomarkers detected in the field samples were VcrA and 1545 for all samples with the exception of O-BH9-A1, where PceA from

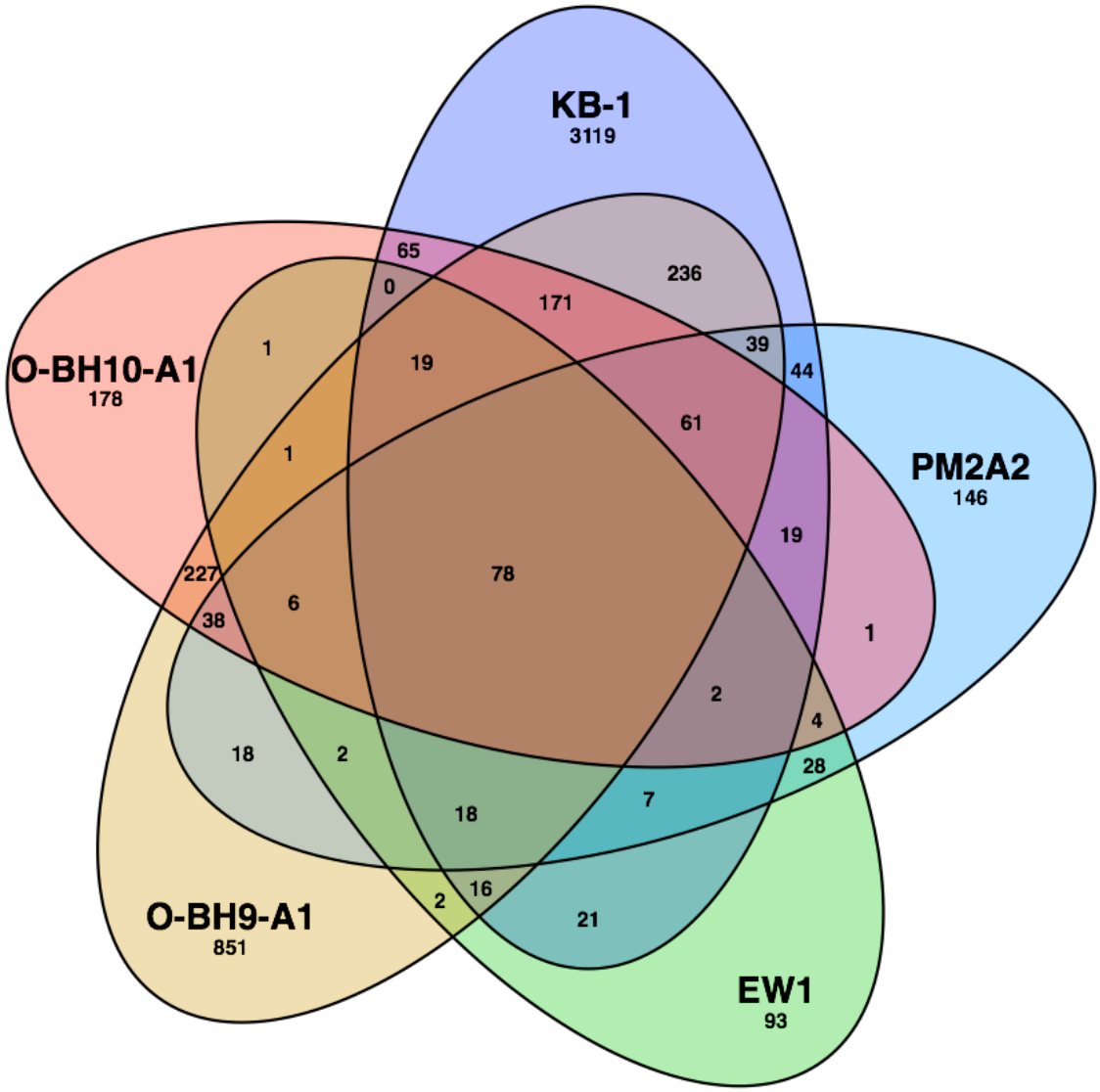

Figure 4. 7. Overlap of detected proteins in the KB-1 mixed culture and the PM2A2, EW1, O-BH9-A1 and O-BH10-A1 field samples. Numbers indicate the number proteins detected. The databases searched include multiple phylogenies beyond *Dehalococcoides*, including methanogens, fermenters, *Geobacter* and other community member. This figure was generated from a template devised by Branko Gruenbaum and rendered by CMG Lee that is licensed under the Creative Commons Attribution-Share Alike 3.0 Unported license.

Geobacter was the highest detected respiratory biomarker (Table 4.2). Figure 4.8 presents how those 15 biomarkers (RDases and HupL) were distributed among the samples. Nine RDases were found only in the KB-1 metaproteome sample and only two (VcrA and the 1545 homolog) were found in all the samples. The VcrA and 1545 homologs were strongly detected in the samples collected within the EISB. However, in wells O-BH9-A1 and O-BH10-A1, a greater number of RDases were detected, and their NSAF scores were more evenly distributed (Table 4.2). The Ni-Fe hydrogenase, HupL, was detected in all samples with the exception of PM2A2, where its NSAF was less than 1.6×10^{-4}. BvcA was strongly detected in the KB-1^{TM}, O-BH9-A1 and O-BH10-A1, samples but not detected in PM2A2 or EW1. The *Geobacter* RDase PceA and the KB1_1 RDase were detected only in the KB-1^{TM} mixed culture and sample O-BH9-A1. Though the *Geobacter* RDase was not detected in all samples, *Geobacter* proteins were (Table A3.4). It is surprising that the *Geobacter* RDase was strongly detected in field sample O-BH9-A1. As seen in Figure 4.2, all four wells have had very low levels of TCE since before the EISB was installed. Consequently, *Geobacter* would presumably not have been actively degrading TCE. Alternatively, localized TCE concentrations could be higher than the groundwater sampling concentrations suggest. Seven of the detected proteins were detected in all samples (Table A3.4). Isocitrate dehydrogenase (Glov_1624) was detected in all four field samples, as well as the KB-1^{TM} sample, and citrate synthase (Glov_1379) was detected in all samples with the exception of O-BH10-A1. The detection of these proteins are important because they have previously been detected in a field proteome study[25], and citrate synthase has been identified as a biomarker of *Geobacter* activity.[28] Additionaly, several oxidoreductases were detected in the proteomic samples: 9 were detected in the KB-1^{TM} sample, 2 of these were detected in all samples except for O-BH10-A1, and 1 in both KB-1^{TM} and EW1 (Table A3.4).

Table 4. 2. Detected Biomarkers in Shotgun Field Samples Compared to the KB-1™ Metaproteome Sample. The NSAF is a sum of NSAF's for all detected homologs.

	NSAF x 10^5				
		Inside EISB		Outside EISB	
Homolog	**KB-1™**	PM2A2	EW1	O-BH9-A1	O-BH10-A1
VcrA	4723	2825	2624	384	516
1545-homolog	4684	382	488	155	140
HupL	959	<16	76	107	197
BvcA	923	<16	<31	105	68
KB1_8, KB1_9	66	<16	<31	<2.6	<7.1
DET0180	62	<16	<31	<2.6	<7.1
KB1_1	57	<16	<31	54	<7.1
TceA	49	<16	<31	<2.6	<7.1
KB1_1549	13	<16	<31	<2.6	<7.1
DET1528	8.4	<16	<31	<2.6	<7.1
KB1_7	7.7	<16	<31	<2.6	<7.1
DET1519	2.2	<16	<31	<2.6	<7.1
DET1538	1.1	<16	<31	<2.6	<7.1
cbdbA80	1.1	<16	<31	<2.6	<7.1
Geobacter PceA	94	<16	<31	537	<7.1

*The detection limit is based on the lowest NSAF for that sample (i.e. if a protein's peptides were only found in one spectra in the whole spectral library).

Strain-Resolution Using Metaproteome Results.

As discussed in Chapter 2, regions of strain variation for the 1545 homolog were observed in the peptides detected for the KB-1™ mixed culture. One 1545 homolog peptide was detected in each of the PM2A2, EW1 and O-BH10-A1 field samples and two were detected in the O-BH9-A1 field sample. These peptides were also detected in the KB-1™ mixed culture sample. The detected peptides did not allow for strain identification (Cornell, VS or Pinellas subgroups) as the PM2A2 peptide and one of the O-BH9-A1 peptides aligned with all three groups and the EW1, O-BH10-A1, and remaining O-BH9-A1 peptides aligned with the Cornell and Pinellas subgroups (Figure 4.9).

With regards to strain variation, the HupL biomarker is also also informative. Although it is highly conserved among DMC strains (91% identity between DMC195 and strain VS, 89%

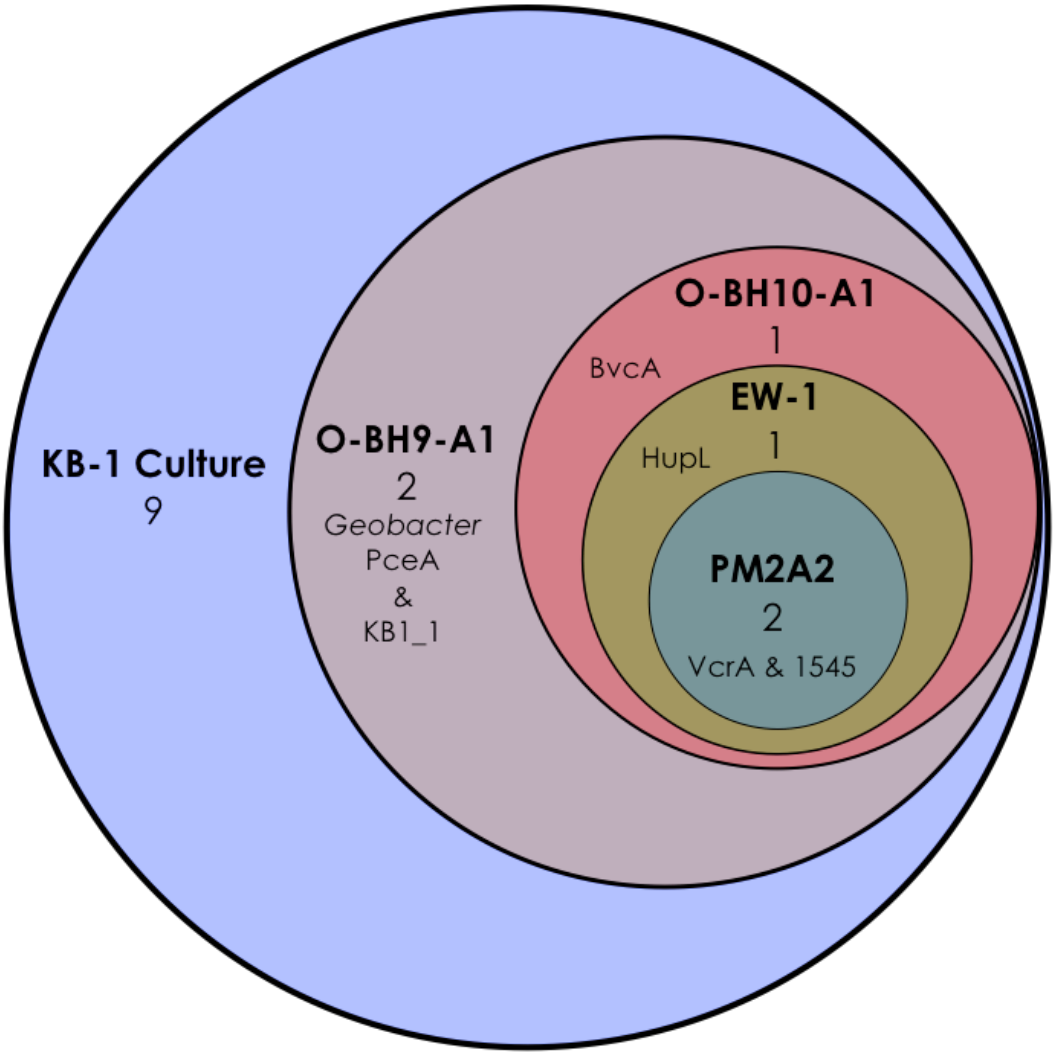

Figure 4. 8. Overlap of detected DHC and *Geobacter* reductive dehalogenase, and HupL proteins in the KB-1 mixed culture and the PM2A2, EW1, O-BH9-A1 and O-BH10-A1 field samples. Numbers indicate the quantity of unique proteins detected.

identity between DMC195 and strains GT, BAV1 and CBDB1, as determined by BLAST), some of the detected peptides are unique to specific DMC subgroups. Of the 74 HupL peptides that were detected in the KB-1^{TM} culture, 14 peptides hit DMC195 alone, 28 peptides align with all five strains, five peptides align with the Pinellas group (CBDB1, GT and BAV1) but not DMC195 and VS, and thirteen peptides align with VS, CBDB1, GT and BAV1 but not DMC195 (Table A3.5). Consequently, DMC strains in KB-1^{TM} could be differentiated by virtue of slight differences in the HupL homologs' peptides. Consensus peptides were generated from

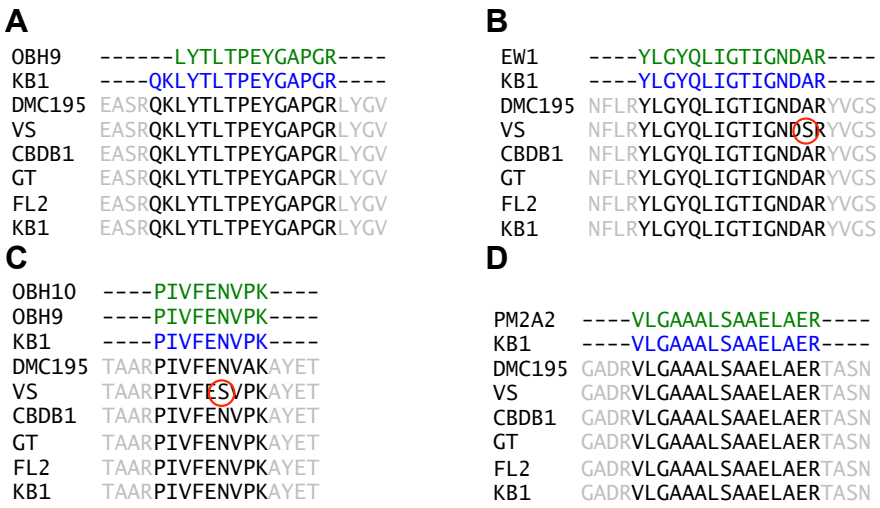

Figure 4. 9. Four regions of the 1545-homolog where peptides were detected in the field samples (green) as compared to peptides detected in the KB-1™ mixed culture sample (blue). Six homologs from DMC genomes and the KB-1 metagenome are shown in black. The amino acids that differ are circled in red if they match the DMC195 sequence and in blue if they match the remaining sequences. Panel A represents region F, Panel B represents region B, Panel C represents region D, and Panel D represents region G in Figure 3.5 .

alignments of detected peptides with available full homolog sequences (Table 4.3). Seven regions of the HupL sequence had strain specificity in the detected peptides (red boxes A-G in Figure 4.10). Four regions were found to be highly conserved (blue boxes H-K in Figure 4.10) and contained multiple detected peptides that aligned with strains from all groups (Cornell, VS and Pinellas). Four HupL peptides were detected in each of the O-BH9-A1 and O-BH10-A1 field samples. These peptides were also detected in the KB-1™ mixed culture sample. One peptide did not allow for strain identification (Cornell, VS or Pinellas subgroups) as it aligned with all strains (Figure 11A) The other three peptides, however, did allow for strain differentiation. The "DGQGVYGPVEQALIGTK" peptide (Figure 11B) aligned with the Pinellas group and not the Cornell or VS groups. The "YENTPYEVGPLAR" and "LAHELSAIYSGR" peptides (Figure 11C-D) aligned with the VS and Pinellas groups, but not the Cornell group. Additionally, it is interesting to note that the peptides detected in the KB-1™ mixed culture in Figure 11B-C both aligned with the Cornell group.

Table 4. 3. Consensus HupL Homolog Peptides Detected in Shotgun KB-1™ Sample. Peptides are highlighted based on their specificity the Cornell group (green) or the Pinellas group (orange), and peptides highlighted in blue are highly conserved.

Peptide Numbers	Consensus Sequence	Spectral Count	Cornell Group	Victoria Group	Pinellas Group			KB1-UT Mixed Culture
			DMC195	VS	CBDB1	GT	BAV1	
15,16,65	VRDNDNPFELVRIV	75	X	X	X	X	X	X
24,27	GVYGPVEQALIGTK	35	X		X	X	X*	X
12,30	ISNYQCVVPTTWNCSPKDGQGVYGPV EQALIGTK	11	X	X		X		
17	DNQGVYGPVEQALIGTK	2	X					
29	IGEPVIADYEIPETAEGMGLWEAPR	9	X					
45,46,51,52,53,74	MVVNYVSGDPLVQQMVNDTLSHFGA GPAALFSTLGR	28	X					
3,20,21	FGAGPAALFSTLGR	43	X	X	X	X	X	X
38,39,40,41,42,43,44, 62,63	MVNDTLAHFGAGPAALFSTLGR	180				X	X	X
47,48,49,50,61,64,73	MVVNYVAGDPVVQKMVN	31		X	X	X	X	X
10,59,72	APRYENTPYEVGPLAR	26		X	X	X	X	X
70	YDGTPYEVGPLAR	6	X					
22	GDTTEYPLNEVTEPEFTK	2	X					
58	TFDPSKITESIK	1	X					
26,36	LFTQGVVSASDLAHR	9	X					
35	LFTQGTVSASDLTLH	15			X	X	X	X
14	DLEASGTNLATR	1	X					
13,25,57	SYGVFDLEANGTNLATR	12		X	X	X	X	X
23,56,66,67,68,69	SVAVVAGGVTSHPSIDSISSFMSK	32			X	X	X	X
34	LAHELSAIYSGR	17		X	X	X	X	X
33	KVAQAAVAH	9	X	X	X	X	X	X
2,4,5,6,7,8,71	ALAAGDMSMLAPFYPRYEGDYRLPK	34	X	X	X	X	X	X
18,19,60	ALDYVDVTEVADYDGTDPELLK	4	X	X	X	X	X	X
9	ALDYVDVTEVADYDGTDPELLK	9	X		X	X	X	X
54,55	NLIQGANYIASH	4	X	X	X	X	X	X
1	AAFGVADKIPNNGR	2			X	X	X	X
11	DAVHITQR	5	X	X	X	X	X	X
28	IEATVDGGEVKDAK	1	X	X	X	X	X	X
31,32,37	MQKIVIDPITRIE	22	X	X	X	X	X	X

*One peptide doesn't hit BAV1

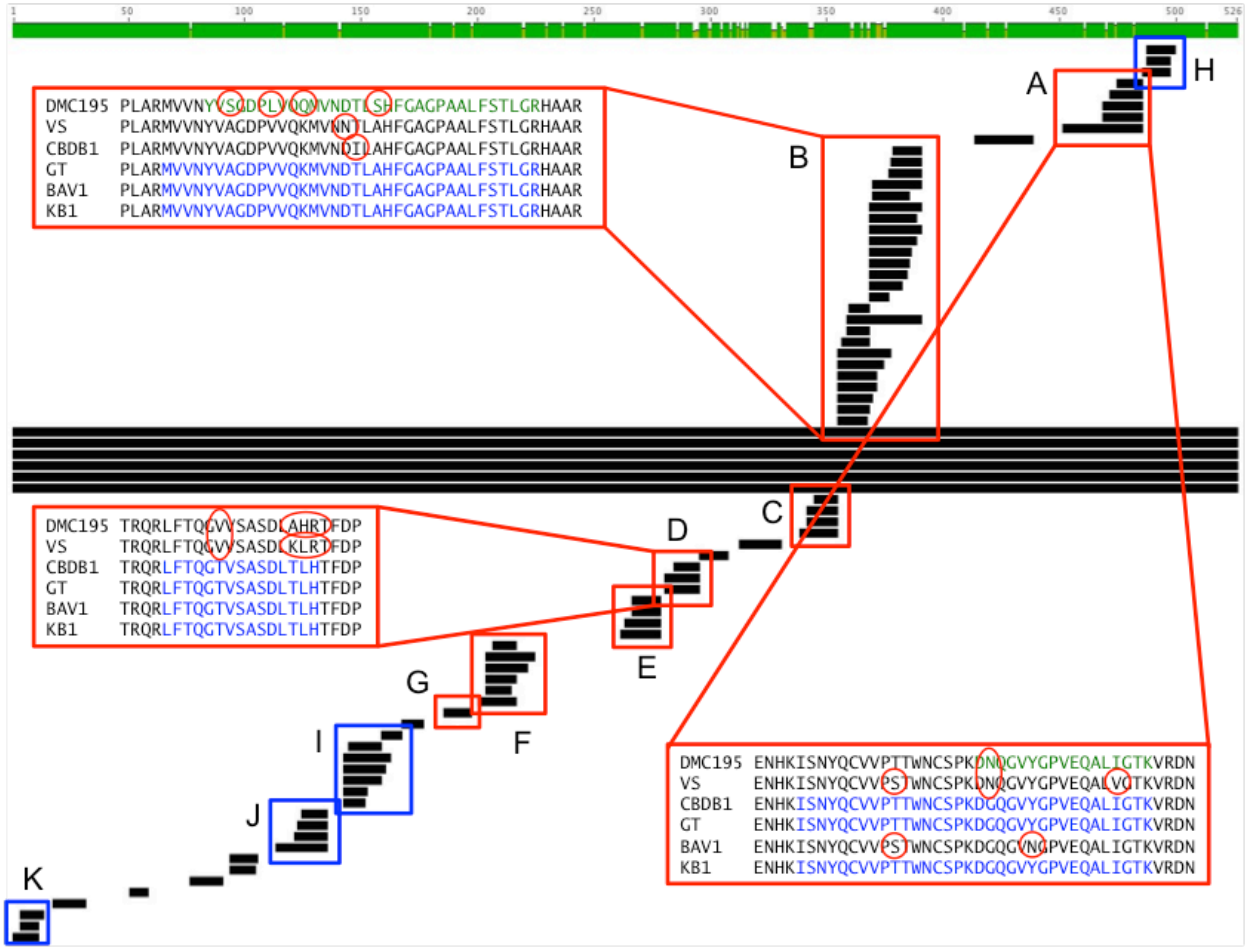

Figure 4. 10. A comparison of HupL-homolog peptides detected in the KB-1 culture sample to the HupL-homolog sequences of DMC195, DMC strains VS, CBDB1, GT, BAV1 and the KB-1 mixed culture. Peptides boxed in red (A-G) show strain specificity, whereas peptides boxed in blue (H-K) are highly conserved and align across all strains. Consensus peptides are highlighted in blue, and variations that were detected are highlighted in green, with the differences circled in red. The consensus sequence is the combined sequence of all detected peptides that align with a strain. This figure was created using Geneious version 5.0.4 created by Biomatters.

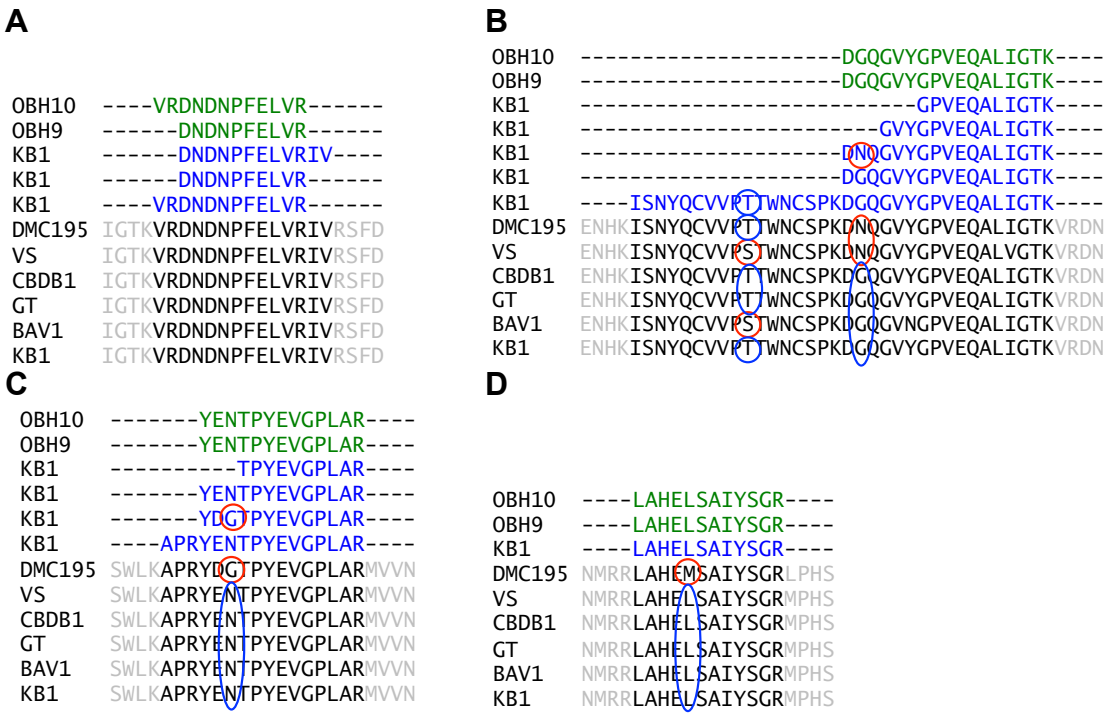

Figure 4. 11. Four regions of the HupL-homolog where peptides were detected in the O-BH9-A1 and O-BH10-A1 field samples (green) as compared to the KB-1 mixed culture sample (blue). The amino acids that differ are circled in red if they match the DMC195 sequence and in blue if they match the remaining sequences. Panel A represents region G in Figure 4.10, and Panel B represents region A in Figure 4.10, Panel C represents region C in Figure 4.10, and Panel D represents region H in Figure 4.10.

The key results of this study are that DMC proteins can be detected in field samples, and that the detected RDases are a subset of those present in the KB-1^{TM} mixed culture that was used to bioaugment the site. Additionally, the most highly detected biomarkers were the same across the board for DNA, RNA and protein (VcrA and the 1545 homolog). However, the advantage that can be seen for proteomic analysis of field samples is for strain differentiation, which could be used to track changes in microbial community composition. Strain differentiation is possible with qPCR of nucleic acids, though multiple primer sets are necessary for each target and "cross-talk" must be carefully considered. Ultimately, a quantitative proteomic biomarker method is the goal. This is the first report of proteomic data from EISB sites undergoing chloroethene

bioremediation and even extends to native populations in nearby wells outside the active EISB zone.

4.E. Acknowledgements

This project was supported by the National Science Foundation (NSF) CBET Program (CBET-0731169). Culture used in this research was provided by Philip C. Dennis at SiREM Laboratories in Guelph, Ontario, Canada. Groundwater samples were provided by Geosyntec Consultants in Guelph, Ontario, Canada. Portions of this research were performed at the Environmental Molecular Sciences Laboratory (EMSL), a DOE/BER national scientific user facility located at Pacific Northwest National Laboratory (PNNL) in Richland, Washington. PNNL is a multi-program national laboratory operated by Battelle for the DOE under Contract DE-ACO5-76RLO 1830.

REFERENCES

(1) Loffler, F. E.; Yan, J.; Ritalahti, K. M.; Adrian, L.; Edwards, E. A.; Konstantinidis, K. T.; Muller, J. A.; Fullerton, H.; Zinder, S. H.; Spormann, A. M. *Dehalococcoides mccartyi* gen. nov., sp. nov., obligate organohalide-respiring anaerobic bacteria, relevant to halogen cycling and bioremediation, belong to a novel bacterial class, Dehalococcoidetes classis nov., within the phylum Chloroflexi. *Int. J. Syst. Evol. Micr.* **2012**.

(2) Hendrickson, E. R.; Payne, J. A.; Young, R. M.; Starr, M. G.; Perry, M. P.; Fahnestock, S.; Ellis, D. E.; Ebersole, R. C. Molecular analysis of *Dehalococcoides* 16S ribosomal DNA from chloroethene-contaminated sites throughout North America and Europe. *Appl. Environ. Microb.* **2002**, *68*, 485–495.

(3) Lovley, D. R. Cleaning up with genomics: applying molecular biology to bioremediation. *Nat Rev Micro* **2003**, *1*, 35–44.

(4) Lu, X.; Wilson, J. T.; Kampbell, D. H. Relationship between *Dehalococcoides* DNA in ground water and rates of reductive dechlorination at field scale. *Water Res.* **2006**, *40*, 3131–3140.

(5) Scheutz, C.; Durant, N.; Dennis, P.; Hansen, M. H.; Jorgensen, T.; Jakobsen, R.; Bjerg, P. L. Concurrent ethene generation and growth of *Dehalococcoides* containing vinyl chloride reductive dehalogenase genes during an enhanced reductive dechlorination field demonstration. *Environ. Sci. Technol* **2008**, *42*, 9302–9309.

(6) Tas, N.; Van Eekert, M. H. .; De Vos, W. M.; Smidt, H. The little bacteria that can–diversity, genomics and ecophysiology of *Dehalococcoides* spp. in contaminated environments. *Microbial Biotechnology*.

(7) Rahm, B. G.; Richardson, R. E. Gene Transcripts As Quantitative Bioindicators of Tetrachloroethene, Trichloroethene, and cis-1,2-Dichloroethene Dehalorespiration Rates. *Environ. Sci. Technol.* **2008**, *42*, 5099–5105.

(8) Lee, P. K. H.; Macbeth, T. W.; Sorenson, K. S.; Deeb, R. A.; Alvarez-Cohen, L. Quantifying Genes and Transcripts To Assess the In Situ Physiology of *Dehalococcoides* spp. in a Trichloroethene-Contaminated Groundwater Site. *Appl. Environ. Microb.* **2008**, *74*, 2728–2739.

(9) Rahm, B. G.; Morris, R. M.; Richardson, R. E. Temporal Expression of Respiratory Genes in an Enrichment Culture Containing *Dehalococcoides ethenogenes*. *Appl. Environ. Microb.* **2006**, *72*, 5486–5491.

(10) Rahm, B. G.; Richardson, R. E. Correlation of respiratory gene expression levels and pseudo-steady-state PCE respiration rates in *Dehalococcoides ethenogenes*. *Environ. Sci. Technol.* **2008**, *42*, 416–421.

(11) Waller, A. S.; Krajmalnik-Brown, R.; Loffler, F. E.; Edwards, E. A. Multiple Reductive-Dehalogenase-Homologous Genes Are Simultaneously Transcribed during Dechlorination by *Dehalococcoides*-Containing Cultures. *Appl. Environ. Microb.* **2005**, *71*, 8257–8264.

(12) Behrens, S.; Azizian, M. F.; McMurdie, P. J.; Sabalowsky, A.; Dolan, M. E.; Semprini, L.; Spormann, A. M. Monitoring abundance and expression of *Dehalococcoides* species chloroethene-reductive dehalogenases in a tetrachloroethene-dechlorinating flow column. *Appl. Environ. Microb.* **2008**, *74*, 5695–5703.

(13) Fung, J. M.; Morris, R. M.; Adrian, L.; Zinder, S. H. Expression of Reductive Dehalogenase Genes in *Dehalococcoides ethenogenes* Strain 195 Growing on Tetrachloroethene, Trichloroethene, or 2,3-Dichlorophenol. *Appl. Environ. Microb.* **2007**, *73*, 4439–4445.
(14) Johnson, D. R.; Lee, P. K. H.; Holmes, V. F.; Fortin, A. C.; Alvarez-Cohen, L. Transcriptional expression of the tceA gene in a *Dehalococcoides*-containing microbial enrichment. *Appl. Environ. Microb.* **2005**, *71*, 7145.
(15) Johnson, D. R.; Lee, P. K. H.; Holmes, V. F.; Alvarez-Cohen, L. An internal reference technique for accurately quantifying specific mRNAs by real-time PCR with application to the tceA reductive dehalogenase gene. *Appl. Environ. Microb.* **2005**, *71*, 3866.
(16) Rowe, A. R.; Heavner, G. L.; Mansfeldt, C. B.; Werner, J. J.; Richardson, R. E. Relating Chloroethene Respiration Rates in *Dehalococcoides* to Protein and mRNA Biomarkers. *Environ. Sci. Technol.* **2012**, *46*, 9388–9397.
(17) Morris, R.; Sowell, S.; Barofsky, D.; Zinder, S.; Richardson, R. Transcription and mass-spectroscopic proteomic studies of electron transport oxidoreductases in *Dehalococcoides ethenogenes*. *Environ. Microbiol.* **2006**, *8*, 1499–1509.
(18) Morris, R. M.; Fung, J. M.; Rahm, B. G.; Zhang, S.; Freedman, D. L.; Zinder, S. H.; Richardson, R. E. Comparative Proteomics of *Dehalococcoides* spp. Reveals Strain-Specific Peptides Associated with Activity. *Appl. Environ. Microb.* **2007**, *73*, 320–326.
(19) Werner, J. J.; Ptak, A. C.; Rahm, B. G.; Zhang, S.; Richardson, R. E. Absolute quantification of *Dehalococcoides* proteins: enzyme bioindicators of chlorinated ethene dehalorespiration. *Environmental Microbiology* **2009**, *11*, 2687–2697.
(20) Mundle, S. O. C.; Johnson, T.; Lacrampe-Couloume, G.; Pérez-de-Mora, A.; Duhamel, M.; Edwards, E. A.; McMaster, M. L.; Cox, E.; Révész, K.; Sherwood Lollar, B. Monitoring Biodegradation of Ethene and Bioremediation of Chlorinated Ethenes at a Contaminated Site Using Compound-Specific Isotope Analysis (CSIA). *Environ. Sci. Technol.* **2012**, *46*, 1731–1738.
(21) Peirson, S. N.; Butler, J. N.; Foster, R. G. Experimental validation of novel and conventional approaches to quantitative real-time PCR data analysis. *Nucleic Acids Res.* **2003**, *31*, 1–7.
(22) Schefe, J. H.; Lehmann, K. E.; Buschmann, I. R.; Unger, T.; Funke-Kaiser, H. Quantitative real-time RT-PCR data analysis: current concepts and the novel "gene expression's C T difference" formula. *J. Mol. Med.* **2006**, *84*, 901–910.
(23) Wiśniewski, J. R.; Zougman, A.; Nagaraj, N.; Mann, M. Universal sample preparation method for proteome analysis. *Nature Methods* **2009**, *6*, 359–362.
(24) Zybailov, B.; Mosley, A. L.; Sardiu, M. E.; Coleman, M. K.; Florens, L.; Washburn, M. P. Statistical Analysis of Membrane Proteome Expression Changes in *Saccharomyces cerevisiae*. *Journal of Proteome Research* **2006**, *5*, 2339–2347.
(25) Wilkins, M. J.; VerBerkmoes, N. C.; Williams, K. H.; Callister, S. J.; Mouser, P. J.; Elifantz, H.; N'Guessan, A. L.; Thomas, B. C.; Nicora, C. D.; Shah, M. B.; Abraham, P.; Lipton, M. S.; Lovley, D. R.; Hettich, R. L.; Long, P. E.; Banfield, J. F. Proteogenomic Monitoring of *Geobacter* Physiology during Stimulated Uranium Bioremediation. *Appl. Environ. Microb.* **2009**, *75*, 6591–6599.

(26) Zila, A. A Molecular Study of Field Bioaugmentation Using the KB-1® Mixed Microbial Consortium: The Application of Real-Time PCR in Analyzing Population Dynamics. Master of Engineering, University of Toronto: Toronto, Ontario, Canada, 2011.
(27) Cheng, D.; He, J. Z. Isolation and Characterization of *Dehalococcoides* sp Strain MB, Which Dechlorinates Tetrachloroethene to trans-1,2-Dichloroethene. *Appl. Environ. Microb.* **2009**, *75*, 5910–5918.
(28) Wilkins, M. J.; Callister, S. J.; Miletto, M.; Williams, K. H.; Nicora, C. D.; Lovley, D. R.; Long, P. E.; Lipton, M. S. Development of a biomarker for *Geobacter* activity and strain composition; Proteogenomic analysis of the citrate synthase protein during bioremediation of U(VI). *Microbial Biotechnology* **2011**, *4*, 55–63.

CHAPTER 5

Summary and Future Directions

5.A. Summary of Research Objectives

The main objective of this study was to test DNA, mRNA and protein as specific and robust biomarkers of anaerobic reductive dechlorination by *Dehalococcoides* strains in predictive modeling, with mixed microbial cultures, and at a field site. The specific objectives undertaken, as given in Chapter 1, to achieve this were:

1) Develop a mechanistic model of the D2 mixed community based on species-specific molecular biological data (DNA and RNA) that also incorporated competitive inhibition.
2) Develop robust empirical relationships between mRNA levels and instantaneous respiration rates in different DMC-containing mixed cultures (D2 and KB-1). This was expected to provide a suite of robust biomarkers of reductive dechlorination that target multiple strains of DMC.
3) Detect field proteomes for DMC (which had not yet been successfully done) and make a comparison of DNA, mRNA and protein biomarker detection in samples from a TCE-contaminated site in Ft. Erie, Canada.

5.B. Summary of Biokinetic Model Development

A comprehensive biokinetic model of a community containing *Dehalococcoides mccartyi* was updated to describe continuously fed reactors with specific biomass levels based on quantitative PCR (qPCR)-based population data (DNA and RNA). The model was calibrated and validated with subsets of chemical and molecular biological data from various continuous feed experiments (n=24) with different loading rates of the electron acceptor (1.5 to 482 μeeq/L-h),

types of electron acceptor [tetrachloroethene (PCE), trichloroethene (TCE), *cis*-dichloroethene (*cis*-DCE)] and electron donor to electron acceptor ratios.

The resulting model predicted the sum of dechlorination products vinyl chloride (VC) and ethene well. However, VC alone was under-predicted and ethene was over-predicted. Consequently, competitive inhibition among chlorinated ethenes was examined and then added to the model. Additionally, as 16S rRNA gene copy numbers did not provide accurate model fits in all cases, we examined whether an improved fit could be obtained if mRNA levels for key functional enzymes could be used to infer respiration rates. The resulting empirically-derived mRNA "adjustment factors" were added to the model for both DMC and the main methanogen in the culture (a *Methanosaeta* species) to provide a more nuanced description of activity. Results of this study suggest that at higher feeding rates, competitive inhibition is important and mRNA provides a more accurate indicator of a population's instantaneous activity than 16S rRNA gene copies alone as biomass estimates. The use of mRNA as a biomarker of specific respiratory activity was especially valuable in cases of high chloroethene concentrations, where there was potential for toxicity to various community members and a purely biokinetic model overpredicted dechlorination and methanogenesis. mRNA levels (McrA for the *Methanosaeta* and HupL for the DMC) served as good biomarkers of methanogenesis and dechlorination rates, and improved model fits significantly. This work demonstrates one possible strategy for integrating quantitative molecular biomarkers into biokinetic modelings of mixed cultures.

5.C. Summary of Biomarker Development

Quantitative reverse-transcriptase polymerase chain reaction (qRT-PCR) data were taken from microcosms containing the KB-1^{TM} consortium, operated under continuous, chlorinated ethene feed conditions, with the aim of clarifying relationships, creating a more robust set of

biomarkers that could be used at field sites bioaugmented with the KB-1™ culture. The key results of this study are that the correlation between respiration rate and mRNA transcript number was upheld for HupL and 16S rRNA, and significant differences were observed for TceA and 1545 when comparing the two mixed cultures studied (KB-1™ and D2). A correlation was also observed for VcrA expression compared to respiration rate in the KB-1™ mixed culture. Additionally, correlation trends for HupL and VcrA were upheld when looking at proteomic ion intensities as compared to respiration rates, though protein changes were not as drastic as they were for mRNA transcripts.

Addition of stressors caused respiration rates to decrease significantly while mRNA degraded more slowly, indicating that transcript abundance alone cannot predict respiration rate in stressed conditions within hours to days following stress. However, both transcriptomic and proteomic data indicated initial recovery of specific DMC strains that have homologs for 1545 and BvcA as opposed to a strain with VcrA.

5.D. Summary of Field Site Proteome

We reported on a successful proteomics-based method for identifying *Dehalococcoides* and *Geobacter* biomarkers of reductive dechlorination at a trichloroethene-contaminated industrial site in Ft. Erie, Ontario that had been bio-augmented with the commercially-available KB-1™ microbial culture. Samples were obtained from two wells with high hydraulic connectivity to the enhanced in-situ bioremediation system, and two with low hydraulic connectivity. The DNA and RNA biomarkers examined were the 16S rRNA gene, a set of reductive dehalogenases, and the highly-conserved Ni-Fe hydrogenase, HupL. Proteomic biomarkers of organohalide respiration were detected in all four field samples' metaproteomes, and the key reductive dehalogenases present in the bioaugmentation culture were the most highly

detected biomarkers, suggesting that deployed DMC strains maintain devotion to high RDase concentrations in the field.

The key results of this study are that DMC proteins can be detected in field samples, that site geochemistry can significantly affect proteome extraction and analysis workflows, and that the detected RDases are the same as those present in the KB-1^{TM} mixed culture that was used to bioaugment the site. Additionally, the most highly detected biomarkers were the same across the board for DNA, RNA and protein (VcrA and the 1545 homolog). However, the advantage that can be seen for proteomic analysis of field samples is for strain differentiation, which could be used to track changes in microbial community composition. Strain differentiation is possible with qPCR of nucleic acids, but multiple primer sets are necessary for each target and "cross-talk" must be carefully considered. Ultimately, a quantitative proteomic biomarker method is the goal. This is the first report of proteomic data from EISB sites undergoing chloroethene bioremediation.

5.E. Methodological Future Directions

Ultimately, absolute quantification of biomarkers in field samples is the goal. Multiple Reaction Monitoring (MRM) has been used successfully to quantify preselected proteomic biomarkers in DMC-containing mixed culture samples.[1,2] MRM is an LC-MS/MS method in which the specific transition ions for specific peptides are targeted and monitored as a function of retention time. Five DMC cultures were used to develop an initial suite of RDase MRM targets: D2, KB-1, CBDB1, BDI and VS. Samples were extracted and digested according to the shotgun proteomics methods reported by Werner and Rowe.[2,3] Shotgun analysis was performed on each sample. The results of the shotgun analyses were compared to a DMC/methanogen database to determine detected peptides. Using software designed for selecting peptide targets

from nanoLC-MS/MS spectra (MRMpilot, ABI), which ranks the detected peptides as likely MRM targets, a list of potential targets was generated using the following criteria:

1. The peptides chosen had been detected by shotgun proteomics with no potential post-translational modifications, no methionine in the sequence, no missed cleavages, and 99% confidence in identification.
2. The peptides were unique to the specific protein when searched across all genomes.

Additionally, Rowe suggested use of internal standards to account for issues with varying retention times for peptide targets in complex culture samples.[4] Field samples are even more complex than mixed culture samples, so isotopically-labeled internal standards for each peptide target were created at the Environmental Molecular Sciences Laboratory (EMSL) at the Pacific Northwest National Laboratory. Such internal standards can help to deal with two results of matrix effects: retention time shift and ion suppression. EMSL has attempted to run MRM on the field samples discussed in Chapter 4, without success as of yet. It is possible that, as discussed in Chapter 4, there was a loss of material during the extraction, and not enough remained for quantification. Also, methods designed for laboratory techniques are often not applicable to environmental samples. Now that shotgun proteomic data is available from field samples, this MRM target list can be expanded and/or modified based on peptides that were detected in the field.

5.F. Suggested Future Research Directions

5.F.1. Biokinetic Model

Syntrophomonas has been shown to produce polyhydroxybutyrate (PHB) granules to store alkanoic acids when they are exposed to a transient substrate supply, like the batch feeding

of our mixed culture.[5,6] A key enzyme in PHB production is PHB synthase (3-hydroxybutyryl-CoA dehydratase (Locus ID: Swol_1936) in *Syntrophomonas)*.[7] The homolog of this gene in the D2 metagenome is PCEOTH_1714030 (IMG-M taxon ID: 2032320001, http://img.jgi.doe.gov/cgi-bin/m/main.cgi). After designing new primers we looked at mRNA expression levels for PHB synthase in these experiments. It was observed that at higher electron donor feeding rates, which correspond to greater amounts of missing eeqs, PHB synthase expression was up-regulated relative to time zero (Figure A1.5 in Appendix I). However, this information was not included in the present version of the model – and butyrate is still not predicted well. Modification of the model to account for this butyrate storage as PHB granules could be useful.

An important characteristic of the D2 mixed culture is competition for hydrogen between DMC195 and *Methanospirillum hungatei*, a hydrogenotrophic methanogen. Empirical trends have been established correlating respiration rate to FrcA and MvrD expression in *Methanospirillum*. Incorporation of this relationship into the biokinetic model could add to its value.

Another point on which the model could be improved is the mRNA adjustment factor. The values we currently are using for mRNA transcript abundance are final time point values. We originally analyzed the initial and final time points to look for a change in biomarker expression. Due to the limited amount of cDNA available from each experiment modeled in Chapter 2, and the high number of targets already analyzed, we were unable to look at more data points.[2,8] The design of new experiments to target the mRNA response in high feed rate conditions could add to the value of the model.

The biokinetic model was successfully modified to utilize DNA-based kinetic

parameters. While this model is applicable to our mixed culture where we have only one strain of DMC present, the highly conserved nature of the 16S rRNA gene among DHC strains makes this model not ideal for field sites where the strain of DMC present may be unknown. The biokinetic model could be modified (and simplified) by reworking the existing kinetic relationships so that they are based on absolute protein levels rather than 16S rRNA gene levels. Enzyme kinetic parameters have already been estimated for the DMC195 RDases TceA and PceA.[2]

5.F.2. Biomarkers of Reductive Dechlorination

In KB-1™, increasing the number and variety of experiments performed will help resolve biomarker trends that have been observed (e.g. the difference 1545 homolog expression between the D2 and KB-1™ mixed cultures). Additionally, evaluation of proteomic data from the field site revealed that BvcA is likely significant at field sites undergoing biostiumulation and/or bioaugmentation. Examination of BvcA expression trends in the KB-1™ mixed culture would be informative. DNA and cDNA stocks are available for the experiments discussed in Chapter 3, and could be analyzed. Additionally, as *Geobacter* is an important member of the KB-1 mixed culture, examination of *Geobacter* 16S rRNA and PceA expression trends, and 16S rRNA gene levels in the KB-1™ culture and field sample stocks that we have would could lead to additional biomarkers of reductive dechlorination.

As noted in Chapter 4, the HupL primers used in this study are specific for DMC195, with at least one mismatch to other strains' homologs. Additional examination of HupL expression trends could be conducted using KB-1™ and field sample DNA and cDNA stocks that we have stored in the lab from the samples/experiments discussed in Chapters 3 and 4. The use of primers that hit all strains would be informative as HupL is a highly conserved gene among DMC strains (like 1545) – this would complement the HupL proteomic data that was

presented.

Contaminated field sites often have more than one type of chlorinated organic contaminant, and understanding the dynamics of these would be interesting. Conducting PSS experiments with multiple electron acceptors (beyond the inhibition studies discussed in Chapter 2), could provide valuable information about biomarkers in more complex environmental systems.

5.F.3. Field Proteomics

It is important to continue to work on a method of absolute quantification of protein in environmental samples. Ideally, one would find a field site and concurrently analyze samples for DNA, RNA, protein and metabolites over time and see if a relationship can be established between respiration rate and biomarker quantities. Additionally, we have recently received shotgun proteomic data from TCE-contaminated field site that had been bioaugmented with Shaw-SDC, a commercially available mixed culture that contains different strains of DMC than the KB-1^{TM} mixed culture. An in depth comparison of these proteomic results to those reported in Chapter 4 would be very informative with regards to biomarkers of anaerobic reductive dechlorination among varying DMC strains.

REFERENCES

(1) Werner, J. J.; Ptak, A. C.; Rahm, B. G.; Zhang, S.; Richardson, R. E. Absolute quantification of Dehalococcoides proteins: enzyme bioindicators of chlorinated ethene dehalorespiration. *Environ. Microbiol.* **2009**, *11*, 2687–2697.

(2) Rowe, A. R.; Heavner, G. L.; Mansfeldt, C. B.; Werner, J. J.; Richardson, R. E. Relating Chloroethene Respiration Rates in *Dehalococcoides* to Protein and mRNA Biomarkers. *Environ. Sci. Technol.* **2012**, *46*, 9388–9397.

(3) Werner, J. J.; Ptak, A. C.; Rahm, B. G.; Zhang, S.; Richardson, R. E. Absolute quantification of *Dehalococcoides* proteins: enzyme bioindicators of chlorinated ethene dehalorespiration. *Environmental Microbiology* **2009**, *11*, 2687–2697.

(4) Rowe, A. R. Molecular Biomarkers for Respiration in *Dehalococcoides ethenogenes* and *Methanospirillum hungatei*: Comparing Protein and Messenger-RNA Abundance in Anaerobes, Cornell University: Ithaca, NY, 2011.

(5) Beccari, M.; Majone, M.; Massanisso, P.; Ramadori, R. A bulking sludge with high storage response selected under intermittent feeding. *Water Res.* **1998**, *32*, 3403–3413.

(6) Beun, J.; Dircks, K.; Van Loosdrecht, M.; Heijnen, J. Poly-[beta]-hydroxybutyrate metabolism in dynamically fed mixed microbial cultures. *Water Res.* **2002**, *36*, 1167–1180.

(7) Dias, J. M. L.; Serafim, L. S.; Lemos, P. C.; Reis, M. A. M.; Oliveira, R. Mathematical modelling of a mixed culture cultivation process for the production of polyhydroxybutyrate. *Biotechnol. Bioeng.* **2005**, *92*, 209–222.

(8) Rowe, A. R.; Mansfeldt, C. B.; Heavner, G.; Richardson, R. E. *Methanospirillum* respiratory mRNA biomarkers correlate with hydrogenotrophic methanogenesis rate during growth and competition for hydrogen in an organochlorine-respiring mixed culture. *Environ. Sci. Technol.* **2012**, 10.1021/es303061y.

APPENDIX I:

Supporting Information for Chapter 2

A1.A. Supporting Tables

Table A1. 1. Experimental Parameters for Model Calibration and Validation

Experiment	Culture Title	Length of Experiment (days)	EA	EA Feed Rate (μeeq/L-h)	ED	ED Feed Rate (μmol/h)	eeq ratio ED/EA as H2*	Average Measured Respiration Rate (μeeq/L-h)
PCE Half Butyrate	PHB1	7	PCE	104	But	1	0.74	84.6
	PHB2			45.7			1.68	39.3
	PHB3			106			0.72	97.2
DCE High	DH1_INHIB	7	DCE	119	But	6	2.03	37.4
	DH2_INHIB			114			1.81	35.6
	DH3_INHIB			127			2.69	46.4
PCE High Low	HLH1_INHIB	2**	PCE	316	But	26	2.62	141
	HLH2_INHIB			482			1.72	156
	HLH1_INHIB			435			1.90	78.6
	HLH2_INHIB	7**		481			1.72	82.3
	HLH3			183			4.52	138
	HLL1			4.9		0.2	4.14	4.9
	HLL2			4.7			4.14	4.8
	HLL3			5.9			3.31	5.9
PCE 0, YE	P0FY01	4	PCE	6.6	none	0	0.00	1.70
	P0FY02			5.4			0.00	1.59
	P0FYY1	7		4.9			2.79	4.54
	P0FYY2			4.7			2.79	4.34
PCE High	HiP1	1	PCE	259	But	26	3.37	141
	HiP2			231			3.78	133
	HiP3			279			3.13	167
TCE 3 Rates	T3A1	4	TCE	34.2	But	4	3.79	34.2
	T3B1			6.9		0.9	5.14	6.9
	T3C1			1.5		0.2	11.40	1.5
DCE-3 Rates	D3A1	1	DCE	36.7	But	4	2.65	36.7
	D3B1	4		8.9		0.9	2.97	8.9
	D3C1			2.3		0.2	5.46	2.3
	D3A2			32.4		4	3.04	32.4
	D3B2			8.2		0.9	3.25	8.2
	D3C2			2.3		0.2	5.37	2.3

* Assumes butyrate → 2 acetate + 2 H_2 as fermentation stoichiometry

** Bottles were modeled for the first two days of the experiment, and also the entire experiment (7 days) – these were treated as different experiments and respiration and feeding rates were calculated for 2 and 7 days, respectively

Table A1. 2. Model improvement by adding competitive inhibition to the model as gauged by χ^2 goodness of fit.

	P0FY01		P0FY02		P0FYY1		P0FYY2		HLL1		HLL2		HLL3	
	No INH	INH	No INH	INH	No INH	INH	No INH	INH	No INH	INH	No INH	INH	No INH	INH
PCE	1.5	0.35	0.49	0.24	48	66	44	52	128	112	121	108	246	213
TCE	0.83	0.057	0.17	0.26	0.13	0.12	0.22	0.21	0.62	0.62	6.8E-4	5.9E-4	0.021	0.021
DCE	107	302	2.5	6.5	5.1	8.9	2.9	4.9	3.3	3.3	2.2	2.1	4.8	4.8
VC	2.6	0.36	2.7	0.35	3.4	3.1	1.5	1.0	4.8	4.1	4.4	3.9	7.1	6.0
ETH	7.1E-4	3.0	0.0035	0.87	1.7	2.3	1.9	2.4	1.8	1.3	2.1	1.5	2.8	2.2
VC+ETH	2.5	0.17	2.7	0.26	1.5	3.0	1.4	1.5	0.39	0.37	0.60	0.58	0.52	0.50
Butyrate	n/a	n/a	n/a	n/a	n/a	n/a	n/a	n/a	3.0	3.0	3.0	3.0	3.0	3.0
Acetate	n/a	n/a	n/a	n/a	n/a	n/a	n/a	n/a	1478	3803	1309	3382	1283	3020
H2	0.075	0.066	0.097	0.088	1.0	1.6	1.7	2.0	0.11	0.10	0.24	0.22	0.27	0.24
Methane	8.4	19	3.83	10	104	99	78	78	81	239	82	396	800	2350
	PHB1		PHB2		PHB3		HLH1_INHIB		HLH2_INHIB		HLH3		HiP1	
	No INH	INH	No INH	INH	No INH	INH	No INH	INH	No INH	INH	No INH	INH	No INH	INH
PCE	431	1390	13376	13068	5623	5556	149	66	295	83	764	30496	30	38
TCE	455	152	6.7	6.4	98	108	1.3	5.2	3703	40	7.3	7.7	11	15
DCE	283	2019	83	79	1823	1626	0.22	1214	18	3472	3.8	340	140	549
VC	42	38	65	65	70	81	20	37	57	67	475	207	3.3	23
ETH	452	36	21	22	169	85	1113	8.6	1971	14	2823	1493	91	4.3
VC+ETH	63	42	37	38	122	125	269	32	604	37	152	105	14	27
Butyrate	n/a	n/a	n/a	n/a	n/a	n/a	42	87	63	118	5751	6666	4968	6851
Acetate	n/a	n/a	n/a	n/a	n/a	n/a	30	19	32	20	210	232	4.6	52
H2	19	19	3.2	3.2	15	17	1.3	1.6	0.53	0.55	0.67	0.51	1.7	4.3
Methane	45	43	108	116	193	192	4126	3811	3115	2853	15094	15001	1165	864

	HiP2		HiP3		T3A1		T3B1		T3C1		D3A2		D3B2	
	No INH	INH	No INH	INH	No INH	INH	No INH	INH	No INH	INH	No INH	INH	No INH	INH
PCE	24	45	175	1212	n/a	n/a	n/a	n/a	n/a	n/a	n/a	n/a	n/a	n/a
TCE	0.0043	4.3	57	8.7	0.65	0.40	0.0021	0.0035	0.0044	0.0044	n/a	n/a	n/a	n/a
DCE	217	868	81	276	27	64	1.6	2.3	0.19	0.18	138	141	22	21
VC	8.2	27	5.7	37	24	6.4	1.1	0.48	0.035	0.027	49	23	1.9	1.6
ETH	58	6.5	61	11	19	2.9	0.057	0.13	0.0037	0.022	38	17	0.77	1.7
VC+ETH	12	33	8.8	47	1.7	1.7	0.33	0.33	0.014	0.014	10	10	1.9	1.9
Butyrate	5448	7427	5961	8257	5505	7702	0.81	1.0	2.0	2.0	2509	2650	0.78	0.81
Acetate	8.7	61	14	77	338	312	6.0	3.1	435	543	804	805	4423	4431
H2	1.7	4.7	1.7	5.3	1.9	1.5	0.18	0.17	0.058	0.066	0.43	0.47	0.048	0.047
Methane	958	711	654	451	114	208	0.19	34	3.7	50	4603	4622	42	43

	D3C2		DH1_INHIB		DH2_INHIB		DH3_INHIB		D3B1		D3C1	
	No INH	INH	No INH	INH	No INH	INH	No INH	INH	No INH	INH	No INH	INH
PCE	n/a	n/a		0		0		0		0		0
TCE	n/a	n/a		0		0		0		0		0
DCE	3.3	3.2		3.8E5		2.9E5		6.2E5		28		3.4
VC	0.17	0.45		394		181		255		1.2		1.9
ETH	0.31	0.54		1.1E5		1.1E5		9.7E4		1.4		0.43
VC+ETH	0.052	0.054		6016		5504		4324		0.52		1.2
Butyrate	2.0	2.0		3.0E4		4.5E4		3.8E4		0.71		2.0
Acetate	596	594		5.6E5		5.7E5		4.6E5		25		206
H2	0.095	0.095		3.7		4.7		2.3		0.038		0.033
Methane	29	29		7.6E5		8.8E5		8.1E5		82		192

*** Green highlighting indicates that the χ^2 value is lower for INH than for no INH for that metabolite.**

Table A1. 3. χ2 values for all metabolites for the complete model (including mRNA adjustment where highlighted in green).

	P0FY01	P0FY02	P0FYY1	P0FYY2	HLL1	HLL2	HLL3	PHB1	PHB2	PHB3
PCE	0.35	0.24	66	52	112	108	213	1390	13068	5556
TCE	0.057	0.26	0.12	0.21	0.62	0.00059	0.021	152	6.4	108
DCE	302	6.5	8.9	4.9	3.3	2.1	4.8	2019	79	1626
VC	0.36	0.35	3.1	1.0	4.1	3.9	6.0	38	65	81
ETH	3.0	0.87	2.3	2.4	1.3	1.5	2.2	36	22	85
VC+ETH	0.17	0.26	3.0	1.5	0.37	0.58	0.50	42	38	125
Butyrate	n/a	n/a	n/a	n/a	3.0	3.0	3.0	n/a	n/a	n/a
Acetate	n/a	n/a	n/a	n/a	3803	3382	3020	n/a	n/a	n/a
H2	0.066	0.088	1.6	2.0	0.10	0.22	0.24	19	3.2	17
Methane	19	10	99	78	239	396	2350	43	116	192

	T3A1	T3B1	T3C1	D3B1	D3C1	D3B2	D3C2	HiP1	HiP2	HiP3
PCE	n/a	n/a	n/a	n/a	n/a	n/a	n/a	38	45	1212
TCE	0.40	0.0035	0.0044	n/a	n/a	n/a	n/a	15	4.3	8.7
DCE	64	2.3	0.18	28	3.4	21	3.2	549	868	276
VC	6.4	0.48	0.027	1.2	1.9	1.6	0.45	23	27	37
ETH	2.9	0.13	0.022	1.4	0.43	1.7	0.54	4.3	6.5	11
VC+ETH	1.7	0.33	0.014	0.52	1.2	1.9	0.054	27	33	47
Butyrate	7702	1.0	2.0	0.71	2.0	0.81	2.0	6851	7427	8257
Acetate	312	3.1	543	25	206	4431	594	52	61	77
H2	1.5	0.17	0.066	0.038	0.033	0.047	0.095	4.3	4.7	5.3
Methane	208	34	50	82	192	43	29	864	711	451

	D3A2	D3A2	HLH2_IN HIB-7days	HLH1_IN HIB-7days	HLH2_IN HIB-7days	HLH2_IN HIB-7days	HLH3
PCE	n/a	n/a	2467	922	2367	392	30496
TCE	n/a	n/a	5.3	20.6	63.7	58.6	7.7
DCE	141	240	2649	85	7733	72	340
VC	23	4	58	198	105	349	207
ETH	17	10	23418	87	62138	98	1493
VC+ETH	10	10	3807	140	9091	444	105
Butyrate	2650	10902	1681	4216	1363	3908	6666
Acetate	805	80	981	8879	2390	13014	232
H2	0.47	0.5	2.6	1.5	1.2	1.1	0.51
Methane	4622	66	141541	283	120472	236	15001

* Green highlighting indicates that mRNA adjustment was included for that bottle.

A1.B. Supporting Figures

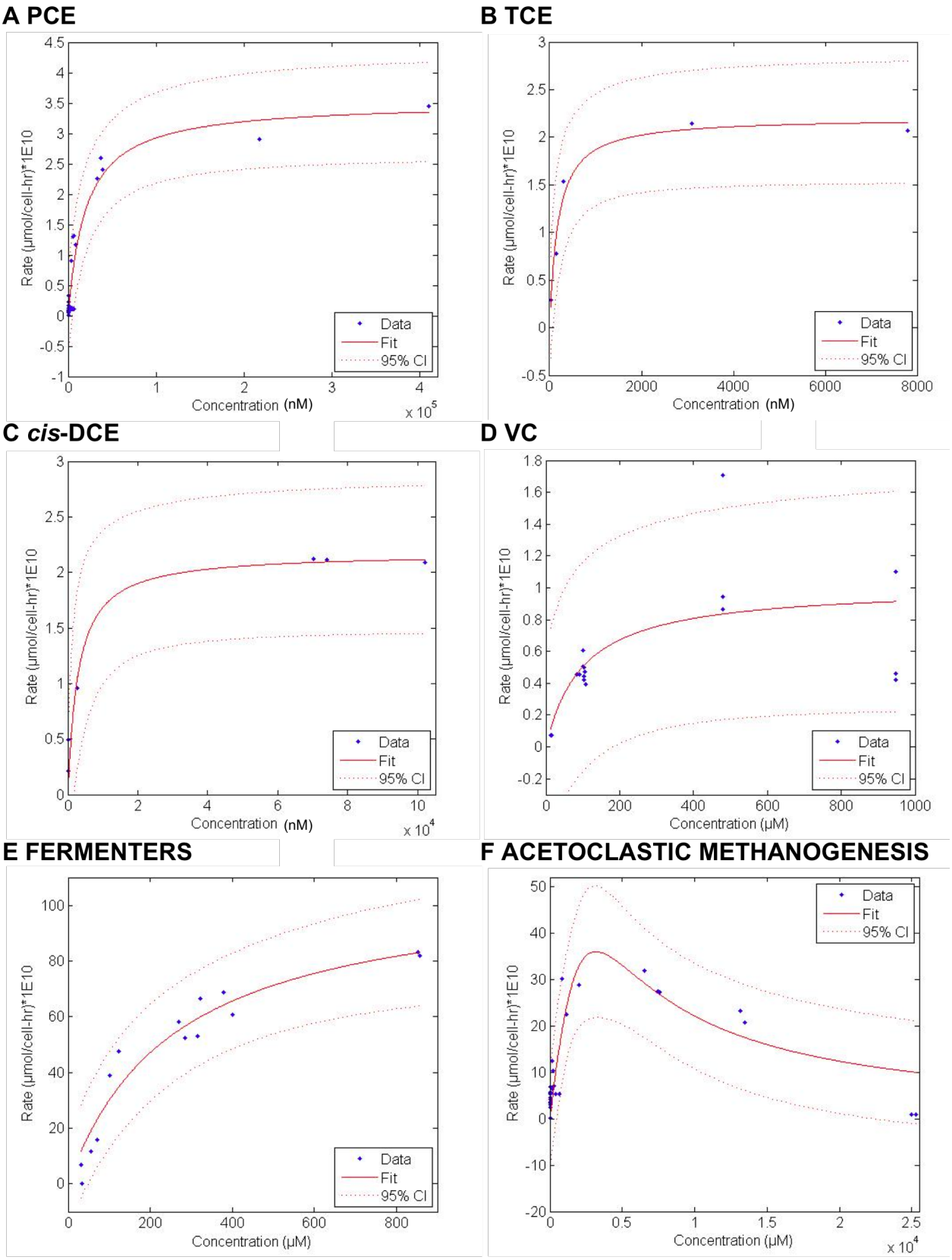

Figure A1. 1. Nonlinear Regressions and 95% Confidence Intervals for Kinetic Parameters.

A

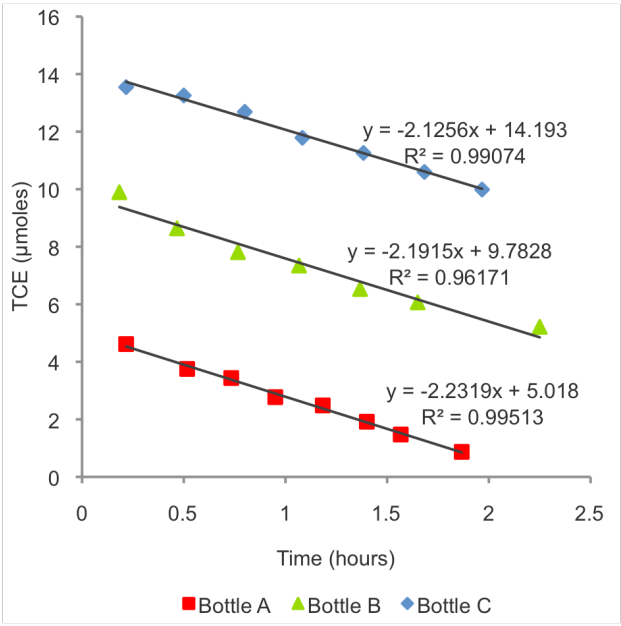

Bottle A – 4.6 umoles TCE, 0 umoles PCE
Bottle B – 9.9 umoles TCE, 8.1 umoles PCE
Bottle C – 14 umoles TCE, 18 umoles PCE

B

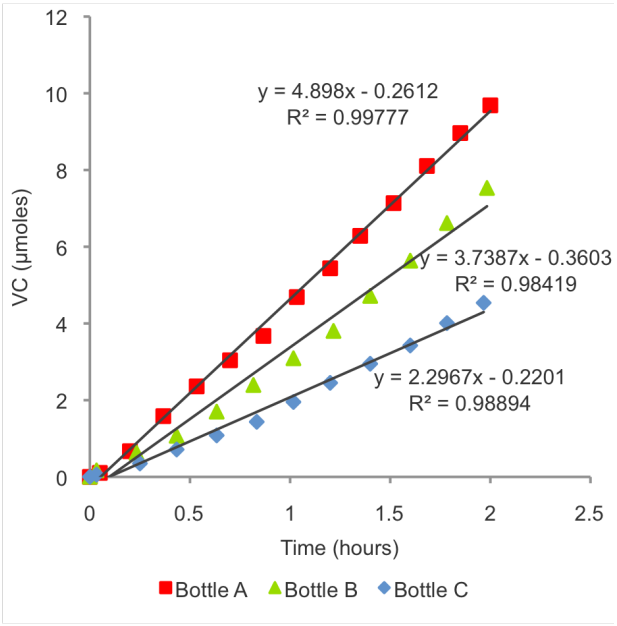

Bottle A – 23 umoles DCE, 0 umoles TCE
Bottle B – 55 umoles DCE, 33 umoles TCE
Bottle C – 25 umoles DCE, 55 umoles TCE

C

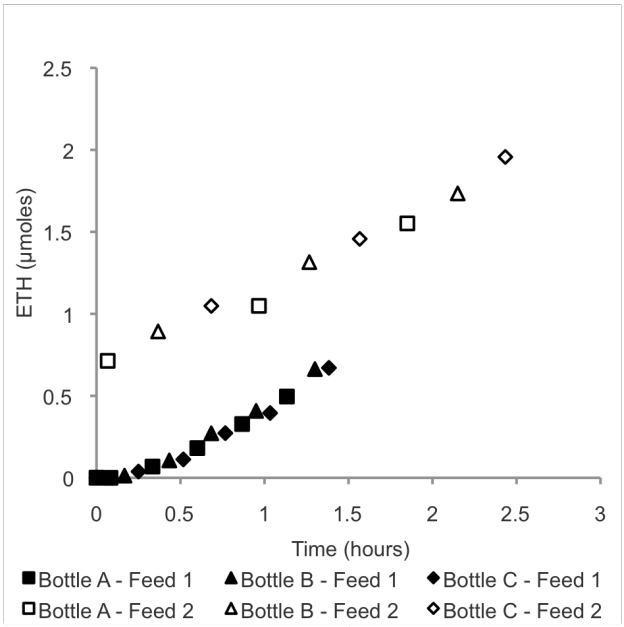

Feed 1 Resp. Rate = 4.8±0.4 µmoles/L-hr
C_{VC}=103 µmoles/L C_{PCE}=0 µmoles/L
Feed 2 Resp. Rate = 4.9±0.3 µmoles/L-hr
C_{VC} =93 µmoles/L C_{PCE} =56 µmoles/L

D

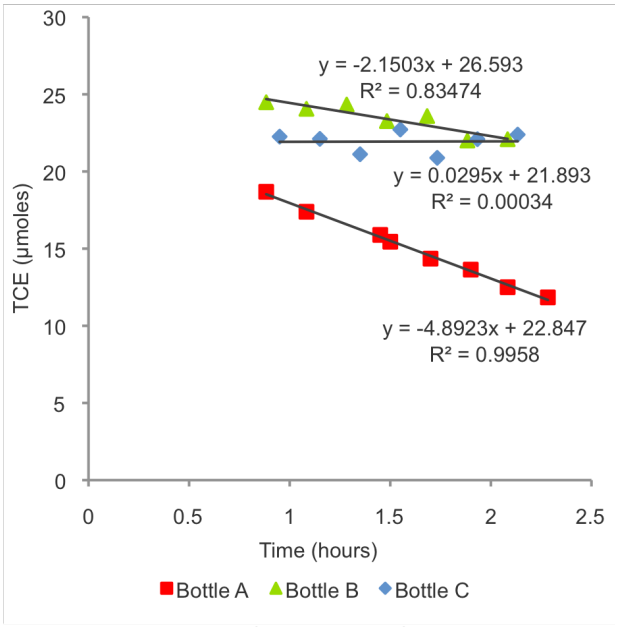

Bottle A – 19 umoles TCE, 0 umoles DCE
Bottle B – 24 umoles TCE, 92 umoles DCE
Bottle C – 22 umoles TCE, 113 umoles DCE

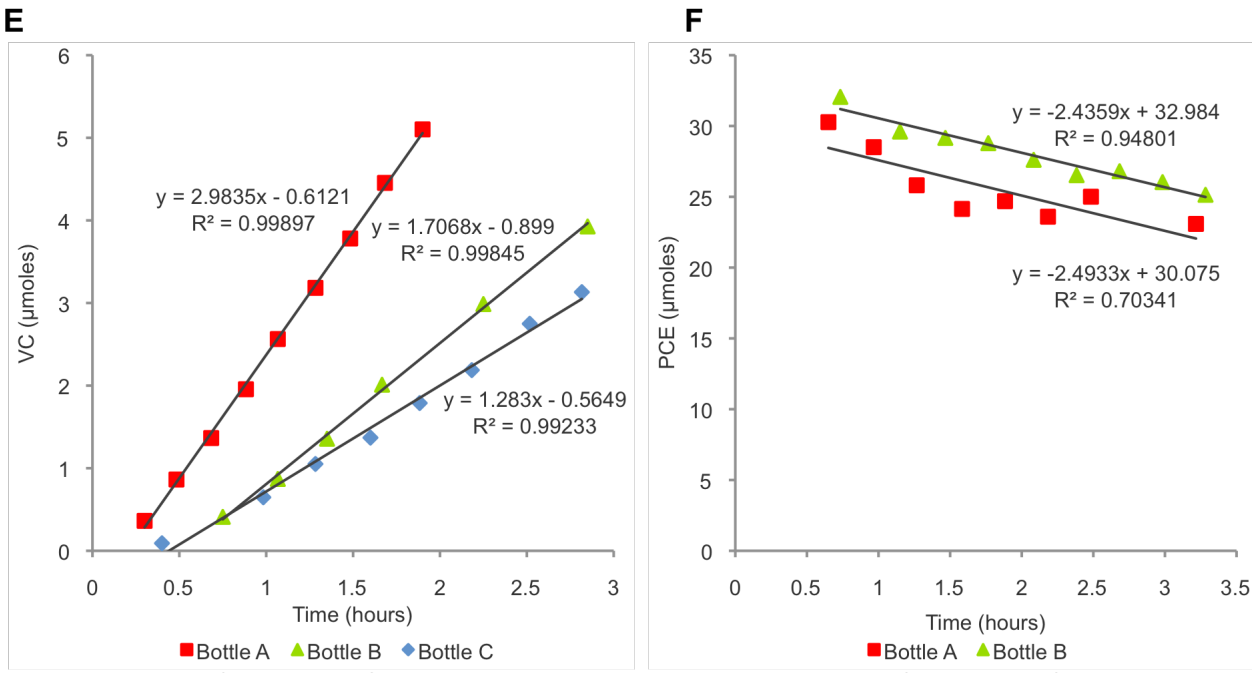

Bottle A – 42umoles DCE, 0 umoles PCE
Bottle B – 60 umoles DCE, 16 umoles PCE
Bottle C – 57 umoles DCE, 10 umoles PCE

Bottle A – 30 umoles PCE, 0 umoles DCE
Bottle B – 32 umoles PCE, 115 umoles DCE

Figure A1. 2. Results of Inhibition Studies.

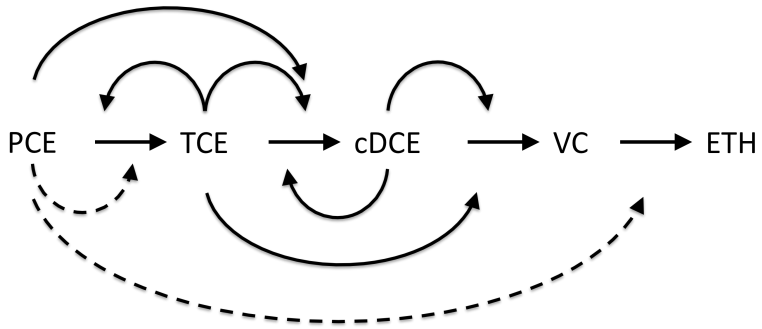

Figure A1. 3. Proposed competitive inhibition model for *D. mccartyi* ecotype Donna II (JGI Taxon ID: 2088090019) among chlorinated ethenes based on inhibition studies. Solid lines show inhibition (e.g. TCE inhibits PCE degradation) and dashed lines show no/weak inhibition observed (e.g. PCE does not inhibit TCE degradation). VC inhibition on TCE, DCE & PCE was not tested.

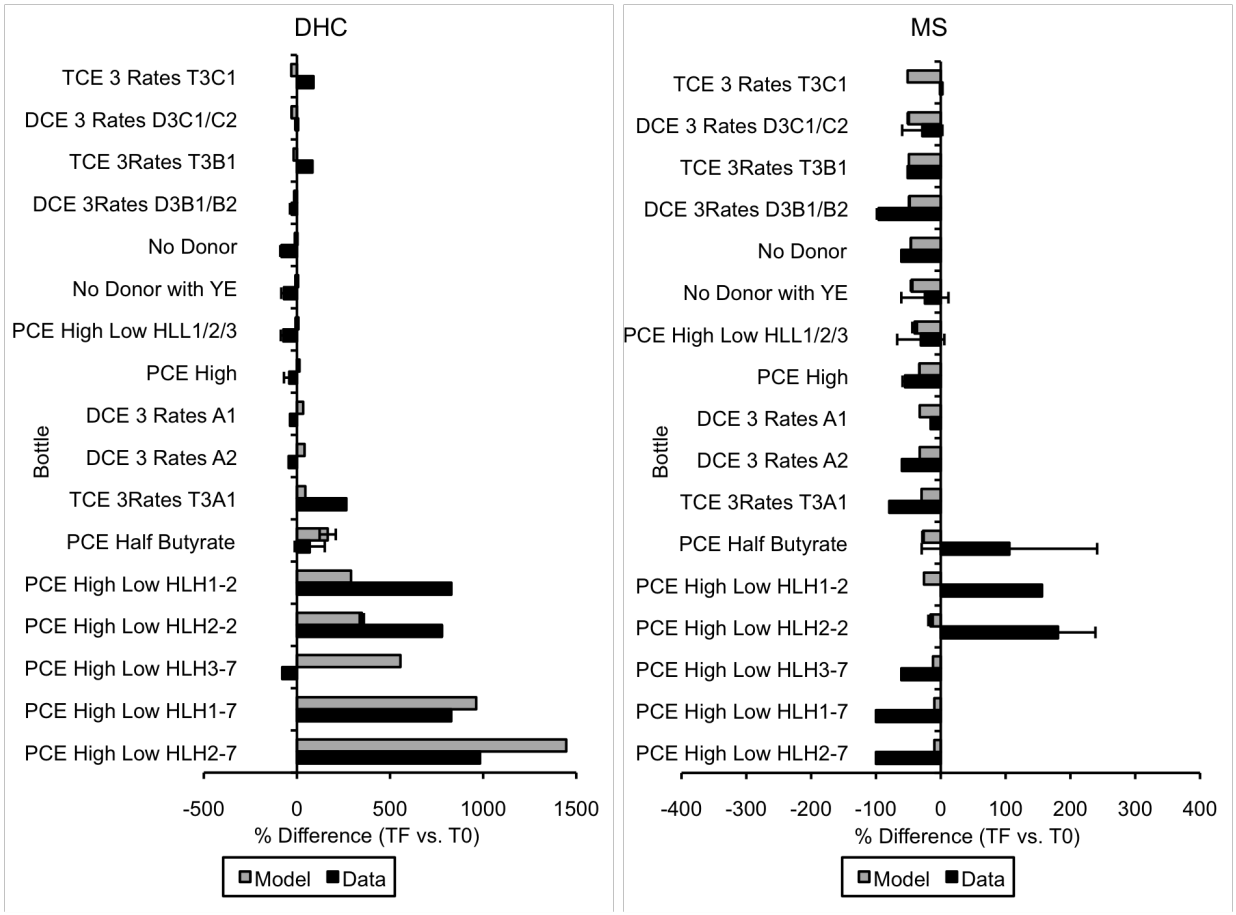

Figure A1. 4. Model biomass predictions (grey) as compared to data (black) measured as the percent difference between the final and initial time points. Data are qPCR-quantified 16S rRNA gene copies per mL of culture. Error bars represent the standard deviation between replicate bottles.

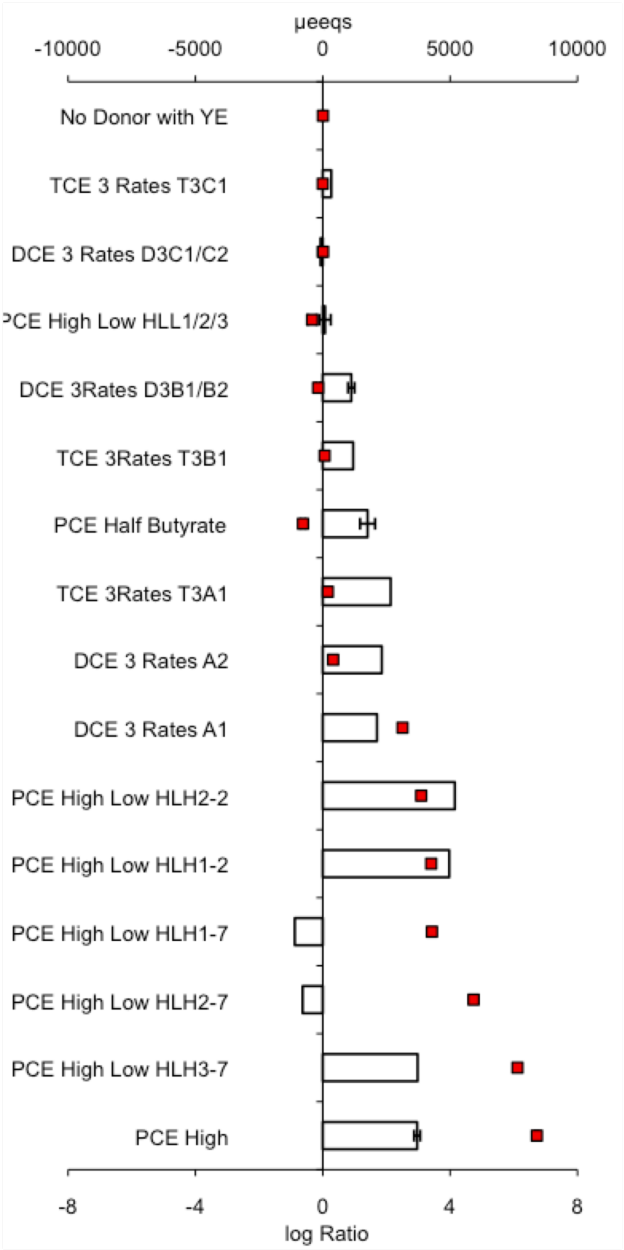

Figure A1. 5. Gene expression of PHB Synthase (bars) compared to missing butyrate eeqs (squares) over the last 24 hours of the experiment. Gene expression is shown as the log ratio of transcript abundance versus the abundance of the gene in the sample prior to feeding.

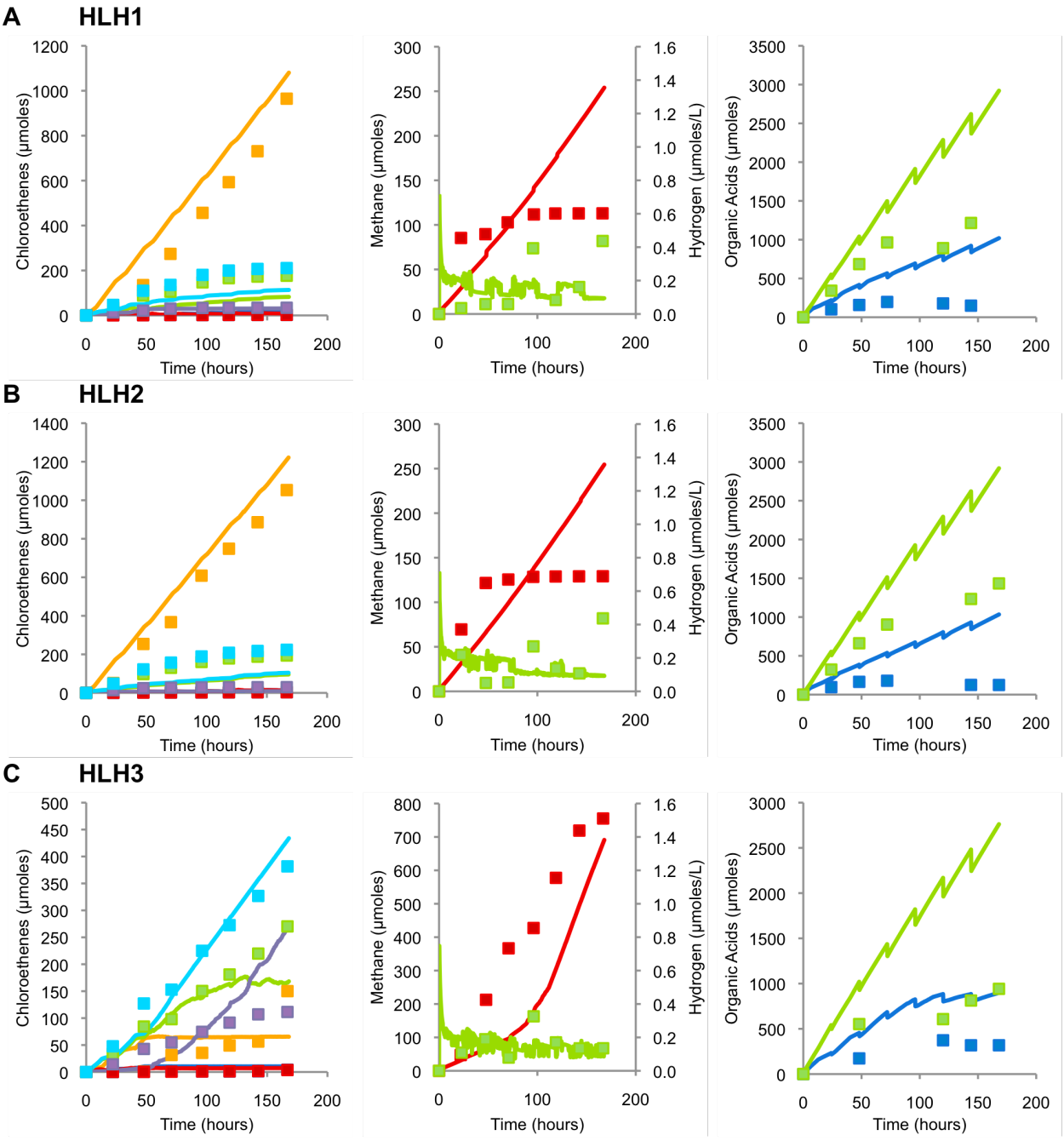
A
HLH1
Chloroethenes (µmoles)
Time (hours)
Methane (µmoles)
Hydrogen (µmoles/L)
Organic Acids (µmoles)
B
HLH2
C
HLH3

D **HLL1**

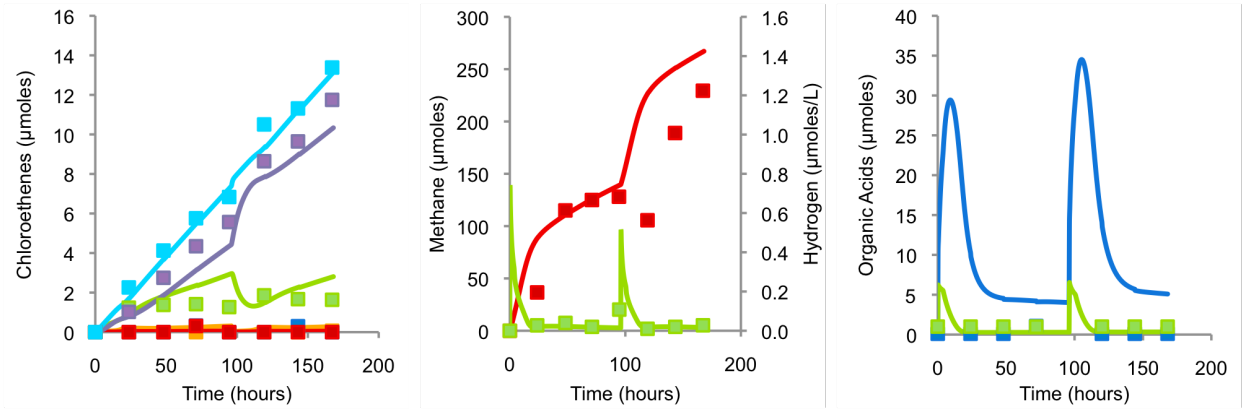

E **HLL2**

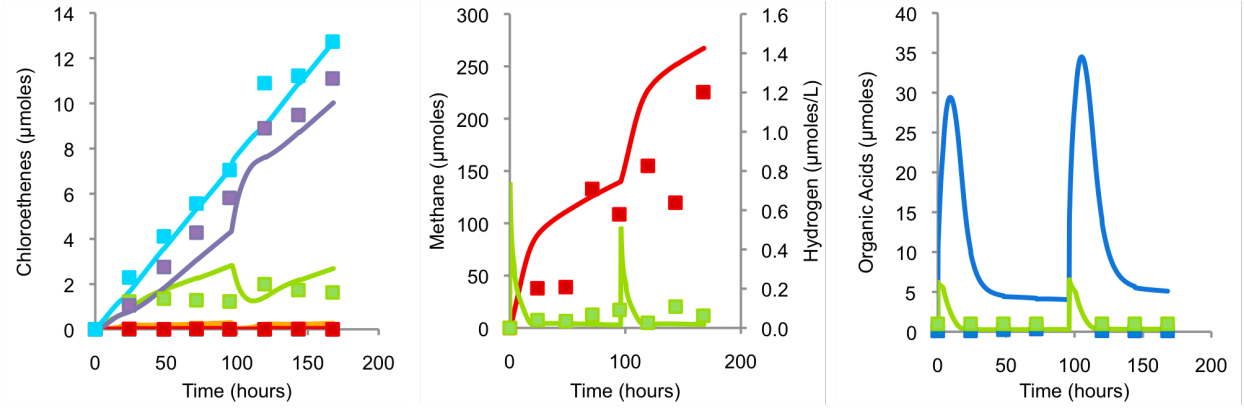

F **HLL3**

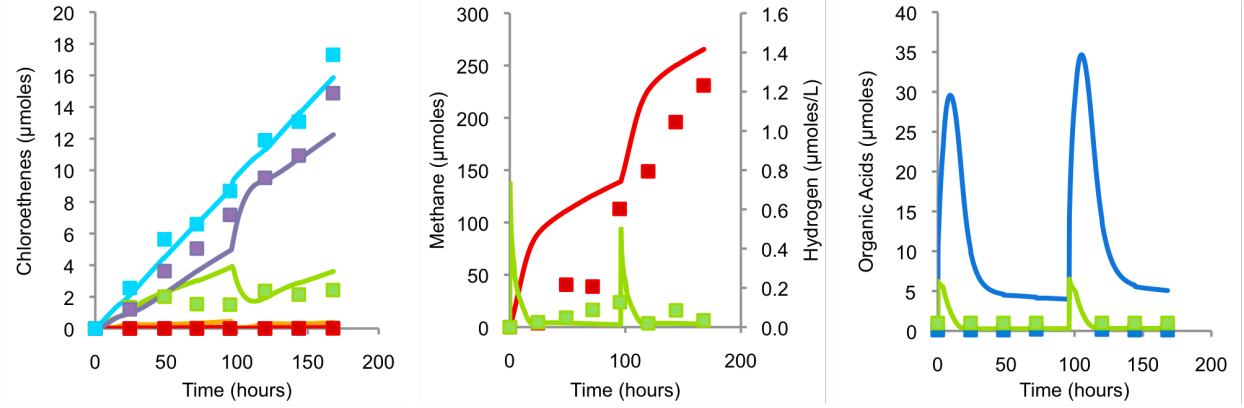

G P0FY01

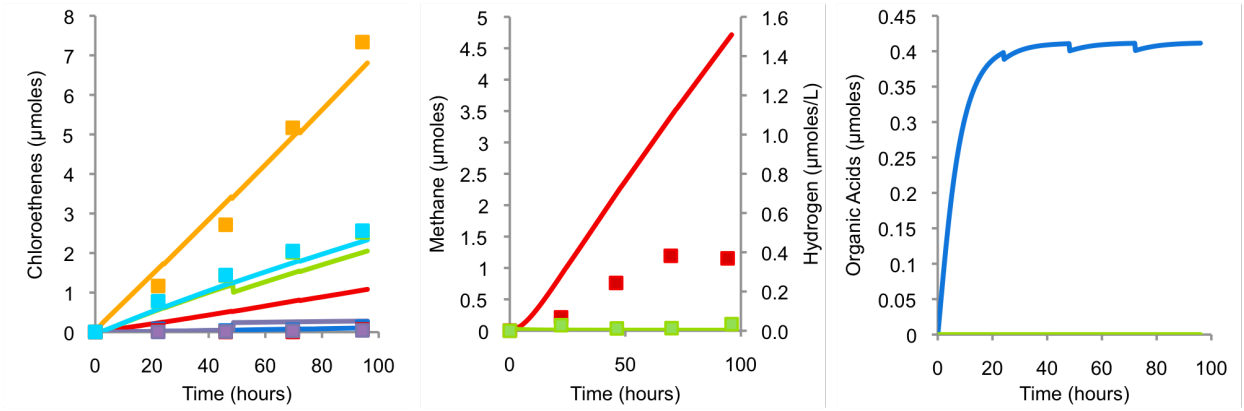

H P0FY02

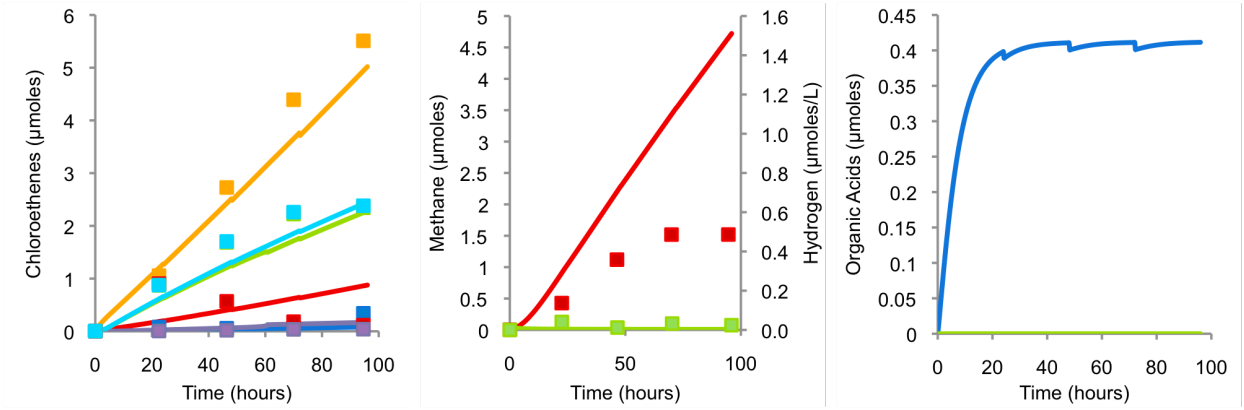

I P0FYY1

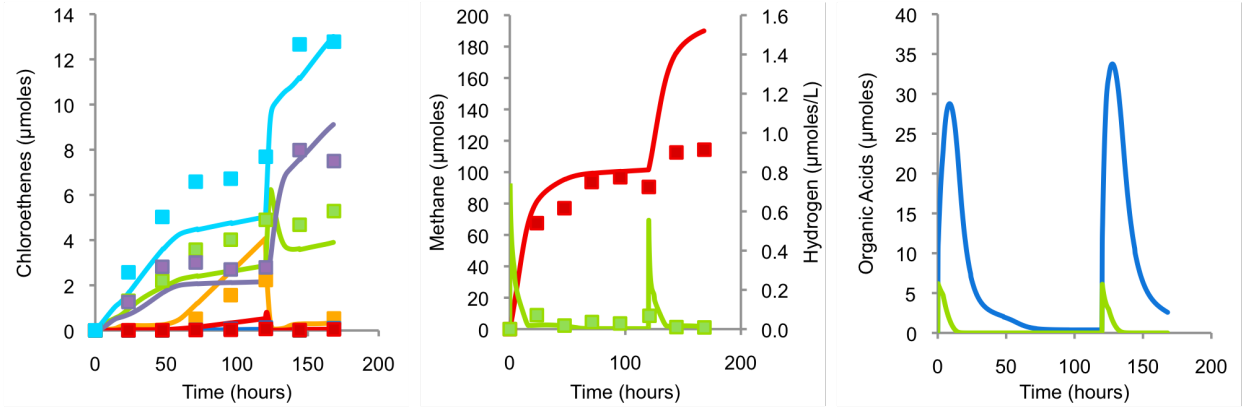

J P0FYY2

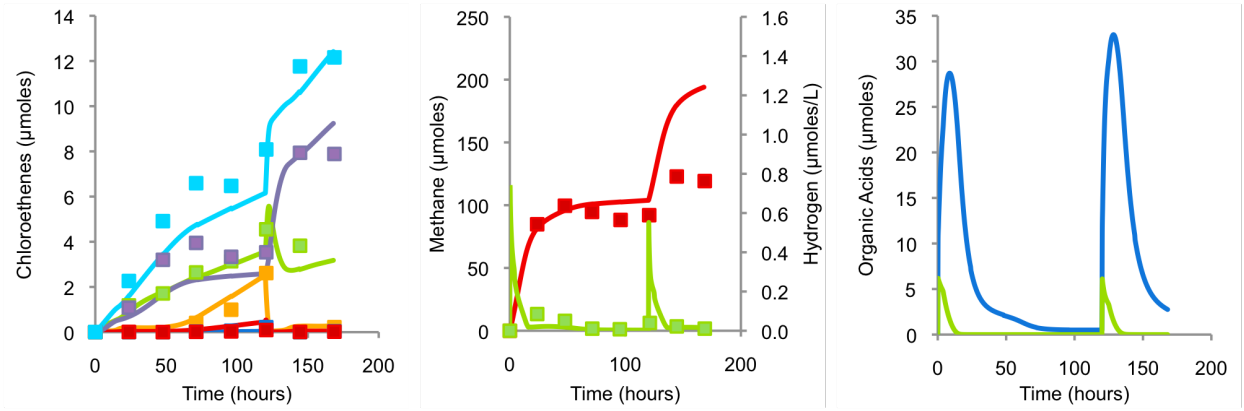

K HiP1

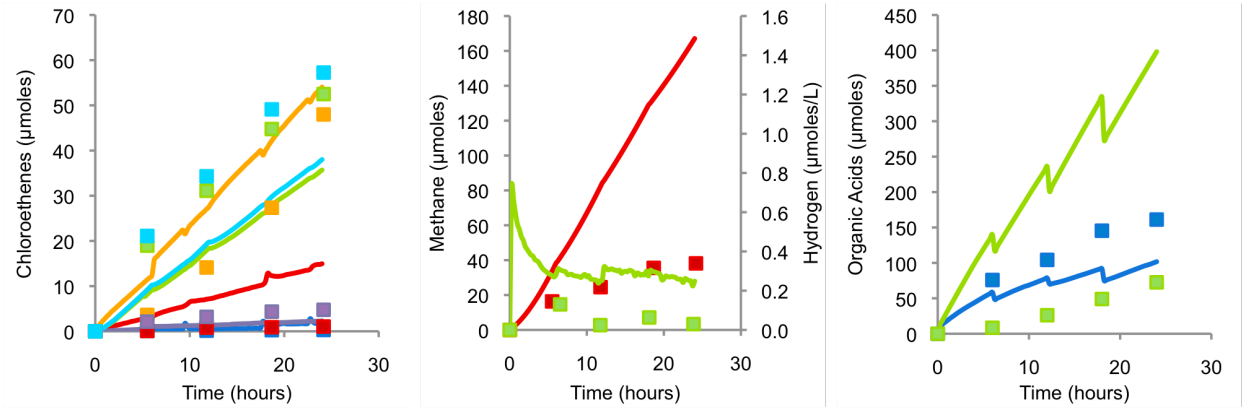

L HiP2

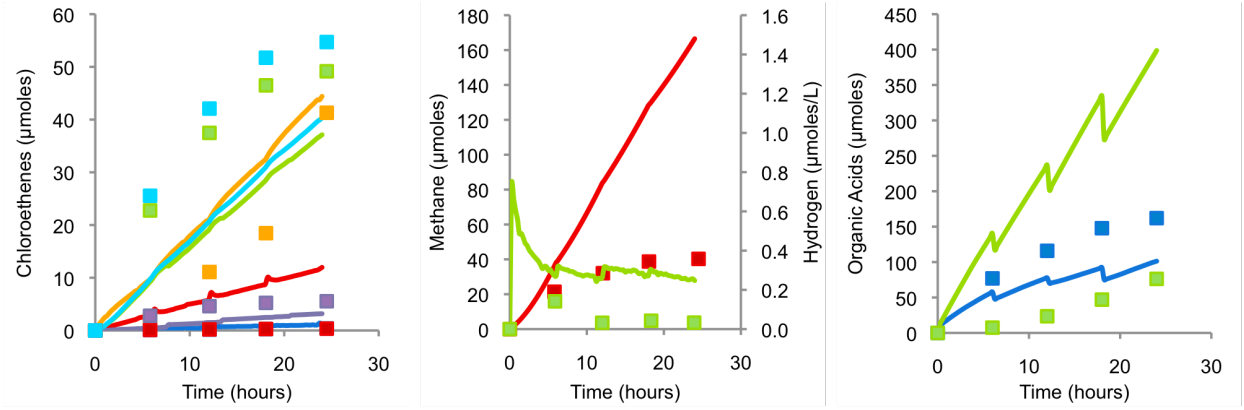

M HiP3

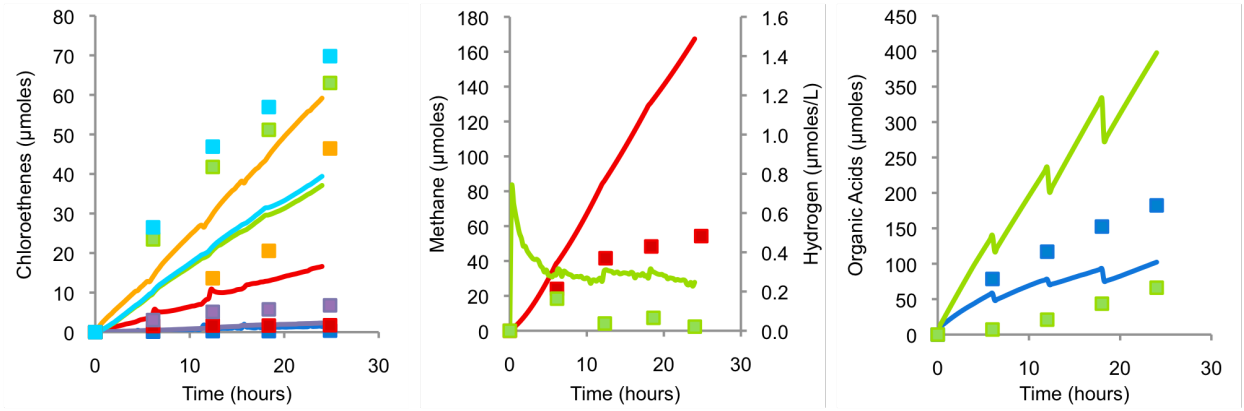

N T3A1

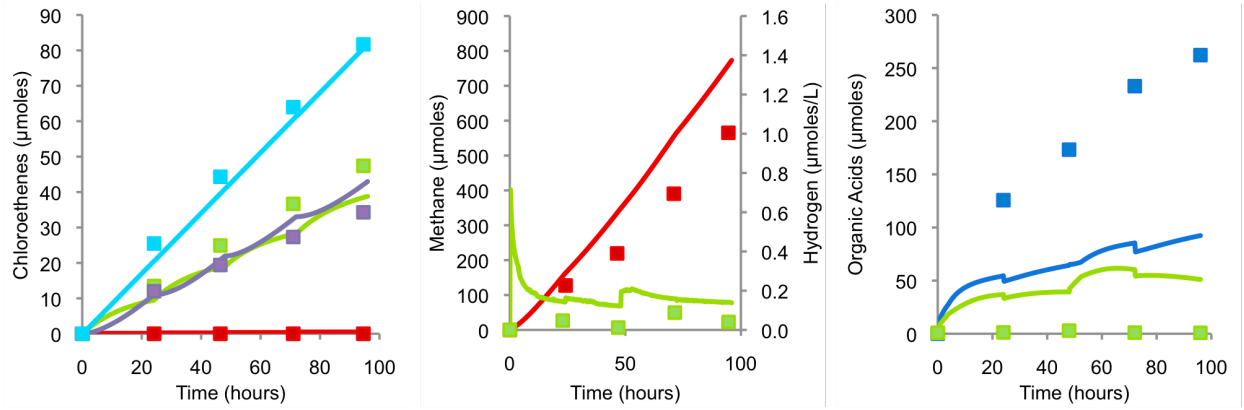

O T3B1

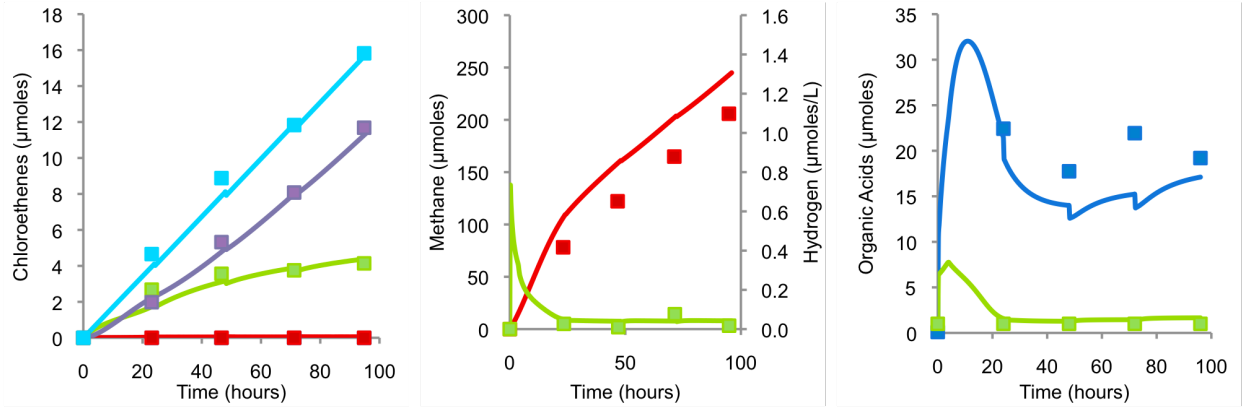

P T3C1

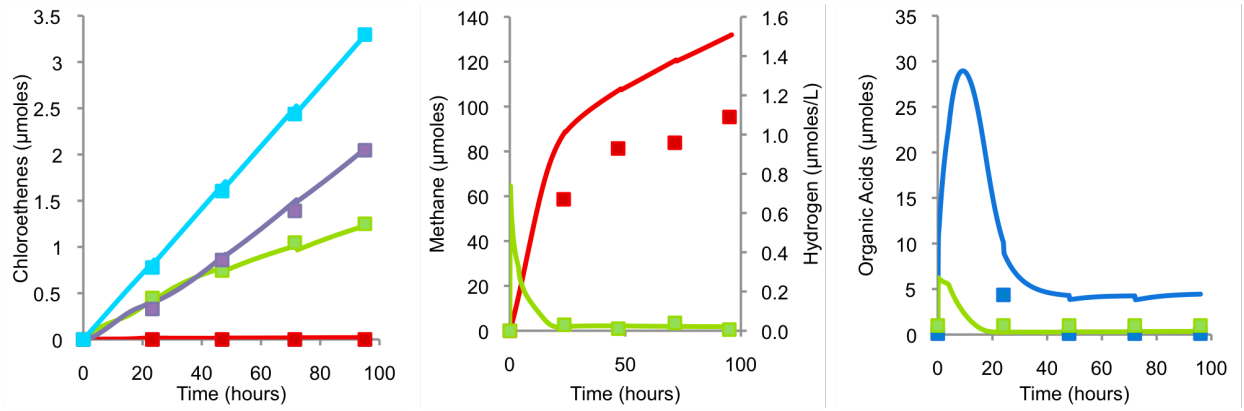

Q D3A2

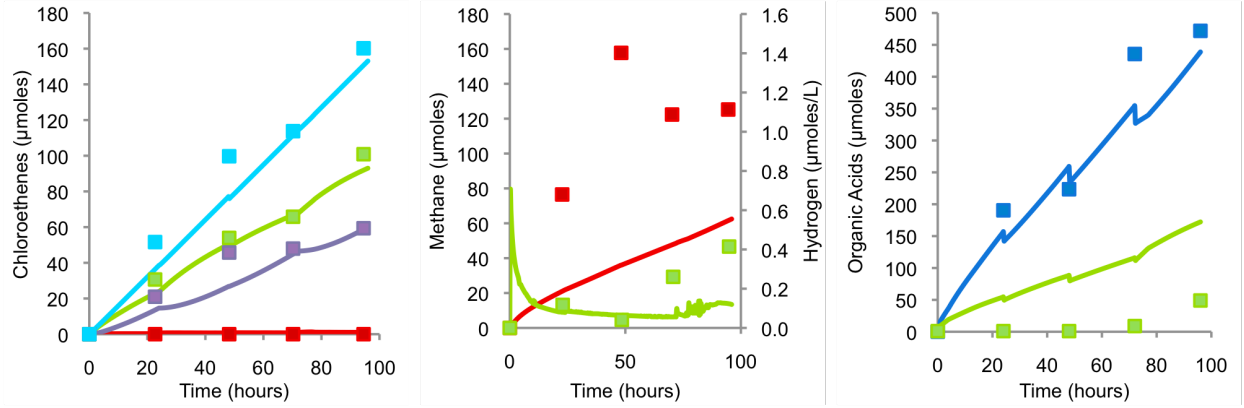

R D3B2

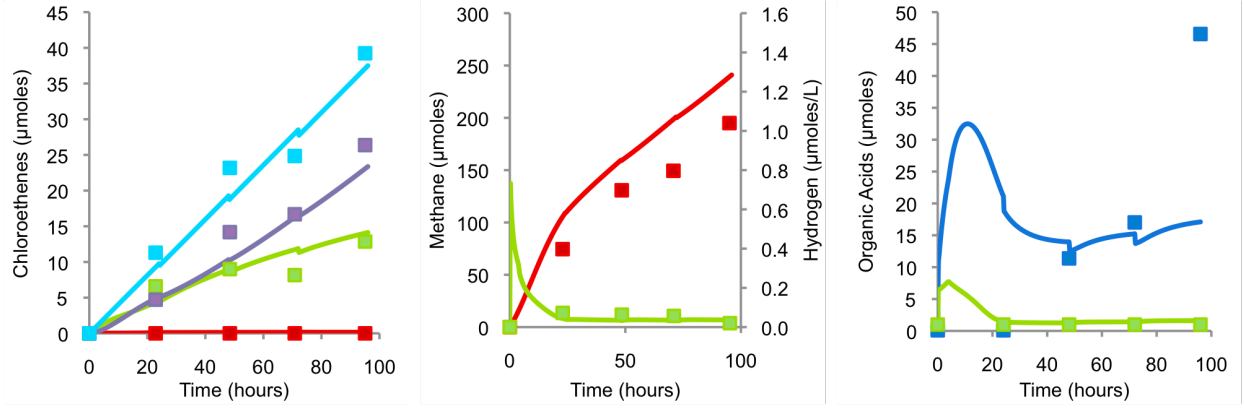

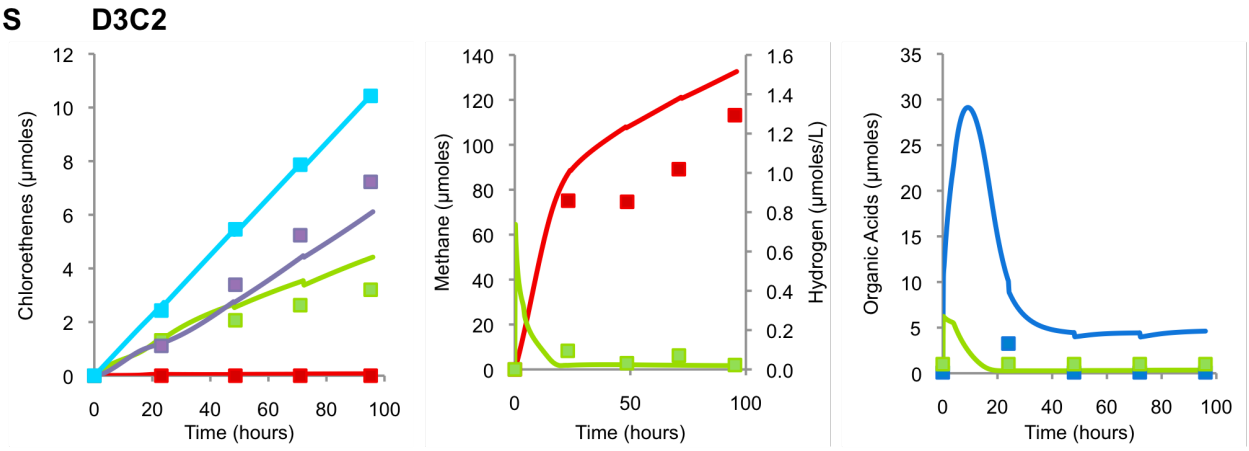

Figure A1. 6. Model fits for experiments listed in Table A1.1. On the left panels, metabolites are colored as follows: PCE (orange), TCE (dark blue), DCE (red), VC (green), ETH (purple), VC+ETH (light blue). On the middle panels, metabolites are colored as follows: methane (red) on the primary axis and hydrogen (green) on the secondary axis. For the right panels, metabolites are colored as follows: butyrate (green), acetate (blue).

A1.C. Supporting Results and Discussion

Competitive Inhibition

Supplemental Figure A1.2A presents the effect of PCE on TCE degradation. As PCE concentrations increased, TCE degradation rates remained constant, indicating that TCE dechlorination was not inhibited by PCE. Conversely, in each case, PCE was not degraded to TCE, indicating that TCE inhibits PCE degradation. Ethene was not produced in any case, however it cannot be determined from this experiment which chloroethenes inhibit VC degradation because multiple are present at any given time. Supplemental Figure A1.2B presents the effect of TCE on DCE degradation. As TCE concentrations increased, DCE degradation rates decreased (shown as production of VC), indicating that TCE inhibits DCE degradation. Ethene was not produced in any case of this experiment, indicating that DCE inhibits VC degradation (inferred from experiments where no TCE was present), and that TCE may also inhibit VC degradation. Supplemental Figure A1.2C presents the effect of PCE on VC degradation.

Respiration rates (shown as production of ETH) were equivalent whether or not PCE was present. Supplemental Figure A1.2D shows the effect of DCE on TCE degradation. As DCE concentrations increased, TCE degradation rates decreased. Supplemental Figure A1.2E shows the effect of PCE on DCE degradation. With the presence of PCE, DCE degradation decreased (shown as production of VC). Supplemental Figure A1.2F shows the effect of DCE on PCE degradation. The presence of DCE does not cause a change in the respiration rate of PCE.

A1.D. Model Equations

The equations that make up the model in the STELLA Software (ISEE Systems) are included below.

ACETATE
Mt_Acetate(t) = Mt_Acetate(t - dt) + (Acetate_Production + Acetate_Pulse_from_FYE - Sampling_Acetate - Acetate_Conversion_to_Methane - Acetate_to_Sink) * dt
INIT Mt_Acetate = Initial_Acetate

DOCUMENT: Reservoir representing acetic acid {µmol}.

INFLOWS:
Acetate_Production =
(fe_Butyrate*(Butyrate_Fermented_to_Acetate+Fermented_Myth_But)*Acetate_Formed_per_Butyrate)+(fe_Lactate*Myth_Lac_Fermented_to_Acetate*Acetate_Formed_per_Lactate)+(fe_Propionate*Propionate_Fermented_to_Acetate*Acetate_Formed_per_Propionate)+(fe_Lactate*Myth_Lac_Fermented_to_Propionate*Acetate_Formed_per_Lactate_to_Propionate)
DOCUMENT: Acetate production from all donors {µmol/hr}. Acetate Produced = Sum of {donor fermentation flow * stoichiometric conversion (HAc/Donor) * fe}. Where fe is the fraction of the donor that is used for energy.

Acetate_Pulse_from_FYE =
PULSE(YE_Acetate,Feed_Time_Donor,Feed_Increment_Time_Donor)
DOCUMENT: This is a pulse input of acetate that is contributed by FYE at each feeding {µmol}.

OUTFLOWS:
Sampling_Acetate =
PULSE(Mt_Acetate*Liquid_Waste_Rate,Waste_Pulse_Time,Waste_Increment_Time)

DOCUMENT: Ten percent (10 mL) of the liquid from the culture is wasted and replaced with 10 mL of fresh basal medium every 4 days (96 hr-dt). This decreases the amount of soluble constituents by 10 percent. Volatile constituents are not affected since they are purged out after each 96 hr period {µmol every 96 hr}.

Acetate_Conversion_to_Methane = (k_Acetate*(McrApercell/McrApercell_MAX)*X_Mt_Acetotrophs*Cw_Acetate)/(Ks_Acetate+Cw_Acetate+Ac_Inhibition*(Cw_Acetate^2)/KI_Ac)
DOCUMENT: Acetate conversion to methane {µmol/hr}.

Acetate_to_Sink = Cw_Acetate*Ks_Acetate_Sink*k_Acetate_Sink*0
Ac_Inhibition = 0
DOCUMENT: Substrate inhibition (Haldane)

Cw_Acetate = Mt_Acetate/Vw {µmol/L}
DOCUMENT: Converter to allow display of acetic acid in concentration units {µmol/L}.

Initial_Acetate = 1E-20
DOCUMENT: Initial amount of acetate present (µmol).

KI_Ac = 1047
Ks_Acetate = 9689
DOCUMENT: Half-velocity coeficient for acetate degradation. 1000 µmol/L. Ohtsubo et al., 1992; Zehnder et al., 1980.

Ks_Acetate_Sink = 1000
DOCUMENT: Half-velocity coeficient for acetate degradation. 1000 µmol/L. Ohtsubo et al., 1992; Zehnder et al., 1980.

k_Acetate = 2.55e-8 {umol/cell-hr}
DOCUMENT: Rate of acetate degradation.

k_Acetate_Sink = 6e-9
DOCUMENT: Rate of acetate degradation.

McrApercell = .392583
McrApercell_MAX = 168.3661 {Ro/mL normalized to T0 DNA}

ACETOTROPHIC METHANOGEN BIOMASS
X_Acetotrophs(t) = X_Acetotrophs(t - dt) + (Biomass_Growth_Acetotrophs - Biomass_Decay_Acetotrophs - Day_4_Waste_X_Acetotrophs) * dt
INIT X_Acetotrophs = Initial_X_Acetotrophs*Initial_Culture_Dilution {cells}

DOCUMENT: Reservoir representing acetotrophic methanogen biomass {mg VSS}.

INFLOWS:
Biomass_Growth_Acetotrophs = Y_Acetotrophs*Acetate_Conversion_to_Methane {mg VSS/hr}
OUTFLOWS:
Biomass_Decay_Acetotrophs = Decay_Acetotrophs*X_Acetotrophs {cells/hr}
Day_4_Waste_X_Acetotrophs = PULSE(X_Acetotrophs*Liquid_Waste_Rate,Waste_Pulse_Time,Waste_Increment_Time) {mg VSS wasted every 96 hr}
DOCUMENT: Ten percent (10 mL) of the liquid from the culture is wasted and replaced with 10 mL of fresh basal medium every 4 days (96 hr). This decreases the amount of soluble constituents by 10 percent. Volatile constituents are not affected since they are purged out after each 96 hr period.

Decay_Acetotrophs = 0.001 {/hr}
DOCUMENT: 0.001/hr. Generic number.

X_Cw_Acetotrophs = X_Acetotrophs/Vw {cells/L}
DOCUMENT: Converter to allow reporting of acetotrophic methanogen biomass as a concentration {mg VSS/L}.

X_Mt_Acetotrophs = X_Acetotrophs {cells}
Y_Acetotrophs = 4.19e5 {cells/umol}

BUTYRIC ACID
Mt_Butyrate(t) = Mt_Butyrate(t - dt) + (Pulse_Butyric_Acid_Feeding + Step_Butyric_Acid_Feeding + Butyrate_Pulse_from_FYE - Day_4_Waste_Butyrate - Butyrate_Fermented_to_Acetate) * dt
INIT Mt_Butyrate = Initial_Butyrate {µmol}

DOCUMENT: Reservoir representing butyric acid {µmol}.

INFLOWS:

Pulse_Butyric_Acid_Feeding =
PULSE((Pulse_Value_Butyric_Acid*Pulse_Butyrate_Feed),Feed_Time_Donor,Feed_Increment_Time_Donor)
DOCUMENT: Pulse input of butyric acid {µmol} beginning at time = 0 hr.

Step_Butyric_Acid_Feeding =
Constant_Butyrate_Feed*STEP(Step_Value_Butyric_Acid,Feed_Time_Donor)
Butyrate_Pulse_from_FYE =
PULSE(YE_Butyrate,Feed_Time_Donor,Feed_Increment_Time_Donor)
OUTFLOWS:
Day_4_Waste_Butyrate =
PULSE(Mt_Butyrate*Liquid_Waste_Rate,Waste_Pulse_Time,Waste_Increment_Time) {µmol every 96 hr}
DOCUMENT: 2.5 mL of the liquid from the culture is removed approixmately every 3 hours for DNA and RNA sampling.

Butyrate_Fermented_to_Acetate =
(k_Butyrate*X_Mt_Butyrate_Fermenters*Cw_Butyrate*Thermo_Factor_Butyrate)/(Ks_Butyrate+Cw_Butyrate)
DOCUMENT: Butyrate fermentation to acetate and hydrogen {µmol/hr}.

Constant_Butyrate_Feed = 0
Cw_Butyrate = Mt_Butyrate/Vw {µmol/L}
DOCUMENT: Converter to allow reporting of butyrate as a concentration {µmol/L}.

Initial_Butyrate = 1E-20
DOCUMENT: The inital amount of butyrate present {µmol}.

Ks_Butyrate = 260.8
DOCUMENT: Half-velocity coefficient for butyrate fermentation. 34.25 µmol/L, Fennell est., 1996.

k_Butyrate = 1.08e-8 {umol butyrate/cell-hr}
Pulse_Butyrate_Feed = 0
Pulse_Value_Butyric_Acid = 44
DOCUMENT: This is the amount of butyric acid fed at each pulse beginning at 0 hr {µmol}.

Step_Value_Butyric_Acid = 0 {umol/hr}

DECHLORINATION
Mg_DCE(t) = Mg_DCE(t - dt) + (- Volat_and_Dissol_DCE - Headspace_Purge_DCE_g) * dt
INIT Mg_DCE = 0 {µmol}

DOCUMENT: Reservoir representing DCE in the gaseous phase {µmol}.

OUTFLOWS:
Volat_and_Dissol_DCE = Inflow_Zero_DCE*Vw*Kla_DCE*((Cg_DCE/Hc_DCE)-Cw_DCE)
DOCUMENT: This biflow simulates the exchange of DCE between the gaseous and liquid phases of the bottle.

Headspace_Purge_DCE_g = PULSE(Mg_DCE,Purge_Pulse_Time,Purge_Increment_Time)
DOCUMENT: The pulse output simulates the purge of PCE in the headspace that remains undechlorinated.

Mg_ETH(t) = Mg_ETH(t - dt) + (- Volat_and_Dissol_ETH - Headspace_Purge_ETH_g) * dt
INIT Mg_ETH = 0 {µmol}

DOCUMENT: Reservoir representing ETH in the gaseous phase {µmol}.

OUTFLOWS:
Volat_and_Dissol_ETH = Inflow_Zero_ETH*Vw*Kla_ETH*((Cg_ETH/Hc_ETH)-Cw_ETH) {µmol/hr}
DOCUMENT: This biflow simulates the exchange of ETH between the gaseous and liquid phases of the bottle.

Headspace_Purge_ETH_g = PULSE(Mg_ETH,Purge_Pulse_Time,Purge_Increment_Time)
DOCUMENT: The pulse output simulates the purge of PCE in the headspace that remains undechlorinated.

Mg_PCE(t) = Mg_PCE(t - dt) + (- Volat_and_Dissol_PCE - Headspace_Purge_PCE_g) * dt
INIT Mg_PCE = 0 {µmol}

DOCUMENT: Reservoir representing PCE in the gaseous phase {µmol}.

OUTFLOWS:
Volat_and_Dissol_PCE = Inflow_Zero_PCE*Vw*Kla_PCE*((Cg_PCE/Hc_PCE)-Cw_PCE)
DOCUMENT: This biflow simulates the exchange of PCE between the gaseous and liquid phases of the bottle.

Headspace_Purge_PCE_g = PULSE(Mg_PCE,Purge_Pulse_Time,Purge_Increment_Time)
DOCUMENT: The pulse output simulates the purge of PCE in the headspace that remains undechlorinated.

Mg_TCE(t) = Mg_TCE(t - dt) + (- Volat_and_Dissol_TCE - Headspace_Purge_TCE_g) * dt
INIT Mg_TCE = 0 {µmol}

DOCUMENT: Reservoir representing TCE in the gaseous phase {µmol}.

OUTFLOWS:
Volat_and_Dissol_TCE = Inflow_Zero_TCE*Vw*Kla_TCE*((Cg_TCE/Hc_TCE)-Cw_TCE)
DOCUMENT: This biflow simulates the exchange of TCE between the gaseous and liquid phases of the bottle.

Headspace_Purge_TCE_g = PULSE(Mg_TCE,Purge_Pulse_Time,Purge_Increment_Time)
DOCUMENT: The pulse output simulates the purge of PCE in the headspace that remains undechlorinated.

Mg_VC(t) = Mg_VC(t - dt) + (- Volat_and_Dissol_VC - Headspace_Purge_VC_g) * dt
INIT Mg_VC = 0 {µmol}

DOCUMENT: Reservoir representing VC in the gaseous phase {µmol}.

OUTFLOWS:
Volat_and_Dissol_VC = Inflow_Zero_VC*Vw*Kla_VC*((Cg_VC/Hc_VC)-Cw_VC) {µmol/hr}
DOCUMENT: This biflow simulates the exchange of VC between the gaseous and liquid phases of the bottle.

Headspace_Purge_VC_g = PULSE(Mg_VC,Purge_Pulse_Time,Purge_Increment_Time)
DOCUMENT: The pulse output simulates the purge of PCE in the headspace that remains undechlorinated.

Mw_DCE(t) = Mw_DCE(t - dt) + (Volat_and_Dissol_DCE + TCE_Dechlorination_to_DCE + Constant_DCE_Feeding + Pulse_DCE_Feeding - DCE_Purge - DCE_Dechlorination_to_VC - DCE_Sampling) * dt
INIT Mw_DCE = Initial_DCE

DOCUMENT: Reservoir representing DCE in the liquid phase {µmol}.

INFLOWS:
Volat_and_Dissol_DCE = Inflow_Zero_DCE*Vw*Kla_DCE*((Cg_DCE/Hc_DCE)-Cw_DCE)
DOCUMENT: This biflow simulates the exchange of DCE between the gaseous and liquid phases of the bottle.

TCE_Dechlorination_to_DCE =
Inflow_Zero_DCE*((k_TCE*(HupLpercell/HupLpercellMAX)*X_Mt_Dechlorinators*Cw_TCE)/(Ks_TCE*TCE_Competitive_Inhibition_Term+Cw_TCE))*((Cw_H2-H2_Threshold_dechlor)/(Ks_H2_Dechlor+(Cw_H2-H2_Threshold_dechlor))) {µmol TCE converted to DCE/hr}
Constant_DCE_Feeding =
STEP(cDCE_Feed_Rate_in_umol_per_hr,Feed_Time_Electron_Acceptor)*Constant_EA_Feed {umol/hr}
Pulse_DCE_Feeding =
PULSE(Pulse_Value_DCE,Feed_Pulse_Time_EA,Feed_Increment_Time_EA)*Pulse_EA_Feed
OUTFLOWS:
DCE_Purge = PULSE(Mw_DCE,Purge_Pulse_Time,Purge_Increment_Time)
DOCUMENT: The pulse output simulates the purge of accumulated DCE from the bottle.

DCE_Dechlorination_to_VC =
Inflow_Zero_VC*((k_DCE*(HupLpercell/HupLpercellMAX)*X_Mt_Dechlorinators*Cw_DCE)/(Ks_DCE*DCE_Competitive_Inhibition_Term+Cw_DCE))*((Cw_H2-H2_Threshold_dechlor)/(Ks_H2_Dechlor+(Cw_H2-H2_Threshold_dechlor))) {µmol DCE converted to VC/hr}
DCE_Sampling =
PULSE(Liquid_Waste_Rate*Cw_DCE*Vw,Waste_Pulse_Time,Waste_Increment_Time)
Mw_ETH(t) = Mw_ETH(t - dt) + (VC_Dechlorination_to_ETH + Volat_and_Dissol_ETH - ETH_Purge - ETH_Sampling) * dt
INIT Mw_ETH = 0 {µmol}

DOCUMENT: Reservoir representing ETH in the liquid phase {µmol}.

INFLOWS:
VC_Dechlorination_to_ETH =
Inflow_Zero_ETH*((k_VC*(HupLpercell/HupLpercellMAX)*X_Mt_Dechlorinators*Cw_VC)/(Ks_VC*VC_Competitive_Inhibition_Term+Cw_VC))*((Cw_H2-H2_Threshold_dechlor)/(Ks_H2_Dechlor+(Cw_H2-H2_Threshold_dechlor))) {µmol VC converted to ETH/hr}

Volat_and_Dissol_ETH = Inflow_Zero_ETH*Vw*Kla_ETH*((Cg_ETH/Hc_ETH)-Cw_ETH)
{µmol/hr}
DOCUMENT: This biflow simulates the exchange of ETH between the gaseous and liquid phases of the bottle.

OUTFLOWS:
ETH_Purge = PULSE(Mw_ETH,Purge_Pulse_Time,Purge_Increment_Time)
DOCUMENT: The pulse output simulates the purge of accumulated ETH from the bottle.

ETH_Sampling =
PULSE(Liquid_Waste_Rate*Cw_ETH*Vw,Waste_Pulse_Time,Waste_Increment_Time)
Mw_PCE(t) = Mw_PCE(t - dt) + (Constant_PCE_Feeding + Volat_and_Dissol_PCE +
Pulse_PCE_Feeding - PCE_Purge - PCE_Dechlorination_to_TCE - PCE_Sampling) * dt
INIT Mw_PCE = Initial_PCE

DOCUMENT: Reservoir representing PCE in the liquid phase {µmol}.

INFLOWS:
Constant_PCE_Feeding =
(STEP(PCE_Feed_Rate_in_umol_per_hr,Feed_Time_Electron_Acceptor))*Constant_EA_Feed
DOCUMENT: Saturated PCE is fed continuously at 5, 10, 20, or 40 ul/min.

Volat_and_Dissol_PCE = Inflow_Zero_PCE*Vw*Kla_PCE*((Cg_PCE/Hc_PCE)-Cw_PCE)
DOCUMENT: This biflow simulates the exchange of PCE between the gaseous and liquid phases of the bottle.

Pulse_PCE_Feeding =
PULSE(Pulse_Value_PCE,Feed_Pulse_Time_EA,Feed_Increment_Time_EA)*Pulse_EA_Feed
OUTFLOWS:
PCE_Purge = PULSE(Mw_PCE,Purge_Pulse_Time,Purge_Increment_Time)
DOCUMENT: The pulse output simulates the purge of PCE that remained undechlorinated from the bottle.

PCE_Dechlorination_to_TCE =
Inflow_Zero_TCE*((k_PCE*(PCE_Tuning)*X_Mt_Dechlorinators*Cw_PCE)/(Ks_PCE*PCE_
Competitive_Inhibition_Term+Cw_PCE+PCE_Inhibition*(Cw_PCE^2)/KI_PCE))*((Cw_H2-
H2_Threshold_dechlor)/(Ks_H2_Dechlor+(Cw_H2-H2_Threshold_dechlor))) {µmol PCE
converted to TCE/hr}
PCE_Sampling =
PULSE(Liquid_Waste_Rate*Cw_PCE*Vw,Waste_Pulse_Time,Waste_Increment_Time)

Mw_TCE(t) = Mw_TCE(t - dt) + (Volat_and_Dissol_TCE + PCE_Dechlorination_to_TCE + ConstantTCE_Feeding + Pulse_TCE_Feeding - TCE_purge - TCE_Dechlorination_to_DCE - TCE_Sampling) * dt
INIT Mw_TCE = Initial_TCE

DOCUMENT: Reservoir representing TCE in the liquid phase {µmol}.

INFLOWS:
Volat_and_Dissol_TCE = Inflow_Zero_TCE*Vw*Kla_TCE*((Cg_TCE/Hc_TCE)-Cw_TCE)
DOCUMENT: This biflow simulates the exchange of TCE between the gaseous and liquid phases of the bottle.

PCE_Dechlorination_to_TCE = Inflow_Zero_TCE*((k_PCE*(PCE_Tuning)*X_Mt_Dechlorinators*Cw_PCE)/(Ks_PCE*PCE_Competitive_Inhibition_Term+Cw_PCE+PCE_Inhibition*(Cw_PCE^2)/KI_PCE))*((Cw_H2-H2_Threshold_dechlor)/(Ks_H2_Dechlor+(Cw_H2-H2_Threshold_dechlor))) {µmol PCE converted to TCE/hr}
ConstantTCE_Feeding = STEP(TCE_Feed_Rate_in_umol_per_hr,Feed_Time_Electron_Acceptor)*Constant_EA_Feed {umol/hr}
Pulse_TCE_Feeding = PULSE(Pulse_Value_TCE,Feed_Pulse_Time_EA,Feed_Increment_Time_EA)*Pulse_EA_Feed
OUTFLOWS:
TCE_purge = PULSE(Mw_TCE,Purge_Pulse_Time,Purge_Increment_Time)
DOCUMENT: The pulse output simulates the purge of accumulated TCE from the bottle.

TCE_Dechlorination_to_DCE = Inflow_Zero_DCE*((k_TCE*(HupLpercell/HupLpercellMAX)*X_Mt_Dechlorinators*Cw_TCE)/(Ks_TCE*TCE_Competitive_Inhibition_Term+Cw_TCE))*((Cw_H2-H2_Threshold_dechlor)/(Ks_H2_Dechlor+(Cw_H2-H2_Threshold_dechlor))) {µmol TCE converted to DCE/hr}
TCE_Sampling = PULSE(Liquid_Waste_Rate*Cw_TCE*Vw,Waste_Pulse_Time,Waste_Increment_Time)
Mw_VC(t) = Mw_VC(t - dt) + (Volat_and_Dissol_VC + DCE_Dechlorination_to_VC - VC_Dechlorination_to_ETH - VC_Purge - VC_Sampling) * dt
INIT Mw_VC = 0 {µmol}

DOCUMENT: Reservoir representing VC in the liquid phase {µmol}.

INFLOWS:
Volat_and_Dissol_VC = Inflow_Zero_VC*Vw*Kla_VC*((Cg_VC/Hc_VC)-Cw_VC) {µmol/hr}

DOCUMENT: This biflow simulates the exchange of VC between the gaseous and liquid phases of the bottle.

DCE_Dechlorination_to_VC =
Inflow_Zero_VC*((k_DCE*(HupLpercell/HupLpercellMAX)*X_Mt_Dechlorinators*Cw_DCE)/(Ks_DCE*DCE_Competitive_Inhibition_Term+Cw_DCE))*((Cw_H2-H2_Threshold_dechlor)/(Ks_H2_Dechlor+(Cw_H2-H2_Threshold_dechlor))) {µmol DCE converted to VC/hr}
OUTFLOWS:
VC_Dechlorination_to_ETH =
Inflow_Zero_ETH*((k_VC*(HupLpercell/HupLpercellMAX)*X_Mt_Dechlorinators*Cw_VC)/(Ks_VC*VC_Competitive_Inhibition_Term+Cw_VC))*((Cw_H2-H2_Threshold_dechlor)/(Ks_H2_Dechlor+(Cw_H2-H2_Threshold_dechlor))) {µmol VC converted to ETH/hr}
VC_Purge = PULSE(Mw_VC,Purge_Pulse_Time,Purge_Increment_Time)
DOCUMENT: The pulse output simulates the purge of accumulated VC from the bottle.

VC_Sampling =
PULSE(Liquid_Waste_Rate*Cw_VC*Vw,Waste_Pulse_Time,Waste_Increment_Time)
Actual_Total_Mass_DCE = Mg_DCE+Mw_DCE {µmol}
DOCUMENT: Mt DCE

Actual_Total_Mass_ETH = Mg_ETH+Mw_ETH {µmol}
DOCUMENT: Mt ETH

Actual_Total_Mass_PCE = Mg_PCE+Mw_PCE {µmol}
DOCUMENT: Mt PCE

Actual_Total_Mass_TCE = Mg_TCE+Mw_TCE {µmol}
DOCUMENT: Mt TCE

Actual_Total_Mass_VC = Mg_VC+Mw_VC {µmol}
DOCUMENT: Mt VC

cDCE_Concentration = 1400 {umol/L}
cDCE_Feed_Rate_in_umol_per_hr =
Feed_Rate_cDCE*60/1E6*cDCE_Concentration*Saturated_Media+Neat_DCE_Feed_Rate*Neat_EA
Cg_DCE = Mg_DCE/Vg {µmol/L}

Cg_DCE_Eq = Cw_DCE*Hc_DCE {µmol/L}
Cg_ETH = Mg_ETH/Vg {µmol/L}
Cg_ETH_Eq = Cw_ETH*Hc_ETH { µmol/L }
Cg_PCE = Mg_PCE/Vg {µmol/L}
Cg_PCE_Eq = Cw_PCE*Hc_PCE { µmol/L}
Cg_TCE = Mg_TCE/Vg {µmol/L}
Cg_TCE_Eq = Cw_TCE*Hc_TCE { µmol/L }
Cg_VC = Mg_VC/Vg {µmol/L}
Cg_VC_Eq = Cw_VC*Hc_VC {µmol/L }
Constant_EA_Feed = 0
Cw_DCE = Mw_DCE/Vw {µmol/L}
Cw_ETH = Mw_ETH/Vw {µmol/L}
Cw_PCE = Mw_PCE/Vw {µmol/L}
Cw_TCE = Mw_TCE/Vw {µmol/L}
Cw_VC = Mw_VC/Vw {µmol/L}
DCE_Competitive_Inhibition_Term = if (DCE_to_VC_Inhibition=0) then 1 else (1+(Cw_TCE/KI_TCE_on_DCE+Cw_PCE/KI_PCE_on_DCE))
DCE_to_VC_Inhibition = 0
Feed_Increment_Time_EA = 24 {hr}
Feed_Pulse_Time_EA = 0 {hr}
Feed_Rate_cDCE = 0
DOCUMENT: The rate at which cDCE is fed to the microcosm (µL/min) beginning at 0 hr until the end of the experiment.

Feed_Rate_PCE = 0
DOCUMENT: The rate at which PCE is fed to the microcosm (µL/min) beginning at 0 hr until the end of the experiment.

HupLpercell = .1
HupLpercellMAX = 20.29
Inflow_Zero_DCE = IF(Headspace_Purge_DCE_g>0)THEN(0)ELSE(1)
DOCUMENT: This converter takes a value of 1 if there is no purge occurring. It takes a value of 0 if there IS a purge event. The purpose of the converter is to zero the flow so that the stock is fully purged.

Inflow_Zero_ETH = IF(Headspace_Purge_ETH_g>0)THEN(0)ELSE(1)
DOCUMENT: This converter takes a value of 1 if there is no purge occurring. It takes a value of 0 if there IS a purge event. The purpose of the converter is to zero the flow so that the stock is fully purged.

Inflow_Zero_PCE = IF(Headspace_Purge_PCE_g>0)THEN(0)ELSE(1)

DOCUMENT: This converter takes a value of 1 if there is no purge occurring. It takes a value of 0 if there IS a purge event. The purpose of the converter is to zero the flow so that the stock is fully purged.

Inflow_Zero_TCE = IF(Headspace_Purge_TCE_g>0)THEN(0)ELSE(1)
DOCUMENT: This converter takes a value of 1 if there is no purge occurring. It takes a value of 0 if there IS a purge event. The purpose of the converter is to zero the flow so that the stock is fully purged.

Inflow_Zero_VC = IF(Headspace_Purge_VC_g>0)THEN(0)ELSE(1)
DOCUMENT: This converter takes a value of 1 if there is no purge occurring. It takes a value of 0 if there IS a purge event. The purpose of the converter is to zero the flow so that the stock is fully purged.

Initial_DCE = 0 {µmol/bottle}
Initial_ETH = 0 { µmol/Bottle }
Initial_PCE = 0 {µmol/Bottle}
Initial_TCE = 0 {µmol/Bottle}
Initial_VC = 0 {µmol/bottle}
KI_DCE_on_TCE = 2.93
KI_DCE_on_VC = 0.160
KI_PCE = 1485 {umol/L}
KI_PCE_on_DCE = 22.2
KI_TCE_on_DCE = 0.358
KI_TCE_on_PCE = 0.358
KI_TCE_on_VC = 0.358
Ks_DCE = 7.66
DOCUMENT: This value is calculated from nonlinear regressions several PSS experiments in file: Nonlinear_Regression.xls.

Ks_H2_Dechlor = 0.1
DOCUMENT: Half-velocity coefficient for H2 for dechlorination, 0.1 µmol/L, Smatlak, 1995.

Ks_PCE = 12.91
DOCUMENT: Half-velocity coefficient for PCE dechlorination, 0.54 µmol/L, Smatlak, 1995; 0.6 µmol/L, Tandoi, 1994.

This value is calculated from nonlinear regressions several PSS experiments in file: Nonlinear_Regression.xls.

Ks_TCE = .134
DOCUMENT: This value is calculated from nonlinear regressions several PSS experiments in file: Nonlinear_Regression.xls.

Ks_VC = 101
DOCUMENT: Half-velocity coefficient for VC, 290 µmol/L, Smatlak, 1995.

Estimated from relative vmax/Ks in Tandoi et al., 1994
and the k/Ks for the pure culture for PCE. 3

{µmol PCE to VC/16S DNA copies-hr}

This value is calculated from nonlinear regressions several PSS experiments in file: Nonlinear_Regression.xls and batch_03_18_09_VC_kinetics.xls.

k_DCE = 2.31E-10
DOCUMENT: Estimated from relative vmax/Ks in Tandoi et al., 1994
and the k/Ks for the pure culture for PCE. 3

{µmol PCE to VC/16S DNA copies-hr}

This value is calculated from nonlinear regressions several PSS experiments in file: Nonlinear_Regression.xls.

k_PCE = 1.98E-10
DOCUMENT: Rate of PCE dechlorination {µmol PCE to VC/16S DNA copies-hr}

1.25E-10 (Rahm, 2008)

This value is calculated from nonlinear regressions several PSS experiments in file: Nonlinear_Regression.xls.

k_TCE = 1.17E-10
DOCUMENT: Estimated from relative vmax/Ks in Tandoi et al., 1994
and the k/Ks for the pure culture for PCE. 3

{µmol PCE to VC/16S DNA copies-hr}

This value is calculated from nonlinear regressions several PSS experiments in file: Nonlinear_Regression.xls.

k_VC = 1.01E-10
DOCUMENT: Estimated from relative vmax/Ks in Tandoi et al., 1994
and the k/Ks for the pure culture for PCE. 3

{µmol PCE to VC/16S DNA copies-hr}

Estimated from relative vmax/Ks in Tandoi et al., 1994
and the k/Ks for the pure culture for PCE. 3

{µmol PCE to VC/16S DNA copies-hr}

This value is calculated from nonlinear regressions several PSS experiments in file:
Nonlinear_Regression.xls and batch_03_18_09_VC_kinetics.xls

Mass_if_HS_Meas_DCE = Cg_DCE*(Vg+(Vw/Hc_DCE)) {µmol}
DOCUMENT: Mt for DCE if determined from a direct measurement of Cg.

Mass_if_HS_Meas_ETH = Cg_ETH* (Vg+(Vw/Hc_ETH)){µmol}
DOCUMENT: Mt for ETH if determined from a direct measurement of Cg.

Mass_if_HS_Meas_PCE = Cg_PCE*(Vg+(Vw/Hc_PCE)) {µmol}
DOCUMENT: Mt for PCE if determined from a direct measurement of Cg.

Mass_if_HS_Meas_TCE = Cg_TCE*(Vg+(Vw/Hc_TCE)) {µmol}
DOCUMENT: Mt for TCE if determined from a direct measurement of Cg.

Mass_if_HS_Meas_VC = Cg_VC*(Vg+(Vw/Hc_VC)) {µmol}
DOCUMENT: Mt for VC if determined from a direct measurement of Cg.

Neat_EA = 0
Neat_PCE_Feed_Rate = 0 {umol/hour}
PCE_Competitive_Inhibition_Term = if (PCE_to_TCE_Inhibition=0) then 1 else
(1+(Cw_TCE/KI_TCE_on_PCE))
PCE_Feed_Rate_in_umol_per_hr =
Feed_Rate_PCE*60/1E6*Saturated_PCE_Concentration*Saturated_Media+Neat_PCE_Feed_Ra
te*Neat_EA
PCE_Inhibition = 0
PCE_to_TCE_Inhibition = 0
PCE_Tuning = IF (Cw_PCE < (10*Ks_PCE)) then 1 ELSE (HupLpercell/HupLpercellMAX)
Pulse_EA_Feed = 0

Pulse_Value_DCE = 0 {umoles}
Pulse_Value_PCE = 0 {umoles}
Pulse_Value_TCE = 0 {umoles}
Saturated_Media = 0
Saturated_PCE_Concentration = 393 {umol/L}
TCE_Competitive_Inhibition_Term = if (TCE_to_DCE_Inhibition=0) then 1 else (1+(Cw_DCE/KI_DCE_on_TCE))
TCE_Feed_Rate_in_umol_per_hr = Feed_Rate_TCE*60/1E6*Saturated_TCE_Concentration*Saturated_Media+Neat_TCE_Feed_Rate*Neat_EA
TCE_to_DCE_Inhibition = 0
VC_Competitive_Inhibition_Term = if (VC_to_ETH_Inhibition=0) then 1 else (1+(Cw_TCE/KI_TCE_on_VC+Cw_DCE/KI_DCE_on_VC))
VC_to_ETH_Inhibition = 0

DECHLORINATOR BIOMASS
X_Dechlorinators(t) = X_Dechlorinators(t - dt) + (Biomass_Growth_Dechlorinators - Biomass_Decay_Dechlorinators - Day_4_Waste_X_Dechlorinators) * dt
INIT X_Dechlorinators = Initial_X_Dechlorinators*Initial_Culture_Dilution

DOCUMENT: Reservoir representing dechlorinator biomass {16S DNA copies}.

INFLOWS:
Biomass_Growth_Dechlorinators = Y_Dechlorinators*(PCE_Dechlorination_to_TCE*H2_per_PCE_Dechlorinated+TCE_Dechlorination_to_DCE*H2_per_TCE_Dechlorinated+DCE_Dechlorination_to_VC*H2_per_DCE_Dechlorinated) {mg VSS/hr}
OUTFLOWS:
Biomass_Decay_Dechlorinators = Decay_Dechlorinators*X_Dechlorinators {cellss/hr}
Day_4_Waste_X_Dechlorinators = PULSE(X_Dechlorinators*Liquid_Waste_Rate,Waste_Pulse_Time,Waste_Increment_Time) {mg VSS wasted every 3 hr}
DOCUMENT: 2.5 mL of the liquid from the culture is wasted for sampling every 3 hours (3 hr-dt). This decreases the mass of soluble constituents by 2.5 percent.

Decay_Dechlorinators = 0.001 {/hr}
DOCUMENT: 0.001/hr. Generic number.

Initial_Culture_Dilution = 1
DOCUMENT: Dilution of initial culture: undiluted = 1, half = 0.5, quarter = 0.25

Initial_X_Dechlorinators = DHC_Initial_Copies/DHC_DNA_Copies_per_Cell {cells}

DOCUMENT: Initial amount of dechlorinator present (cells).

X_Cw_Dechlorinators = X_Dechlorinators/Vw {mg VSS/L}
DOCUMENT: Converter to allow reporting of dechlorinator biomass as a concentration {16S DNA copies/L}.

X_Mt_Dechlorinators = X_Dechlorinators {16S DNA copies}
Y_Dechlorinators = 1.6e8
DOCUMENT: Yield for dechlorinators. {16S DNA copies/µmol H2 used.}

1.6E8 (Rahm, 2007)

DONOR FERMENTER BIOMASS
X_Butyrate_Fermenters(t) = X_Butyrate_Fermenters(t - dt) +
(Biomass_Growth_Butyrate_Fermenters - Biomass_Decay_Butyrate_Fermenters -
Day_4_Waste_X_Butyrate_Fermenters) * dt
INIT X_Butyrate_Fermenters = Initial_X_Butyrate_Fermenters*Initial_Culture_Dilution {cells}

DOCUMENT: Reservoir representing butyrate fermenter biomass {copies}.

INFLOWS:
Biomass_Growth_Butyrate_Fermenters =
Y_Butyrate_Fermenters*Butyrate_Fermented_to_Acetate {copies/hr}
OUTFLOWS:
Biomass_Decay_Butyrate_Fermenters = X_Butyrate_Fermenters*Decay_Butyrate_Fermenters
{cells/hr}
Day_4_Waste_X_Butyrate_Fermenters =
PULSE(X_Butyrate_Fermenters*Liquid_Waste_Rate,Waste_Pulse_Time,Waste_Increment_Ti
me) {copies wasted every 96 hr}
DOCUMENT: Ten percent (10 mL) of the liquid from the culture is wasted and replaced with 10 mL of fresh basal medium every 4 days (96 hr-dt). This decreases the amount of soluble constituents by 10 percent. Volatile constituents are not affected since they are purged out after each 96 hr period.

Decay_Butyrate_Fermenters = 0.001 {/hr}
DOCUMENT: 0.001/hr. Generic number.

Fermenters_DNA_Copies_per_Cell = 3
DOCUMENT: The number of copies of the 16S gene per cell.

Fermenters_Initial_Copies = 4.93e9 {copies in 100 mL}
DOCUMENT: Initial copies of 16S gene in 100 mL of culture.

Initial_X_Butyrate_Fermenters = Fermenters_Initial_Copies/Fermenters_DNA_Copies_per_Cell {cells}
DOCUMENT: Initial amount of butyrate fermenter biomass present (copies).

X_Cw_Butyrate_Fermenters = X_Butyrate_Fermenters/Vw {cells/L}
DOCUMENT: Converter to allow reporting of butyrate fermenter biomass as a concentration {copies/L}.

X_Mt_Butyrate_Fermenters = X_Butyrate_Fermenters {cells}
Y_Butyrate_Fermenters = 1.26E6 {cells/umol butyrate}
DOCUMENT: Yield for butyrate fermenters.

GLOBAL INPUTS
Butyrate_µeq_per_µmol = 4 {µeq/µmol HBu}
Cw_Bicarbonate = 0.0714 {mol/L}
DOCUMENT: Bicarbonate concentration in the basal salts medium {mol/L}.

Ethanol_µeq_per_µmol = 4 {µeq/µmol EtOH}
Feed_Increment_Time_Donor = 12 {hr}
DOCUMENT: This is the increment of time {hr} between feedings.

Feed_Time_Donor = 0 {hr}
DOCUMENT: The pulse feed time is the time {hr} at which the first feed pulse occurs.

Feed_Time_Electron_Acceptor = 0 {hr}
DOCUMENT: The time {hr} when the first input of electron acceptor occurs.

g_CH4 = 10^(Salt_Out_CH4*Ionic_Strength)
DOCUMENT: Activity coefficent for the nonionic compound, CH4.

g_H2 = 10^(Salt_Out_H2*Ionic_Strength)
DOCUMENT: Activity coefficent for the nonionic compound, H2.

g_ionic_Z1 = 10^(-(0.5*Z^2*Ionic_Strength^0.5)/(1+Ionic_Strength^0.5))
DOCUMENT: Activity coefficient for ionic compounds with a charge of 1. Calculated using the Guntelburg approximation.

H2_Threshold_dechlor = 0.0015 {µmol/L}
DOCUMENT: Estimate, Fennell, 1997 from FYE- or non-fed cultures.

H2_Threshold_meth = 0.008 {µmol/L}
DOCUMENT: Estimate, Fennell, 1997.

H2_Threshold_unknown_sink = 0.0001 {µmol/L}
Hc_CH4 = 33.1
DOCUMENT: pseudo-dimensionless, DiStefano, 1992

Hc_DCE = 0.190
DOCUMENT: dimensionless, for cis-1,2-DCE, 30C

Hc_ETH = 9
DOCUMENT: pseudo-dimensionless, DiStefano, 1992

Hc_H2 = 52.7
DOCUMENT: Young, 1981

Hc_PCE = 0.917
DOCUMENT: dimensionless, 30C

Hc_TCE = 0.491
DOCUMENT: dimensionless, 30C

Hc_VC = 1.264
DOCUMENT: dimensionless, 30C

Ionic_Strength = 0.0856
DOCUMENT: Estimated for the basal salts medium {eq/L}.

Kla_CH4 = 50 {/hr}
DOCUMENT: Smatlak, 1995

Kla_DCE = 38.2 {/hr}
DOCUMENT: Estimated from the molar volume and Equation 9-26 of Schwarzenbach et al., 1993, and the relationship developed by Smatlak, 1995. 38.2 (/hr)

Kla_ETH = 60 {/hr}
DOCUMENT: Smatlak, 1995 60 (/hr)

Kla_H2 = 69.3 {/hr}
DOCUMENT: Smatlak, 1995

Kla_PCE = 25 {/hr}
DOCUMENT: Smatlak, 1995 25 (/hr)

Kla_TCE = 36 {/hr}
DOCUMENT: Estimated from the molar volume and Equation 9-26 of Schwarzenbach et al., 1993, and the relationship developed by Smatlak, 1995. 36 (/hr)

Kla_VC = 40 {/hr}
DOCUMENT: Smatlak, 1995 40 (/hr)

Lactate_ueq_per_umol = 4 {µeeq/µmol Lac}
Liquid_Waste_Rate = 0.025
DOCUMENT: 2.5 mL of the liquid is removed for sampling.

PCE_µeq_per_µmol = 8 {µeq/µmol PCE}
pH = 7.3
DOCUMENT: Typical pH of the system.

Propionate_µeq_per_µmol = 6 {µeq/µmol Prop}
Purge_Increment_Time = 24 {hours}

DOCUMENT: Time increment for purging the bottles.

Purge_Pulse_Time = 24 {hours}
DOCUMENT: Time at which the first purge occurs.

R = 0.00831441 {kJ/mol-K}
DOCUMENT: For thermodynamic calculations.

R2 = 0.082054 {L-atm/mol-K}
DOCUMENT: To convert Cg (μmol/L) to partial pressure (atm).

Salt_Out_CH4 = 0.135 {L/mol}
DOCUMENT: Salt effect parameter for CH4 in aqueous NaCl solution from a review of various studies. In Solubility Data Series, Vol 27/28, Methane, C.L. Young, editor, 1987, Pergamon Press, page 70.

Salt_Out_H2 = 0.102 {L/mol}
DOCUMENT: Salt effect parameter for H2 in aqueous NaCl solution from a review of various studies. In Solubility Data Series, Vol 5/6, Hydrogen and Deuterium, C.L. Young, editor, 1981, Pergamon Press, page 32.

Temp = 308.15 {K}
DOCUMENT: Temperature, K

Vg = 0.12 {L}
DOCUMENT: Volume {L} of the gaseous headspace of the serum bottle

Vw = 0.1 {L}
DOCUMENT: Volume {L} of the aqueous contents of the serum bottle.

Waste_Increment_Time = 3 {hr}
DOCUMENT: This is the time {hr} that elapses between wasting events.

Waste_Pulse_Time = 0 {hr}
DOCUMENT: This is the initial time {hr} at which all sampling events occur. The waste event occurs just prior to feeding, that's why the event is set at 3-dt.

YE_HAc_µmol_per_uL = 0.0689 {µmol Acetic acid/uL YE added}
DOCUMENT: Acetic acid produced by addition of YE .

YE_HBu_µmol_per_uL = 0.0665 {µmol Butyric acid/uL YE added}
DOCUMENT: Butyric acid produced by YE added. Table 5.12 of Donna's thesis.

YE_Prop_µmol_per_uL = 0.0160 {µmol Propionic acid/uL YE }
DOCUMENT: Propionic acid formed from YE addition.

YE_µeq_per_uL = 2.03 {µeq contributed/ mg YE }
DOCUMENT: The amount of reducing equivalents added by YE . From 1/18/10 batch experiment (and 3/4/09 no donor PSS) (1.03 ueeq/ul). It was assumed that 10% of reduction equivalents were channelled to synthesis. (1.14*0.9=1.03)

Z = 1
DOCUMENT: Charge on ionic species

HYDROGEN
Mt_Hydrogen(t) = Mt_Hydrogen(t - dt) + (Hydrogen_Production + Pulse_Hydrogen_Feeding + Step_Hydrogen_Feeding - H2_For_Dechlorination - H2_For_Methanogenesis - Purging_H2 - H2_for_Unknown_Sink - Sampling_Hydrogen) * dt
INIT Mt_Hydrogen = Initial_H2

DOCUMENT: This reservoir represents all gaseous and aqueous hydrogen plus the aqueous formate that is in equilibrium with the aqueous hydrogen.

INFLOWS:
Hydrogen_Production = (fe_Butyrate*(Butyrate_Fermented_to_Acetate+Fermented_Myth_But)*H2_per_Butyrate_Fermented_to_Acetate)+(fe_Lactate*Myth_Lac_Fermented_to_Acetate*H2_per_Lactate_Fermented_to_Acetate)+(fe_Propionate*Propionate_Fermented_to_Acetate*H2_per_Propionate__Fermented_to_Acetate) {µmol/hr}
DOCUMENT: Hydrogen production from all donors.
Hydrogen Produced = Sum of {donor fermentation flow * stoichiometric conversion (H2/Donor) * fe}
Where fe is the fraction of the donor that is used for energy.

Pulse_Hydrogen_Feeding =
PULSE(Pulse_Value_Hydrogen,Feed_Time_Donor,Feed_Increment_Time_Donor)
Step_Hydrogen_Feeding =
Constant_Hydrogen_Feed*STEP(Step_Value_Hydrogen,Feed_Time_Donor)
OUTFLOWS:
H2_For_Dechlorination =
(PCE_Dechlorination_to_TCE*H2_per_PCE_Dechlorinated+TCE_Dechlorination_to_DCE*H2_per_TCE_Dechlorinated+DCE_Dechlorination_to_VC*H2_per_DCE_Dechlorinated+VC_Dechlorination_to_ETH*H2_per_VC_Dechlorinated)/fe_H2_to_Dechlorination {µmol/hr}
H2_For_Methanogenesis = (k_H2_methane*X_Mt_Hydrogenotrophic_Methanogens*(Cw_H2-H2_Threshold_meth))/(Ks_H2_methane+(Cw_H2-H2_Threshold_meth)) {µmol/hr}
Purging_H2 = PULSE(Mt_Hydrogen,Purge_Pulse_Time,Purge_Increment_Time) {µmol wasted every 96 hr}
DOCUMENT: The pulse output simulates the purge of hydrogen from the bottle every 4 days (96 hr-dt).

H2_for_Unknown_Sink = Cw_H2*k_H2_Unknown_Sink*Initial_Culture_Dilution
Sampling_Hydrogen =
PULSE(Cw_H2*Liquid_Waste_Rate*Vw,Waste_Pulse_Time,Waste_Increment_Time) {µmol wasted or sampled}
Cg_H2 = Mt_Hydrogen/((Vw/Hc_H2)+Vg) {µmol/L}
Constant_Hydrogen_Feed = 2 {umol/hr}
Cw_H2 = Mt_Hydrogen/(Vw+(Hc_H2*Vg)) {µmol/L}
fe_H2_to_Dechlorination = 0.9023
DOCUMENT: fe -- fraction of hydrogen used for energy

H2_atm = Cg_H2*R2*Temp/1E6 {atm}
H2_per_DCE_Dechlorinated = 1 {µmol Hydrogen/µmol DCE converted to VC}
H2_per_PCE_Dechlorinated = 1 {µmol Hydrogen/µmol PCE converted to TCE}
H2_per_TCE_Dechlorinated = 1 {µmol Hydrogen/µmol TCE converted to DCE}
H2_per_VC_Dechlorinated = 1 {µmol Hydrogen/µmol VC Dechlorinated to ETH }
Initial_H2 = 1E-20 {µmol/bottle }
Ks_H2_methane = 0.5
DOCUMENT: Half-velocity coefficient for hydrogen conversion to methane. An average value of 0.96 µmol/L was reported by Smatlak, 1995; however, a slightly lower value was used for modeling.

k_H2_methane = 9.41e-10 {µmol H2/cell-hr}
k_H2_Unknown_Sink = 1
Pulse_Value_Hydrogen = 0
DOCUMENT: This is the amount of hydrogen fed {µmol} at each pulse beginning at 0 hr and occurring every 48 hr.

Step_Value_Hydrogen = 0.5

HYDROGENOTROPHIC METHANOGEN BIOMASS
X_Hydrogenotrophic_Methanogens(t) = X_Hydrogenotrophic_Methanogens(t - dt) +
(Biomass_Growth_Hydrogenotrophic_Methanogens -
Biomass_Decay_Hydrogenotrophic_Methanogens -
Day_4_Waste_X_Hydrogenotrophic_Methanogens) * dt
INIT X_Hydrogenotrophic_Methanogens =
Initial_X_Hydrogenotrophic_Methanogens*Initial_Culture_Dilution {cells}

DOCUMENT: Reservoir representing hydrogenotrophic methanogen biomass {mg VSS}.

INFLOWS:
Biomass_Growth_Hydrogenotrophic_Methanogens =
Y_Hydrogenotrophic_Methanogens*H2_For_Methanogenesis {cells/hr}
OUTFLOWS:
Biomass_Decay_Hydrogenotrophic_Methanogens =
Decay_Hydrogenotrophic_Methanogens*X_Hydrogenotrophic_Methanogens {cells/hr}
Day_4_Waste_X_Hydrogenotrophic_Methanogens =
PULSE(X_Hydrogenotrophic_Methanogens*Liquid_Waste_Rate,Waste_Pulse_Time,Waste_Increment_Time) {mg VS wasted every 96 hr}
DOCUMENT: Ten percent (10 mL) of the liquid from the culture is wasted and replaced with 10 mL of fresh basal medium every 4 days (96 hrs). This decreases the amount of soluble constituents by 10 percent. Volatile constituents are not affected since they are purged out after each 96 hr period.

Decay_Hydrogenotrophic_Methanogens = 0.001 {/hr}
DOCUMENT: 0.001/hr. Generic number.

Hydrogenotrophic_Methanogens_DNA_Copies_per_Cell = 4
DOCUMENT: The number of copies of the 16S gene per cell.

Initial_X_Hydrogenotrophic_Methanogens =
Hydrogenotrophic_Methanogens_Initial_Copies/Hydrogenotrophic_Methanogens_DNA_Copies_per_Cell {cells}
DOCUMENT: Initial amount of hydrogenotrophic methanogen biomass present (DNA copies). 4 copies/cell

X_Cw_Hydrogenotrophic_Methanogens = X_Hydrogenotrophic_Methanogens/Vw {cells/L}

DOCUMENT: Converter to allow reporting of hydrogenotrophic methanogen biomass as a concentration (mg VSS/L).

X_Mt_Hydrogenotrophic_Methanogens = X_Hydrogenotrophic_Methanogens {cells}
Y_Hydrogenotrophic_Methanogens = 6.08e7 {cells/umol}

METHANE FROM ACETATE
Mt_Methane_From_Acetate(t) = Mt_Methane_From_Acetate(t - dt) +
(Methane_Production_From_Acetate - Purging_Methane_from_Acetate -
Sampling_Methane_from_Acetate) * dt
INIT Mt_Methane_From_Acetate = Initial_Methane/2

DOCUMENT: Reservoir representing methane formed by acetotrophic methanogens {µmol}.

INFLOWS:
Methane_Production_From_Acetate =
Inflow_Zero_Methane_From_Acetate*Acetate_Conversion_to_Methane*fe_Acetate
DOCUMENT: Methane production from acetate. Methane Produced = {HAc to Methane flow * fe}. Where fe is the fraction of the donor that is used for energy.

OUTFLOWS:
Purging_Methane_from_Acetate =
PULSE(Mt_Methane_From_Acetate,Purge_Pulse_Time,Purge_Increment_Time)
DOCUMENT: The pulse output simulates the purge of methane formed from acetate from the bottle.

Sampling_Methane_from_Acetate =
PULSE(Cw_Methane_From_Acetate*Liquid_Waste_Rate*Vw,Waste_Pulse_Time,Waste_Increment_Time)
Cg_Methane_From_Acetate = Mt_Methane_From_Acetate/((Vw/Hc_CH4)+Vg) {µmol/L}
Cw_Methane_From_Acetate = Mt_Methane_From_Acetate/(Vw+(Hc_CH4*Vg)) {µmol/L}
fe_Acetate = 0.9582
DOCUMENT: fe -- fraction of acetate for energy

Inflow_Zero_Methane_From_Acetate =
IF(Purging_Methane_from_Acetate>0)THEN(0)ELSE(1)
DOCUMENT: This converter takes a value of 1 if there is no purge occurring. It takes a value of 1E-20 if there IS a purge event. The purpose of the converter is to zero the flow so that the stock is fully purged.

METHANE FROM HYDROGEN
Mt_Methane_From_H2(t) = Mt_Methane_From_H2(t - dt) + (Methane_Production_From_H2 - Purging_Methane_From_H2 - Sampling_Methane_from_H2) * dt
INIT Mt_Methane_From_H2 = Initial_Methane/2

DOCUMENT: Reservoir representing methane produced by hydrogenotrophic methanogens {µmol}.

INFLOWS:
Methane_Production_From_H2 = Inflow_Zero_Methane_From_H2*fe_H2*H2_For_Methanogenesis*H2_To_CH4_Molar_Conversion_Factor {µmol/hr}
DOCUMENT: Methane production from hydrogen. Methane Produced = {H2 for Methanogenesis * stoichiometric conversion (CH4/H2) * fe}. Where fe is the fraction of the donor that is used for energy.

OUTFLOWS:
Purging_Methane_From_H2 = PULSE(Mt_Methane_From_H2,Purge_Pulse_Time,Purge_Increment_Time)
DOCUMENT: The pulse output simulates the purge of methane formed from hydrogen from the bottle.

Sampling_Methane_from_H2 = PULSE(Cw_Methane_From_H2*Liquid_Waste_Rate*Vw,Waste_Pulse_Time,Waste_Increment_Time)
Cg_Methane_from_H2 = Mt_Methane_From_H2/((Vw/Hc_CH4)+Vg) {µmol/L}
Cw_Methane_From_H2 = Mt_Methane_From_H2/(Vw+(Hc_CH4*Vg)) {µmol/L}
fe_H2 = 0.8877
DOCUMENT: fe -- fraction of hydrogen used for energy

H2_to_CH4_Molar_Conversion_Factor = 0.25 {µmol CH4 Formed per µmol H2}
Inflow_Zero_Methane_From_H2 = IF(Purging_Methane_From_H2>0)THEN(0)ELSE(1)
DOCUMENT: This converter takes a value of 1 if there is no purge occurring. It takes a value of 0 if there IS a purge event. The purpose of the converter is to zero the flow so that the stock is fully purged.

MYTHICAL FERMENTABLE SUBSTRATE POOL

Mythical_Fermentable_Butyrate(t) = Mythical_Fermentable_Butyrate(t - dt) + (Pulse_YE_But_Feed + Endogenous_Decay_to_Butyrate - Fermented_Myth_But - But_Waste) * dt
INIT Mythical_Fermentable_Butyrate = 0

INFLOWS:
Pulse_YE_But_Feed = PULSE(Fraction_of_YE_pool_treated_as_butyrate*YE_Unknown/Butyrate_µeq_per_µmol,Feed_Time_Donor,Feed_Increment_Time_Donor)
Endogenous_Decay_to_Butyrate = (Total_Biomass_Decay)*fraction_decaying_biomass_to_mythical_pools*1000/mg_VSS_per_mmol_VSS*Endog_Decay*Fraction_of_ED_pool_treated_as_butyrate {µmol/hr}
OUTFLOWS:
Fermented_Myth_But = (k_Butyrate*X_Mt_Butyrate_Fermenters*Cw_Myth_But*Thermo_Factor_Butyrate)/(Ks_Butyrate+Cw_Myth_But)
But_Waste = PULSE(Mythical_Fermentable_Butyrate*Liquid_Waste_Rate,Waste_Pulse_Time,Waste_Increment_Time) {µmol every 96 hr}
Mythical_Fermentable_Lactate(t) = Mythical_Fermentable_Lactate(t - dt) + (Pulse_YE_Lac_Feed + Endogenous_Decay_to_Lactate - Lac_Waste - Myth_Lac_Fermented_to_Acetate - Myth_Lac_Fermented_to_Propionate) * dt
INIT Mythical_Fermentable_Lactate = 0

INFLOWS:
Pulse_YE_Lac_Feed = PULSE(Fraction_of_YE_pool_treated_as_lactate*YE_Unknown/Lactate_ueq_per_umol,Feed_Time_Donor,Feed_Increment_Time_Donor)
Endogenous_Decay_to_Lactate = (Total_Biomass_Decay)*fraction_decaying_biomass_to_mythical_pools*1000/mg_VSS_per_mmol_VSS*Endog_Decay*Fraction_of_ED_pool_treated_as_lactate {µmol/hr}
OUTFLOWS:
Lac_Waste = PULSE(Mythical_Fermentable_Lactate*Liquid_Waste_Rate,Waste_Pulse_Time,Waste_Increment_Time) {µmol every 96 hr}
Myth_Lac_Fermented_to_Acetate = (k_Lactate_to_Acetate*X_Mt_Butyrate_Fermenters*Cw_Myth_Lac*Thermo_Factor_Lac_to_Acetate)/(Ks_Lactate_to_Acetate+Cw_Myth_Lac)
Myth_Lac_Fermented_to_Propionate = (k_Lactate_to_Propionate*X_Mt_Butyrate_Fermenters*Cw_Myth_Lac*Thermo_Factor_Lactate_to_Propionate)/(Ks_Lactate_to_Propionate+Cw_Myth_Lac)
Ac_Methanogens_mgVSS_per_cell = 4.37e-10 {mgVSS/cell}
DOCUMENT: Calculated in file protein_to_cell_conversion.xls

Constant_Endogenous_Decay = 0

Const_End_Decay = 0.006815
Cw_Myth_But = Mythical_Fermentable_Butyrate/Vw {µmol/L}
Cw_Myth_Lac = Mythical_Fermentable_Lactate/Vw {µmol/L}
Dechlroinators_mgVSS_per_cell = 2.688e-11 {mgVSS/cell}
DOCUMENT: Calculated in file protein_to_cell_conversion.xls

Endog_Decay = 0
Fermenters_mgVSS_per_cell = 7.855e-10 {mgVSS/cell}
DOCUMENT: Calculated in file protein_to_cell_conversion.xls

fraction_decaying_biomass_to_mythical_pools = .5
Fraction_of_ED_pool_treated_as_butyrate = 0
Fraction_of_ED_pool_treated_as_lactate = 1-Fraction_of_ED_pool_treated_as_butyrate
Fraction_of_YE_pool_treated_as_butyrate = .5
Fraction_of_YE_pool_treated_as_lactate = 1-Fraction_of_YE_pool_treated_as_butyrate
H2_Methanogens_mgVSS_per_cell = 5.998e-10 {mgVSS/cell}
DOCUMENT: Calculated in file protein_to_cell_conversion.xls

Ks_Lactate_to_Acetate = 2.5
DOCUMENT: Half-velocity coefficient for lactate fermentation. 2.52 µmol/L, Fennell, est., 1996. 4x for 25C

Ks_Lactate_to_Propionate = 2.5
k_Lactate_to_Acetate = 1.7e-9
DOCUMENT: Apparent rate of lactate degradation was 2.67 {µmol lactate/mg VSS-hr, est., Fennell}.

This occurred under a thermodynamic ceiling (ave) of -50 kJ/mol lactate fermented (on average) for the 1:1 TISs and -50 kJ/mol for the 2:1 TISs. Delta G critical was set at -19 kJ/mol and the thermo factor was calculated for each condition. There is less lactate-degrader biomass than the total VSS measured. From my biomass estimates the lactate degraders make up 27.4 % for 1:1 TISs and 33.9 % for 2:1 TISs, of the total biomass in the bottle.

The rate that would be observed in the absence of a thermodynamic limit and accounting for the fraction of relevant biomass is:
rate = apparent rate/(thermo factor*fraction of relevant VSS).

AVE k = 8.57 µmol/mg lactate VSS-hr Halved for 25C

k_Lactate_to_Propionate = 1.7e-9
mg_VSS_per_mmol_VSS = 113.12 { mg VSS/mmol C5H7O2N }

Total_Biomass_Decay =
(Biomass_Decay_Acetotrophs*Ac_Methanogens_mgVSS_per_cell+Biomass_Decay_Butyrate_Fermenters*Fermenters_mgVSS_per_cell+Biomass_Decay_Dechlorinators*Dechlroinators_mgVSS_per_cell+Biomass_Decay_Hydrogenotrophic_Methanogens*H2_Methanogens_mgVSS_per_cell)*Variable_Endognenous_Decay+Const_End_Decay*Constant_Endogenous_Decay
DOCUMENT: Default is 0.005958

Variable_Endognenous_Decay = 0

PROPIONIC ACID
Mt_Propionate(t) = Mt_Propionate(t - dt) + (Propionate_Production + Propionic_Acid_Feeding - Day_4_Waste_Propionate - Propionate_Fermented_to_Acetate) * dt
INIT Mt_Propionate = Initial_Propionate {µmol}

DOCUMENT: Reservoir representing propionic acid {µmol}.

INFLOWS:
Propionate_Production =
fe_Lactate*Myth_Lac_Fermented_to_Propionate*Propionate_Formed_per_Lactate
DOCUMENT: Propionate production from all donors. Propionate Produced = Sum of {donor fermentation flow * stoichiometric conversion (Prop/Donor) * fe}. Where fe is the fraction of the donor that is used for energy.

Propionic_Acid_Feeding =
PULSE((Pulse_Value_Propionic_Acid+YE_Propionate),Feed_Pulse_Time_Donor,Feed_Increment_Time)
DOCUMENT: Pulse input of propionic acid {µmol} beginning at time = 0 hr and occurring every 48 hr thereafter.

OUTFLOWS:
Day_4_Waste_Propionate =
PULSE(Mt_Propionate*Liquid_Waste_Rate,Waste_Pulse_Time,Waste_Increment_Time)
DOCUMENT: Ten percent (10 mL) of the liquid from the culture is wasted and replaced with 10 mL of fresh basal medium every 4 days (96 hr). This decreases the amount of soluble constituents by 10 percent. Volatile constituents are not affected since they are purged out after each 96 hr period. Units are µmol every 96 hr.

Propionate_Fermented_to_Acetate =
(k_Propionate*X_Mt_Butyrate_Fermenters*Cw_Propionate*Thermo_Factor_Propionate)/(Ks_Propionate+Cw_Propionate) {µmol/hr}
Cw_Propionate = Mt_Propionate/Vw {µmol/L}

DOCUMENT: Converter to allow reporting of propionic acid as a concentration {µmol/L}.

Feed_Increment_Time = 1000 {hr}
DOCUMENT: This is the increment of time {hr} between feedings.

Feed_Pulse_Time_Donor = 0 {hr}
DOCUMENT: The pulse feed time is the time {hr} at which the first feed pulse occurs.

Initial_Propionate = 1E-20
DOCUMENT: Initial amount of propionate present (µmol).

Ks_Propionate = 11.3
DOCUMENT: Half-velocity coefficient for propionate fermentation. 11.3 µmol/L Fennell, est. 1996. 4x for 25C

k_Propionate = 4.4e-10 {umol/cell-hr}
DOCUMENT: Apparent rate of propionate degradation was 0.096 {µmol propionate/mg VSS-hr, est., Fennell}.

This occurred under a thermodynamic ceiling (ave) of -20 kJ/mol propionate fermented (on average) for the 1:1 TISs and -27 kJ/mol for the 2:1 TISs. Delta G critical was set at -19 kJ/mol and the thermo factor was calculated for each condition. There is less propionate-degrader biomass than the total VSS measured. From my biomass estimates the propionate degraders make up 6.2 % for 1:1 TISs and 6.5% for 2:1 TISs, of the total biomass in the bottle.

The rate that would be observed in the absence of a thermodynamic limit and accounting for the fraction of relevant biomass is:
rate = apparent rate/(thermo factor*fraction of relevant VSS).

AVE k = 2.21 µmol/mg propionate VSS-hr Halved for 25C

Propionate_Formed_per_Lactate = (2/3) {µmol Propionate/µmol Lactate converted to Propionate}
Pulse_Value_Propionic_Acid = 0
DOCUMENT: This is the amount of propionic acid fed {µmol} at each pulse beginning at 0 hr and occurring every 48 hr.

THERMODYNAMICS
Cw_Hydrogen_Ion = 10^-pH
delta_G_critical_Butyrate = -19 {kJ/mol butyrate}
DOCUMENT: The maximum value that delta G can acquire that still provides the organism with enough energy to make ATP. Analysis of butyrate data--degradation proceeds at delta G values of -20 kJ/mol butyrate. Arbitrarily used a value 5 % higher.

delta_G_critical_Lactate_to_Acetate = -19 {kJ/mol lactate}
DOCUMENT: The maximum value that delta G can acquire that still provides the organism with enough energy to make ATP.

delta_G_critical_Lactate_to_Propionate = -19 {kJ/mol lactate}
delta_G_critical_Propionate_to_Acetate = -19 {kJ/mol propionate}
DOCUMENT: The maximum value that delta G can acquire that still provides the organism with enough energy to make ATP. Analysis of propionate data--degradation proceeds at delta G values of -20 kJ/mol propionate. Arbitrarily used a value 5 % higher.

delta_G_rxn_Butyrate =
delta_G_zero_Butyrate+(R*Temp*LOGN((g_ionic_Z1*Cw_Hydrogen_Ion*(g_ionic_Z1*Cw_Acetate/1E6)^2*(g_H2*Cw_H2/1E6)^2)/(g_ionic_Z1*(Cw_Butyrate+Cw_Myth_But)/1E6)))
delta_G_rxn_Lactate_to_Acetate =
delta_G_zero_Lactate_to_Acetate+R*Temp*LOGN((g_ionic_Z1*Cw_Hydrogen_Ion*g_ionic_Z1*Cw_Bicarbonate*g_ionic_Z1*Cw_Acetate/1E6*(g_H2*Cw_H2/1E6)^2)/(g_ionic_Z1*Cw_Myth_Lac/1E6))
delta_G_rxn_Lactate_to_Propionate =
delta_G_zero_Lactate_to_Propionate+R*Temp*LOGN(((g_ionic_Z1*Cw_Hydrogen_Ion)^(1/3)*(g_ionic_Z1*Cw_Acetate/1E6)^(1/3)*(g_ionic_Z1*Cw_Bicarbonate)^(1/3)*(g_ionic_Z1*Cw_Propionate/1E6)^(2/3))/(g_ionic_Z1*(Cw_Myth_Lac)/1E6))
delta_G_rxn_Propionate =
delta_G_zero_Propionate+R*Temp*LOGN((g_ionic_Z1*Cw_Acetate/1E6*(g_H2*Cw_H2/1E6)^3*g_ionic_Z1*Cw_Hydrogen_Ion*g_ionic_Z1*Cw_Bicarbonate)/(g_ionic_Z1*Cw_Propionate/1E6))
{kJ/mol}
delta_G_zero_Butyrate = 123.16 {kJ/mol}
DOCUMENT: delta G zero at 35C

delta_G_zero_Lactate_to_Acetate = 71.01 {kJ/mol}
DOCUMENT: delta G zero at 35C

delta_G_zero_Lactate_to_Propionate = -40.26 {kJ/mol}
DOCUMENT: delta G zero at 35C

delta_G_zero_Propionate = 166.9 {kJ/mol}
DOCUMENT: delta G zero at 35C

one_minus_expGRT_Butyrate = 1-EXP((delta_G_rxn_Butyrate-
delta_G_critical_Butyrate)/(R*Temp))
one_minus_expGRT_Lac = 1-EXP((delta_G_rxn_Lactate_to_Acetate-
delta_G_critical_Lactate_to_Acetate)/(R*Temp))
one_minus_expGRT_Lactate_to_Propionate = 1-EXP((delta_G_rxn_Lactate_to_Propionate-
delta_G_critical_Lactate_to_Propionate)/(R*Temp))
one_minus_expGRT_Propionate = 1-EXP((delta_G_rxn_Propionate-
delta_G_critical_Propionate_to_Acetate)/(R*Temp))
Thermo_Factor_Butyrate =
IF(one_minus_expGRT_Butyrate>=0)THEN(one_minus_expGRT_Butyrate)ELSE(0)
Thermo_Factor_Lactate_to_Propionate =
IF(one_minus_expGRT_Lactate_to_Propionate>=0)THEN(one_minus_expGRT_Lactate_to_Pr
opionate)ELSE(0)
Thermo_Factor_Lac_to_Acetate =
IF(one_minus_expGRT_Lac>=0)THEN(one_minus_expGRT_Lac)ELSE(0)
Thermo_Factor_Propionate =
IF(one_minus_expGRT_Propionate>=0)THEN(one_minus_expGRT_Propionate)ELSE(0.00000
001)

YEAST EXTRACT
YE_Acetate = YE_Addition_uL*YE_HAc_µmol_per_uL {µmol Acetate added by YE}
YE_Addition_uL = 100 {mg/L}
DOCUMENT: Designates the mass YE added (mg).
Typically, the following additions were made:

	YE Addition
as nutrient source (low)	20 mg/L = 2 mg in 100 mL
as donor (high)	200 mg/L = 20 mg in 100 mL

Typical FYE acetate, propionate, butyrate, and reducing equivalents concentrations are entered in the model. These can be changed if other measurements become available.

YE_Butyrate = YE_Addition_uL*YE_HBu_µmol_per_uL {µmol butyric acid added from YE}
DOCUMENT: A measurable amount butyric acid is produced when YE is added.

YE_Propionate = YE_Addition_uL*YE_Prop_µmol_per_uL {µmol Propionate added by YE}

YE_Unknown = YE_Addition_uL*(YE_µeq_per_uL-
Butyrate_µeq_per_µmol*YE_HBu_µmol_per_uL-
Propionate_µeq_per_µmol*YE_Prop_µmol_per_uL) {unknown µeeq added from YE}
DOCUMENT: This model represents all unaccounted for reducing equivalents added by YE (excluding the reducing equivalents that are added as measurable butyric acid or propionic acid) as going to a "mythical fermentable substrate pool" that is treated with the thermodynamics of both butyrate and lactate, but does not contribute to the measureable pools of those substrates.

In this way, YE Unknown represents a pool of slowly released reducing euivalents donated by FYE that we are unable to completely quantify. Some of this is higher fatty acids, some is probably carbohydrate and protein.

Not in a sector
Acetate_Formed_per_Butyrate = 2 {µmol Acetate Formed/µmol Butyrate Fermented to Acetate}
Acetate_Formed_per_Lactate = 1 {µmol Acetate formed/µmol Lactate Fermented to Acetate}
Acetate_Formed_per_Lactate_to_Propionate = (1/3) { µmol Acetate formed/µmol Lactate Fermented to Propionate }
Acetate_Formed_per_Propionate = 1 {µmol acetate formed/µmol propionate}
Acetotrophs_DNA_Copies_per_Cell = 2
DOCUMENT: The number of copies of the 16S gene per cell.

Acetotrophs_Initial_Copies = 1.13e10{copies in 100 mL}
DOCUMENT: Initial copies of 16S gene in 100 mL of culture.

Cg_Total_Methane = Cg_Methane_from_H2+Cg_Methane_From_Acetate
Cw_Total_Methane = Cw_Methane_From_H2+Cw_Methane_From_Acetate
DHC_DNA_Copies_per_Cell = 1
DOCUMENT: DHC has one copy of the 16S gene per cell.

DHC_Initial_Copies = 2.73e10 {copies in 100 mL}
DOCUMENT: Initial copies of 16S gene in 100 mL of culture.

Feed_Rate_TCE = 0
DOCUMENT: The rate at which TCE is fed to the microcosm (µL/min) beginning at 0 hr until the end of the experiment.

fe_Butyrate = 0.9753
DOCUMENT: fe -- the fraction of the donor butyrate that is used for energy

fe_Lactate = 0.9482
DOCUMENT: fe -- fraction of lactate used for energy

fe_Propionate = 0.9818
DOCUMENT: fe -- fraction of propionate used for energy

H2_per_Butyrate_Fermented_to_Acetate = 2 {µmol H2/µmol Butyrate Fermented To Acetate}
H2_per_Lactate_Fermented_to_Acetate = 2 {µmol H2/µmol Lactate Fermented to Acetate}
H2_per_Propionate__Fermented_to_Acetate = 3 {µmol H2/µmol Propionate Fermented to Acetate}
H2_Threshold_Term = ((Cw_H2-H2_Threshold_dechlor)/(Ks_H2_Dechlor+(Cw_H2-H2_Threshold_dechlor)))
Hydrogenotrophic_Methanogens_Initial_Copies = 6.78e10 {copies in 100 mL}
DOCUMENT: Initial copies of 16S gene in 100 mL of culture.

Initial_Methane = 0 {µmol/Bottle}
Initial_X_Acetotrophs = Acetotrophs_Initial_Copies/Acetotrophs_DNA_Copies_per_Cell {cells}
DOCUMENT: Initial amount of acetotrophic methanogen biomass present {DNA copies}.

Mt_Total_Methane = Mt_Methane_From_H2+Mt_Methane_From_Acetate
Neat_DCE_Feed_Rate = 0 {umol/hr}
Neat_TCE_Feed_Rate = 0 {umol/hr}
Saturated_TCE_Concentration = 810 {umol/L}
VC_Inhibition_Term = k_VC/(Ks_VC*(1+(Cw_TCE/KI_TCE_on_VC+Cw_DCE/KI_DCE_on_VC))+Cw_VC)

APPENDIX II:

Supporting Information for Chapter 3

A2.A. Supporting Tables

Table A2. 1. mRNA biomarker targets with qPCR primer sequence and annealing temperature

Strain Targeted	Gene ID	Gene Name	Annotation	Primer Sequence (5'-3')	Annealing temp.	Amplicon length	Reference
All DMC strains	DET_DE16S	16S rRNA	16S ribosomal RNA	GGAGCGTGTGGTTTAATTCGATGC (sense) GCCCAAGATATAAAGGCCATGCTG (anti-sense)	60°C	270 bp	Fung, et al., 2007
Dehalococcoides mccartyi st. 195	DET0110	HupL	[Ni/Fe] hydrogenase, group 1, large subunit (EC:1.12.99.6)	TGACGTTATTGCAGTAGCTGAGT (sense) CACACCATAGCTGAGCAGGTT (anti-sense)	55°C	82 BP	Fung, et al., 2007
All DMC strains except MB	DET1545	1545	Reductive dehalogenase, putative	CGCTGCCGAACTGGCTGAAA (sense) GTTTTTACCGGAGCGGGGTC (anti-sense)	60°C	144 bp	This study
Dehalococcoides mccartyi st. 195 and FL2	DET0079	TceA	Reductive dehalogenase	TAATATATGCCGCCACGAATGG (sense) AATCGTATACCAAGGCCCGAGG (anti-sense)	60°C	317 bp	Fung, et al., 2007
DMC strains VS and GT *Dehalococcoides* containing mixed cultures KB-1 and ANAS	DCKB1_96900	VcrA	Reductive dehalogenase	GAAAGCTCAGCCGATGACTC (sense) TGGTTGAGGTAGGGTGAAAG (anti-sense)	60°C	205 bp	Waller, et al., 2005

Table A2. 2. Long amplicon targets for qPCR standards with primer sequence and annealing temperature

Organism	Gene ID	Gene Name	Annotation	Primer Sequence	Annealing temp.	Amplicon length	Reference
Dehalococcoides mccartyi st. 195	DET_DE16S	16S rRNA	16S ribosomal RNA	GATGAACGCTAGCGGCG (sense) GGTTGGCACATCGACTTCAA (anti-sense)	50°C	1377 bp	Hendrickson et al., 2002
All DHC strains except MB	DET1545	1545	Reductive dehalogenase, putative	TCAGCCGCGTCCCTGGTG (sense) GGCTTCACCCAGACCGGC (anti-sense)	50°C	823 bp	This study
Dehalococcoides mccartyi st. 195	DET0079	TceA	Reductive dehalogenase	ACGCCAAAGTGCGAAAAGC (sense) TAATCTATTCCATCCTTTCTC (anti-sense)	50°C	1732 bp	He et al., 2003
DMC strains VS and GT *Dehalococcoides* containing mixed cultures KB-1 and ANAS	DCKB1_9690 0	VcrA	Reductive dehalogenase	CTATGAAGGCCCTCCAGATGC (sense) GTAACAGCCCCAATATGCCAAGTA (anti-sense)	50°C	1482 bp	Muller et al., 2004

Table A2. 3. 1545 peptides detected in KB-1™culture sample and the DMC strain homologs that they match. Peptides highlighted in orange are specific for the Pinellas Group, peptides highlighted in green are specific for the Cornell Group.

Peptide No.	Peptide Sequence	Spectral Count in KB-1™ Culture	Cornell Group DMC195	Victoria Group VS	Pinellas Group	
					CBDB1, GT, KB-1 Mixed Culture	FL2
13	IPLFNTYFYK	2			X	X
27	NIPLFNTYFYK	2			X	X
28	NVSLFNTYFYK	2	X			
26	NIPLFNTYFY	1			X	X
10	GTIANIPLFNTYFYK	6			X	X
9	GTIANIPLFNTY	3			X	X
14	LPLEPTHPIDAGIYR	1	X	X	X	X
21	LYGVLTDLPLEPTHPIDAGIYR	11	X	X	X	X
20	LYGVLTDLPLEPTHPIDAGIY	2	X	X	X	X
19	LYGVLTDLPLEPTHPID	1	X	X	X	X
37	TPEYGAPGR	2	X	X	X	X
36	TLTPEYGAPGRLYGVL	1	X	X	X	X
45	YTLTPEYGAPGR	2	X	X	X	X
25	LYTLTPEYGAPGRLYGVLTD	3	X	X	X	X
24	LYTLTPEYGAPGRLYGVL	1	X	X	X	X
23	LYTLTPEYGAPGRLY	1	X	X	X	X
22	LYTLTPEYGAPGR	1	X	X	X	X
30	QKLYTLTPEYGAPGR	5	X	X	X	X
46	YVGSEGGAAIMAGLGEASR	268	X	X	X	X
12	IGTIGNDARYVGSEGGAAIMAGLGEASR	5	X		X	X
31	QLIGTIGNDAR	1	X		X	X
44	YLGYQLIGTIGNDAR	136	X		X	X
32	SAGTLLGGMANGNTFYN	1			X	X
34	STQGSNELWR	1	X	X	X	X
15	LSTQGSNELWR	1	X	X	X	
11	IALSTQGSNELWR	1	X	X	X	
18	LVIPNVPLWEIALSTQGSNELWR	3	X	X	X	
17	LVIPNVPLWEIALSTQ	1	X	X	X	
16	LVIPNVPLWEIAL	1	X	X	X	
29	PIVFENVPK	1			X	X
43	YIGTTIPVTAARPIVFE	1			X	X
42	YIGTTIPVTAARPIVF	1			X	X
41	WTGTPEEASR	5	X		X	X
40	VSQGTSPGWAETK	2		X	X	
33	SNYPGYTYR	1	X	X	X	X
35	TASNYPGYTYR	12	X	X	X	X
5	ALSAAELAERTASNYPGYTYR	1	X	X	X	X
4	ALSAAELAER	7	X	X	X	X
2	AALSAAELAER	1	X	X	X	X
1	AAALSAAELAER	2	X	X	X	X

8	GAAALSAAELAER	5	X	X	X	X
39	VLGAAALSAAELAERTASNYPGYTYR	14	X	X	X	X
38	VLGAAALSAAELAER	38	X	X	X	X
3	AIYYGADR	1		X	X	X
7	ERPIDDPTIEVDF	1	X	X	X	X
6	DTAVQPRPWWVK	4	X	X	X	X

A2.B. Supporting Figures

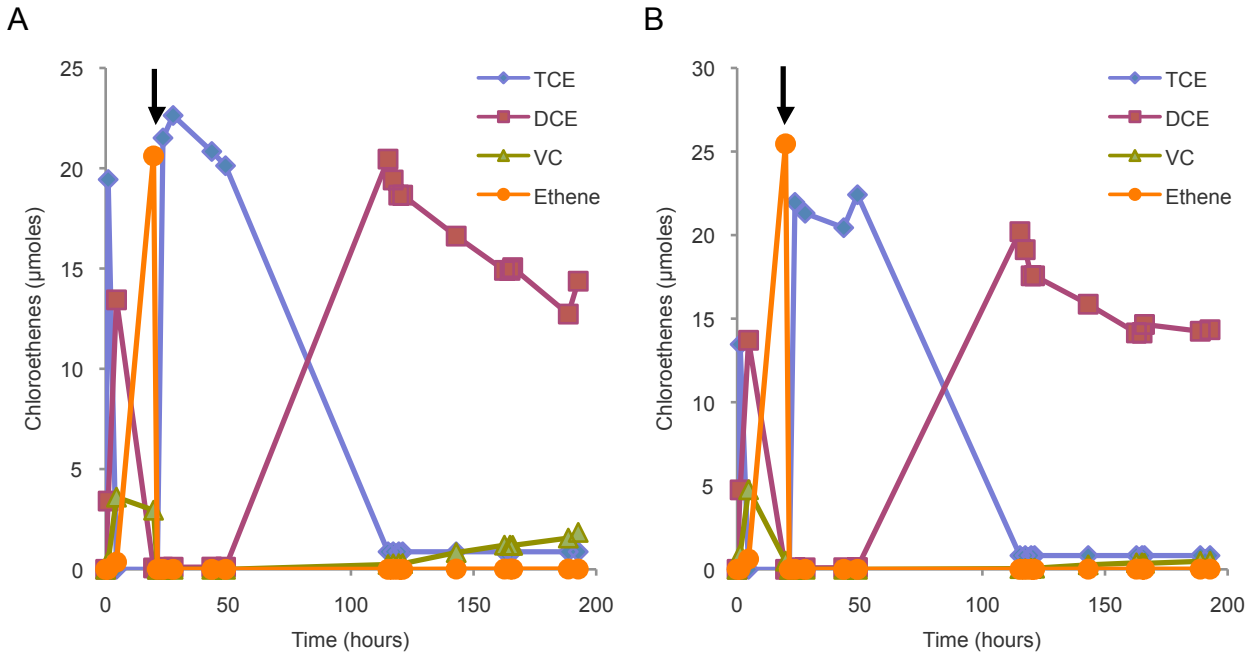

Figure A2. 1. Timecourses of chloroethene data for stressed bottles C1 (A) and C2 (B). The arrow indicates when the bottles were purged, TCE re-fed, and the oxygen was added.

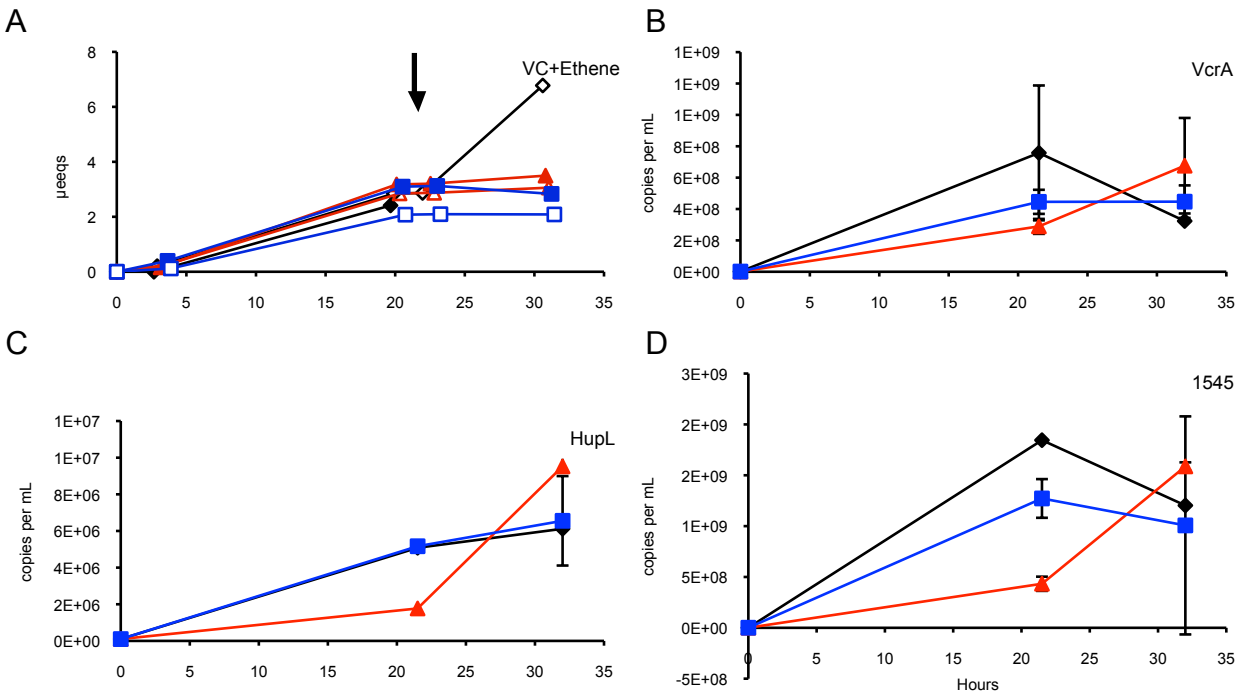

Figure A2. 2. Timecourses of metabolite and mRNA concentrations for specific targets in acid stress experiments. The control is in black, and the stressed bottles are in red (sacrificed ~12 hours after stress) and blue (sacrificed at end of the experiment). The arrow indicates when the stress was added. Error bars represent standard error of duplicate reactors.

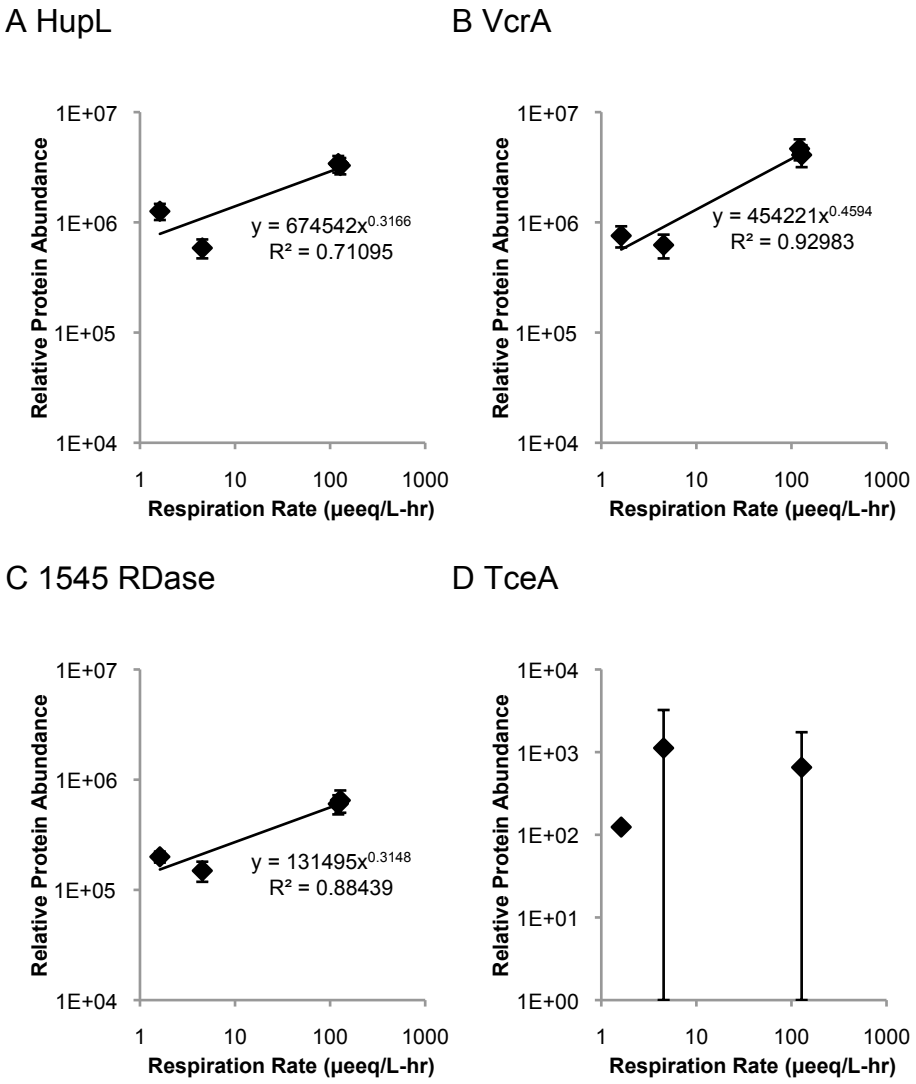

Figure A2. 3. Relative protein abundance vs. steady-state respiration rates (µeeq/L-hr): hydrogenase HupL (A); and reductive dehalogenases VcrA (B), 1545 (C), and TceA (D) for the KB-1 culture. The relative protein abundance is measured as TMT ion intensity. Error bars represent standard deviations of detected homologs. Power trend lines are displayed where appropriate. Note different scale in for TceA (D).

APPENDIX III:

Supporting Information for Chapter 4

A3.A. Supporting Tables

Table A3. 1. mRNA biomarker and long amplicon targets with primer sequence and annealing temperature.

Organism	Gene ID	Gene Name	Annotation	Primer Sequence	Annealing temp.	Amplicon length	Reference
Dehalococcoides mccartyi st. 195	DET1559	1559	Reductive dehalogenase, putative	CAATTAAAGTGGGTGGTTGGGCTG (sense) ATCTGTGCCCATATCATCTTGCGG (anti-sense)	60°C	241 bp	Fung, et al., 2007
DMC st. BAV1 and KB-1 Mixed Culture	BAV1_0847	BvcA	Reductive dehalogenase	AAAAGCACTTGGCTATCAAGGAC (sense) CCAAAAGCACCACCAGGTC (anti-sense)	60°C	92 bp	Ritalahti, et al., 2006
DMC st. BAV1 and KB-1 Mixed Culture	BAV1_0847	BvcA	Reductive dehalogenase	TGCCTCAAGTACAGGTGGT (sense) ATTGTGGAGGACCTACCT (anti-sense)	50°C	838 bp	Muller et al., 2004

Table A3.2. Proteins detected in field samples, but not in KB-1 culture sample that were identified as part of the KB-1 metagenome

		Spectral Counts				NSAF			
Protein ID	Description	PM2A2	EW1	O-BH9-A1	O-BH10-A1	PM2A2	EW1	O-BH9-A1	O-BH10-A1
2013915854	Inorganic pyrophosphatase(EC:3.6.1.1)	3	1	5	1	0.00270055	0.00152288	0.00096784	0.00043616
2013887565	Predicted metal-dependent hydrolase of the TIM-barrel fold	1	1	1	0	0.00083975	0.00142064	0.00018057	0
2013921552	ATP synthase F1 subcomplex alpha subunit	1	0	2	1	0.00432088	0	0.00185826	0.00209355
2013897406	Uncharacterized conserved protein	1	0	7	4	0.00126409	0	0.00190274	0.00244989
2013889415	Formate-tetrahydrofolate ligase (EC 6.3.4.3)	1	0	6	1	0.00093932	0	0.00121191	0.00045512
2013907866	DNA-directed RNA polymerase, beta' subunit/160 kD subunit	1	0	1	1	0.00083094	0	0.00017868	0.00040261
2013890743	DNA-directed RNA polymerase subunit beta' (EC 2.7.7.6)(EC:2.7.7.6)	1	0	1	1	0.00077159	0	0.00016592	0.00037385
2013904178	DNA-directed RNA polymerase subunit beta' (EC 2.7.7.6)	1	0	1	1	0.00064931	0	0.00013962	0.0003146
2013889773	DNA-directed RNA polymerase subunit beta' (EC 2.7.7.6)(EC:2.7.7.6)	1	0	1	1	0.00060317	0	0.0001297	0.00029225
2013890583	Formate-tetrahydrofolate ligase (EC 6.3.4.3)(EC:6.3.4.3)	1	0	8	1	0.00039281	0	0.00067573	0.00019032
2013901217	DNA-directed RNA polymerase subunit beta' (EC 2.7.7.6)(EC:2.7.7.6)	1	0	1	1	0.00021333	0	4.5873E-05	0.00010336
2013901240	SSU ribosomal protein S19P	1	1	0	0	0.00282915	0.0047862	0	0
2013927386	DNA-directed RNA polymerase, alpha subunit/40 kD subunit	1	1	0	0	0.00203118	0.00343625	0	0
2013914702	hypothetical protein	1	1	0	0	0.00118233	0.00200021	0	0
2013894518	2-isopropylmalate synthase (EC 2.3.3.13)	1	1	0	0	0.00105622	0.00178685	0	0
2013907806	Glyceraldehyde-3-phosphate dehydrogenase/erythrose-4-phosphate dehydrogenase(EC:1.2.1.59)	1	1	0	0	0.00101127	0.00171081	0	0
2013921549	ATP synthase F1 subcomplex alpha subunit (EC:3.6.3.14)	2	0	2	0	0.00300821	0	0.00064686	0
2013917586	glyceraldehyde-3-phosphate dehydrogenase (EC 1.2.1.12)	1	0	1	0	0.00144029	0	0.00030971	0
2013893216	glyceraldehyde-3-phosphate dehydrogenase (EC 1.2.1.12)	1	0	1	0	0.00123775	0	0.00026616	0
2013897390	Dihydropteroate synthase (EC 2.5.1.15)(EC:2.5.1.15)	1	0	1	0	0.00084272	0	0.00018121	0
2013892646	glutamate dehydrogenase (NADP) (EC 1.4.1.4)	1	0	3	0	0.0007031	0	0.00045357	0
Dehalococcoides_KB1_0466	hypothetical protein	0	0	20	12	0	0	0.02044082	0.02763481
Dehalococcoides_KB1_0757	Uncharacterized conserved protein	0	0	17	14	0	0	0.00998546	0.01852909
Dehalococcoides_KB1_1396	hypothetical protein	0	0	30	33	0	0	0.00934793	0.02316943
Dehalococcoides_KB1_0767	Methyl-accepting chemotaxis protein (MCP) signaling domain.	0	0	9	2	0	0	0.00766531	0.00383817
Dehalococcoides_KB1_0984	hypothetical protein	0	0	10	3	0	0	0.00681361	0.0046058
Dehalococcoides_KB1_0691	hypothetical protein	0	0	7	1	0	0	0.00638776	0.00205616
Dehalococcoides_KB1_0679	hypothetical protein	0	0	8	2	0	0	0.00498557	0.00280842
Dehalococcoides_KB1_1419	ABC-type dipeptide/oligopeptide/nickel transport systems, permease components	0	0	24	17	0	0	0.00402114	0.00641792
Dehalococcoides_KB1_0756	Predicted flavin-nucleotide-binding protein structurally related to pyridoxine 5'-phosphate oxidase	0	0	10	2	0	0	0.00381359	0.00171858
Dehalococcoides_KB1_1110	hydrogenase accessory protein HypB	0	0	16	9	0	0	0.00375061	0.00475369
Dehalococcoides_KB1_0844	hypothetical protein	0	0	3	2	0	0	0.0034068	0.00511756
Dehalococcoides_KB1_0313	hypothetical protein	0	0	14	9	0	0	0.00292012	0.00422982
Dehalococcoides_KB1_0104	hypothetical protein	0	0	7	4	0	0	0.00248413	0.00319847
Dehalococcoides_KB1_0069	Superfamily II DNA and RNA helicases(EC:3.6.4.13)	0	0	6	7	0	0	0.0024529	0.00644812
Dehalococcoides_KB1_0649	hypothetical protein	0	0	2	3	0	0	0.00243343	0.00822465
Dehalococcoides_KB1_0607	hypothetical protein	0	0	8	3	0	0	0.00222183	0.00187736
Dehalococcoides_KB1_0281	phenylacetate-CoA ligase (EC 6.2.1.30)(EC:6.2.1.30)	0	0	10	4	0	0	0.00211165	0.00190322
Dehalococcoides_KB1_1477	Uncharacterized conserved protein	0	0	10	9	0	0	0.00198841	0.00403232
Dehalococcoides_KB1_0713	Glutamate decarboxylase and related PLP-dependent proteins(EC:4.1.1.25)	0	0	8	1	0	0	0.00197496	0.00055626
Dehalococcoides_KB1_0252	Osmosensitive K+ channel histidine kinase	0	0	5	4	0	0	0.00182507	0.00328986
2013897235	phosphate-binding protein	0	0	10	4	0	0	0.00179937	0.00162176
Dehalococcoides_KB1_1184	hypothetical protein	0	0	8	3	0	0	0.00174708	0.00147622
Dehalococcoides_KB1_1434	hypothetical protein	0	0	1	1	0	0	0.00164845	0.00371436
2013918649	Inorganic pyrophosphatase	0	0	7	5	0	0	0.00149671	0.00240889
Dehalococcoides_KB1_1343	Uncharacterized membrane protein	0	0	5	2	0	0	0.00138114	0.00124481
Dehalococcoides_KB1_0477	6,7-dimethyl-8-ribityllumazine synthase (EC 2.5.1.9) (EC:2.5.1.-)	0	0	1	1	0	0	0.00127755	0.00287863
Dehalococcoides_KB1_0978	nucleotidyltransferase(EC:5.4.2.8)	0	0	3	3	0	0	0.00125661	0.00283144
Dehalococcoides_KB1_1243	Iron-sulfur cluster assembly accessory protein	0	0	3	2	0	0	0.00124639	0.00187228
Dehalococcoides_KB1_1275	hypothetical protein	0	0	2	1	0	0	0.00114836	0.00129376
Dehalococcoides_KB1_0678	hypothetical protein	0	0	1	1	0	0	0.00111091	0.00250315
2013897691	Inorganic pyrophosphatase(EC:3.6.1.1)	0	0	12	7	0	0	0.00110094	0.00144707
Dehalococcoides_KB1_0114	Uncharacterized conserved protein	0	0	3	1	0	0	0.001002	0.00075258
Dehalococcoides_KB1_1389	Predicted membrane protein	0	0	5	5	0	0	0.00089028	0.00200601
Dehalococcoides_KB1_0253	PAS/PAC sensor hybrid histidine kinase (EC 2.7.3.-)	0	0	1	1	0	0	0.00081114	0.0018277
Dehalococcoides_KB1_0072	hypothetical protein	0	0	2	1	0	0	0.00079847	0.00089957
Dehalococcoides_KB1_1120	hypothetical protein	0	0	1	2	0	0	0.0007515	0.00338662
Dehalococcoides_KB1_0481	4Fe-4S binding domain.	0	0	1	1	0	0	0.00069057	0.00155601

Table A3.2. Proteins detected in field samples, but not in KB-1 culture sample that were identified as part of the KB-1 metagenome

		Spectral Counts				NSAF			
Protein ID	Description	PM2A2	EW1	O-BH9-A1	O-BH10-A1	PM2A2	EW1	O-BH9-A1	O-BH10-A1
Dehalococcoides_KB1_gi147669671	DNA polymerase III, beta subunit (EC 2.7.7.7)(EC:2.7.7.7)	0	0	4	3	0	0	0.00068593	0.00115918
Dehalococcoides_KB1_1441	hypothetical protein	0	0	2	1	0	0	0.00067685	0.00076255
2013924844	ATP synthase F1 subcomplex beta subunit (EC:3.6.3.14)	0	0	3	2	0	0	0.00065797	0.00098837
2013890641	vacuolar-type H(+)-translocating pyrophosphatase	0	0	9	2	0	0	0.0006496	0.00032527
2013907225	glucose-6-phosphate isomerase (EC 5.3.1.9)(EC:5.3.1.9)	0	0	3	1	0	0	0.00064145	0.00048178
Dehalococcoides_KB1_0380	Nitroreductase	0	0	2	1	0	0	0.00058402	0.00065797
Dehalococcoides_KB1_0464	Phage terminase-like protein, large subunit	0	0	4	3	0	0	0.00057906	0.00097857
Dehalococcoides_KB1_1099	Methylase involved in ubiquinone/menaquinone biosynthesis	0	0	3	1	0	0	0.00055146	0.00041419
Dehalococcoides_KB1_1163	ABC-type dipeptide transport system, periplasmic component	0	0	6	2	0	0	0.00055146	0.00041419
2013926526	ABC-type branched-chain amino acid transport systems, periplasmic component	0	0	2	3	0	0	0.0005351	0.00180856
2013902062	vacuolar-type H(+)-translocating pyrophosphatase(EC:3.6.1.1)	0	0	7	5	0	0	0.00052145	0.00083925
2013909265	FOG: Ankyrin repeat	0	0	2	1	0	0	0.00050596	0.00057002
2013918220	hypothetical protein	0	0	1	1	0	0	0.00050596	0.00114005
Dehalococcoides_KB1_1502	Superfamily II DNA/RNA helicases, SNF2 family	0	0	9	6	0	0	0.00048058	0.00072191
Dehalococcoides_KB1_0289	hypothetical protein(EC:6.2.1.20,EC:2.3.1.40)	0	0	1	1	0	0	0.00044826	0.00101004
Dehalococcoides_KB1_0545	hypothetical protein	0	0	1	1	0	0	0.00043677	0.00098415
Dehalococcoides_KB1_1235	hypothetical protein	0	0	1	1	0	0	0.00041546	0.00093614
Dehalococcoides_KB1_1167	Predicted transcriptional regulator	0	0	2	1	0	0	0.00035243	0.00039705
Dehalococcoides_KB1_0398	RepB plasmid partitioning protein.	0	0	2	1	0	0	0.00034412	0.00038769
Dehalococcoides_KB1_0051	Predicted secreted protein	0	0	1	1	0	0	0.00034068	0.00076763
Dehalococcoides_KB1_1344	translation elongation factor 2 (EF-2/EF-G)	0	0	4	2	0	0	0.00029928	0.00033717
Dehalococcoides_KB1_0598	ATPase, PilT family	0	0	2	2	0	0	0.00028629	0.00064507
2013919419	Predicted alternative tryptophan synthase beta-subunit (paralog of TrpB)(EC:4.2.1.20)	0	0	1	1	0	0	0.0002839	0.00063969
Dehalococcoides_KB1_0982	hypothetical protein	0	0	1	1	0	0	0.00027623	0.00062241
Dehalococcoides_KB1_0861	ribonuclease III, bacterial(EC:3.1.26.3)	0	0	1	2	0	0	0.00026478	0.00119321
Dehalococcoides_KB1_1004	Calcineurin-like phosphoesterase.	0	0	1	1	0	0	0.00023768	0.00053556
2013889522	Flagellin and related hook-associated proteins	0	0	1	2	0	0	0.00023019	0.00103734
Dehalococcoides_KB1_0930	CO dehydrogenase/acetyl-CoA synthase complex, beta subunit(EC:1.2.7.4)	0	0	2	4	0	0	0.00021426	0.00096558
Dehalococcoides_KB1_0958	Type I restriction-modification system methyltransferase subunit	0	0	3	3	0	0	0.00019884	0.00044804
Dehalococcoides_KB1_1028	hypothetical protein	0	0	1	1	0	0	0.00017501	0.00039433
Dehalococcoides_KB1_0126	Zn-dependent oligopeptidases	0	0	1	2	0	0	0.00016327	0.00073575
Dehalococcoides_KB1_1288	transposase, IS4 family	0	0	1	1	0	0	0.0001558	0.00035105
2013894233	pilus retraction protein PilT	0	0	1	1	0	0	0.00014274	0.00032163
Dehalococcoides_KB1_0290	L-serine deaminase	0	0	1	1	0	0	0.00013924	0.00031375
Dehalococcoides_KB1_0531	CRISPR-associated helicase Cas3/CRISPR-associated HD domain protein	0	0	2	1	0	0	0.00013924	0.00015687
Dehalococcoides_KB1_0254	Methyl-accepting chemotaxis protein	0	0	1	2	0	0	0.00012525	0.00056444
2013898331	transcription termination factor Rho	0	0	1	1	0	0	0.0001194	0.00026903
Dehalococcoides_KB1_1003	MiaB-like tRNA modifying enzyme YliG, TIGR01125	0	0	1	2	0	0	0.00011667	0.00052578
Dehalococcoides_KB1_0520	NAD-dependent aldehyde dehydrogenases	0	0	1	1	0	0	0.00010668	0.00024039
Dehalococcoides_KB1_1418	ABC-type oligopeptide transport system, periplasmic component	0	0	1	2	0	0	9.1581E-05	0.00041271
Dehalococcoides_KB1_0648	hypothetical protein	0	0	1	2	0	0	6.9057E-05	0.0003112
2013897455	Cation/multidrug efflux pump	0	0	1	1	0	0	5.0898E-05	0.00011469
2013894190	SSU ribosomal protein S19P	1	0	0	0	0.00267021	0	0	0
2013890390	SSU ribosomal protein S19P	1	0	0	0	0.00258313	0	0	0
2013894970	RecA protein	1	0	0	0	0.00224197	0	0	0
2013888949	ribosomal subunit interface protein	1	0	0	0	0.00218026	0	0	0
2013890439	Excinuclease ABC subunit C	1	0	0	0	0.00214098	0	0	0
2013910571	Pyruvate:ferredoxin oxidoreductase and related 2-oxoacid:ferredoxin oxidoreductases, alpha subunit(EC:1.2.7.3)	1	0	0	0	0.00214098	0	0	0
2013892817	LSU ribosomal protein L14P	1	0	0	0	0.00210308	0	0	0
2013919529	RecA protein	1	0	0	0	0.00199705	0	0	0
2013921384	dTDP-glucose pyrophosphorylase	1	0	0	0	0.00199705	0	0	0
2013918285	Regulator of polyketide synthase expression	1	0	0	0	0.00172209	0	0	0
2013908996	ATP-dependent Lon protease, bacterial type	1	0	0	0	0.00154317	0	0	0
2013898022	2-methylthioadenine synthetase(EC:1.3.1.74)	1	0	0	0	0.00144908	0	0	0
2013890404	membrane protease FtsH catalytic subunit (EC 3.4.24.-)(EC:3.4.24.-)	1	0	0	0	0.00139793	0	0	0
2013910401	Predicted oxidoreductases of the aldo/keto reductase family	1	0	0	0	0.00138168	0	0	0
2013892367	Uncharacterized conserved protein	1	0	0	0	0.00127768	0	0	0
2013906296	hypothetical protein	1	0	0	0	0.00126409	0	0	0
2013890368	ATP:corrinoid adenosyltransferase(EC:2.5.1.17)	1	0	0	0	0.00109013	0	0	0

Table A3.2. Proteins detected in field samples, but not in KB-1 culture sample that were identified as part of the KB-1 metagenome

		Spectral Counts				NSAF			
Protein ID	Description	PM2A2	EW1	O-BH9-A1	O-BH10-A1	PM2A2	EW1	O-BH9-A1	O-BH10-A1
2013924473	DNA-directed RNA polymerase subunit beta (EC 2.7.7.6)	1	0	0	0	0.00104232	0	0	0
2013901027	hypothetical protein	1	0	0	0	0.0009902	0	0	0
2013913368	Serine/threonine protein kinase	1	0	0	0	0.00095059	0	0	0
2013903685	Transcriptional regulator	1	0	0	0	0.00090361	0	0	0
2013905808	membrane protease FtsH catalytic subunit (EC 3.4.24.-)(EC:3.4.24.-)	2	0	0	0	0.00090189	0	0	0
2013888745	hypothetical protein	1	0	0	0	0.00088675	0	0	0
2013892796	Predicted kinase(EC:2.7.1.100)	1	0	0	0	0.00087051	0	0	0
2013890331	conserved hypothetical protein	1	0	0	0	0.00073804	0	0	0
2013890277	hexulose-6-phosphate synthase (EC 4.1.2.-)(EC:4.3.-)	1	0	0	0	0.00069084	0	0	0
2013905466	hypothetical protein	1	0	0	0	0.00051107	0	0	0
2013893913	LVIVD repeat.	1	0	0	0	0.00038959	0	0	0
2013902394	chromosome segregation protein SMC, common bacterial type	1	0	0	0	0.00019624	0	0	0
2013913624	hypothetical protein(EC:2.4.1.1)	0	1	0	0	0	0.00893425	0	0
2013898280	Propanediol dehydratase, large subunit	0	1	0	0	0	0.00502552	0	0
2013914672	hypothetical protein	0	2	0	0	0	0.00434639	0	0
2013892803	hypothetical protein	0	1	0	0	0	0.00358965	0	0
2013920411	LSU ribosomal protein L12P	0	1	0	0	0	0.00321633	0	0
2013919925	3-dehydroquinate dehydratase	0	1	0	0	0	0.00289238	0	0
2013913325	prepilin-type N-terminal cleavage/methylation domain	0	1	0	0	0	0.00275371	0	0
2013888664	hypothetical protein	0	1	0	0	0	0.00259381	0	0
2013908070	DNA polymerase III, delta subunit	0	1	0	0	0	0.00257719	0	0
2013895369	Ethanolamine utilization protein	0	1	0	0	0	0.00243661	0	0
2013898572	Threonyl-tRNA synthetase(EC:6.1.1.3)	0	1	0	0	0	0.00229738	0	0
2013886535	Sugar kinases, ribokinase family(EC:2.7.1.45)	0	1	0	0	0	0.00227142	0	0
2013910907	hypothetical protein	0	1	0	0	0	0.0021732	0	0
2013924136	Response regulator containing CheY-like receiver, AAA-type ATPase, and DNA-binding domains	0	1	0	0	0	0.0021732	0	0
2013924272	hypothetical protein	0	1	0	0	0	0.00209396	0	0
2013909693	Methionyl-tRNA synthetase	0	1	0	0	0	0.0018613	0	0
2013921260	nitrate oxidoreductase alpha subunit(EC:1.7.99.4)	0	1	0	0	0	0.0016277	0	0
2013899303	Phytoene dehydrogenase and related proteins(EC:1.3.99.23)	0	1	0	0	0	0.00156436	0	0
2013910033	ABC-type Fe3+ transport system, permease component	0	1	0	0	0	0.00155228	0	0
2013904102	hypothetical protein	0	1	0	0	0	0.00134014	0	0
2013887109	Uncharacterized conserved protein	0	1	0	0	0	0.00124087	0	0
2013889455	Predicted oxidoreductases (related to aryl-alcohol dehydrogenases)	0	1	0	0	0	0.00122574	0	0
2013892141	hypothetical protein	0	1	0	0	0	0.00094598	0	0
2013894585	Uncharacterized conserved protein	0	1	0	0	0	0.00080088	0	0
2013891234	formylmethanofuran dehydrogenase, subunit A (EC 1.2.99.5)(EC:1.2.99.5)	0	1	0	0	0	0.00070164	0	0
2013922320	Inorganic pyrophosphatase	0	0	4	0	0	0	0.00163527	0
Dehalococcoides_KB1_0547	hypothetical protein	0	0	3	0	0	0	0.00148841	0
Dehalococcoides_KB1_0390	hypothetical protein	0	0	2	0	0	0	0.0014195	0
2013903984	transcriptional regulator, AsnC family	0	0	2	0	0	0	0.00134479	0
Dehalococcoides_KB1_1384	Fe2+/Zn2+ uptake regulation proteins	0	0	3	0	0	0	0.0011356	0
2013906972	Bacterial regulatory proteins, crp family.	0	0	1	0	0	0	0.00108728	0
Dehalococcoides_KB1_0381	hypothetical protein	0	0	1	0	0	0	0.00108728	0
Dehalococcoides_KB1_0532	hypothetical protein	0	0	1	0	0	0	0.00088107	0
2013897737	Anti-anti-sigma regulatory factor (antagonist of anti-sigma factor)	0	0	2	0	0	0	0.00087354	0
2013924355	translation elongation factor 1A (EF-1A/EF-Tu)	0	0	1	0	0	0	0.0008517	0
Dehalococcoides_KB1_0568	hypothetical protein	0	0	1	0	0	0	0.00082423	0
2013916922	hypothetical protein	0	0	1	0	0	0	0.00074061	0
Dehalococcoides_KB1_0149	ABC-type tungstate transport system, periplasmic component	0	0	1	0	0	0	0.00074061	0
Dehalococcoides_KB1_0718	Kef-type K+ transport system, predicted NAD-binding component	0	0	2	0	0	0	0.00074061	0
Dehalococcoides_KB1_0546	hypothetical protein	0	0	1	0	0	0	0.00070003	0
Dehalococcoides_KB1_0732	hypothetical protein	0	0	1	0	0	0	0.00065515	0
Dehalococcoides_KB1_0693	Uncharacterized conserved protein	0	0	2	0	0	0	0.00063089	0
Dehalococcoides_KB1_0248	2-polyprenylphenol hydroxylase and related flavodoxin oxidoreductases	0	0	2	0	0	0	0.00062702	0
Dehalococcoides_KB1_0124	hypothetical protein	0	0	1	0	0	0	0.00061569	0
Dehalococcoides_KB1_0288	hypothetical protein	0	0	1	0	0	0	0.00061569	0
Dehalococcoides_KB1_1285	hypothetical protein	0	0	1	0	0	0	0.00061569	0
Dehalococcoides_KB1_0603	Predicted nucleotidyltransferases	0	0	2	0	0	0	0.00060476	0

Table A3.2. Proteins detected in field samples, but not in KB-1 culture sample that were identified as part of the KB-1 metagenome

		Spectral Counts				NSAF			
Protein ID	Description	PM2A2	EW1	O-BH9-A1	O-BH10-A1	PM2A2	EW1	O-BH9-A1	O-BH10-A1
Dehalococcoides_KB1_0634	adenine phosphoribosyltransferase (EC 2.4.2.7)(EC:2.4.2.7)	0	0	2	0	0	0	0.00059768	0
Dehalococcoides_KB1_0294	(tRNA)	0	0	1	0	0	0	0.00059421	0
2013896961	SSU ribosomal protein S15P	0	0	1	0	0	0	0.00058738	0
2013925736	hypothetical protein	0	0	1	0	0	0	0.00058071	0
Dehalococcoides_KB1_0967	hypothetical protein	0	0	1	0	0	0	0.00057418	0
Dehalococcoides_KB1_1251	Membrane-associated phospholipid phosphatase	0	0	2	0	0	0	0.00057097	0
2013926064	Uncharacterized anaerobic dehydrogenase	0	0	1	0	0	0	0.00056156	0
2013926954	hypothetical protein	0	0	1	0	0	0	0.00056156	0
Dehalococcoides_KB1_0909	Uncharacterized protein conserved in archaea	0	0	1	0	0	0	0.00054948	0
2013917932	Bacterial nucleoid DNA-binding protein	0	0	1	0	0	0	0.00053792	0
2013901364	hypothetical protein	0	0	1	0	0	0	0.00053231	0
Dehalococcoides_KB1_0755	hypothetical protein	0	0	1	0	0	0	0.00052683	0
2013891002	methyl-accepting chemotaxis sensory transducer	0	0	1	0	0	0	0.00052145	0
Dehalococcoides_KB1_0265	hypothetical protein	0	0	1	0	0	0	0.00051618	0
Dehalococcoides_KB1_0605	hypothetical protein	0	0	2	0	0	0	0.00049856	0
2013909812	translation elongation factor P (EF-P)	0	0	1	0	0	0	0.00047759	0
Dehalococcoides_KB1_0428	hypothetical protein	0	0	1	0	0	0	0.00047759	0
2013921870	hypothetical protein	0	0	1	0	0	0	0.00047317	0
2013892533	hypothetical protein	0	0	1	0	0	0	0.00044826	0
2013919981	methyl-accepting chemotaxis sensory transducer	0	0	2	0	0	0	0.00043864	0
Dehalococcoides_KB1_0492	transcriptional regulator, MarR family	0	0	1	0	0	0	0.00042943	0
2013918440	osmosensitive K+ channel signal transduction histidine kinase (EC 2.7.3.-)(EC:2.7.13.3)	0	0	1	0	0	0	0.00042233	0
2013924817	methyl-accepting chemotaxis sensory transducer	0	0	2	0	0	0	0.00041716	0
Dehalococcoides_KB1_0843	Membrane-bound serine protease (ClpP class)	0	0	1	0	0	0	0.00040557	0
2013896217	fructose-bisphosphate aldolase (EC 4.1.2.13)	0	0	1	0	0	0	0.00039614	0
2013910658	ribosomal protein S3, bacterial type	0	0	1	0	0	0	0.00039614	0
2013916826	Methyl-accepting chemotaxis protein	0	0	2	0	0	0	0.00039461	0
Dehalococcoides_KB1_0537	Uncharacterized conserved protein, contains double-stranded beta-helix domain	0	0	1	0	0	0	0.00039309	0
Dehalococcoides_KB1_1166	camphor resistance protein CrcB	0	0	1	0	0	0	0.00039309	0
2013925418	ABC-type spermidine/putrescine transport systems, ATPase components(EC:3.6.3.30)	0	0	1	0	0	0	0.00039009	0
2013919291	SSU ribosomal protein S2P	0	0	1	0	0	0	0.00038714	0
Dehalococcoides_KB1_1442	hypothetical protein	0	0	1	0	0	0	0.00038136	0
2013896780	methyl-accepting chemotaxis sensory transducer	0	0	1	0	0	0	0.00037853	0
2013905159	Formate-tetrahydrofolate ligase (EC 6.3.4.3)	0	0	1	0	0	0	0.00037575	0
Dehalococcoides_KB1_1031	(tRNA)	0	0	1	0	0	0	0.00037575	0
Dehalococcoides_KB1_0752	Uncharacterized protein conserved in archaea	0	0	1	0	0	0	0.0003703	0
2013891098	hypothetical protein	0	0	1	0	0	0	0.00036243	0
2013911992	L-lysine 2,3-aminomutase (EC 5.4.3.2)(EC:5.4.3.2)	0	0	1	0	0	0	0.00036243	0
Dehalococcoides_KB1_gi147668718	hypothetical protein	0	0	1	0	0	0	0.00036243	0
Dehalococcoides_KB1_0658	cytochrome c-type biogenesis protein CcsB	0	0	2	0	0	0	0.00036115	0
Dehalococcoides_KB1_0476	Pyruvate decarboxylase and related thiamine pyrophosphate-requiring enzymes(EC:4.1.1.74)	0	0	1	0	0	0	0.00035001	0
Dehalococcoides_KB1_0121	hypothetical protein	0	0	1	0	0	0	0.00032549	0
Dehalococcoides_KB1_0599	Divergent AAA domain.	0	0	2	0	0	0	0.00032039	0
2013922125	Excinuclease ABC subunit A	0	0	1	0	0	0	0.00031939	0
Dehalococcoides_KB1_0518	PAS fold.	0	0	1	0	0	0	0.00031939	0
Dehalococcoides_KB1_0635	RNA polymerase, sigma 38 subunit, RpoS	0	0	2	0	0	0	0.00031939	0
2013900081	hypothetical protein	0	0	1	0	0	0	0.0003174	0
2013908081	Nucleoside-diphosphate-sugar epimerases	0	0	1	0	0	0	0.0003174	0
2013910540	hypothetical protein	0	0	1	0	0	0	0.0003174	0
2013904811	Signal transduction histidine kinase(EC:2.7.13.3)	0	0	1	0	0	0	0.00031544	0
Dehalococcoides_KB1_0556	hypothetical protein	0	0	1	0	0	0	0.00031544	0
Dehalococcoides_KB1_0957	Dual specificity phosphatase, catalytic domain.	0	0	1	0	0	0	0.00031544	0
Dehalococcoides_KB1_1478	hypothetical protein	0	0	1	0	0	0	0.00031351	0
2013919004	SSU ribosomal protein S2P	0	0	1	0	0	0	0.0003116	0
Dehalococcoides_KB1_0436	Methylase involved in ubiquinone/menaquinone biosynthesis	0	0	1	0	0	0	0.0003116	0
2013907314	Adenylosuccinate lyase	0	0	1	0	0	0	0.00030784	0
Dehalococcoides_KB1_0513	Predicted Fe-S oxidoreductase	0	0	2	0	0	0	0.00030784	0
Dehalococcoides_KB1_0606	hypothetical protein	0	0	1	0	0	0	0.00030784	0
Dehalococcoides_KB1_1096	IMP cyclohydrolase (EC 3.5.4.10)/phosphoribosylaminoimidazolecarboxamide formyltransferase (EC 2.1.2.3)(EC:3.5.4.10,EC:2.1.2.3)	0	0	3	0	0	0	0.00029884	0

Table A3.2. Proteins detected in field samples, but not in KB-1 culture sample that were identified as part of the KB-1 metagenome

		Spectral Counts				NSAF			
Protein ID	Description	PM2A2	EW1	O-BH9-A1	O-BH10-A1	PM2A2	EW1	O-BH9-A1	O-BH10-A1
2013913035	dephospho-CoA kinase(EC:2.7.1.24)	0	0	1	0	0	0	0.00029369	0
Dehalococcoides_KB1_0859	hypothetical protein(EC:1.-)	0	0	1	0	0	0	0.00029201	0
2013896939	LSU ribosomal protein L10P	0	0	1	0	0	0	0.00029035	0
2013922871	bacterial translation initiation factor 2 (bIF-2)	0	0	1	0	0	0	0.00028871	0
2013897736	Adenylate kinase and related kinases	0	0	1	0	0	0	0.00028233	0
Dehalococcoides_KB1_1393	cob(I)yrinic acid a,c-diamide adenosyltransferase (EC 2.5.1.17)(EC:2.5.1.17)	0	0	1	0	0	0	0.00028078	0
2013926981	Long-chain acyl-CoA synthetases (AMP-forming)(EC:6.2.1.3)	0	0	1	0	0	0	0.00027327	0
2013920505	Na+-transporting NADH:ubiquinone oxidoreductase, subunit NqrC(EC:1.6.5.-)	0	0	1	0	0	0	0.00027182	0
Dehalococcoides_KB1_0400	Cysteine sulfinate desulfinase/cysteine desulfurase and related enzymes(EC:2.8.1.7)	0	0	2	0	0	0	0.0002711	0
2013903325	Methyl-accepting chemotaxis protein	0	0	1	0	0	0	0.00026896	0
Dehalococcoides_KB1_1398	Predicted membrane protein	0	0	1	0	0	0	0.00026896	0
Dehalococcoides_KB1_0644	hypothetical protein	0	0	1	0	0	0	0.00026616	0
Dehalococcoides_KB1_0979	nucleotidyltransferase(EC:5.4.2.8)	0	0	1	0	0	0	0.00026478	0
2013902483	bacterial translation initiation factor 2 (bIF-2)	0	0	1	0	0	0	0.00026341	0
Dehalococcoides_KB1_0383	exodeoxyribonuclease III (xth)	0	0	1	0	0	0	0.00026341	0
2013919343	ketoisovalerate ferredoxin oxidoreductase, alpha subunit (EC 1.2.7.7)(EC:1.2.7.7,EC:1.2.7.1)	0	0	1	0	0	0	0.00026072	0
2013899885	Signal transduction histidine kinase	0	0	1	0	0	0	0.0002594	0
Dehalococcoides_KB1_0925	hexulose-6-phosphate isomerase (EC 5.-.-.-)(EC:5.3.1.27)	0	0	1	0	0	0	0.00025679	0
2013922809	ATPases with chaperone activity, ATP-binding subunit	0	0	1	0	0	0	0.00025551	0
Dehalococcoides_KB1_1030	HD-GYP domain	0	0	1	0	0	0	0.00025551	0
Dehalococcoides_KB1_1190	Methylase of chemotaxis methyl-accepting proteins	0	0	1	0	0	0	0.00025298	0
Dehalococcoides_KB1_1240	(tRNA)	0	0	2	0	0	0	0.00025112	0
2013902564	Chemotaxis protein CheC, inhibitor of MCP methylation(EC:2.7.13.3)	0	0	1	0	0	0	0.0002505	0
Dehalococcoides_KB1_1366	riboflavin synthase, alpha subunit	0	0	1	0	0	0	0.00024928	0
2013909306	Adenylate kinase (EC 2.7.4.3)(EC:2.7.4.3)	0	0	1	0	0	0	0.00024687	0
2013911334	Methyl-accepting chemotaxis protein	0	0	1	0	0	0	0.00024451	0
2013912791	succinyl-CoA synthetase (ADP-forming) alpha subunit (EC 6.2.1.5)(EC:6.2.1.5)	0	0	1	0	0	0	0.00024334	0
2013915885	Predicted hydrocarbon binding protein (contains V4R domain)	0	0	1	0	0	0	0.00024334	0
2013920114	Methyl-accepting chemotaxis protein	0	0	1	0	0	0	0.00024334	0
2013889373	Predicted EndoIII-related endonuclease	0	0	1	0	0	0	0.00024219	0
2013892724	Uncharacterized conserved protein	0	0	1	0	0	0	0.00024219	0
2013902429	methyl-accepting chemotaxis sensory transducer	0	0	1	0	0	0	0.00024105	0
2013924856	Acyl-CoA dehydrogenases	0	0	1	0	0	0	0.00024105	0
2013898891	transaldolase (EC 2.2.1.2)(EC:2.2.1.2)	0	0	1	0	0	0	0.00023768	0
2013925970	Adenylate kinase (EC 2.7.4.3)(EC:2.7.4.6)	0	0	1	0	0	0	0.00023768	0
2013906802	rod shape-determining protein MreB	0	0	1	0	0	0	0.00022813	0
2013916436	hypothetical protein	0	0	1	0	0	0	0.00022712	0
2013897935	Response regulators consisting of a CheY-like receiver domain and a winged-helix DNA-binding domain	0	0	1	0	0	0	0.00022512	0
Dehalococcoides_KB1_1556	(tRNA)	0	0	1	0	0	0	0.00022413	0
Dehalococcoides_KB1_0642	PAS domain S-box	0	0	1	0	0	0	0.00022315	0
Dehalococcoides_KB1_0838	hypothetical protein	0	0	1	0	0	0	0.00022122	0
Dehalococcoides_KB1_1241	(tRNA)	0	0	2	0	0	0	0.00022122	0
2013892303	conserved hypothetical protein TIGR00266	0	0	1	0	0	0	0.00021932	0
2013905952	Preprotein translocase subunit SecD	0	0	1	0	0	0	0.00021932	0
2013891361	Acetyl-CoA carboxylase, carboxyltransferase component (subunits alpha and beta)(EC:6.4.1.3)	0	0	1	0	0	0	0.00021117	0
2013892577	5'-nucleotidase/2',3'-cyclic phosphodiesterase and related esterases	0	0	1	0	0	0	0.0002103	0
2013920436	Pyruvate:ferredoxin oxidoreductase and related 2-oxoacid:ferredoxin oxidoreductases, beta subunit(EC:1.2.7.-)	0	0	1	0	0	0	0.00020858	0
Dehalococcoides_KB1_0708	hypothetical protein	0	0	1	0	0	0	0.00020689	0
2013894937	Inorganic pyrophosphatase(EC:3.6.1.1)	0	0	1	0	0	0	0.00020606	0
Dehalococcoides_KB1_0943	TrkA-C domain.	0	0	1	0	0	0	0.00020606	0
2013888407	phosphomethylpyrimidine kinase/thiamine-phosphate pyrophosphorylase(EC:2.7.4.7,EC:2.7.1.49)	0	0	2	0	0	0	0.00020564	0
2013905077	Long-chain acyl-CoA synthetases (AMP-forming)	0	0	1	0	0	0	0.00020279	0
2013895251	Predicted phage phi-C31 gp36 major capsid-like protein	0	0	1	0	0	0	0.0002004	0
2013919189	pilus retraction protein PilT	0	0	1	0	0	0	0.00019962	0
2013900813	methyl-accepting chemotaxis sensory transducer	0	0	1	0	0	0	0.00019731	0
2013913570	ATPases with chaperone activity, ATP-binding subunit	0	0	1	0	0	0	0.00019357	0
2013892255	Predicted sugar kinase(EC:2.7.1.23)	0	0	1	0	0	0	0.00019139	0
Dehalococcoides_KB1_1338	HAD-superfamily hydrolase, subfamily IIB	0	0	1	0	0	0	0.00018857	0
Dehalococcoides_KB1_1439	hypothetical protein	0	0	1	0	0	0	0.00018788	0

Table A3.2. Proteins detected in field samples, but not in KB-1 culture sample that were identified as part of the KB-1 metagenome

		Spectral Counts				NSAF			
Protein ID	Description	PM2A2	EW1	O-BH9-A1	O-BH10-A1	PM2A2	EW1	O-BH9-A1	O-BH10-A1
2013898537	AraC-type DNA-binding domain-containing proteins	0	0	1	0	0	0	0.00018719	0
2013920006	Histidinol-phosphate/aromatic aminotransferase and cobyric acid decarboxylase	0	0	1	0	0	0	0.00018719	0
Dehalococcoides_KB1_0517	molybdopterin molybdochelatase	0	0	1	0	0	0	0.00017931	0
Dehalococcoides_KB1_0591	Histidine kinase-, DNA gyrase B-, and HSP90-like ATPase.	0	0	1	0	0	0	0.00017561	0
2013888472	porphobilinogen synthase (EC 4.2.1.24)	0	0	1	0	0	0	0.00017091	0
2013887775	tyrosine recombinase XerD subunit	0	0	1	0	0	0	0.00016921	0
2013895260	hypothetical protein	0	0	1	0	0	0	0.000167	0
2013893825	methyl-accepting chemotaxis sensory transducer	0	0	1	0	0	0	0.00016327	0
2013896388	ABC-type Fe3+-siderophore transport system, permease component	0	0	1	0	0	0	0.00016223	0
Dehalococcoides_KB1_0699	4-hydroxybenzoate polyprenyltransferase and related prenyltransferases	0	0	1	0	0	0	0.00016172	0
2013889225	Pyruvate:ferredoxin oxidoreductase and related 2-oxoacid:ferredoxin oxidoreductases, alpha subunit(EC:1.2.7.1)	0	0	1	0	0	0	0.0001592	0
2013889770	DNA-directed RNA polymerase subunit beta' (EC 2.7.7.6)(EC:2.7.7.6)	0	0	1	0	0	0	0.00015346	0
2013900244	hypothetical protein	0	0	1	0	0	0	0.00015074	0
2013898474	phosphate-binding protein	0	0	1	0	0	0	0.00014986	0
Dehalococcoides_KB1_0645	Predicted Fe-S oxidoreductases	0	0	1	0	0	0	0.00014476	0
2013902338	methyl-accepting chemotaxis sensory transducer	0	0	1	0	0	0	0.00014395	0
Dehalococcoides_KB1_0444	Type II secretory pathway, ATPase PulE/Tfp pilus assembly pathway, ATPase PilB	0	0	1	0	0	0	0.00014395	0
2013886641	Predicted pyridoxal phosphate-dependent enzyme apparently involved in regulation of cell wall biogenesis	0	0	1	0	0	0	0.00014039	0
2013904894	Methyl-accepting chemotaxis protein	0	0	1	0	0	0	0.00013924	0
2013901979	Predicted cation transporter	0	0	1	0	0	0	0.00013737	0
2013898076	methyl-accepting chemotaxis sensory transducer	0	0	1	0	0	0	0.00013273	0
2013892468	probable carbamoyltransferase YgeW	0	0	1	0	0	0	0.00012905	0
Dehalococcoides_KB1_1151	tryptophan synthase, beta chain (EC 4.2.1.20)(EC:4.2.1.20)	0	0	1	0	0	0	0.00012808	0
2013903898	Type II secretory pathway, component PulF	0	0	1	0	0	0	0.00012744	0
2013891998	glucose-6-phosphate isomerase (EC 5.3.1.9)(EC:5.3.1.9)	0	0	1	0	0	0	0.00012618	0
Dehalococcoides_KB1_0411	hypothetical protein	0	0	1	0	0	0	0.00012618	0
2013898676	methyl-accepting chemotaxis sensory transducer	0	0	1	0	0	0	0.00012556	0
Dehalococcoides_KB1_0054	formate dehydrogenase, beta subunit (F420) (EC 1.2.99.-)(EC:1.2.1.2)	0	0	1	0	0	0	0.00012284	0
2013888559	Methyl-accepting chemotaxis protein	0	0	1	0	0	0	0.00011996	0
Dehalococcoides_KB1_0479	homoserine dehydrogenase (EC 1.1.1.3)(EC:1.1.1.3)	0	0	1	0	0	0	0.00011641	0
2013904551	hydroxylamine reductase(EC:1.7.-)	0	0	1	0	0	0	0.00010781	0
Dehalococcoides_KB1_1100	tRNA(Ile)-lysidine synthetase, N-terminal domain/tRNA(Ile)-lysidine synthetase, C-terminal domain(EC:6.3.4.-)	0	0	1	0	0	0	0.00010736	0
2013887338	PAS domain S-box	0	0	1	0	0	0	0.00010387	0
Dehalococcoides_KB1_1125	(tRNA)	0	0	1	0	0	0	0.000102	0
2013903859	Uncharacterized protein containing caspase domain	0	0	1	0	0	0	0.0001002	0
2013887511	GH3 auxin-responsive promoter.	0	0	1	0	0	0	9.4111E-05	0
2013898088	Methyl-accepting chemotaxis protein	0	0	1	0	0	0	9.1745E-05	0
2013891922	Methyl-accepting chemotaxis protein	0	0	1	0	0	0	9.0606E-05	0
Dehalococcoides_KB1_0261	(tRNA)	0	0	1	0	0	0	8.7654E-05	0
2013890586	aspartyl-tRNA synthetase (EC 6.1.1.12)	0	0	1	0	0	0	8.5455E-05	0
Dehalococcoides_KB1_0717	(tRNA)	0	0	1	0	0	0	8.5312E-05	0
Dehalococcoides_KB1_0522	PAS domain S-box	0	0	1	0	0	0	8.4746E-05	0
2013898297	Pyruvate:ferredoxin oxidoreductase and related 2-oxoacid:ferredoxin oxidoreductases, beta subunit(EC:1.2.7.-)	0	0	1	0	0	0	8.2423E-05	0
2013887814	ABC-type multidrug transport system, ATPase and permease components	0	0	1	0	0	0	8.0476E-05	0
2013898204	PAS domain S-box	0	0	1	0	0	0	7.7077E-05	0
2013893126	valyl-tRNA synthetase(EC:6.1.1.9)	0	0	1	0	0	0	5.8071E-05	0
2013898202	PAS domain S-box	0	0	1	0	0	0	5.3121E-05	0
2013924115	Inorganic pyrophosphatase(EC:3.6.1.1)	0	0	0	1	0	0	0	0.00225775
Dehalococcoides_KB1_1265	Uncharacterized protein conserved in bacteria	0	0	0	2	0	0	0	0.00223583
Dehalococcoides_KB1_0740	hypothetical protein	0	0	0	3	0	0	0	0.00209355
Dehalococcoides_KB1_1187	Polyribonucleotide nucleotidyltransferase (polynucleotide phosphorylase)	0	0	0	1	0	0	0	0.00171858
2013890550	hypothetical protein	0	0	0	1	0	0	0	0.00166877
2013897153	hypothetical protein	0	0	0	2	0	0	0	0.00165676
Dehalococcoides_KB1_0703	hypothetical protein	0	0	0	1	0	0	0	0.00162176
2013927261	hypothetical protein	0	0	0	1	0	0	0	0.00155601
Dehalococcoides_KB1_0432	Molybdopterin biosynthesis enzyme	0	0	0	1	0	0	0	0.00149539
2013918651	Inorganic pyrophosphatase(EC:3.6.1.1)	0	0	0	1	0	0	0	0.00147622
2013890398	Uncharacterized conserved protein	0	0	0	2	0	0	0	0.00120571
Dehalococcoides_KB1_0165	Site-specific recombinase XerD	0	0	0	1	0	0	0	0.00119943

Table A3.2. Proteins detected in field samples, but not in KB-1 culture sample that were identified as part of the KB-1 metagenome

		Spectral Counts				NSAF			
Protein ID	Description	PM2A2	EW1	O-BH9-A1	O-BH10-A1	PM2A2	EW1	O-BH9-A1	O-BH10-A1
Dehalococcoides_KB1_0369	hypothetical protein	0	0	0	2	0	0	0	0.00115724
2013924820	hypothetical protein	0	0	0	1	0	0	0	0.00112887
2013897067	hypothetical protein	0	0	0	1	0	0	0	0.00111791
2013913331	Major Facilitator Superfamily.	0	0	0	2	0	0	0	0.00110187
2013910586	Dinucleotide-utilizing enzymes involved in molybdopterin and thiamine biosynthesis family 1	0	0	0	1	0	0	0	0.00102808
Dehalococcoides_KB1_0674	hypothetical protein	0	0	0	1	0	0	0	0.00097581
2013905185	Inorganic pyrophosphatase(EC:3.6.1.1)	0	0	0	1	0	0	0	0.00081088
Dehalococcoides_KB1_0680	hypothetical protein	0	0	0	1	0	0	0	0.00081088
Dehalococcoides_KB1_0980	DNA uptake lipoprotein	0	0	0	1	0	0	0	0.0007833
Dehalococcoides_KB1_1165	MarR family.	0	0	0	1	0	0	0	0.00076255
2013914409	Inorganic pyrophosphatase(EC:3.6.1.1)	0	0	0	1	0	0	0	0.0007477
Dehalococcoides_KB1_0328	DNA gyrase subunit B (EC 5.99.1.3)(EC:5.99.1.3)	0	0	0	1	0	0	0	0.00070641
Dehalococcoides_KB1_0960	hypothetical protein	0	0	0	1	0	0	0	0.00068539
2013900716	hypothetical protein	0	0	0	1	0	0	0	0.00066558
2013905888	hypothetical protein	0	0	0	1	0	0	0	0.00062921
Dehalococcoides_KB1_0557	Predicted membrane protein	0	0	0	1	0	0	0	0.00060923
Dehalococcoides_KB1_0098	Fe-S oxidoreductase	0	0	0	1	0	0	0	0.00058449
2013919678	Flagellin and related hook-associated proteins	0	0	0	1	0	0	0	0.00056444
2013926699	hypothetical protein	0	0	0	1	0	0	0	0.00055093
Dehalococcoides_KB1_0242	Type II secretory pathway, component PulF	0	0	0	1	0	0	0	0.00053308
2013926622	Excinuclease ABC subunit A	0	0	0	1	0	0	0	0.00049207
2013903815	Inorganic pyrophosphatase(EC:3.6.1.1)	0	0	0	1	0	0	0	0.00047581
2013905763	carbamoyl-phosphate synthase large subunit(EC:6.3.4.16,EC:6.3.5.5)	0	0	0	1	0	0	0	0.00046058
Dehalococcoides_KB1_0246	Uncharacterized conserved protein containing a ferredoxin-like domain	0	0	0	1	0	0	0	0.00045875
2013904402	amino acid-binding protein	0	0	0	1	0	0	0	0.00045155
2013890454	bacterial translation initiation factor 2 (bIF-2)	0	0	0	1	0	0	0	0.00043288
2013886582	ABC-type polysaccharide/polyol phosphate export systems, permease component	0	0	0	1	0	0	0	0.00042646
Dehalococcoides_KB1_1326	Flagellar basal body rod protein	0	0	0	1	0	0	0	0.000389
2013891805	Uncharacterized protein conserved in bacteria	0	0	0	1	0	0	0	0.00035429
2013897192	Glycosyltransferase	0	0	0	1	0	0	0	0.00034372
2013897593	Transposase IS66 family.	0	0	0	1	0	0	0	0.00030301
Dehalococcoides_KB1_0971	pyruvate ferredoxin oxidoreductase, alpha subunit (EC 1.2.7.1)(EC:1.2.7.1)	0	0	0	1	0	0	0	0.00029986
2013902794	OB-fold nucleic acid binding domain.	0	0	0	1	0	0	0	0.00027547
2013904608	Sugar phosphate permease	0	0	0	1	0	0	0	0.00027547
2013896782	Sep-tRNA:Cys-tRNA synthase (EC 2.5.1.-)(EC:2.5.1.73)	0	0	0	1	0	0	0	0.00025531
Dehalococcoides_KB1_0850	Indolepyruvate ferredoxin oxidoreductase, alpha and beta subunits(EC:1.2.7.8)	0	0	0	1	0	0	0	0.0002419
2013898224	5'-3' exonuclease (including N-terminal domain of PolI)(EC:2.7.7.7)	0	0	0	1	0	0	0	0.00022489
2013900730	Predicted signaling protein consisting of a modified GGDEF domain and a DHH domain	0	0	0	1	0	0	0	0.00017526
2013892730	hypothetical protein	0	0	0	1	0	0	0	8.1605E-05

Table A3.3. Proteins detected in all five samples (KB-1 mixed culture, PM2A2, EW1, O-BH9-A1 and O-BH10-A1)

			Spectral Counts					NSAF				
Protein ID	Homolog	Description	KB1	PM2A2	EW1	O-BH9-A1	O-BH10-A1	KB1	PM2A2	EW1	O-BH9-A1	O-BH10-A1
gi|157326512	VcrA	reductive dehalogenase	984	10	6	9	6	1.08E-02	4.67E-03	4.74E-03	9.04E-04	1.36E-03
DehalGT_1237	VcrA	reductive dehalogenase	984	10	6	9	6	1.06E-02	4.58E-03	4.65E-03	8.86E-04	1.33E-03
2013896112	VcrA	reductive dehalogenase	949	10	6	9	6	1.03E-02	4.58E-03	4.65E-03	8.86E-04	1.33E-03
gi|77176887	VcrA	reductive dehalogenase	854	10	5	8	5	9.53E-03	4.72E-03	4.00E-03	8.13E-04	1.14E-03
2013887519		hypothetical protein	1695	8	6	30	33	9.23E-03	1.85E-03	2.34E-03	1.49E-03	3.69E-03
gi|77176860	1545	reductive dehalogenase	553	1	1	2	1	6.41E-03	4.91E-04	8.31E-04	2.11E-04	2.38E-04
FL2_RdhA6	1545	reductive dehalogenase	551	1	1	2	1	6.39E-03	4.91E-04	8.31E-04	2.11E-04	2.38E-04
2013897436	1545	reductive dehalogenase	560	1	1	2	1	6.28E-03	4.75E-04	8.04E-04	2.04E-04	2.30E-04
cbdbA1638	1545	reductive dehalogenase	560	1	1	2	1	6.28E-03	4.75E-04	8.04E-04	2.04E-04	2.30E-04
DehalGT_1353	1545	reductive dehalogenase	560	1	1	2	1	6.28E-03	4.75E-04	8.04E-04	2.04E-04	2.30E-04
2013895580		translation elongation factor 1A (EF-1A/EF-Tu)(EC:3.6.5.3)	196	8	8	1	3	4.43E-03	7.67E-03	1.30E-02	2.06E-04	1.39E-03
2013887541		chaperonin GroL	312	5	5	24	17	3.26E-03	2.21E-03	3.74E-03	2.28E-03	3.65E-03
Glov_1331		translation elongation factor Tu	213	7	8	3	6	3.02E-03	4.20E-03	8.12E-03	3.87E-04	1.74E-03
Glov_1344		translation elongation factor Tu	213	7	8	3	6	3.02E-03	4.20E-03	8.12E-03	3.87E-04	1.74E-03
DET1428		co-chaperonin GroEL	231	5	5	20	12	2.41E-03	2.21E-03	3.74E-03	1.90E-03	2.57E-03
PCEOTH_831740		ATP synthase F1 subcomplex beta subunit(EC:3.6.3.14)	40	1	3	6	2	2.14E-03	2.26E-03	1.15E-02	2.92E-03	2.19E-03
PCEOTH_2517890		ATP synthase F1 subcomplex beta subunit(EC:3.6.3.14)	34	1	3	6	2	2.01E-03	2.50E-03	1.27E-02	3.23E-03	2.42E-03
Glov_3170		ATP synthase F1, beta subunit (EC:3.6.3.14)	148	3	4	14	7	1.76E-03	1.51E-03	3.41E-03	1.52E-03	1.71E-03
2013899565		degV family protein	82	1	1	20	12	1.65E-03	8.52E-04	1.44E-03	3.66E-03	4.95E-03
PCEOTH_619260		ketol-acid reductoisomerase (EC 1.1.1.86)(EC:1.1.1.86)	28	2	1	1	1	1.37E-03	4.13E-03	3.50E-03	4.44E-04	1.00E-03
PCEOTH_1287470		translation elongation factor 1A (EF-1A/EF-Tu)(EC:3.6.5.3)	33	11	7	5	1	1.31E-03	1.85E-02	2.00E-02	1.81E-03	8.17E-04
Glov_2019		Phosphopyruvate hydratase (EC:4.2.1.11)	94	3	1	3	3	1.22E-03	1.65E-03	9.33E-04	3.56E-04	8.01E-04
PCEOTH_2434430		translation elongation factor 1A (EF-1A/EF-Tu)(EC:3.6.5.3)	30	11	7	5	1	1.17E-03	1.82E-02	1.95E-02	1.77E-03	8.00E-04
PCEOTH_726050		ATP synthase F1 subcomplex beta subunit(EC:3.6.3.14)	28	1	3	6	2	1.16E-03	1.75E-03	8.87E-03	2.25E-03	1.69E-03
PCEOTH_3043890		ATP synthase F1 subcomplex beta subunit(EC:3.6.3.14)	49	1	3	6	3	1.13E-03	9.74E-04	4.94E-03	1.26E-03	1.42E-03
2013897074		ketol-acid reductoisomerase (EC 1.1.1.86)(EC:1.1.1.86)	64	2	1	3	2	1.08E-03	1.43E-03	1.21E-03	4.62E-04	6.94E-04
PCEOTH_878390		ATP synthase F1 subcomplex beta subunit(EC:3.6.3.14)	24	1	3	7	2	9.97E-04	1.76E-03	8.93E-03	2.65E-03	1.71E-03
PCEDHC_06710		BNR/Asp-box repeat./Fibronectin type III domain.	174	1	1	10	3	9.75E-04	2.37E-04	4.02E-04	5.11E-04	3.45E-04
2013888620		ATP synthase F1 subcomplex beta subunit (EC:3.6.3.14)	43	2	4	7	2	9.50E-04	1.87E-03	6.33E-03	1.41E-03	9.07E-04
PCEOTH_660870		ATP synthase F1 subcomplex beta subunit(EC:3.6.3.14)	23	1	3	10	2	9.35E-04	1.72E-03	8.74E-03	3.70E-03	1.67E-03
DET1407		BNR/Asp-box repeat domain protein	165	1	1	10	3	9.25E-04	2.37E-04	4.02E-04	5.11E-04	3.45E-04
PCEOTH_240310		ATP synthase F1 subcomplex beta subunit(EC:3.6.3.14)	27	2	3	6	2	8.66E-04	2.72E-03	6.89E-03	1.75E-03	1.32E-03
PCEOTH_145020		ATP synthase F1 subcomplex beta subunit(EC:3.6.3.14)	19	1	1	1	1	7.61E-04	1.70E-03	2.87E-03	3.65E-04	8.22E-04
DET0831		ketol-acid reductoisomerase(EC:1.1.1.86)	43	2	1	1	1	7.27E-04	1.43E-03	1.21E-03	1.54E-04	3.47E-04
PCEOTH_2733910		ATP synthase F1 subcomplex beta subunit(EC:3.6.3.14)	58	1	3	8	4	7.12E-04	5.20E-04	2.64E-03	8.95E-04	1.01E-03
PCEOTH_512590		Molecular chaperone	15	1	2	5	2	6.58E-04	1.86E-03	6.28E-03	2.00E-03	1.80E-03
2013890562		ABC-type Fe3+-hydroxamate transport system, periplasmic component	41	1	1	7	1	6.57E-04	6.79E-04	1.15E-03	1.02E-03	3.29E-04
Glov_1624		isocitrate dehydrogenase, NADP-dependent (EC:1.1.1.42)	82	2	1	1	1	6.20E-04	6.41E-04	5.42E-04	6.89E-05	1.55E-04
2013900253		chaperonin GroL	58	3	3	8	6	5.97E-04	1.31E-03	2.21E-03	7.50E-04	1.27E-03
2013917999		ATP synthase F1 subcomplex beta subunit (EC:3.6.3.14)	28	3	4	6	4	5.78E-04	2.62E-03	5.91E-03	1.13E-03	1.69E-03
2013895374		ATP synthase F1 subcomplex alpha subunit (EC:3.6.3.14)	43	2	1	1	3	5.66E-04	1.12E-03	9.44E-04	1.20E-04	8.11E-04
2013922024		LSU ribosomal protein L12P	9	3	3	3	2	4.04E-04	5.70E-03	9.65E-03	1.23E-03	1.84E-03
PCEOTH_1239690		Chaperonin GroEL (HSP60 family)	7	1	1	3	1	3.36E-04	2.03E-03	3.44E-03	1.31E-03	9.84E-04
PCEOTH_1796930		Chaperonin GroEL (HSP60 family)	10	1	1	9	7	2.98E-04	1.26E-03	2.14E-03	2.45E-03	4.29E-03
Swol_2343		ribosomal protein L7/L12	6	3	4	3	1	2.69E-04	5.70E-03	1.29E-02	1.23E-03	9.21E-04
PCEOTH_2546790		LSU ribosomal protein L12P	6	3	3	2	3	2.67E-04	5.66E-03	9.57E-03	8.11E-04	2.74E-03
PCEOTH_682880		Chaperonin GroEL (HSP60 family)	7	1	1	3	1	2.55E-04	1.54E-03	2.61E-03	9.95E-04	7.48E-04
Glov_2829		chaperone protein DnaK	28	1	2	6	3	2.46E-04	3.72E-04	1.26E-03	4.80E-04	5.41E-04
PCEOTH_2665550		chaperonin GroL	23	4	1	7	9	2.39E-04	1.76E-03	7.46E-04	6.64E-04	1.92E-03

			Spectral Counts					NSAF				
Protein ID	Homolog	Description	KB1	PM2A2	EW1	O-BH9-A1	O-BH10-A1	KB1	PM2A2	EW1	O-BH9-A1	O-BH10-A1
PCEOTH_2525800		LSU ribosomal protein L12P	4	3	3	2	1	2.27E-04	7.20E-03	1.22E-02	1.03E-03	1.16E-03
PCEOTH_1371030		LSU ribosomal protein L12P	4	3	3	2	1	1.84E-04	5.84E-03	9.89E-03	8.38E-04	9.44E-04
PCEOTH_1752910		LSU ribosomal protein L12P	4	3	3	3	2	1.84E-04	5.84E-03	9.89E-03	1.26E-03	1.89E-03
2013890519		DNA-directed RNA polymerase subunit beta' (EC 2.7.7.6)	31	1	1	2	3	1.34E-04	1.84E-04	3.10E-04	7.89E-05	2.67E-04
PCEOTH_821690		Methyl-accepting chemotaxis protein	2	1	1	3	1	1.10E-04	2.33E-03	3.94E-03	1.50E-03	1.13E-03
PCEOTH_1250520		methyl-accepting chemotaxis sensory transducer	2	1	1	3	3	9.93E-05	2.10E-03	3.56E-03	1.36E-03	3.06E-03
PCEOTH_1120670		Methyl-accepting chemotaxis protein	2	1	1	2	1	9.84E-05	2.08E-03	3.53E-03	8.97E-04	1.01E-03
PCEOTH_288530		Methyl-accepting chemotaxis protein	2	1	1	2	1	9.27E-05	1.96E-03	3.32E-03	8.45E-04	9.52E-04
PCEOTH_2999900		methyl-accepting chemotaxis sensory transducer	2	1	1	2	1	8.37E-05	1.77E-03	3.00E-03	7.63E-04	8.59E-04
PCEOTH_2283790		methyl-accepting chemotaxis sensory transducer	2	1	1	2	1	7.90E-05	1.67E-03	2.83E-03	7.20E-04	8.11E-04
PCEOTH_1104500		Methyl-accepting chemotaxis protein	2	1	1	2	1	7.63E-05	1.62E-03	2.73E-03	6.95E-04	7.83E-04
PCEOTH_2380250		Methyl-accepting chemotaxis protein	2	1	1	2	1	7.29E-05	1.54E-03	2.61E-03	6.64E-04	7.48E-04
PCEOTH_1462300		translation elongation factor 1A (EF-1A/EF-Tu)(EC:3.6.5.3)	1	4	2	10	4	7.19E-05	1.22E-02	1.03E-02	6.55E-03	5.90E-03
PCEOTH_1229430		Methyl-accepting chemotaxis protein	2	1	1	3	1	7.19E-05	1.52E-03	2.58E-03	9.83E-04	7.38E-04
PCEOTH_866620		Methyl-accepting chemotaxis protein	2	1	1	3	1	7.06E-05	1.49E-03	2.53E-03	9.64E-04	7.24E-04
PCEOTH_2310650		Methyl-accepting chemotaxis protein	2	1	1	2	1	6.60E-05	1.40E-03	2.36E-03	6.01E-04	6.77E-04
PCEOTH_1721300		Methyl-accepting chemotaxis protein	2	1	1	2	1	6.17E-05	1.31E-03	2.21E-03	5.62E-04	6.33E-04
2013896472		methyl-accepting chemotaxis sensory transducer	2	1	1	2	1	5.94E-05	1.26E-03	2.13E-03	5.41E-04	6.09E-04
PCEOTH_2679690		Methyl-accepting chemotaxis protein	2	1	1	3	1	5.78E-05	1.22E-03	2.07E-03	7.90E-04	5.94E-04
PCEOTH_411580		Methyl-accepting chemotaxis protein	2	1	1	3	1	5.15E-05	1.09E-03	1.84E-03	7.03E-04	5.28E-04
2013910496		Methyl-accepting chemotaxis protein	2	1	1	3	1	5.05E-05	1.07E-03	1.81E-03	6.91E-04	5.19E-04
PCEOTH_323630		Methyl-accepting chemotaxis protein	2	1	1	3	1	4.86E-05	1.03E-03	1.74E-03	6.64E-04	4.98E-04
PCEOTH_904410		acetyl-coenzyme A synthetase (EC 6.2.1.1)(EC:6.2.1.1)	2	3	1	15	2	4.51E-05	2.86E-03	1.61E-03	3.08E-03	9.25E-04
2013905002		ATP synthase F1 subcomplex alpha subunit (EC:3.6.3.14)	1	1	1	2	2	4.38E-05	1.86E-03	3.14E-03	7.98E-04	1.80E-03
PCEOTH_1323510		Methyl-accepting chemotaxis protein	2	1	1	2	1	3.94E-05	8.34E-04	1.41E-03	3.59E-04	4.04E-04
PCEOTH_335150		Methyl-accepting chemotaxis protein	2	1	1	3	1	3.03E-05	6.42E-04	1.09E-03	4.14E-04	3.11E-04
2013887853		ABC-type oligopeptide transport system, periplasmic component	3	2	3	16	9	3.02E-05	8.52E-04	2.16E-03	1.47E-03	1.86E-03
Glov_3335		methyl-accepting chemotaxis sensory transducer	2	1	1	2	1	2.61E-05	5.53E-04	9.35E-04	2.38E-04	2.68E-04
2013903892		Tfp pilus assembly protein, ATPase PilM	1	1	1	4	2	1.14E-05	4.81E-04	8.14E-04	4.14E-04	4.66E-04

Table A3.4.*Geobacter* proteins detected in samples

		Spectral Counts					NSAF				
Protein ID	**Description**	KB1	PM2A2	EW1	O-BH9-A1	O-BH10-A1	KB1	PM2A2	EW1	O-BH9-A1	O-BH10-A1
Glov_3706	Hypothetical protein MTH865	111	1	0	0	0	5.66E-03	3.03E-03	0	0	0
Glov_0477	hypothetical protein	63	0	0	0	0	3.43E-03	0	0	0	0
Glov_1331	translation elongation factor Tu	213	7	8	3	6	2.14E-03	4.18E-03	7.80E-03	3.79E-04	1.71E-03
Glov_1344	translation elongation factor Tu	213	7	8	3	6	2.14E-03	4.18E-03	7.80E-03	3.79E-04	1.71E-03
Glov_2929	chaperonin GroEL	289	2	0	16	6	2.10E-03	8.62E-04	0	1.46E-03	1.23E-03
Glov_1794	Rubrerythrin	66	0	0	0	0	1.56E-03	0	0	0	0
Glov_3170	ATP synthase F1, beta subunit (EC:3.6.3.14)	148	3	4	14	7	1.25E-03	1.51E-03	3.28E-03	1.49E-03	1.67E-03
Glov_3311	response regulator receiver protein	38	0	0	0	0	1.24E-03	0	0	0	0
Glov_1338	ribosomal protein L7/L12	35	1	0	1	1	1.10E-03	1.88E-03	0	3.97E-04	8.93E-04
Glov_1625	malate dehydrogenase, NAD-dependent (EC:1.1.1.37)	75	8	4	2	0	9.29E-04	5.89E-03	4.81E-03	3.12E-04	0
Glov_2019	Phosphopyruvate hydratase (EC:4.2.1.11)	94	3	1	3	3	8.68E-04	1.64E-03	8.96E-04	3.48E-04	7.83E-04
Glov_1629	pyruvate ferredoxin/flavodoxin oxidoreductase (EC:1.2.7.3)	28	0	4	1	0	6.15E-04	0	8.54E-03	2.76E-04	0
Glov_3371	flagellin domain protein	41	0	0	0	1	5.93E-04	0	0	0	4.09E-04
Glov_1518	hypothetical protein	34	0	0	0	0	5.64E-04	0	0	0	0
Glov_0345	Acetyl-CoA hydrolase (EC:3.1.2.1)	73	0	0	0	0	5.47E-04	0	0	0	0
Glov_3009	cold-shock DNA-binding domain protein	8	1	1	0	0	4.82E-04	3.58E-03	5.85E-03	0	0
Glov_3186	cold-shock DNA-binding domain protein	8	1	1	0	0	4.75E-04	3.53E-03	5.76E-03	0	0
Glov_3086	hypothetical protein	15	0	0	0	0	4.66E-04	0	0	0	0
Glov_3460	hypothetical protein	8	0	0	0	0	4.48E-04	0	0	0	0
Glov_1624	**isocitrate dehydrogenase, NADP-dependent (EC:1.1.1.42)**	82	2	1	1	1	4.40E-04	6.37E-04	5.21E-04	6.74E-05	1.52E-04
Glov_1597	acetyl-CoA carboxylase, biotin carboxyl carrier protein	17	0	0	0	0	4.33E-04	0	0	0	0
Glov_2870	**reductive dehalogenase**	43	0	0	27	0	3.33E-04	0	0	2.63E-03	0
Glov_2872	**reductive dehalogenase**	43	0	0	27	0	3.33E-04	0	0	2.63E-03	0
Glov_3724	NADPH-dependent FMN reductase	17	0	0	0	0	3.17E-04	0	0	0	0
Glov_1210	phosphate acetyltransferase (EC:2.3.1.8)	26	0	0	1	0	3.11E-04	0	0	1.50E-04	0
Glov_2402	phosphopantetheine-binding	6	0	0	0	0	3.06E-04	0	0	0	0
Glov_0505	thioredoxin	8	0	0	0	0	2.92E-04	0	0	0	0
Glov_3172	ATP synthase F1, alpha subunit (EC:3.6.3.14)	34	2	0	1	3	2.69E-04	9.42E-04	0	9.96E-05	6.73E-04
Glov_1879	nitrogen regulatory protein P-II	7	0	0	0	1	2.49E-04	0	0	0	1.00E-03
Glov_2928	chaperonin Cpn10	6	0	0	0	0	2.49E-04	0	0	0	0
Glov_1627	pyruvate flavodoxin/ferredoxin oxidoreductase domain protein (EC:1.2.7.3)	22	0	2	0	0	2.32E-04	0	2.05E-03	0	0
Glov_2165	sigma 54 modulation protein/ribosomal protein S30EA	10	0	0	0	0	2.20E-04	0	0	0	0
Glov_3013	Acetyl-CoA hydrolase (EC:3.1.2.1)	27	0	0	0	0	2.07E-04	0	0	0	0
Glov_1929	trigger factor	21	0	0	0	0	1.90E-04	0	0	0	0
Glov_1797	Rubrerythrin	9	0	0	0	0	1.86E-04	0	0	0	0
Glov_3257	LamB porin family protein, putative	23	0	0	0	0	1.86E-04	0	0	0	0
Glov_1934	3-oxoacyl-(acyl-carrier-protein) synthase 2 (EC:2.3.1.179)	19	0	0	0	0	1.84E-04	0	0	0	0
Glov_1379	**Citrate (Si)-synthase (EC:2.3.3.1)**	20	5	1	3	0	1.81E-04	2.69E-03	8.78E-04	3.41E-04	0
Glov_1216	6,7-dimethyl-8-ribityllumazine synthase (EC:2.5.1.78)	7	0	0	0	0	1.80E-04	0	0	0	0
Glov_1887	aconitate hydratase 2 (EC:4.2.1.3)	37	0	1	0	0	1.75E-04	0	4.58E-04	0	0
Glov_2829	chaperone protein DnaK	28	1	2	6	3	1.74E-04	3.70E-04	1.21E-03	4.70E-04	5.28E-04
Glov_3611	Nucleoside-diphosphate kinase (EC:2.7.4.6)	6	1	0	0	0	1.73E-04	1.71E-03	0	0	0
Glov_1149	molybdopterin oxidoreductase (EC:1.2.7.-)	37	0	0	0	0	1.72E-04	0	0	0	0
Glov_1768	aminotransferase class I and II (EC:2.6.1.1)	16	0	0	0	0	1.60E-04	0	0	0	0
Glov_3351	flagellar FlaF family protein	5	0	0	0	0	1.59E-04	0	0	0	0
Glov_2222	Ferritin Dps family protein (EC:1.16.3.1)	7	0	0	0	0	1.58E-04	0	0	0	0
Glov_1935	acyl carrier protein	3	0	0	0	0	1.55E-04	0	0	0	0
Glov_3350	thioredoxin reductase (EC:1.8.1.9)	12	0	0	0	0	1.50E-04	0	0	0	0
Glov_2213	succinate dehydrogenase or fumarate reductase, flavoprotein subunit (EC:1.3.99.1)	24	0	1	0	0	1.50E-04	0	6.05E-04	0	0
Glov_3497	hypothetical protein	3	0	0	0	0	1.47E-04	0	0	0	0
Glov_2501	ketol-acid reductoisomerase (EC:1.1.1.86)	12	0	0	0	0	1.41E-04	0	0	0	0
Glov_3134	NADH dehydrogenase (ubiquinone) 24 kDa subunit (EC:1.6.5.3)	6	0	0	0	0	1.40E-04	0	0	0	0
Glov_1711	hypothetical protein	5	0	0	0	0	1.28E-04	0	0	0	0

		Spectral Counts					NSAF				
Protein ID	**Description**	KB1	PM2A2	EW1	O-BH9-A1	O-BH10-A1	KB1	PM2A2	EW1	O-BH9-A1	O-BH10-A1
Glov_0349	Methionine adenosyltransferase (EC:2.5.1.6)	12	0	0	0	0	1.23E-04	0	0	0	0
Glov_1360	ribosomal protein S8	4	0	0	0	0	1.21E-04	0	0	0	0
Glov_1696	Peroxiredoxin (EC:1.11.1.15)	7	0	0	0	0	1.19E-04	0	0	0	0
Glov_1345	ribosomal protein S10	3	0	0	0	0	1.17E-04	0	0	0	0
Glov_1951	protein of unknown function DUF1255	3	0	0	0	0	1.15E-04	0	0	0	0
Glov_3175	H+transporting two-sector ATPase B/B' subunit (EC:3.6.3.14)	4	0	0	0	0	1.13E-04	0	0	0	0
Glov_1859	amino acid-binding ACT domain protein	4	1	0	1	0	1.11E-04	1.65E-03	0	3.50E-04	0
Glov_1628	thiamine pyrophosphate protein domain protein TPP-binding (EC:1.2.7.3)	7	0	0	0	0	1.02E-04	0	0	0	0
Glov_0475	alkyl hydroperoxide reductase/ Thiol specific antioxidant/ Mal allergen (EC:1.11.1.15)	5	0	0	0	0	1.00E-04	0	0	0	0
Glov_1343	translation elongation factor G	17	0	0	0	1	9.77E-05	0	0	0	1.63E-04
Glov_1932	Glycine hydroxymethyltransferase (EC:2.1.2.1)	10	0	0	0	0	9.59E-05	0	0	0	0
Glov_3216	peptide deformylase (EC:3.5.1.88)	4	0	0	0	0	9.59E-05	0	0	0	0
Glov_2143	heat shock protein Hsp90	15	0	0	0	0	9.27E-05	0	0	0	0
Glov_2760	phosphoribosylaminoimidazolecarboxamide formyltransferase/IMP cyclohydrolase (EC:3.5.4.10, EC:2.1.2.3)	12	0	0	0	0	9.20E-05	0	0	0	0
Glov_2318	ribonucleoside-diphosphate reductase, adenosylcobalamin-dependent (EC:1.17.4.1)	17	0	0	0	0	9.08E-05	0	0	0	0
Glov_2709	translation elongation factor Ts	7	1	0	0	0	8.95E-05	7.60E-04	0	0	0
Glov_2830	GrpE protein	4	0	0	0	0	8.79E-05	0	0	0	0
Glov_1832	methyl-accepting chemotaxis sensory transducer	8	0	0	3	1	8.53E-05	0	0	4.02E-04	3.02E-04
Glov_1335	ribosomal protein L11	3	0	0	0	2	8.46E-05	0	0	0	1.60E-03
Glov_3462	Phosphoenolpyruvate carboxykinase (GTP) (EC:4.1.1.32)	13	0	0	0	0	8.39E-05	0	0	0	0
Glov_2678	phospho-2-dehydro-3-deoxyheptonate aldolase (EC:2.5.1.54)	7	0	0	0	0	8.21E-05	0	0	0	0
Glov_0377	hypothetical protein	4	0	0	0	0	8.16E-05	0	0	0	0
Glov_1052	Rubrerythrin	3	0	0	0	0	7.96E-05	0	0	0	0
Glov_1640	type IV pilus assembly protein PilM	7	0	0	0	0	7.91E-05	0	0	0	0
Glov_1347	ribosomal protein L4/L1e	4	0	0	0	0	7.72E-05	0	0	0	0
Glov_0348	3-isopropylmalate dehydrogenase (EC:1.1.1.85)	7	0	0	0	0	7.67E-05	0	0	0	0
Glov_3251	Adenylosuccinate synthase (EC:6.3.4.4)	8	0	0	0	0	7.40E-05	0	0	0	0
Glov_2608	ribosomal protein S18	2	0	0	0	0	7.23E-05	0	0	0	0
Glov_2058	Rhodanese domain protein	7	0	0	0	0	7.18E-05	0	0	0	0
Glov_2531	aspartate kinase (EC:2.7.2.4)	7	0	0	0	0	6.89E-05	0	0	0	0
Glov_2455	ribosomal protein L19	2	0	0	0	0	6.69E-05	0	0	0	0
Glov_2638	branched-chain amino acid aminotransferase (EC:2.6.1.42)	6	0	0	0	0	6.65E-05	0	0	0	0
Glov_1686	Dinitrogenase iron-molybdenum cofactor biosynthesis protein	2	0	0	0	0	6.63E-05	0	0	0	0
Glov_0106	NADH:flavin oxidoreductase/NADH oxidase (EC:1.-)	6	0	0	0	0	6.59E-05	0	0	0	0
Glov_1362	ribosomal protein L18	2	0	0	0	0	6.52E-05	0	0	0	0
Glov_2315	PhoH family protein	7	0	0	0	0	6.34E-05	0	0	0	0
Glov_2708	ribosomal protein S2	4	0	0	0	0	6.19E-05	0	0	0	0
Glov_1599	glycine cleavage system H protein	2	0	0	0	0	6.17E-05	0	0	0	0
Glov_2606	Dinitrogenase iron-molybdenum cofactor biosynthesis protein	2	0	0	0	0	6.17E-05	0	0	0	0
Glov_3325	2-isopropylmalate synthase (EC:2.3.3.13)	8	0	0	0	0	6.13E-05	0	0	0	0
Glov_0035	thiamine biosynthesis protein ThiS	1	0	0	0	0	6.03E-05	0	0	0	0
Glov_2627	cold-shock DNA-binding domain protein	1	0	0	0	0	6.03E-05	0	0	0	0
Glov_1373	DNA-directed RNA polymerase, alpha subunit (EC:2.7.7.6)	5	0	0	2	0	5.85E-05	0	0	2.94E-04	0
Glov_2077	hypothetical protein	1	0	0	0	0	5.77E-05	0	0	0	0
Glov_3169	ATP synthase F1, epsilon subunit (EC:3.6.3.14)	2	0	0	0	0	5.77E-05	0	0	0	0
Glov_1025	transcription termination factor Rho	6	0	0	4	1	5.75E-05	0	0	4.82E-04	2.71E-04
Glov_1372	ribosomal protein S4	3	0	0	0	0	5.74E-05	0	0	0	0
Glov_1674	Polyribonucleotide nucleotidyltransferase (EC:2.7.7.8)	10	1	0	0	0	5.66E-05	3.36E-04	0	0	0
Glov_1214	Homoserine dehydrogenase (EC:1.1.1.3)	6	0	0	0	0	5.44E-05	0	0	0	0
Glov_1795	catalase/peroxidase HPI (EC:1.11.1.6, EC:1.11.1.7)	10	0	0	0	0	5.41E-05	0	0	0	0
Glov_2950	hypothetical protein	6	0	0	0	0	5.40E-05	0	0	0	0
Glov_3484	nitrogen-fixing NifU domain protein	1	0	0	0	0	5.38E-05	0	0	0	0
Glov_1705	4Fe-4S ferredoxin iron-sulfur binding domain protein	4	0	0	0	0	5.27E-05	0	0	0	0
Glov_3312	methyl-accepting chemotaxis sensory transducer	7	0	0	2	1	5.22E-05	0	0	1.88E-04	2.11E-04

		Spectral Counts					NSAF				
Protein ID	**Description**	KB1	PM2A2	EW1	O-BH9-A1	O-BH10-A1	KB1	PM2A2	EW1	O-BH9-A1	O-BH10-A1
Glov_0177	iron-containing alcohol dehydrogenase	5	0	0	0	0	5.19E-05	0	0	0	0
Glov_1342	ribosomal protein S7	2	0	0	0	0	5.10E-05	0	0	0	0
Glov_1880	glutamine synthetase, type I (EC:6.3.1.2)	6	0	0	0	0	5.08E-05	0	0	0	0
Glov_2464	proposed homoserine kinase (EC:5.4.2.1)	5	0	0	0	0	4.98E-05	0	0	0	0
Glov_1593	Tetratricopeptide TPR_2 repeat protein	4	0	0	0	0	4.97E-05	0	0	0	0
Glov_0343	hypothetical protein	3	0	0	0	0	4.85E-05	0	0	0	0
Glov_1831	CheW protein	2	0	0	0	0	4.74E-05	0	0	0	0
Glov_3137	NADH-quinone oxidoreductase, B subunit (EC:1.6.5.3)	2	0	0	0	0	4.71E-05	0	0	0	0
Glov_2206	phosphopantetheine-binding	1	0	0	0	0	4.68E-05	0	0	0	0
Glov_0987	peptidyl-prolyl cis-trans isomerase cyclophilin type (EC:5.2.1.8)	2	0	0	0	0	4.65E-05	0	0	0	0
Glov_0761	outer membrane chaperone Skp (OmpH)	2	0	0	0	0	4.63E-05	0	0	0	0
Glov_1337	ribosomal protein L10	2	0	0	0	0	4.57E-05	0	0	0	0
Glov_3370	flagellin domain protein	3	0	0	0	0	4.34E-05	0	0	0	0
Glov_1647	Chorismate mutase (EC:5.4.99.5)	1	0	0	0	0	4.19E-05	0	0	0	0
Glov_2145	ribosomal protein S1	6	0	0	0	0	4.17E-05	0	0	0	0
Glov_2639	histone family protein DNA-binding protein	1	0	0	1	0	4.14E-05	0	0	5.21E-04	0
Glov_1328	3-hydroxyisobutyrate dehydrogenase (EC:1.1.1.31, EC:1.1.1.60)	3	0	0	0	0	4.14E-05	0	0	0	0
Glov_2671	Glycine dehydrogenase (decarboxylating) (EC:1.4.4.2)	5	0	0	0	0	4.14E-05	0	0	0	0
Glov_1667	NusA antitermination factor	4	0	0	0	0	4.13E-05	0	0	0	0
Glov_3043	dihydrodipicolinate synthase (EC:4.2.1.52)	3	0	0	0	0	4.12E-05	0	0	0	0
Glov_3272	DegT/DnrJ/EryC1/StrS aminotransferase (EC:2.6.1.87)	4	0	0	0	0	4.11E-05	0	0	0	0
Glov_0641	hypothetical protein	1	0	0	0	0	4.10E-05	0	0	0	0
Glov_1119	ATP phosphoribosyltransferase (EC:2.4.2.17)	3	0	0	0	0	4.10E-05	0	0	0	0
Glov_0101	Pirin domain protein	3	0	0	0	0	3.98E-05	0	0	0	0
Glov_3149	ornithine carbamoyltransferase (EC:2.1.3.3)	3	0	0	0	0	3.94E-05	0	0	0	0
Glov_1949	methionyl-tRNA synthetase (EC:6.1.1.10)	5	0	0	0	0	3.92E-05	0	0	0	0
Glov_0586	protein of unknown function DUF47	2	0	0	0	0	3.88E-05	0	0	0	0
Glov_1689	Cobyrinic acid ac-diamide synthase	3	0	0	0	0	3.87E-05	0	0	0	0
Glov_0694	hypothetical protein	1	0	0	0	0	3.86E-05	0	0	0	0
Glov_1352	ribosomal protein S3	2	0	0	0	0	3.79E-05	0	0	0	0
Glov_2084	dihydroorotase, multifunctional complex type (EC:3.5.2.3)	4	0	0	0	0	3.74E-05	0	0	0	0
Glov_3139	glutamate-1-semialdehyde-2,1-aminomutase (EC:5.4.3.8)	4	0	0	0	0	3.72E-05	0	0	0	0
Glov_3684	Cobyrinic acid ac-diamide synthase	2	0	0	0	0	3.68E-05	0	0	0	0
Glov_3613	Ribulose-phosphate 3-epimerase (EC:5.1.3.1)	2	0	0	0	0	3.60E-05	0	0	0	0
Glov_0147	nickel-dependent hydrogenase large subunit (EC:1.12.99.6)	5	0	0	0	0	3.56E-05	0	0	0	0
Glov_3161	recA protein	3	3	0	0	0	3.55E-05	2.11E-03	0	0	0
Glov_1693	Dinitrogenase iron-molybdenum cofactor biosynthesis protein	1	0	0	0	0	3.55E-05	0	0	0	0
Glov_2705	histidine triad (HIT) protein	1	0	0	0	0	3.49E-05	0	0	0	0
Glov_1336	ribosomal protein L1	2	0	0	0	0	3.41E-05	0	0	0	0
Glov_1872	ribosomal protein L20	1	0	0	0	0	3.40E-05	0	0	0	0
Glov_0401	transcriptional regulator, TraR/DksA family	1	0	0	0	0	3.37E-05	0	0	0	0
Glov_1029	peptide chain release factor 1	3	0	0	0	0	3.36E-05	0	0	0	0
Glov_1943	peptidase M42 family protein (EC:3.2.1.4)	3	0	0	0	0	3.35E-05	0	0	0	0
Glov_0347	aspartate-semialdehyde dehydrogenase (EC:1.2.1.11)	3	0	0	0	0	3.26E-05	0	0	0	0
Glov_1370	ribosomal protein S13	1	0	0	0	0	3.26E-05	0	0	0	0
Glov_0002	DNA polymerase III, beta subunit (EC:2.7.7.7)	3	0	0	0	0	3.21E-05	0	0	0	0
Glov_2673	glycine cleavage system H protein	1	0	0	0	0	3.21E-05	0	0	0	0
Glov_2212	4Fe-4S ferredoxin iron-sulfur binding domain protein (EC:1.3.99.1)	2	0	0	0	0	3.17E-05	0	0	0	0
Glov_2283	endoribonuclease L-PSP	1	0	0	0	0	3.16E-05	0	0	0	0
Glov_2434	response regulator receiver protein	1	0	0	0	0	3.16E-05	0	0	0	0
Glov_3253	hypothetical protein	4	0	0	0	0	3.12E-05	0	0	0	0
Glov_3135	NADH dehydrogenase I, D subunit (EC:1.6.5.3)	3	0	0	0	0	3.06E-05	0	0	0	0
Glov_0624	CoA-binding domain protein	1	0	0	0	0	3.01E-05	0	0	0	0
Glov_2600	aminotransferase class I and II (EC:2.6.1.1)	3	0	0	0	0	3.01E-05	0	0	0	0

		Spectral Counts					NSAF				
Protein ID	**Description**	KB1	PM2A2	EW1	O-BH9-A1	O-BH10-A1	KB1	PM2A2	EW1	O-BH9-A1	O-BH10-A1
Glov_0585	hybrid cluster protein (EC:1.7.-)	4	0	0	0	0	2.99E-05	0	0	0	0
Glov_2647	hybrid cluster protein (EC:1.7.-)	4	0	0	0	0	2.99E-05	0	0	0	0
Glov_2697	hypothetical protein	1	0	0	0	0	2.97E-05	0	0	0	0
Glov_1319	translation elongation factor G	5	0	0	0	0	2.87E-05	0	0	0	0
Glov_2028	putative signal transduction protein	2	0	0	0	0	2.85E-05	0	0	0	0
Glov_0121	Cupin 2 conserved barrel domain protein	1	0	0	0	0	2.82E-05	0	0	0	0
Glov_3191	ribosomal protein L13	1	0	0	0	0	2.80E-05	0	0	0	0
Glov_3411	single-strand binding protein	1	0	0	0	0	2.72E-05	0	0	0	0
Glov_0689	OmpA/MotB domain protein	3	0	0	0	0	2.69E-05	0	0	0	0
Glov_1933	sugar-phosphate isomerase, RpiB/LacA/LacB family (EC:5.3.1.6)	1	0	0	0	0	2.67E-05	0	0	0	0
Glov_1262	Malate dehydrogenase (oxaloacetate-decarboxylating) (NADP(+))., Phosphate acetyltransferase (EC:1.1.1.40)	5	0	0	0	0	2.64E-05	0	0	0	0
Glov_1265	hypothetical protein	2	0	0	0	0	2.63E-05	0	0	0	0
Glov_0699	PpiC-type peptidyl-prolyl cis-trans isomerase (EC:5.2.1.8)	2	0	0	0	0	2.61E-05	0	0	0	0
Glov_2868	peptidylprolyl isomerase FKBP-type	2	0	0	1	0	2.56E-05	0	0	1.61E-04	0
Glov_1964	Fructose-bisphosphatase (EC:3.1.3.11)	2	0	0	0	1	2.53E-05	0	0	0	3.57E-04
Glov_2078	transcription elongation factor GreA	1	0	1	0	0	2.52E-05	0	2.44E-03	0	0
Glov_0661	molybdopterin oxidoreductase	5	0	0	0	0	2.46E-05	0	0	0	0
Glov_1363	ribosomal protein S5	1	0	0	0	0	2.46E-05	0	0	0	0
Glov_3123	Roadblock/LC7 family protein	1	0	0	0	0	2.46E-05	0	0	0	0
Glov_1904	inhibitor of MCP methylation-like protein	1	0	0	0	0	2.44E-05	0	0	0	0
Glov_0828	Rubrerythrin	1	0	0	0	0	2.41E-05	0	0	0	0
Glov_2804	transketolase (EC:2.2.1.1)	4	0	0	0	0	2.39E-05	0	0	0	0
Glov_2802	phospho-2-dehydro-3-deoxyheptonate aldolase (EC:2.5.1.54)	2	0	0	0	0	2.35E-05	0	0	0	0
Glov_0911	phospho-2-dehydro-3-deoxyheptonate aldolase (EC:2.5.1.54)	2	0	0	0	0	2.33E-05	0	0	0	0
Glov_1970	hypothetical protein	2	0	0	0	0	2.29E-05	0	0	0	0
Glov_3678	nicotinate-nucleotide/dimethylbenzimidazole phosphoribosyltransferase (EC:2.4.2.21)	2	0	0	0	0	2.27E-05	0	0	0	0
Glov_2113	hypothetical protein	1	0	0	0	0	2.26E-05	0	0	0	0
Glov_3081	Adenosylcobinamide kinase (EC:2.7.1.156, EC:2.7.7.62)	1	0	0	0	0	2.25E-05	0	0	0	0
Glov_2087	D-3-phosphoglycerate dehydrogenase (EC:1.1.1.95)	3	0	0	0	0	2.23E-05	0	0	0	0
Glov_1838	dTDP-4-dehydrorhamnose 3,5-epimerase (EC:5.1.3.13)	1	0	0	0	0	2.20E-05	0	0	0	0
Glov_2776	methyl-accepting chemotaxis sensory transducer	3	0	0	3	1	2.19E-05	0	0	2.76E-04	2.07E-04
Glov_2505	dihydroxy-acid dehydratase (EC:4.2.1.9)	3	0	0	0	0	2.16E-05	0	0	0	0
Glov_3324	hexapeptide transferase family protein	1	0	0	0	0	2.14E-05	0	0	0	0
Glov_2007	Tetratricopeptide TPR_2 repeat protein	1	0	0	0	0	2.09E-05	0	0	0	0
Glov_3146	hypothetical protein	2	0	0	0	0	2.03E-05	0	0	0	0
Glov_3549	methyl-accepting chemotaxis sensory transducer	2	0	0	3	3	2.02E-05	0	0	3.82E-04	8.59E-04
Glov_0462	maf protein	1	0	0	0	0	2.00E-05	0	0	0	0
Glov_3174	H+transporting two-sector ATPase B/B' subunit (EC:3.6.3.14)	1	0	0	0	0	1.99E-05	0	0	0	0
Glov_3179	putative rRNA methylase	1	0	0	0	0	1.99E-05	0	0	0	0
Glov_0105	flavoprotein WrbA	1	0	0	0	0	1.95E-05	0	0	0	0
Glov_2151	hypothetical protein	1	0	0	0	0	1.94E-05	0	0	0	0
Glov_3040	aminotransferase class I and II (EC:2.6.1.83)	2	0	0	0	0	1.94E-05	0	0	0	0
Glov_1927	ATP-dependent Clp protease, ATP-binding subunit ClpX	2	0	0	1	1	1.90E-05	0	0	1.19E-04	2.69E-04
Glov_0359	O-acetylhomoserine/O-acetylserine sulfhydrylase (EC:2.5.1.49)	2	0	0	0	0	1.86E-05	0	0	0	0
Glov_3165	homoaconitate hydratase family protein (EC:4.2.1.35, EC:4.2.1.33)	2	0	0	0	0	1.86E-05	0	0	0	0
Glov_3372	hypothetical protein	1	0	0	0	0	1.86E-05	0	0	0	0
Glov_3252	Histidine--tRNA ligase	2	0	0	0	0	1.85E-05	0	0	0	0
Glov_3335	methyl-accepting chemotaxis sensory transducer	2	1	1	2	1	1.85E-05	5.50E-04	8.98E-04	2.33E-04	2.62E-04
Glov_0822	Histidinol dehydrogenase (EC:1.1.1.23)	2	0	0	0	0	1.84E-05	0	0	0	0
Glov_1858	Phenylacetate--CoA ligase (EC:6.2.1.30)	2	0	0	0	0	1.83E-05	0	0	0	0
Glov_3208	transcriptional regulator, TraR/DksA family	1	0	0	0	0	1.82E-05	0	0	0	0
Glov_0990	protein of unknown function DUF512	2	0	0	0	0	1.79E-05	0	0	0	0
Glov_1207	exsB protein	1	0	0	0	0	1.78E-05	0	0	0	0
Glov_1598	acetyl-CoA carboxylase, biotin carboxylase (EC:6.4.1.2, EC:6.3.4.14)	2	0	0	0	0	1.78E-05	0	0	0	0

		Spectral Counts					NSAF				
Protein ID	**Description**	KB1	PM2A2	EW1	O-BH9-A1	O-BH10-A1	KB1	PM2A2	EW1	O-BH9-A1	O-BH10-A1
Glov_0573	Glutamate dehydrogenase (NADP(+)) (EC:1.4.1.4)	2	0	1	2	0	1.78E-05	0	8.62E-04	2.23E-04	0
Glov_1614	HAD-superfamily hydrolase, subfamily IA, variant 3 (EC:5.4.2.6)	1	0	0	0	0	1.78E-05	0	0	0	0
Glov_3726	haloacid dehalogenase, type II (EC:3.8.1.2)	1	0	0	0	0	1.74E-05	0	0	0	0
Glov_3145	argininosuccinate lyase (EC:4.3.2.1)	2	0	0	0	0	1.74E-05	0	0	0	0
Glov_1040	type IV pilus assembly PilZ	1	0	0	0	0	1.69E-05	0	0	0	0
Glov_1303	diguanylate cyclase	1	0	0	0	0	1.68E-05	0	0	0	0
Glov_2786	two component, sigma54 specific, transcriptional regulator, Fis family	2	0	0	0	0	1.66E-05	0	0	0	0
Glov_1245	protein of unknown function DUF28	1	0	0	0	0	1.61E-05	0	0	0	0
Glov_1618	Triose-phosphate isomerase (EC:5.3.1.1)	1	0	0	0	0	1.58E-05	0	0	0	0
Glov_1891	methyl-accepting chemotaxis sensory transducer	2	0	0	3	1	1.56E-05	0	0	2.95E-04	2.21E-04
Glov_1021	methyl-accepting chemotaxis sensory transducer	2	0	0	3	1	1.54E-05	0	0	2.90E-04	2.17E-04
Glov_2484	Indole-3-glycerol-phosphate synthase (EC:4.1.1.48)	1	0	0	0	0	1.50E-05	0	0	0	0
Glov_3042	Dihydrodipicolinate reductase (EC:1.3.1.26)	1	0	0	0	0	1.50E-05	0	0	0	0
Glov_0149	methyl-accepting chemotaxis sensory transducer	2	0	0	3	1	1.49E-05	0	0	2.82E-04	2.11E-04
Glov_0338	protein of unknown function DUF152	1	0	0	0	0	1.49E-05	0	0	0	0
Glov_1286	methyl-accepting chemotaxis sensory transducer	2	0	0	4	1	1.48E-05	0	0	3.72E-04	2.09E-04
Glov_0882	methyl-accepting chemotaxis sensory transducer	2	0	0	4	1	1.47E-05	0	0	3.71E-04	2.08E-04
Glov_0889	methyl-accepting chemotaxis sensory transducer	2	0	0	3	1	1.47E-05	0	0	2.78E-04	2.08E-04
Glov_2961	methyl-accepting chemotaxis sensory transducer	2	0	0	3	1	1.47E-05	0	0	2.77E-04	2.08E-04
Glov_0572	Electron transfer flavoprotein alpha/beta-subunit	1	0	0	0	0	1.47E-05	0	0	0	0
Glov_3132	molybdopterin oxidoreductase (EC:1.6.5.3, EC:1.2.1.43, EC:1.2.1.2)	3	0	0	0	0	1.46E-05	0	0	0	0
Glov_1039	putative signal transduction protein	1	0	0	0	0	1.46E-05	0	0	0	0
Glov_1349	ribosomal protein L2	1	0	0	0	0	1.45E-05	0	0	0	0
Glov_1733	methyl-accepting chemotaxis sensory transducer	3	0	0	1	1	1.45E-05	0	0	6.08E-05	1.37E-04
Glov_1340	DNA-directed RNA polymerase, beta' subunit (EC:2.7.7.6)	5	3	0	3	3	1.44E-05	5.12E-04	0	1.08E-04	2.44E-04
Glov_1659	dTDP-4-dehydrorhamnose reductase (EC:1.1.1.133)	1	0	0	0	0	1.44E-05	0	0	0	0
Glov_3214	metal dependent phosphohydrolase	1	0	0	0	0	1.41E-05	0	0	0	0
Glov_0461	methyl-accepting chemotaxis sensory transducer	2	0	0	3	1	1.40E-05	0	0	2.64E-04	1.98E-04
Glov_1735	methyl-accepting chemotaxis sensory transducer	3	0	0	1	1	1.37E-05	0	0	5.76E-05	1.30E-04
Glov_3152	acetylglutamate kinase (EC:2.7.2.-, EC:2.7.2.8)	1	0	0	0	0	1.36E-05	0	0	0	0
Glov_1013	RNA polymerase, sigma 70 subunit, RpoD family	2	0	0	0	0	1.36E-05	0	0	0	0
Glov_3047	phosphoribosylaminoimidazole-succinocarboxamide synthase (EC:6.3.2.6)	1	0	0	0	0	1.34E-05	0	0	0	0
Glov_0515	TPR repeat-containing protein	1	0	0	0	0	1.33E-05	0	0	0	0
Glov_0368	pyruvate flavodoxin/ferredoxin oxidoreductase domain protein (EC:1.2.7.-)	4	3	0	3	0	1.33E-05	5.94E-04	0	1.26E-04	0
Glov_2304	dihydroorotate dehydrogenase family protein (EC:1.3.98.1)	1	0	0	0	0	1.31E-05	0	0	0	0
Glov_1024	cysteine synthase (EC:2.5.1.47, EC:2.5.1.47)	1	0	0	0	0	1.30E-05	0	0	0	0
Glov_3375	Tetratricopeptide TPR_2 repeat protein	1	0	0	0	0	1.30E-05	0	0	0	0
Glov_2548	response regulator receiver modulated CheW protein	1	0	0	0	0	1.27E-05	0	0	0	0
Glov_0765	oxidoreductase domain protein	1	0	0	0	0	1.27E-05	0	0	0	0
Glov_2044	ATPase associated with various cellular activities AAA_3 (EC:3.6.3.-)	1	0	0	0	0	1.27E-05	0	0	0	0
Glov_1758	hypothetical protein	1	0	0	0	0	1.26E-05	0	0	0	0
Glov_2522	ATP-dependent metalloprotease FtsH (EC:3.4.24.-)	2	0	0	2	0	1.25E-05	0	0	1.58E-04	0
Glov_2277	Polyprenyl synthetase (EC:2.5.1.90)	1	0	0	0	0	1.24E-05	0	0	0	0
Glov_1869	threonyl-tRNA synthetase (EC:6.1.1.3)	2	0	0	0	0	1.23E-05	0	0	0	0
Glov_0949	fructose-1,6-bisphosphate aldolase, class II (EC:4.1.2.13)	1	0	0	0	0	1.22E-05	0	0	0	0
Glov_3555	response regulator receiver modulated GAF sensor protein	1	0	0	0	0	1.22E-05	0	0	0	0
Glov_0418	3-oxoacyl-(acyl-carrier-protein) synthase III (EC:2.3.1.180)	1	0	0	0	0	1.22E-05	0	0	0	0
Glov_1882	tryptophanyl-tRNA synthetase (EC:6.1.1.2)	1	0	0	0	0	1.21E-05	0	0	0	0
Glov_3525	methyl-accepting chemotaxis sensory transducer	2	0	0	3	1	1.21E-05	0	0	2.28E-04	1.71E-04
Glov_1041	methyl-accepting chemotaxis sensory transducer	2	0	0	3	1	1.20E-05	0	0	2.27E-04	1.70E-04
Glov_1616	glyceraldehyde-3-phosphate dehydrogenase, type I (EC:1.2.1.12)	1	0	0	0	0	1.19E-05	0	0	0	0
Glov_1873	phenylalanyl-tRNA synthetase, alpha subunit (EC:6.1.1.20)	1	0	1	0	0	1.18E-05	0	1.14E-03	0	0
Glov_2597	Agmatine deiminase (EC:3.5.3.12)	1	0	0	0	0	1.17E-05	0	0	0	0
Glov_3496	signal recognition particle-docking protein FtsY	1	0	0	0	0	1.16E-05	0	0	0	0

		Spectral Counts					NSAF				
Protein ID	**Description**	KB1	PM2A2	EW1	O-BH9-A1	O-BH10-A1	KB1	PM2A2	EW1	O-BH9-A1	O-BH10-A1
Glov_0762	UDP-3-O-(3-hydroxymyristoyl) glucosamine N-acyltransferase (EC:2.3.1.-)	1	0	0	0	0	1.15E-05	0	0	0	0
Glov_0385	methyl-accepting chemotaxis sensory transducer	2	0	0	3	1	1.14E-05	0	0	2.15E-04	1.61E-04
Glov_3188	N-acetyl-gamma-glutamyl-phosphate reductase (EC:1.2.1.-, EC:1.2.1.38)	1	0	0	0	0	1.12E-05	0	0	0	0
Glov_3345	Alanine--glyoxylate transaminase (EC:2.6.1.-)	1	0	0	0	0	1.12E-05	0	0	0	0
Glov_3260	methylmalonyl-CoA mutase, large subunit (EC:5.4.99.2)	2	0	0	0	0	1.12E-05	0	0	0	0
Glov_0625	Radical SAM domain protein	1	0	0	0	0	1.11E-05	0	0	0	0
Glov_1592	3-dehydroquinate synthase (EC:4.2.3.4)	1	0	0	0	0	1.11E-05	0	0	0	0
Glov_3721	Methionine synthase vitamin-B12 independent (EC:2.1.1.14)	1	0	0	0	0	1.09E-05	0	0	0	0
Glov_1842	peptidase M29 aminopeptidase II (EC:3.4.11.-)	1	0	0	0	0	1.09E-05	0	0	0	0
Glov_2698	hypothetical protein	1	0	0	0	0	1.08E-05	0	0	0	0
Glov_0659	hypothetical protein	1	0	0	0	0	1.06E-05	0	0	0	0
Glov_3071	Cystathionine gamma-synthase (EC:4.4.1.8)	1	0	0	0	0	1.06E-05	0	0	0	0
Glov_2433	aldehyde oxidase and xanthine dehydrogenase molybdopterin binding	2	0	0	0	0	1.04E-05	0	0	0	0
Glov_2486	response regulator receiver protein	1	0	0	0	0	1.03E-05	0	0	0	0
Glov_0664	cell division protein FtsZ	1	0	0	0	0	1.03E-05	0	0	0	0
Glov_2714	1-deoxy-D-xylulose 5-phosphate reductoisomerase (EC:1.1.1.267)	1	0	0	0	0	1.02E-05	0	0	0	0
Glov_2723	DNA polymerase III, alpha subunit (EC:2.7.7.7)	3	0	0	0	0	1.01E-05	0	0	0	0
Glov_1380	creatinase (EC:3.4.13.9)	1	0	0	0	0	1.00E-05	0	0	0	0
Glov_0756	ribonuclease, Rne/Rng family (EC:3.1.26.12)	1	0	0	0	1	5.37E-06	0	0	0	1.52E-04
Glov_1339	DNA-directed RNA polymerase, beta subunit (EC:2.7.7.6)	2	1	0	0	0	5.31E-06	1.58E-04	0	0	0
Glov_1669	translation initiation factor IF-2	1	0	0	1	0	4.19E-06	0	0	5.27E-05	0
Glov_1350	ribosomal protein S19	0	2	0	0	0	0	5.14E-03	0	0	0
Glov_1356	ribosomal protein L14	0	1	0	0	0	0	1.94E-03	0	0	0
Glov_0693	hypothetical protein	0	1	0	0	0	0	1.79E-03	0	0	0
Glov_0827	V-type H(+)-translocating pyrophosphatase (EC:3.6.1.1)	0	4	2	21	5	0	1.39E-03	1.14E-03	1.54E-03	8.28E-04
Glov_0552	LemA family protein	0	1	0	0	0	0	1.22E-03	0	0	0
Glov_1256	LemA family protein	0	1	0	0	0	0	1.22E-03	0	0	0
Glov_0516	hypothetical protein	0	1	0	0	0	0	8.41E-04	0	0	0
Glov_2635	hypothetical protein	0	1	0	0	0	0	5.36E-04	0	0	0
Glov_2615	hydro-lyase, Fe-S type, tartrate/fumarate subfamily, beta subunit (EC:4.2.1.2)	0	1	0	0	0	0	4.36E-04	0	0	0
Glov_1115	TonB-dependent receptor	0	1	0	0	0	0	3.35E-04	0	0	0
Glov_1301	hypothetical protein	0	0	1	0	0	0	0	1.15E-03	0	0
Glov_1450	type II secretion system protein	0	0	1	0	0	0	0	9.54E-04	0	0
Glov_1926	histone family protein DNA-binding protein	0	0	0	1	0	0	0	0	5.44E-04	0
Glov_2215	histone family protein DNA-binding protein	0	0	0	1	0	0	0	0	5.27E-04	0
Glov_0426	hypothetical protein	0	0	0	1	0	0	0	0	5.21E-04	0
Glov_0080	hypothetical protein	0	0	0	1	0	0	0	0	3.19E-04	0
Glov_0373	transaldolase (EC:2.2.1.2)	0	0	0	1	0	0	0	0	2.34E-04	0
Glov_2763	phosphomethylpyrimidine kinase (EC:2.5.1.3, EC:2.7.4.7, EC:2.7.1.49)	0	0	0	2	0	0	0	0	2.03E-04	0
Glov_0812	protein of unknown function DUF124	0	0	0	1	0	0	0	0	1.87E-04	0
Glov_1143	Uroporphyrin-III C/tetrapyrrole (Corrin/Porphyrin) methyltransferase (EC:2.1.1.198)	0	0	0	1	0	0	0	0	1.80E-04	0
Glov_2718	succinyl-CoA synthetase, alpha subunit (EC:6.2.1.5)	0	0	0	1	0	0	0	0	1.72E-04	0
Glov_0262	ATPase associated with various cellular activities AAA_5 (EC:6.6.1.2)	0	0	0	1	0	0	0	0	1.63E-04	0
Glov_0618	phosphate binding protein	0	0	0	1	0	0	0	0	1.56E-04	0
Glov_1890	histidine kinase	0	0	0	1	0	0	0	0	1.30E-04	0
Glov_1754	acetate kinase (EC:2.7.2.1)	0	0	0	1	0	0	0	0	1.19E-04	0
Glov_2552	DEAD/DEAH box helicase domain protein	0	0	0	1	0	0	0	0	1.16E-04	0
Glov_3519	DEAD/DEAH box helicase domain protein (EC:3.6.4.13)	0	0	0	1	0	0	0	0	1.15E-04	0
Glov_0890	putative sigma54 specific transcriptional regulator	0	0	0	1	0	0	0	0	9.21E-05	0
Glov_0808	glucosamine/fructose-6-phosphate aminotransferase, isomerizing (EC:2.6.1.16)	0	0	0	1	0	0	0	0	8.21E-05	0
Glov_1399	SSS sodium solute transporter superfamily	0	0	0	1	0	0	0	0	7.57E-05	0
Glov_1397	SSS sodium solute transporter superfamily	0	0	0	1	0	0	0	0	7.52E-05	0
Glov_0932	methyl-accepting chemotaxis sensory transducer	0	0	0	1	0	0	0	0	7.07E-05	0
Glov_2507	methyl-accepting chemotaxis sensory transducer	0	0	0	1	0	0	0	0	6.11E-05	0

		Spectral Counts					NSAF				
Protein ID	**Description**	KB1	PM2A2	EW1	O-BH9-A1	O-BH10-A1	KB1	PM2A2	EW1	O-BH9-A1	O-BH10-A1
Glov_3227	osmosensitive K+ channel signal transduction histidine kinase (EC:2.7.13.3)	0	0	0	1	0	0	0	0	5.62E-05	0
Glov_1550	multi-sensor hybrid histidine kinase	0	0	0	1	0	0	0	0	5.03E-05	0
Glov_2093	TPR repeat-containing protein	0	0	0	1	0	0	0	0	2.92E-05	0
Glov_0472	nitrogen regulatory protein P-II	0	0	0	0	1	0	0	0	0	1.00E-03
Glov_2675	glycine cleavage system T protein (EC:2.1.2.10)	0	0	0	0	1	0	0	0	0	3.07E-04
Glov_3051	peptidase S16 lon domain protein	0	0	0	0	1	0	0	0	0	1.36E-04
Glov_2533	TPR repeat-containing protein	0	0	0	0	1	0	0	0	0	1.10E-04

Table A3. 5. HupL peptides detected in KB-1 culture sample and the DMC strain homologs that they hit. Peptides highlighted in orange are specific for the Pinellas Group, peptides highlighted in green are specific for the Cornell Group.

Peptide Number	Sequence	Spectral Counts	DMC195	VS	CBDB1	GT	BAV1	KB-1
16	DNDNPFELVRIV	1	X	X	X	X	X	X
15	DNDNPFELVR	4	X	X	X	X	X	X
65	VRDNDNPFELVR	70	X	X	X	X	X	X
24	GPVEQALIGTK	24	X		X	X	X	X
27	GVYGPVEQALIGTK	11	X		X	X		X
12	DGQGVYGPVEQALIGTK	7			X	X		X
30	ISNYQCVVPTTWNCSPKDGQGVYGPVEQALIGTK	4			X	X		X
17	DNQGVYGPVEQALIGTK	2	X					
29	IGEPVIADYEIPETAEGMGLWEAPR	9	X					
46	MVNDTLSHFGAGPAALFSTLGR	20	X					
45	MVNDTLSHFGAGPAALFSTL	1	X					
74	YVSGDPLVQQMVNDTLSHFGAGPAALFSTLGR	4	X					
53	MVVNYVSGDPLVQQMVNDTLSHF	1	X					
52	MVVNYVSGDPLVQQMVNDTL	1	X					
51	MVVNYVSGDPLVQQMVN	1	X					
3	AGPAALFSTLGR	1	X	X	X	X	X	X
21	GAGPAALFSTLGR	13	X	X	X	X	X	X
20	FGAGPAALFSTLGR	29	X	X	X	X	X	X
63	VNDTLAHFGAGPAALFSTLGR	3				X	X	X
62	VNDTLAHFGAGPAALF	1				X	X	X
44	MVNDTLAHFGAGPAALFSTLGR	126				X	X	X
43	MVNDTLAHFGAGPAALFSTL	8				X	X	X
42	MVNDTLAHFGAGPAALFS	3				X	X	X
41	MVNDTLAHFGAGPAALF	15				X	X	X
40	MVNDTLAHFGAGPAAL	15				X	X	X
39	MVNDTLAHFGAGPA	8				X	X	X
38	MVNDTLAH	1				X	X	X

61	VAGDPVVQK	2		X	X	X	X	X
73	YVAGDPVVQK	5		X	X	X	X	X
64	VNYVAGDPVVQK	2		X	X	X	X	X
50	MVVNYVAGDPVVQKMVN	1		X	X	X	X	X
49	MVVNYVAGDPVVQKM	2		X	X	X	X	X
48	MVVNYVAGDPVVQK	18		X	X	X	X	X
47	MVVNYVAGDPVVQ	1		X	X	X	X	X
59	TPYEVGPLAR	7		X	X	X	X	X
72	YENTPYEVGPLAR	18		X	X	X	X	X
70	YDGTPYEVGPLAR	6	X					
10	APRYENTPYEVGPLAR	1		X	X	X	X	X
22	GDTTEYPLNEVTEPEFTK	2	X					
58	TFDPSKITESIK	1	X					
26	GVVSASDLAHR	1	X					
36	LFTQGVVSASDLAHR	8	X					
35	LFTQGTVSASDLTLH	15			X	X	X	X
14	DLEASGTNLATR	1	X					
13	DLEANGTNLATR	3		X	X	X	X	X
25	GVFDLEANGTNLATR	2		X	X	X	X	X
57	SYGVFDLEANGTNLATR	7		X	X	X	X	X
23	GGVTSHPSID	2	X	X	X	X	X	X
69	VVAGGVTSHPSIDSISSFMSK	4			X	X	X	X
68	VVAGGVTSHPSIDSISSF	2			X	X	X	X
67	VVAGGVTSHPSID	14	X	X	X	X	X	X
66	VVAGGVTSHPS	1	X	X	X	X	X	X
56	SVAVVAGGVTSHPSID	9	X	X	X	X	X	X
34	LAHELSAIYSGR	17		X	X	X	X	X
33	KVAQAAVAH	9	X	X	X	X	X	X
71	YEGDYRLPK	7	X	X	X	X	X	X
2	AAGDMSMLAPFYPR	5	X	X	X	X	X	X

8	ALAAGDMSMLAPFYPRYEGD	4	X	X	X	X	X	X
7	ALAAGDMSMLAPFYPRYE	1	X	X	X	X	X	X
6	ALAAGDMSMLAPFYPR	12	X	X	X	X	X	X
5	ALAAGDMSML	4	X	X	X	X	X	X
4	ALAAGDMSM	1	X	X	X	X	X	X
18	DYDGTDPELLK	2	X	X	X	X	X	X
60	VADYDGTDPELLK	1	X	X	X	X	X	X
19	EVADYDGTDPELLK	1	X	X	X	X	X	X
9	ALDYVDVTEVADYDGTDPELLK	9	X		X	X	X	X
55	NLIQGANYIASH	3	X	X	X	X	X	X
54	NLIQGANYIAS	1	X	X	X	X	X	X
1	AAFGVADKIPNNGR	2			X	X	X	X
11	DAVHITQR	5	X	X	X	X	X	X
28	IEATVDGGEVKDAK	1	X	X	X	X	X	X
32	IVIDPITRIE	16	X	X	X	X	X	X
31	IVIDPITR	2	X	X	X	X	X	X
37	MQKIVIDPITR	4	X	X	X	X	X	X